Untersuchungen antiviraler Mechanismen bei Influenzavirus-Infektionen

Dissertation

der Mathematisch-Naturwissenschaftlichen Fakultät
der Eberhard Karls Universität Tübingen
zur Erlangung des Grades eines
Doktors der Naturwissenschaften
(Dr. rer. nat.)

vorgelegt von
Emanuel Haasbach
aus Lindlar

Tübingen
2012

Tag der mündlichen Qualifikation:	27.06.2012
Dekan:	Prof. Dr. Wolfgang Rosenstiel
1. Berichterstatter:	Prof. Dr. Oliver Planz
2. Berichterstatter:	Prof. Dr. Hans-Georg Rammensee

Omnibus muribus, quibus erat in studiorum eorum elaborando mortem obeundum.

ZUSAMMENFASSUNG

Saisonale Influenza-Erkrankungen sind jährlich weltweit für circa 300.000 Todesfälle verantwortlich. Die Influenza-A-Virusinfektion behandelt man derzeit prophylaktisch mittels Impfungen oder therapeutisch mittels antiviralen Substanzen. Die Stammzusammensetzung des Impfstoffes muss jedes Jahr neu angepasst und verabreicht werden. Dieses dauert vom ersten Auftreten eines neuen saisonalen Influenzavirus-Stammes bis hin zum fertigen Impfstoff ca. 4-6 Monate. Ein weiteres Problem ist zudem die zunehmende Resistenzbildung zirkulierender Influenzaviren gegenüber den sich auf dem Markt befindlichen antiviralen Medikamenten. Diese Resistenzbildung macht es erforderlich, neue antiviral wirkende Substanzen und Ansatzpunkte zu entwickeln, die diese Probleme lösen.

Durch diese Dissertation konnten neue Einblicke in die zellulären und immunologischen Mechanismen während einer Influenza-A-Virusinfektion erlangt werden. Einerseits wurde gezeigt, dass die Inhibition des Proteasoms durch einen spezifischen Proteasominhibitor (VL01) zu einer verminderten Zytokin-/Chemokin-Ausschüttung, sowie zu einer Reduktion der Viruslast führt. Andererseits konnte durch exogene Gabe niedriger IFN-α Dosen das angeborene Immunsystem so aktiviert werden, dass ein antiviraler Status generiert wurde, der es dem Immunsystem ermöglicht, schnell auf eine Influenzavirus-Infektion zu reagieren. Weitere Untersuchungen zur Pathogenese von Influenza-A-Viren zeigten, dass die Viren in der Lage sind, dendritische Zellen zu infizieren, die wiederum in den Thymus einwandern und die T-Zellentwicklung stören. Dies führt letztendlich zu einem der Pathogenitätsmechanismen, der Lymphopenie.

Durch Impfstudien in knock-out Mäusen konnten immunologische Mechanismen identifiziert werden, die für die Kreuzprotektion eine wichtige Rolle spielen. Hierbei liegt der $CD4^+$-T-Zellantwort eine wichtige Aufgabe zugrunde.

Während einer Influenzavirus-Infektion kommt es häufig zu Influenza-assoziierten Sekundärinfektionen, wie z.B. bakteriellen Koinfektionen mit Pneumokokken oder Staphylokokken. Ein in diesem Zusammenhang bislang noch nicht aufgeklärtes Phänomen ist das des Influenza-assoziierten Schlaganfalls. Unsere Untersuchungen deuten daraufhin, dass die durch das Influenzavirus induzierte Hyperzytokinämie das Volumen des Schlaganfalls signifikant vergrößert. Wird im Mausmodell die Hyperzytokinämie durch exogene Substanzen reduziert, so verringert sich ferner das Infarktvolumen.

Zusammenfassend ist festzuhalten, dass die Ergebnisse aus dem Zellkultur- sowie Tiermodell eine Basis darstellen, um weiterführende klinische Studien durchführen zu können, so dass ein Transfer vom Tiermodell zum Menschen möglicht ist.

UNTERSUCHUNGEN ANTIVIRALER MECHANISMEN BEI INFLUENZAVIRUS-INFEKTIONEN

Heutzutage sterben jährlich weltweit ca. 300.000 Menschen an einer Influenzavirus-Infektion. Allein in Deutschland sind es jährlich über 7000 Todesopfer (Zucs et al., 2005). Kommt es zu einer Epidemie oder Pandemie, muss mit wesentlich höheren Erkrankungs- und Todesraten gerechnet werden.

Das Influenza-A-Virus gehört zu der Familie der Orthomyxoviridae. Sie verursachen akute respiratorische Beschwerden sowohl in Menschen als auch in Tieren. Es sind umhüllte Viren mit einem in acht Segmente unterteilten Einzelstrang-RNA-Genom in Negativ-Orientierung. Dies kodiert für elf Proteine. Das Influenza-A-Virus ist in verschiedene Subtypen klassifiziert, basierend auf ihrer Antigenität der Hämaglutin- (HA) und Neuraminidase- (NA) Gene. Zurzeit sind 16 HA- (H1-16) und 9 NA-Subtypen (N1-9) bekannt, was zu einer hohen genetischen Diversität führt (Fouchier et al., 2005).

Die im Jahre 2009 aufgetretene pandemische Influenza (Schweinegrippe) wurde von der Weltgesundheitsorganisation (WHO) auf die zweithöchste Stufe (Stufe 5) der Pandemierisikoskala eingestuft. Stufe 5 bedeutet, dass das Influenza-A-H1N1-Virus Erkrankungen und Todesfälle beim Menschen verursachte, wobei größtenteils keine Immunabwehr in der Bevölkerung bestand. Weiterhin konnte das Virus leicht von Mensch zu Mensch übertragen werden.

Während einer Influenza-A-Virusinfektion kommt es zu einer verstärkten Ausschüttung von Zytokinen und Chemokinen, die primär in die Lunge und ins Blut sezerniert werden und dort zu einer immunologischen Dysfunktion (Hyperzytokinämie) führen (Cheung et al., 2002; Chotpitayasunondh et al., 2005; Droebner et al., 2008; Tumpey et al., 2000; Wong and Yuen, 2006). Während dieser Hyperzytokinämie werden verschiedene Zytokine/Chemokine vorrangig durch alveolare Epithelzellen sowie alveolare Makrophagen sezerniert, die wie z.B. IL-1β, IL-6, IL-8, TNF-α, MCP-1, MIP-1, MIP2 und RANTES (de Jong et al., 2006; Lam et al., 2010; Szretter et al., 2007). Diese ziehen unter anderem neutrophile Granulozyten (Neutrophile) an und lösen eine Entzündungsreaktion in den Alveolen aus (Tate et al., 2008). Solche Entzündungsreaktionen führen zu Gewebeschäden, die wiederum die Lungenfunktion beeinträchtigen. .

Das Auftreten von pandemischen Influenza-A-Viren oder Reassortanten zwischen pandemischen und saisonalen sowie aviären Influenza-A-H5N1-Viren gibt Anlass zur Besorgnis. Zwischen dem ersten Nachweis des neuen Virus und der Bereitstellung des

passenden Impfstoffes vergehen durchschnittlich ca. 4-6 Monate. In dieser Zeit ist es unabdingbar, dass eine ärztliche Versorgung der betroffenen Patienten gewährleistet ist. Aus diesem Grund ist es wichtig, antivirale Substanzen bereitzustellen, die diese zeitliche Lücke bestmöglich schließen. Die antiviralen Medikamente, die momentan gegen Influenzaviren zugelassen sind, sind Tamiflu®/Relenza® (Neuraminidasehemmer) sowie Amantadin® (M2-Membranprotein-hemmer). In den vergangenen Jahren nahm die Resistenzentwicklung der zirkulierenden Influenzaviren gegenüber diesen Medikamenten zu (Hurt et al., 2009a; Hurt et al., 2009b; Le et al., 2005; McKimm-Breschkin et al., 2007; Meijer et al., 2009; Rameix-Welti et al., 2008; Sheu et al., 2010). Diese Resistenzbildungen spiegeln einen dringlichen Bedarf an optimierten und effektiveren antiviralen Medikamenten wieder. Um diesem Bedarf gerecht zu werden, müssen innovative Strategien entwickelt werden.

Aufgrund der hohen Mutationsrate des Influenzavirus und der daraus schnell entstehenden Resistenzbildung, ist die Strategie, bei der Suche nach neuen antiviralen Substanzen auf zelleigene Faktoren zu setzen, äußerst vielversprechend. Die Inhibierung von zelleigenen Faktoren, welche das Virus benötigt, um effektiv replizieren zu können, öffnet einen innovativen Ansatz zur Entwicklung von neuen antiviralen Substanzen.

Es wurde bereits gezeigt, dass Influenza-A-Viren zelleigene Faktoren für eine effiziente Replikation benötigen (Ludwig, 2011; Ludwig and Planz, 2008; Shaw, 2011). Folglich ist es sinnvoll, einen solchen Ansatz zu verfolgen, um innovative, wirksame und kostengünstige antivirale Substanzen zu entwickeln.

Während einer Influenzavirus-Infektion stehen dem angeborenen Immunsystem für die Bekämpfung des Virus zwei wichtige Mechanismen zur Verfügung. Einerseits ist dies die RNA Helikase RIG-I, als Rezeptor für intrazelluläre virale doppelsträngige RNA und andererseits die Familie der Toll-like-Rezeptoren. Werden Toll-like-Rezeptoren induziert, kommt es zur Aktivierung verschiedener Transkriptionsfaktoren wie z.B. NF-κB, IRF3 und IRF7. Diese Transkriptionsfaktoren wiederum induzieren die Produktion von Interferonen (IFN´s) (Seth et al., 2006). Interferone gehören zu den effektivsten zelleigenen, antiviral wirkenden Stoffen, die die Vermehrung und Ausbreitung von Viren verhindern können (Goodbourn et al., 2000; Randall and Goodbourn, 2008). Das enorme antivirale Potential der Interferone zeigt sich in der Tatsache, dass viele Virusarten z.B. Influenza-Viren, Newcastle Disease Viren, Masern-Viren und die respiratorischen Synzytial-Viren, die die zelluläre Produktion von Interferonen inhibieren oder mittels viruseigenen Proteinen blockieren. Im Falle einer Influenza-A-Virusinfektion wirkt das Nichtstrukturprotein 1 (NS1) inhibierend auf die Interferonantwort (Huang et al., 2003; Lo et al., 2005; Palosaari et al., 2003; Wang et al.,

2000). Typ I Interferone, Interferon- α und -β, werden von Zellen als Antwort auf eine virale Infektion ausgeschüttet. Ihr Wirkmechanismus ist sowohl autokrin als auch parakrin und bewirkt eine Expression von hunderten IFN-stimulierenden antiviral wirkenden Genen (ISG). Dies ISG´s sind unter anderem involviert in die Hochregulierung der durch doppelsträngige RNA aktivierten Proteine. Hierzu zählt die Proteinkinase R (PKR), die zum Stopp der Proteinbiosynthese führt, die 2´,5´-oligoadenylat Synthetase (OAS), die RNaseL, die den Abbau der mRNA induzieren, und das Mx Protein (Haller et al., 2009; Silverman, 2007). Die Type I Interferone besitzen zusätzlich zu ihren direkten, antiviralen Eigenschaften noch die Fähigkeit, die Expression verschiedenster Zytokine und Chemokine zu regulieren. Dies bewirkt eine zusätzliche Rekrutierung von Monozyten/Makrophagen an den Ort der Infektion. IFN-α/β erhöht ferner die Antigenpräsentation auf Makrophagen und dendritischen Zellen. Zusätzlich wird die IL-12 Rezeptor-Expression und die Typ II Interferonantwort induziert (Matikainen et al., 1999; Rogge et al., 1997; Stark et al., 1998). Folglich spielen die Typ I Interferone eine wichtige Rolle in der angeborenen sowie in der adaptiven Immunantwort.

Neben den direkten Folgen einer Influenzavirus-Infektion wie z.B. hohes Fieber, starke Kopfschmerzen oder starke Gelenk-, Muskelschmerzen spielen immer mehr die so genannten Influenza-assoziierten Erkrankungen eine wichtige Rolle. Zu denen zählen unter anderem bakterielle Koinfektionen mit Pneumokokken oder Staphylokokken sowie das akute progressive Lungenversagen (*Acute Respiratory Distress Syndrome*, ARDS) (Lopez Cde et al., 2009; Xu et al., 2006). Weiterhin gibt es Krankheiten, die durch vermeintlich unabhängige Erkrankungen verstärkt und/oder ausgelöst werden können. Ein solches Beispiel ist der Schlaganfall. Der Schlaganfall ist eine lebensbedrohende Erkrankung des Gehirns, die jährlich Millionen Menschen das Leben kostet. Zu einem Schlaganfall kommt es, wenn die Blutversorgung des Gehirns unterbrochen wird. Aufgrund des Mangels an Glukose und Sauerstoff kann es zu permanenten neurologischen Schäden kommen. Es gibt viele Risikofaktoren die einen Schlaganfall auslösen können, dazu zählt unter anderem auch eine Influenza-A-Virusinfektion. Das Auftreten von Schlaganfällen ist nahe mit dem Auftreten von Infektionen des Respirationstrakts gekoppelt. Die Zeit zwischen den ersten Symptomen einer respiratorischen Infektion und einem Schlaganfall beträgt zum Teil nur wenige Tage (Grau et al., 1998; Grau et al., 1995; Smeeth et al., 2004). Studien konnten zeigen, dass eine Impfung gegen Influenza-A-Viren das Risiko eines Schlaganfalls sowie die daraus resultierende Todesrate reduziert (Grau et al., 2005; Nichol et al., 2003; Wang et al., 2007). Ein Schlaganfall ereignet sich oft parallel zu Krankheiten, bei denen eine systemische

Inflammation vorliegt, z.B. Atherosklerose, Adipositas oder Infektionskrankheiten wie z.B. Influenzavirus-Infektionen (Emsley and Hopkins, 2008).
Aus diesem Grund bestand ein Projekt meiner Dissertation darin, zu untersuchen, welchen Einfluss eine Influenza-A-Virusinfektion auf die Ausbreitung des Schlaganfalls hat. Die dadurch erhaltenen Hinweise könnten zu einem Ansatzpunkt für eine geeignete Therapie im Zusammenhang mit dieser Indikation führen. Ein weiteres Ziel war es, neue antivirale Strategien zu untersuchen, die eine Influenzavirus-Infektion minimieren oder verhindern.
Des Weiteren war ein Ziel meiner Arbeit, neue Einblicke in die immunologischen und pathologischen Prozesse während einer Influenza-A-Virusinfektion zu erlangen. Hierzu zählt das Verständnis zur Entstehung der Lymphopenie sowie die immunologischen Mechanismen, die für die Kreuzprotektion nach einer Impfung wichtig sind.

Untersuchungen zur Wirksamkeit neuartiger antiviraler Substanzen gegen Influenza-A-Viren

In meiner Dissertation habe ich zwei neue Ansätze verfolgt, um antiviral wirkende Substanzen zu identifizieren. In dem einen Ansatz war es das Ziel, durch die Hemmung des Proteasoms, und somit eines zelleigenen Faktors, die Viruslast zu reduzieren. Der zweite innovative Ansatz zielte auf die unterstützende Wirkung des Immunsystems durch die Behandlung mittels niedriger Mengen exogenem IFN-α ab.
In vorangegangenen Arbeiten der Arbeitsgruppe wurde mittels des COX-1-Inhibitors Acetylsalicylsäure (ASS) gezeigt, dass durch Inhibierung des zelleigenen Transkriptionsfaktors NF-κB die Virusreplikation gehemmt werden kann. Ein Ziel meiner Dissertation war es, weitere zelluläre Faktoren zu finden, deren Inhibierung einen antiviralen Effekt zeigen. Aufgrund dieses Ziels sollte die Hemmung des Proteasoms und deren Folgen auf die NF-κB-Aktivität sowie die Virusreplikation untersucht werden. Ich verwendete für meine Arbeiten den synthetisch hergestellten Proteasominhibitor VL-01 der Firma ViroLogik GmbH, Erlangen. Diese Substanz inhibiert selektiv das 26S-Proteasom, welches die zentrale proteolytische Komponente des Ubiquitin-Proteasom-System (UPS) darstellt. Die Fähigkeit solcher Substanzen, das Proteasom und gleichzeitig die NF-κB-Aktivität zu inhibieren, ist bekannt (Breccia and Alimena, 2010; Vink et al., 2006; Yu and Kem, 2010). Während einer Influenzavirus-Infektion agiert NF-κB als ein Induktor für proapoptotische Faktoren wie zum Beispiel *TNF-related apoptosis-inducing ligand* (TRAIL) oder FasL, gefolgt von Caspase-Aktivitäten. Diese Caspase-Aktivität führt zu einem erhöhten nuklearen Export von viralen

Ribonukleoproteinen (RNPs), welche essenziell für eine effiziente Virusreplikation sind. Wird die Caspase- und/oder die NF-κB-Aktivität inhibiert, so werden die RNP´s im Zellkern zurückgehalten und die virale Replikation ist gestört (Mazur et al., 2007; Wurzer et al., 2003). In meinen Versuchen mit dem Proteasominhibitor VL-01 konnte ich zeigen, dass eine Behandlung von Influenzavirus-infizierten humanen Lungenkarziomzellen (A549) mit VL-01 ein Zurückhalten der viralen RNP´s verursachte (Publikation # 1; Abb. 6). Einhergehend mit der Retention der vRNP´s konnte ich eine VL-01 Dosis-abhängige Reduktion des Virustiters sowie die Inhibition des Proteasoms bei nicht toxischen Konzentrationen in verschiedenen Zelltypen zeigen (Publikation #1; Abb. 1).

Neben Untersuchungen im Zellkultursystem wurden auch *in vivo* Experimente durchgeführt. Um mögliche toxische Effekte *in vivo* bei einer systemischen Gabe ausschließen zu können, wurde VL-01 mittels eines Verneblungsgerätes oral verabreicht. Diese lokale Applikation ermöglicht es, die Substanz nur am Ort der Infektion zu applizieren. Im Mausmodell konnte nach einer Influenza-A-Virusinfektion eine VL-01 Dosis-abhängige Reduktion des Virustiters in der Lunge nachgewiesen werden. Eine effektive und *in vivo* nicht toxische Menge von 14,1 mg/kg wurde ermittelt. Bei dieser Menge konnte der Virustiter in der Lunge um mehr als 90% (1,1 ± 0,3 $\log_{10}$ pfu) reduziert werden (Publikation #1; Abb. 2). Aufgrund der verringerten Viruslast in den Lungen stellte sich die Frage, ob diese Reduktion ein Einfluss auf den Krankheitsverlauf sowie auf die Überlebensrate hatte. Zur Beantwortung dieser Frage wurden Mäuse für vier Tage beginnend eine Stunde vor der Infektion und im weiteren Verlauf alle 12 Stunden mit VL-01 behandelt. Anhand der Überlebenskurve sowie dem Gewichtsverlauf und dem klinischen Index konnte festgestellt werden, dass 50% der mit VL-01 behandelten Mäuse vor einer tödlichen Infektion geschützt waren, wohingegen Mäuse, welchen nur das Lösungsmittel verabreicht wurde, alle verstorben sind (Publikation #1; Abb. 4). Um Rückschlüsse auf den Wirkmechanismus von VL-01 ziehen zu können, wurde der Einfluss der für die Influenza typische Hyperzytokinämie untersucht. Hierzu wurden Mäuse systemisch mit Lipopolysaccharid (LPS) oder dem hochpathogenen aviären Influenza-A-H5N1-Virus, A/Mallard/Bavaria/1/2006, infiziert und mit VL-01 behandelt. Die Menge an proinflammatorischen Zytokinen und Chemokinen (IL-1α/β, IL-6, MIP-1β, RANTES and TNF-α) waren nach 1,5 und 3 Stunden nach LPS Gabe sowie nach 12, 30 und 72 Stunden nach Influenzavirus-Infektion zum Teil drastisch reduziert (Publikation #1; Abb. 5).

Durch meine Arbeit konnte gezeigt werden, dass eine lokale Aerosol-Behandlung mit einem Proteasominhibitor sowohl die Proteasom- als auch die NF-κB-Aktivität während einer Influenza-A-Virusinfektion inhibiert bzw. reduziert. Resultierend daraus kommt es zu einer

Reduktion der Zytokine und Chemokine sowie der Viruslast, was folglich zu einer erhöhten Überlebensrate führt.
Ein sich bereits auf dem Markt befindlicher Proteasominhibitor ist Valcade®. Er wird zur Therapie des multiplen Myeloms (Plasmozytom) eingesetzt. Die intravenöse Gabe erfolgt zweimal wöchentlich über einen Zeitraum von zwei Wochen mit bis zu acht Behandlungszyklen. Aufgrund dieser Daten wäre der kurzzeitige und lokale Einsatz von Proteasominhibitoren (z.B. VL-01) bei schweren humanen Influenzafällen denkbar. Sie könnten als antivirale Substanzen eingesetzt werden, da sie sowohl die Virusreplikation als auch die Hyperzytokinämie hemmen.

Den zweiten innovativen Ansatz, den ich verfolgt habe, ist der, der unterstützenden Wirkung des Immunsystems durch die Behandlung mit niedrigen Mengen exogenem IFN-α. Interferone werden bereits zur Therapie verschiedenster Erkrankungen eingesetzt. Hierzu zählen z.B. chronische Hepatitis B-, sowie akute und chronische Hepatitis C-Infektionen (IFN-α), Multiple Sklerose (IFN-β) und Osteopetrose (IFN-γ). Die Behandlung mit Interferonen birgt aufgrund der hohen Dosen (5.000.000 U/Tag) die Gefahr von starken Nebenwirkungen.
Untersuchungen im Tiermodell sowie im Menschen zeigten, dass radioaktiv-markiertes IFN-α nach oraler Gabe im kompletten Mund- und Rachenraum, im Serum sowie in der Niere, Leber und im Herz nachgewiesen werden konnte (Diez et al., 1987; Schellekens et al., 2001). Die orale Anwendung von IFN-α führt zur Aktivierung von natürlichen Killerzellen, zytotoxischen T-Zellen und B-Zellen sowie zur weiteren Produktion von Interferonen (Cummins et al., 2005). Die intranasale Behandlung von Patienten in Osteuropa und Russland mit IFN-α, die an viralen respiratorischen Erkrankungen litten, zeigte eine Reduktion der Viruslast (Imanishi et al., 1980; Isomura et al., 1982; Saito et al., 1985).
Es stellt sich die Frage: Hat eine intranasale Behandlung mit einer niedrigen IFN-α Dosis einen antiviralen Effekt, um sowohl *in vitro* als auch *in vivo* vor einer hochpathogenen sowie einer saisonalen Influenza-A-Virusinfektion zu schützen?
Für die *in vitro* Studien habe ich Mausfibroblasten (MC57) und A549-Zellen mit Spezies-spezifischem IFN-α in aufsteigender Konzentration behandelt und entweder mit dem aviären hochpathogenen Influenza-A-H5N1-Virus A/mute swan/Germany/R1349/07 oder dem humanen pandemischen Influenza-A-H1N1-Virus A/Hamburg/4/2009 infiziert. Nach 24, 48 und 72 Stunden konnte eine signifikante Reduktion der Virusmenge nachgewiesen werden (Publikation # 2; Abb.1). Um das Potential von IFN-α im Vergleich zu Tamiflu®

(Oseltamivir) beurteilen zu können, habe ich die Konzentrationen der beiden Substanzen bestimmt, bei denen der Virustiter zu 50% reduziert wird (IC_{50}). Die IC_{50}-Bestimmung erfolgte mit drei unterschiedlichen Influenzavirus-Stämmen, A/mute swan/Germany/R1349/07 (H5N1, SN1), A/goosander/Bavaria/20/2006 (H5N1, GSB1) und A/Hamburg/4/2009 (H1N1, SH4). Tabelle 1 in der Publikation # 2 zeigt, dass nur zwei der drei Stämme sensitiv auf Tamiflu® reagieren (SN1 und SH4), wohingegen die Replikation aller drei Stämme durch IFN-α gehemmt wird.

Um das antivirale Potential von IFN-α *in vivo* zu testen, wurden Mäuse 72, 48, 24 oder 8 Stunden vor der Infektion mit 1000 U IFN-α intranasal behandelt. 48 Stunden nach der Infektion wurde der Virustiter in der Lunge bestimmt, sowie die Leber und Milz auf toxische Veränderungen untersucht (Publikation # 2; Abb. 3b, c). Es zeigte sich eine Korrelation zwischen dem Behandlungszeitpunkt und dem ermittelten Virustiter in der Lunge. Je kürzer der Zeitraum zwischen der IFN-α Behandlung und der Infektion, desto niedriger war der Virustiter (Publikation 2 #; Abb. 3a). Durch eine Einfachbehandlung konnte der Virustiter in der Lunge um über 90% (1,18 ± 0,61 $\log_{10}$ pfu/ml) reduziert werden. Nach einer Dreifachbehandlung (56, 32 und 8 Stunden von Infektion) hingegen konnte der Virustiter bis zu 99% (2,04 ± 0,15 $\log_{10}$ pfu/ml) verringert werden (Publikation 2 #; Abb. 4). Die Versuche zeigten bei einer dreimaligen intranasalen Gabe von 1000 U IFN-α vor einer normalerweise letalen Influenza-A-H5N1-Virus-Infektion und einer zweimaligen Nachbehandlung eine Überlebensrate von 75%. Im Vergleich dazu verstarben alle Mäuse, die mit Lösungsmittel behandelt wurden, nach der Infektion (Publikation 2 #; Abb. 5b). Anhand des Gewichtsverlaufs und dem klinischen Index der beiden Mausgruppen war deutlich ein unterschiedlicher Krankheitsverlauf zu erkennen. Die IFN-α behandelten Mäuse zeigten nur leichte Krankheitssymptome sowie kaum Änderungen im Gewicht (Publikation 2 #; Abb. 5c, d). Das identische experimentelle Setup wurde verwendet, um den Effekt von einer exogenen niedrigen IFN-α Dosis auf den endogenen IFN-α Level im Serum behandelter Mäuse zu untersuchen. Somit konnte festgestellt werden, ob die exogene IFN-α Gabe die zelleigene Typ I Interferon Antwort verstärkt. Dazu wurde Mäusen an unterschiedlichen Zeitpunkten prä- und post-Infektion (-56, -44, -20, 16, 36, 60 und 84 Stunden) Serum entnommen und auf IFN-α untersucht. Mit zunehmender Anzahl der Behandlungen prä-Infektion (-56, -32 und -8 Stunden) zeigte sich eine Erhöhung des IFN-α Spiegels im Serum. Nach der Infektion sank der IFN-α Spiegel leicht (16 und 36 Stunden), stieg aber nach 60 bzw. 84 Stunden wieder an (Publikation 2 #; Abb. 6a). Dies lässt darauf schließen, dass durch die Translation des viralen NS1 Proteins die Typ I Interferon Antwort und somit die Sekretion des endogenen IFN-α´s

und -β´s unterdrückt wird. Augenscheinlich ist die angeborene Immunantwort durch die Vorbehandlung mit IFN-α soweit aktiviert, dass die ISG´s induziert werden. Durch die Induktion der ISG´s kommt es zur Aktivierung von Transkriptionsfaktoren, die wiederum die PKR und OAS hochregulieren, was letztendlich dazu führt, dass die Viruslast reduziert wird. Dies zeigen ebenfalls die relativen Quantifizierungen von IFN-α, OAS und RNaseL RNA nach dreimaliger IFN-α Behandlung in der Mauslunge. Die jeweilige mRNA Expression zeigte eine Erhöhung in IFN-α behandelten Mäusen im Vergleich zu unbehandelten Kontrollmäusen (Publikation 2 #; Abb. 6b). Basierend auf diesen Ergebnissen liegt die Vermutung nahe, dass durch die intranasale Gabe von einer niedrigen IFN-α Dosis endogenes IFN-α produziert wird, was wiederum die ISG´s am Ort der Infektion induziert und somit die Viruslast reduziert.

Somit konnte ich in meiner Arbeit zeigen, dass *in vivo* eine intranasale Behandlung mit einer Niedrigdosis von IFN-α einen antiviralen Status als Teil der „first line of defense“ induziert, um vor einer schweren Influenza-A-Virusinfektion zu schützen.

Untersuchungen zum Infarktvolumen während einer Influenza-A-Virusinfektion

Der Schlaganfall wird durch verschiedene Risikofaktoren gesteuert. Hierzu gehören auch Influenzavirus-Infektionen oder andere respiratorische Infektionen. Die Frage, die sich stellt ist: Welchen Einfluss hat die Influenza-A-Virusinfektion auf den Krankheitsverlauf während eines Schlaganfalls und welcher Mechanismus liegt dem zugrunde? Wir konnten im Mausmodell zeigen, dass nach einer Infektion mit dem humanen Influenza-A-Virus (A/Puerto Rico/8/1934 (H1N1, PR8)) das Ausmaß des induzierten Schlaganfalls im Vergleich zu nicht-infizierten Mäusen drastisch gestiegen ist. Mäusen, bei denen drei, vier oder fünf Tage nach Influenzavirus-Infektion ein Schlaganfall induziert wurde, zeigten signifikante Unterschiede im Infarktvolumen (Publikation 3 #; Abb. 1). Bei immunhistologischen Untersuchungen des Gehirns sowie beim Virusnachweis im Gehirn oder Blut infizierter Mäuse konnte kein Virus nachgewiesen werden. Lediglich in der Lunge konnte Virus detektiert werden (Publikation 3 #; Abb. 2a). Ein direkter Einfluss des Virus auf das Infarktvolumen ist somit vermutlich nicht gegeben. Veränderungen, die das Ausmaß weiterhin beeinflussen, sind physiologischer Natur z.B. Sauerstoffsättigung, partieller Sauerstoffdruck sowie die Körpertemperatur. Untersuchungen dieser Parameter bei infizierten und nicht-infizierten Mäusen ergaben keine Erklärung des verstärkten Infarktvolumens (Publikation 3 #; Abb. 2b-d). Aufgrund der Hyperzytokinämie während einer Influenzavirus-Infektion wurden Zytokine in der Lunge, im

Plasma und im Gehirn infizierter und unter Schlaganfall leidender Mäuse sowie deren jeweiligen Kontrollgruppen, untersucht. In der Lunge infizierter Mäuse fanden wir erhöhte Konzentrationen von MIP-1α, MIP2, IL-6, IL-1β, MCP-1 und RANTES im Vergleich zu nicht-infizierten Mäusen (Publikation 3 #; Abb. 3a, linke Spalte). Im Plasma fanden sich nur erhöhte Level an RANTES jeweils nach Infektion, unabhängig davon, ob den Mäusen ein Schlaganfall induziert wurde oder nicht (Publikation 3 #; Abb. 3a, mittlere Spalte). Im Gehirn kommt es nach einer Influenzavirus-Infektion allein zu keiner signifikanten Veränderung im Zytokin/Chemokin-Niveau. Während eines Schlaganfalls hingegen kommt es in infizierten Mäusen zu einer signifikanten Hochregulierung von IL-1β, MCP-1 und MIP-2 (Publikation 3 #; Abb. 3a, rechte Spalte) sowie G-CSF, MIP1-β und TNF-α (Publikation 3 #; Anlage 1a, c, d, rechte Spalte). Aufgrund der erhöhten Menge an RANTES und der Tatsache, dass kein direkter Einfluss des Virus (kein Virus im Gehirn) zu erkennen war, stellte sich die Frage, ob RANTES in der Lage ist, in einem Schlaganfall-relevanten Zellmodell die Expression von Zytokinen/Chemokinen zu induzieren. Hierzu wurden primäre Gliazellen und endotheliale Gehirnzellen (bEnd.) unter Sauerstoff-Glukose Entzug (*oxygen-glucose deprivation (OGD)*) in einem *in vitro* Modell für Schlaganfall mit oder ohne RANTES inkubiert. RANTES und OGD Behandlungen in Gliazellen alleine induzieren die Ausschüttung von MIP-2, wobei eine Kombination der beiden keinen additiven Effekt zeigte. Im Gegensatz zu Gliazellen führt eine Einzelbehandlung endothelialer Gehirnzellen mit RANTES oder OGD zu keinem Effekt. Bei einer Kombinationsbehandlung hingegen lässt sich ein gesteigerter Effekt in Hinblick auf die MIP-2 Expression erkennen (Publikation 3 #; Abb. 3b, c). Dieser Effekt könnte die verstärkte Expression von MIP-2 im Gehirn erklären. Die Zytokine MIP-2, IL-1β und MCP-1, welche während eines Schlaganfalls und einer Influenzavirus-Infektion im Gehirn hochreguliert werden, sind bei der Rekrutierung von Neutrophilen involviert (Chen et al., 1994; Connolly et al., 1996; McColl et al., 2007; Murikinati et al., 2010). Durch immunhistologische Untersuchungen konnten wir zeigen, dass in diesem Bereich verstärkt Neutrophile zu finden waren, die die Matrix-Metalloprotease 9 (MMP-9) exprimieren (Publikation 3 #; Abb. 4c). Dies lässt vermuten, dass die durch die Influenzavirus-Infektion ausgeschütteten Zytokine, z.B. MIP-2, Neutrophile rekrutieren, die wiederum die MMP-9 exprimieren. Die MMP-9 sind an der Degradation der extrazellulären Matrix (Kollagen IV) im Bereich der Blut-Hirn-Schranke beteiligt. Nach einer Influenzavirus-Infektion konnte im Bereich des Schlaganfalls durch eine spezifische Färbung eine reduzierte Kollagen-IV-Menge gezeigt werden. Des Weiteren trat bei infizierten Mäusen eine verstärkte IgG-Extravasation in diesen Bereich im Vergleich zu nicht-infizierten Mäusen auf (Publikation 3 #; Abb. 4d). Diese Ergebnisse

weisen darauf hin, dass die durch die Influenzavirus-Infektion induzierten Zytokine und Chemokine Neutrophile aktivieren, diese wiederum MMP´s ausschütten, welche die Blut-Hirn-Schranke permeabel machen, und es somit im Bereich des Schlaganfalls zu Schäden kommt.

Während einer Influenzavirus-Infektion produzieren epitheliale Lungenzellen sowie Makrophagen den Großteil der induzierten Zytokine und Chemokine. Beide Zelltypen exprimieren den *α7 nicotinic acetylcholine receptor* (GTS-21-R), welcher für die Zytokin- und Chemokinfreisetzung verantwortlich ist. Durch den Antagonist GTS-21 kann diese inhibiert werden (Paleari et al., 2009; Tracey, 2009). Aufgrund dieser Tatsachen sollte in den anschließenden Untersuchungen untersucht werden, inwieweit die gezielte Inhibierung von Zytokinen das Infarktvolumen beeinflusst. Durch *in vitro* Untersuchungen konnten wir zeigen, dass eine Dosis-abhängige Behandlung von Influenzavirus-infizierten humanen Lungenkarzinomzellen (A549) mit GTS-21 zu einem erhöhten Zellüberleben führt. Gleichzeitig wurde die RANTES Freisetzung in infizierten Zellen GTS-21 dosis-abhängig minimiert (Publikation 3 #; Abb. 5a, b). Diese inhibitorischen Effekte konnten ebenfalls *in vivo* gezeigt werden. Influenzavirus infizierte Mäuse wurden an Tag drei nach Infektion, direkt und sechs Stunden nach Induktion des Schlaganfalls intraperitoneal mit 10mg/kg GTS-21 behandelt. Ähnlich wie in den Zellkulturexperimenten konnte eine Reduktion von RANTES im Plasma von Influenzavirus-infizierten Mäusen beobachtet werden. In Gehirnen von Influenzavirus-infizierten und Schlaganfall-induzierten Mäusen konnte eine Reduktion von IL-1β, MCP-1 und MIP-2 gemessen werden (Publikation 3 #; Abb. 5c). Bedeutsam ist die Tatsache, dass durch die GTS-21 Behandlung das Infarktvolumen bei infizierten Mäusen signifikant reduziert werden konnte, wohingegen das Infarktvolumen in nicht-infizierten Mäusen nicht beeinflusst wurde (Publikation 3 #; Abb. 5d). Dies lässt darauf schließen, dass die gezielte Inhibierung der Zytokine und Chemokine auf Transkriptionsebene durch GTS-21 spezifisch die Influenzavirus induzierte Freisetzung der Zytokine und Chemokine verhindert, die Rekrutierung der MMP-9 exprimierenden Neutrophilen hemmt und somit das Infarktvolumen minimiert.

Untersuchungen zur Beteiligung der $CD4^+$-T-Zellantwort an der Kreuzprotektion

Impfungen sind zurzeit die effektivste Möglichkeit, einer Influenzavirus-Infektion vorzubeugen. Jährlich wird von der ständigen Impfkommission (STIKO) eine Empfehlung für die notwendige Influenzaimpfung abgegeben. Diese Empfehlung kann aber erst dann gegeben

werden, wenn bekannt ist, welche Virusstämme in der kommenden Grippesaison für die Infektion verantwortlich sind. Spontane Änderungen oder zusätzlich auftretende Virusstämme (Schweinegrippe) können Probleme bei der Bereitstellung des passenden Impfvirus darstellen. Mit Hilfe einer Impfung ist möglich, über die sich in der Impfung befindlichen Viren hinaus, ein Schutz gegen neue unbekannte Virusstämme zu generieren. Eine solche Eigenschaft wird als Kreuzprotektion bezeichnet.

Aufgrund der zeitlich problematischen Bereitstellung des Impfvirus ist es wichtig, die immunologischen Mechanismen, die der Impfung zugrunde liegen, besser zu verstehen. Wie bereits aus der Literatur bekannt, spielt die durch die Impfung induzierte B-Zellantwort eine wichtige Rolle (Dormitzer et al., 2011). Darüber hinaus ist zu untersuchen, welche weiteren Immunzellen, z.B. $CD4^+$-T-Zellen, ebenfalls eine Rolle während der Impfung spielen und ob sie einen Einfluss auf die Kreuzprotektion haben.

Um dies zu untersuchen, wurden unterschiedliche Mausstämme (Wildtyp, Antikörper-defiziente (µMT), $CD4^+$- und $CD8^+$-T-Zell-defiziente), entweder mit dem niedrig pathogenen Influenza-A-H5N2- oder dem aviären hochpathogenen Influenza-A-H5N1-Virus infiziert. Wurden diese Mausstämme mit dem niedrig pathogenen H5N2 Virus infiziert, kam es weder zum Tod noch zum Gewichtsverlust. Wurden die Mäuse hingegen mit dem hochpathogenen H5N1 Virus infiziert, zeigten sich schwere Krankheitssymptome bis hin zum Tod (Publikation # 4; Fig. 2 und Table 1-3). Aufgrund der apathogenen Eigenschaft des H5N2 Virus wurde dieses für die folgenden Untersuchungen als Lebend-Impfvirus verwendet. Alle Mausstämme wurden mit dem H5N2 Impfvirus infiziert und für 80 Tage beobachtet. Nach dieser Zeit wurden die Mäuse mit der 100-fachen MLD_{50} (Maus-Letalen-Dosis 50%) des hochpathogenen H5N1 Virus infiziert. Alle Antikörper-defizienten (µMT), sowie 50% der $CD4^+$-T-Zell-defizienten Mäuse starben. Ein 100%iger Schutz konnte nur bei den $CD8^+$-T-Zell-defizienten und Wildtyp Mäusen beobachtet werden (Publikation # 4; Fig. 3, 4). Um die Kreuzprotektion zu untersuchen, wurde den Mäusen Serum entnommen und auf Virus-spezifische Antikörper hin untersucht. Der Hämagglutinin-Antikörpertiter in allen drei Mausstämmen zeigte eine humorale Antwort sowohl gegen das Impfvirus als auch gegen das „Challenge-Virus“ (Publikation # 4; Fig. 3, 5). Durch diese Arbeit konnte gezeigt werden, dass für eine Kreuzprotektion nicht nur die virus-spezifischen Antikörper vorhanden sein müssen, sondern vielmehr eine $CD4^+$-T-Zellantwort induziert werden muss. Ist das Immunsystem nicht in der Lage, Antikörper zu generieren oder besitzt keine $CD4^+$-T-Zellantwort (µMT- oder $CD4^+$-T-Zell-defiziente Mäuse), liegt die Letalität im Mausmodell bei 50 - 100%, während bei Wildtyp oder $CD8^+$-T-Zell-defizienten Mäusen eine Letalität von

0% festzustellen war. Dies zeigt, dass die Antikörperbildung hilfe-abhängig ist und scheinbar hilfe-unabhängige neutralisierende Antikörper eine untergeordnete Rolle spielen. Den $CD8^+$-T-Zellen kommt bei der Kreuzprotektion eine eher untergeordnete Rolle zu. Andererseits sind $CD8^+$-T-Zellen für das Immunsystem unabdingbar um das Virus zu eliminieren (Doherty et al., 2006).
Diese Untersuchungen geben erste Hinweise zur Entwicklung zukünftiger Impfstoffe, die die $CD4^+$-T-Zellantwort verstärkt induzieren, um somit eine Kreuzprotektion zu ermöglichen.

Untersuchungen zur T-Zellentwicklung während einer Influenza-A-Virusinfektion

Im Verlaufe der saisonalen Influenza werden meist Menschen infiziert, deren Immunsystem auf unterschiedlichste Art geschwächt ist. So sind beispielsweise Kleinkinder, ältere Menschen oder immunsupprimierte Personen verstärkt betroffen. Bei einer hochpathogenen Influenzavirus-Infektion hingegen werden meist junge Menschen (13-15 Jahre) infiziert (Kandun et al., 2008; Smallman-Raynor and Cliff, 2007). Die Ursachen hierfür sind weitestgehend noch nicht bekannt. Ein ebenfalls wichtiger und unaufgeklärter Mechanismus während einer Influenza-A-H5N1-Infektionen im Menschen ist die drastische Reduktion der Lymphozyten, bekannt als Lymphopenie. Aus diesem Grund haben wir den Ort der T-Zellentwicklung, den Thymus, während einer hoch pathogenen aviären Influenzavirus-(HPAIV) Infektion näher untersucht. Während einer HPAIV Infektion konnte eine signifikante Reduktion der Leukozyten im Thymus festgestellt werden. Diese Abnahme konnte ebenfalls anhand der Volumenänderung der Thymi beobachtet werden, was bei niedrig pathogenen Influenzavirus-Stämmen nicht beobachtet werden konnte (Publikation # 5; Fig.1 c-g). Die Expression von Chemokinen und Adhäsionsmolekülen, die für die T-Zellentwicklung wichtig sind, waren ebenfalls nur nach HPAIV Infektion verändert. Weiterhin konnten Influenzavirus spezifische zytotoxische $CD8^+$-T-Zellen sowie infektiöses Virus im Thymus nachgewiesen werden (Publikation # 5; Fig. 2 – 5 und Tab. 1).
Wir konnten zeigen, dass dendritische Zellen (DC) infiziert werden und somit als „Transportmittel“ für das Virus fungieren, um in den Thymus zu gelangen. Hierfür wurden C57Bl/6-GFP^+ Mäuse mit einem HPAIV infiziert, dendritische Zellen aus der Lunge isoliert und anschließend in C57Bl/6-GFP^- Mäuse transferiert. Drei Tage später wurden DC´s aus der Lunge und aus dem Thymus der Empfängermaus isoliert und mittels Fluoreszenzmikroskopie nach GFP^+ DC´s untersucht. Interessanterweise konnten GPF^+ DC´s sowohl in der Lunge als auch im Thymus nachgewiesen werden (Publikation # 5; Fig. 6, 7). Anhand der Daten lässt

sich zeigen, dass hochpathogene aviäre Influenzaviren in der Lage sind, den Thymus über den „Transporter“, die dendritische Zelle, zu erreichen. Dort greifen sie in die dort stattfindende T-Zellentwicklung ein, was zur Lymphopenie führt, gefolgt von einer Atrophie des Thymus.
Sialinsäure-Rezeptoren auf der Zelloberfläche dienen dem Influenza-Virus als Andockpunkt für die Rezeptor-vermittelte Aufnahme in die Zelle. Diese, für die Influenzavirus-Infektion nötigen Sialinsäure-Rezeptoren, haben wir nicht nur auf murinem Thymusgewebe gefunden, sondern auch auf humanem Thymusgewebe (Publikation # 5; Fig. 4b). Dies lässt die Schlussfolgerung zu, dass eine teilweise Übertragung unseres Mausmodells auf den Menschen möglich ist.

Schlussfolgerung

Untersuchungen zur Pathogenese sowie zur Immunantwort nach einer Impfung, durchgeführt mit einem Lebend-Impfvirus, ergaben neue Erkenntnisse, welche ein weiterführendes Verständnis während einer Influenzavirus-Infektion ermöglichen. Diese Erkenntnisse geben Hinweise darauf, dass bei der Entwicklung zukünftiger Impfstoffe gegen Influenzaviren verstärkt auf die Aktivierung der $CD4^+$-T-Zellantwort hingearbeitet werden sollte. Im Mausmodell zeigte sich diese als notwendig, um eine Kreuzprotektion gegen andere Influenza-A-Virusstämme zu generieren.
Weiterhin konnte ich zeigen, dass eine lokale Behandlung mit einer niedrigen IFN-α Dosis zu einer signifikanten Reduktion der Viruslast sowie zur Erhöhung der Überlabensrate führt. Im Vergleich zur Hochdosis-Interferontherapie im humanen Bereich, konnten im Mausmodel keine Nebenwirkungen beobachtet werden. Eine solch lokale Behandlung wäre in einer möglichst frühen Phase der Infektion denkbar, sodass das Immunsystem durch die IFN-α Gabe gestärkt wird und das Virus schneller eliminiert werden kann.
Während einer Influenzavirus-Infektion kommt es zur Hyperzytokinämie, welche einen nicht unerheblichen Teil zur Pathogenese beiträgt. Hierbei sind vor allem die Sekundärinfektionen während bzw. nach einer Influenza zu nennen. Ein Beispiel, welches ich in meiner Dissertation bearbeitet habe, ist die lebensbedrohende Erkrankung des Gehirns, der Schlaganfall. Tritt während einer Influenzavirus-Infektion ein Schlaganfall auf, kommt es aufgrund der Hyperzytokinämie zu einem signifikant vergrößerten Infarktvolumen. Wird die Zytokin-/Chemokinlast durch GTS-21 Gabe reduziert, kann das Infarktvolumen verringert werden. GTS-21 wirkt hauptsächlich hemmend auf die Zytokin/Chemokinfreisetzung und hat keine signifikanten antiviralen Eigenschaften. Eine Möglichkeit, um Sekundärinfektionen

entgegen zu treten, wäre die Behandlung mit Substanzen, die bivalente Eigenschaften aufweisen. Sie sollten einerseits die Viruslast reduzieren und andererseits die inflammatorischen Dysfunktionen regulieren.

Anhand meiner Untersuchungen konnte ich zeigen, dass der Proteasominhibitor VL-01 solch bivalente Eigenschaften besitzt. VL-01 kann sowohl die Viruslast in Influenza-infizierten Mäusen reduzieren, als auch die Freisetzung der Zytokine/Chemokine vermindern. Diese Eigenschaften können innovative Einsatzmöglichkeiten in der Bekämpfung von Influenzavirus-Infektionen sowie deren Sekundärerkrankungen eröffnen.

Grundsätzlich ist festzuhalten, dass durch meine Dissertation neue Aspekte der Pathogenese sowie der Bekämpfung von Influenzaviren mittels neuartiger antiviraler Substanzen und Strategien dargelegt worden sind. In Zukunft besteht die Möglichkeit diese Ergebnisse aus Zellkultur- und Tiermodell als Grundlage zu nutzen, um neue innovative Behandlungsmethoden zu etablieren, die die Gefahr vor einer Influenzavirus-Infektion minimieren.

LITERATUR

Breccia, M., and G. Alimena. 2010. NF-kappaB as a potential therapeutic target in myelodysplastic syndromes and acute myeloid leukemia. *Expert Opin Ther Targets* 14:1157-1176.

Chen, H., M. Chopp, R.L. Zhang, G. Bodzin, Q. Chen, J.R. Rusche, and R.F. Todd, 3rd. 1994. Anti-CD11b monoclonal antibody reduces ischemic cell damage after transient focal cerebral ischemia in rat. *Ann Neurol* 35:458-463.

Cheung, C.Y., L.L. Poon, A.S. Lau, W. Luk, Y.L. Lau, K.F. Shortridge, S. Gordon, Y. Guan, and J.S. Peiris. 2002. Induction of proinflammatory cytokines in human macrophages by influenza A (H5N1) viruses: a mechanism for the unusual severity of human disease? *Lancet* 360:1831-1837.

Chotpitayasunondh, T., K. Ungchusak, W. Hanshaoworakul, S. Chunsuthiwat, P. Sawanpanyalert, R. Kijphati, S. Lochindarat, P. Srisan, P. Suwan, Y. Osotthanakorn, T. Anantasetagoon, S. Kanjanawasri, S. Tanupattarachai, J. Weerakul, R. Chaiwirattana, M. Maneerattanaporn, R. Poolsavathitikool, K. Chokephaibulkit, A. Apisarnthanarak, and S.F. Dowell. 2005. Human disease from influenza A (H5N1), Thailand, 2004. *Emerg.Infect.Dis.* 11:201-209.

Connolly, E.S., Jr., C.J. Winfree, T.A. Springer, Y. Naka, H. Liao, S.D. Yan, D.M. Stern, R.A. Solomon, J.C. Gutierrez-Ramos, and D.J. Pinsky. 1996. Cerebral protection in homozygous null ICAM-1 mice after middle cerebral artery occlusion. Role of neutrophil adhesion in the pathogenesis of stroke. *J Clin Invest* 97:209-216.

Cummins, J.M., G.S. Krakowka, and C.G. Thompson. 2005. Systemic effects of interferons after oral administration in animals and humans. *Am J Vet Res* 66:164-176.

de Jong, M.D., C.P. Simmons, T.T. Thanh, V.M. Hien, G.J. Smith, T.N. Chau, D.M. Hoang, N.V. Chau, T.H. Khanh, V.C. Dong, P.T. Qui, B.V. Cam, d.Q. Ha, Y. Guan, J.S. Peiris, N.T. Chinh, T.T. Hien, and J. Farrar. 2006. Fatal outcome of human influenza A (H5N1) is associated with high viral load and hypercytokinemia. *Nat.Med.* 12:1203-1207.

Diez, R.A., B. Perdereau, and E. Falcoff. 1987. From old results to new perspectives: a look at interferon's fate in the body. *J Interferon Res* 7:553-557.

Doherty, P.C., S.J. Turner, R.G. Webby, and P.G. Thomas. 2006. Influenza and the challenge for immunology. *Nat Immunol* 7:449-455.

Dormitzer, P.R., G. Galli, F. Castellino, H. Golding, S. Khurana, G. Del Giudice, and R. Rappuoli. 2011. Influenza vaccine immunology. *Immunol Rev* 239:167-177.

Droebner, K., S.J. Reiling, and O. Planz. 2008. Role of hypercytokinemia in NF-kappaB p50-deficient mice after H5N1 influenza A virus infection. *J Virol* 82:11461-11466.

Emsley, H.C., and S.J. Hopkins. 2008. Acute ischaemic stroke and infection: recent and emerging concepts. *Lancet Neurol* 7:341-353.

Fouchier, R.A., V. Munster, A. Wallensten, T.M. Bestebroer, S. Herfst, D. Smith, G.F. Rimmelzwaan, B. Olsen, and A.D. Osterhaus. 2005. Characterization of a novel influenza A virus hemagglutinin subtype (H16) obtained from black-headed gulls. *J Virol* 79:2814-2822.

Goodbourn, S., L. Didcock, and R.E. Randall. 2000. Interferons: cell signalling, immune modulation, antiviral response and virus countermeasures. *J Gen Virol* 81:2341-2364.

Grau, A.J., F. Buggle, H. Becher, E. Zimmermann, M. Spiel, T. Fent, M. Maiwald, E. Werle, M. Zorn, H. Hengel, and W. Hacke. 1998. Recent bacterial and viral infection is a risk factor for cerebrovascular ischemia: clinical and biochemical studies. *Neurology* 50:196-203.

Grau, A.J., F. Buggle, S. Heindl, C. Steichen-Wiehn, T. Banerjee, M. Maiwald, M. Rohlfs, H. Suhr, W. Fiehn, H. Becher, and et al. 1995. Recent infection as a risk factor for cerebrovascular ischemia. *Stroke* 26:373-379.

Grau, A.J., B. Fischer, C. Barth, P. Ling, C. Lichy, and F. Buggle. 2005. Influenza vaccination is associated with a reduced risk of stroke. *Stroke* 36:1501-1506.

Haller, O., P. Staeheli, and G. Kochs. 2009. Protective role of interferon-induced Mx GTPases against influenza viruses. *Rev Sci Tech* 28:219-231.

Huang, Z., S. Krishnamurthy, A. Panda, and S.K. Samal. 2003. Newcastle disease virus V protein is associated with viral pathogenesis and functions as an alpha interferon antagonist. *J Virol* 77:8676-8685.

Hurt, A.C., J. Ernest, Y.M. Deng, P. Iannello, T.G. Besselaar, C. Birch, P. Buchy, M. Chittaganpitch, S.C. Chiu, D. Dwyer, A. Guigon, B. Harrower, I.P. Kei, T. Kok, C. Lin, K. McPhie, A. Mohd, R. Olveda, T. Panayotou, W. Rawlinson, L. Scott, D. Smith, H. D'Souza, N. Komadina, R. Shaw, A. Kelso, and I.G. Barr. 2009a. Emergence and spread of oseltamivir-resistant A(H1N1) influenza viruses in Oceania, South East Asia and South Africa. *Antiviral Res* 83:90-93.

Hurt, A.C., J.K. Holien, and I.G. Barr. 2009b. In vitro generation of neuraminidase inhibitor resistance in A(H5N1) influenza viruses. *Antimicrob Agents Chemother* 53:4433-4440.

Imanishi, J., T. Karaki, O. Sasaki, A. Matsuo, K. Oishi, C.B. Pak, T. Kishida, S. Toda, and H. Nagata. 1980. The preventive effect of human interferon-alpha preparation on upper respiratory disease. *J Interferon Res* 1:169-178.

Isomura, S., T. Ichikawa, M. Miyazu, H. Naruse, M. Shibata, J. Imanishi, A. Matsuo, T. Kishida, and T. Karaki. 1982. The preventive effect of human interferon-alpha on influenza infection; modification of clinical manifestations of influenza in children in a closed community. *Biken J* 25:131-137.

Kandun, I.N., E. Tresnaningsih, W.H. Purba, V. Lee, G. Samaan, S. Harun, E. Soni, C. Septiawati, T. Setiawati, E. Sariwati, and T. Wandra. 2008. Factors associated with case fatality of human H5N1 virus infections in Indonesia: a case series. *Lancet* 372:744-749.

Lam, W.Y., A.C. Yeung, I.M. Chu, and P.K. Chan. 2010. Profiles of cytokine and chemokine gene expression in human pulmonary epithelial cells induced by human and avian influenza viruses. *Virol J* 7:344.

Le, Q.M., M. Kiso, K. Someya, Y.T. Sakai, T.H. Nguyen, K.H. Nguyen, N.D. Pham, H.H. Ngyen, S. Yamada, Y. Muramoto, T. Horimoto, A. Takada, H. Goto, T. Suzuki, Y. Suzuki, and Y. Kawaoka. 2005. Avian flu: isolation of drug-resistant H5N1 virus. *Nature* 437:1108.

Lo, M.S., R.M. Brazas, and M.J. Holtzman. 2005. Respiratory syncytial virus nonstructural proteins NS1 and NS2 mediate inhibition of Stat2 expression and alpha/beta interferon responsiveness. *J Virol* 79:9315-9319.

Lopez Cde, H., R.F. Roca, and J.V. Daunis. 2009. [Pneumonia and the acute respiratory distress syndrome due to influenza A (H1N1) virus]. *Med Intensiva* 33:455-458.

Ludwig, S. 2011. Disruption of virus-host cell interactions and cell signaling pathways as an anti-viral approach against influenza virus infections. *Biol Chem* 392:837-847.

Ludwig, S., and O. Planz. 2008. Influenza viruses and the NF-kappaB signaling pathway - towards a novel concept of antiviral therapy. *Biol Chem* 389:1307-1312.

Matikainen, S., T. Sareneva, T. Ronni, A. Lehtonen, P.J. Koskinen, and I. Julkunen. 1999. Interferon-alpha activates multiple STAT proteins and upregulates proliferation-associated IL-2Ralpha, c-myc, and pim-1 genes in human T cells. *Blood* 93:1980-1991.

Mazur, I., W.J. Wurzer, C. Ehrhardt, S. Pleschka, P. Puthavathana, T. Silberzahn, T. Wolff, O. Planz, and S. Ludwig. 2007. Acetylsalicylic acid (ASA) blocks influenza virus propagation via its NF-kappaB-inhibiting activity. *Cell Microbiol.* 9:1683-1694.

McColl, B.W., S.M. Allan, and N.J. Rothwell. 2007. Systemic inflammation and stroke: aetiology, pathology and targets for therapy. *Biochem Soc Trans* 35:1163-1165.

McKimm-Breschkin, J.L., P.W. Selleck, T.B. Usman, and M.A. Johnson. 2007. Reduced sensitivity of influenza A (H5N1) to oseltamivir. *Emerg.Infect.Dis.* 13:1354-1357.

Meijer, A., A. Lackenby, O. Hungnes, B. Lina, S. van-der-Werf, B. Schweiger, M. Opp, J. Paget, J. van-de-Kassteele, A. Hay, and M. Zambon. 2009. Oseltamivir-resistant influenza virus A (H1N1), Europe, 2007-08 season. *Emerg Infect Dis* 15:552-560.

Murikinati, S., E. Juttler, T. Keinert, D.A. Ridder, S. Muhammad, Z. Waibler, C. Ledent, A. Zimmer, U. Kalinke, and M. Schwaninger. 2010. Activation of cannabinoid 2 receptors protects against cerebral ischemia by inhibiting neutrophil recruitment. *FASEB J* 24:788-798.

Nichol, K.L., J. Nordin, J. Mullooly, R. Lask, K. Fillbrandt, and M. Iwane. 2003. Influenza vaccination and reduction in hospitalizations for cardiac disease and stroke among the elderly. *N Engl J Med* 348:1322-1332.

Paleari, L., F. Sessa, A. Catassi, D. Servent, G. Mourier, G. Doria-Miglietta, E. Ognio, M. Cilli, L. Dominioni, M. Paolucci, A. Calcaterra, A. Cesario, S. Margaritora, P. Granone, and P. Russo. 2009. Inhibition of non-neuronal alpha7-nicotinic receptor reduces tumorigenicity in A549 NSCLC xenografts. *Int J Cancer* 125:199-211.

Palosaari, H., J.P. Parisien, J.J. Rodriguez, C.M. Ulane, and C.M. Horvath. 2003. STAT protein interference and suppression of cytokine signal transduction by measles virus V protein. *J Virol* 77:7635-7644.

Rameix-Welti, M.A., V. Enouf, F. Cuvelier, P. Jeannin, and W.S. van der. 2008. Enzymatic properties of the neuraminidase of seasonal H1N1 influenza viruses provide insights for the emergence of natural resistance to oseltamivir. *PLoS.Pathog.* 4:e1000103.

Randall, R.E., and S. Goodbourn. 2008. Interferons and viruses: an interplay between induction, signalling, antiviral responses and virus countermeasures. *J Gen Virol* 89:1-47.

Rogge, L., L. Barberis-Maino, M. Biffi, N. Passini, D.H. Presky, U. Gubler, and F. Sinigaglia. 1997. Selective expression of an interleukin-12 receptor component by human T helper 1 cells. *J Exp Med* 185:825-831.

Saito, H., H. Takenaka, S. Yoshida, T. Tsubokawa, A. Ogata, F. Imanishi, and J. Imanishi. 1985. Prevention from naturally acquired viral respiratory infection by interferon nasal spray. *Rhinology* 23:291-295.

Schellekens, H., G. Geelen, J.F. Meritet, C. Maury, and M.G. Tovey. 2001. Oromucosal interferon therapy: relationship between antiviral activity and viral load. *J Interferon Cytokine Res* 21:575-581.

Seth, R.B., L. Sun, and Z.J. Chen. 2006. Antiviral innate immunity pathways. *Cell Res* 16:141-147.

Shaw, M.L. 2011. The host interactome of influenza virus presents new potential targets for antiviral drugs. *Rev Med Virol* 21:358-369.

Sheu, T.G., V.M. Deyde, R.J. Garten, A.I. Klimov, and L.V. Gubareva. 2010. Detection of antiviral resistance and genetic lineage markers in influenza B virus neuraminidase using pyrosequencing. *Antiviral Res* 85:354-360.

Silverman, R.H. 2007. Viral encounters with 2',5'-oligoadenylate synthetase and RNase L during the interferon antiviral response. *J Virol* 81:12720-12729.

Smallman-Raynor, M., and A.D. Cliff. 2007. Avian influenza A (H5N1) age distribution in humans. *Emerg.Infect.Dis.* 13:510-512.

Smeeth, L., S.L. Thomas, A.J. Hall, R. Hubbard, P. Farrington, and P. Vallance. 2004. Risk of myocardial infarction and stroke after acute infection or vaccination. *N Engl J Med* 351:2611-2618.

Stark, G.R., I.M. Kerr, B.R. Williams, R.H. Silverman, and R.D. Schreiber. 1998. How cells respond to interferons. *Annu Rev Biochem* 67:227-264.

Szretter, K.J., S. Gangappa, X. Lu, C. Smith, W.J. Shieh, S.R. Zaki, S. Sambhara, T.M. Tumpey, and J.M. Katz. 2007. Role of host cytokine responses in the pathogenesis of avian H5N1 influenza viruses in mice. *J.Virol.* 81:2736-2744.

Tate, M.D., A.G. Brooks, and P.C. Reading. 2008. The role of neutrophils in the upper and lower respiratory tract during influenza virus infection of mice. *Respir Res* 9:57.

Tracey, K.J. 2009. Reflex control of immunity. *Nat Rev Immunol* 9:418-428.

Tumpey, T.M., X. Lu, T. Morken, S.R. Zaki, and J.M. Katz. 2000. Depletion of lymphocytes and diminished cytokine production in mice infected with a highly virulent influenza A (H5N1) virus isolated from humans. *J.Virol.* 74:6105-6116.

Vink, J., J. Cloos, and G.J. Kaspers. 2006. Proteasome inhibition as novel treatment strategy in leukaemia. *Br J Haematol* 134:253-262.

Wang, C.S., S.T. Wang, C.T. Lai, L.J. Lin, and P. Chou. 2007. Impact of influenza vaccination on major cause-specific mortality. *Vaccine* 25:1196-1203.

Wang, X., M. Li, H. Zheng, T. Muster, P. Palese, A.A. Beg, and A. Garcia-Sastre. 2000. Influenza A virus NS1 protein prevents activation of NF-kappaB and induction of alpha/beta interferon. *J Virol* 74:11566-11573.

Wong, S.S., and K.Y. Yuen. 2006. Avian influenza virus infections in humans. *Chest* 129:156-168.

Wurzer, W.J., O. Planz, C. Ehrhardt, M. Giner, T. Silberzahn, S. Pleschka, and S. Ludwig. 2003. Caspase 3 activation is essential for efficient influenza virus propagation. *EMBO J.* 22:2717-2728.

Xu, T., J. Qiao, L. Zhao, G. Wang, G. He, K. Li, Y. Tian, M. Gao, J. Wang, H. Wang, and C. Dong. 2006. Acute respiratory distress syndrome induced by avian influenza A (H5N1) virus in mice. *Am J Respir Crit Care Med* 174:1011-1017.

Yu, X., and D.C. Kem. 2010. Proteasome inhibition during myocardial infarction. *Cardiovasc Res* 85:312-320.

Zucs, P., U. Buchholz, W. Haas, and H. Uphoff. 2005. Influenza associated excess mortality in Germany, 1985-2001. *Emerg Themes Epidemiol* 2:6.

DANKSAGUNG

Bedanken möchte ich mich bei Herrn Prof. Dr. rer. nat. Oliver Planz für das sehr interessante Dissertationsthema, sowie für die Möglichkeit zur Erlangung des Doktortitels. Olli, im Jahr 2009 hast du mich in einem unserer unzähligen wissenschaftlichen Gespräche einmal als Michael Ballack der Arbeitsgruppe bezeichnet. Zu diesem Zeitpunkt spielte Ballack in England beim FC Chelsea eine super Session aber es gelangen ihm keine Tore. Ähnlich war es in dieser Zeit mit meinen Projekten. Alles lief, aber der Abschluss, die Veröffentlichung, wurde nicht stark genug verfolgt. Nach langem und teils mühsamen Coachen deinerseits gelang es in den letzten Jahren, drei Tore und zwei Torvorlagen zu erzielen. Diese Erfolge konnten nur mithilfe deiner Unterstützung in Form von Zirkeltraining (paper writing), Trainingslagern (Kongresse & Meetings) sowie Teamcoaching (organisatorische Aufgaben) gelingen. Aus diesem Grunde nochmals vielen Dank.

Mein Dank geht weiterhin an Herrn Prof. Dr. rer. nat. Hans-Georg Rammensee für die Bereitschaft zur Begutachtung dieser Dissertation.

Herrn Prof. Dr. med. vet. Lothar Stitz, Institutsleiter des Friedrich-Loeffler-Institutes Bundesforschungsinstitut für Tiergesundheit in Tübingen, möchte ich für die Bereitstellung des Arbeitsplatzes danken.

Herrn Prof. Dr. med. Markus Schwaninger und Dr. med. Sajjad Muhammad danke ich für die interessante und äußerst produktive Zusammenarbeit im Schlaganfall Projekt.

Mein Dank gilt ebenfalls der Erlanger Firma ViroLogik GmbH, insbesondere deren „Influenza Research Department“, namentlich Dr. rer. nat. Ralf Kircheis und Dr. rer. nat. Eva-Katharina Pauli.

Großer Dank gilt allen aktuellen und ehemaligen Mitgliedern unserer Arbeitsgruppe für die fortwährend heiteren und abwechslungsreichen Tage im sonst so tristen Laborleben. Dank an Dr. rer. nat. Karoline Dröbner. Karo, ich war 2006 dein erster Praktikant, von dort an hast du mich stets gelehrt, dass man fokussiert an die Arbeit herangehen muss und sich somit manche Widrigkeiten erspart. Du hast mich in die Welt der Tierversuche eingearbeitet und mir stets gezeigt, wohin die Reise gehen soll. Weiterer Dank gilt Carmen Müller. Durch dich Carmen, habe ich gelernt in der Arbeitswelt mit Menschen umzugehen. Deine Art und Weise mir

teilweise Dinge klarzumachen, teils sehr direkt teils schonend, hat mir all die Jahre sehr imponiert. Deine wohlstrukturierte Arbeitsweise spiegelt sich stets in exzellenten Ergebnissen wieder. Hierfür nochmals vielen Dank. Dipl. Biol. Annette Vogel bin ich besonderen Dank verpflichtet. Annette, ich erinnere mich immer wieder sehr gerne an unsere wilden, hochspekulativen und vom Wahn getriebenen Gespräche im Pausenraum. Dabei ging es nicht immer nur um die Arbeit, vielmehr waren es Gespräche die mir Mut und Zuversicht für die anstehenden Projekte gaben. Experimentell kannst du mir in so manchen Dingen etwas vormachen, weshalb ich immer froh für deine Hilfe war. Gedankt sei auch Ulrich Wulle, der Fels in der FLI-Brandung. Deine ruhige und besonnene Art, Uli, holte mich das ein oder andere Mal, wenn mal wieder nichts geklappt hat, wieder auf den Boden der Tatsachen zurück und machte mir deutlich, dass es noch etwas anderes außer der Arbeit gibt. Vielen Dank.

Vielen herzlichen Dank auch an die zahlreichen anderen netten Kolleginnen und Kollegen des FLI, allen voran PD. Dr. rer. nat. Michael Knittler, Dr. rer. nat. Benjamin Petsch, Elizabeta Zirdum, Alexander Rassochin, Sina Korn, Waldemar und Karl Schleicher.

PUBLIKATIONSLISTE

Haasbach, E., Pauli, E. K., Spranger, R., Mitzner, D., Schubert, U., Kircheis, R., Planz, O. (2011). Antiviral activity of the proteasome inhibitor VL-01 against influenza A viruses. *Antiviral Res* 91(3), 304-13.

Haasbach, E., Droebner, K., Vogel, A. B., and Planz, O. (2011). Low-Dose Interferon Type I Treatment Is Effective Against H5N1 and Swine-Origin H1N1 Influenza A Viruses In Vitro and In Vivo. *J Interferon Cytokine Res* 31(6), 515-25.

Muhammad*, S., **Haasbach*, E.**, Kotchourko, M., Strigli, A., Krenz, A., Ridder, D. A., Vogel, A. B., Marti, H. H., Al-Abed, Y., Planz, O., and Schwaninger, M. (2011). Influenza virus infection aggravates stroke outcome. *Stroke* 42(3), 783-91.

Vogel, A. B., **Haasbach, E.**, Reiling, S. J., Droebner, K., Klingel, K., and Planz, O. (2010). Highly pathogenic influenza virus infection of the thymus interferes with T lymphocyte development. *J Immunol* 185(8), 4824-34.

Droebner, K., **Haasbach, E.**, Fuchs, C., Weinzierl, A. O., Stevanovic, S., Buttner, M., and Planz, O. (2008). Antibodies and CD4(+) T-cells mediate cross-protection against H5N1 influenza virus infection in mice after vaccination with a low pathogenic H5N2 strain. *Vaccine* 26(52), 6965-74.

PUBLICATION #1:

Antiviral activity of the proteasome inhibitor VL-01 against Influenza A viruses

Emanuel Haasbach[a,b], Eva-Katharina Pauli[b], Robert Spranger[b], David Mitzner[b,c], Ulrich Schubert[b,c], Ralf Kircheis[b], Oliver Planz[a,d*]

[a] Friedrich-Loeffler-Institut, Institute of Immunology, Paul-Ehrlich Str. 28, 72076 Tuebingen, Germany

[b] ViroLogik GmbH, Innovation Centre for Medical Technology and Pharmaceuticals, Henkestr. 91, 91052 Erlangen, Germany

[c] Clinical and Molecular Virology, Friedrich-Alexander-University of Erlangen-Nuernberg, Schloßgarten 4, 91054 Erlangen, Germany

[d] University of Tuebingen, Interfaculty Institute for Cell Biology, Department of Immunology, Auf der Morgenstelle 15, 72076 Tuebingen, Germany

*Corresponding author: Prof. Dr. Oliver Planz
University of Tuebingen, Interfaculty Institute for Cell Biology,
Department of Immunology,
Auf der Morgenstelle 15
D-72076 Tuebingen, Germany
Tel: +49-7071-29 80995
Fax: +49-7071-29 5653
E-mail: oliver.planz@uni-tuebingen.de

Keywords: Influenza A virus; proteasome inhibitor; drug-resistance

Abstract

The appearance of highly pathogenic avian influenza A viruses of the H5N1 subtype being able to infect humans and the 2009 H1N1 pandemic reveals the urgent need for new and efficient countermeasures against these viruses. The long-term efficacy of current antivirals is often limited, because of the emergence of drug-resistant virus mutants. A growing understanding of the virus-host interaction raises the possibility to explore alternative targets involved in the viral replication. In the present study we show that the proteasome inhibitor VL-01 leads to reduction of influenza virus replication in human lung adenocarcinoma epithelial cells (A549) as demonstrated with three different influenza virus strains, A/Puerto Rico/8/34 (H1N1) (EC_{50} value of 1.7 µM), A/Regensburg/D6/09 (H1N1v) (EC_{50} value of 2.4 µM) and A/Mallard/Bavaria/1/2006 (H5N1) (EC_{50} value of 0.8 µM). In *in vivo* experiments we could demonstrate that VL-01-aerosol-treatment of BALB/c mice with 14.1 mg/kg results in no toxic side effects, reduced progeny virus titers in the lung (1.1 ± 0.3 $\log_{10}$ pfu) and enhanced survival of mice after infection with a 5-fold MLD_{50} of the human influenza A virus strain A/Puerto Rico/8/34 (H1N1) up to 50%. Furthermore, treatment of mice with VL-01 reduced the cytokine release of IL-α/-β, IL-6, MIP-1 β, RANTES and TNF- α induced by LPS or highly pathogen avian H5N1 influenza A virus. The present data demonstrates an antiviral effect of VL-01 *in vitro* and *in vivo* and the ability to reduce influenza virus induced cytokines and chemokines.

1. Introduction

H1N1 influenza viruses are a major topic of human health care, especially after the last H1N1 pandemic. Additionally, highly pathogenic avian influenza (HPAI) H5N1 virus infection leads to high lethality in humans, as a result of extensive alveolar immune inflammatory infiltrates, causing tissue damage that compromises lung function. The H5N1 virus infection results in high levels of inflammatory cytokines and chemokines, due to an immune dysregulation (hypercytokinemia) (Cheung et al., 2002; Chotpitayasunondh et al., 2005; Droebner et al., 2008; Tumpey et al., 2000; Wong and Yuen, 2006). Elevated levels of cytokines and chemokines, including IP10, MIG, MCP-1, IL-6, IL-8 and RANTES, have been observed in human cell lines, mice and macaques infected with H5N1 influenza virus (Chan et al., 2005; de Jong et al., 1997; Kobasa et al., 2007).

The pandemic situation of the last years clearly demonstrates that influenza A virus infection is still a major risk for the public health. The possibility of a new emerging pandemic influenza A virus strain or reassortment between the pandemic and seasonal or avian A/H5N1 influenza virus strain is indeed a frightening but not unlikely event. Since vaccines will not be available in the first six months after a pandemic outbreak, there is a strong need for effective antivirals. Today, neuraminidase-inhibitors such as oseltamivir represent the most common clinically approved medication against influenza A viruses. In the recent past the number of reports in which drug-resistant influenza A viruses were described increased. (Hurt et al., 2009; Le et al., 2005; McKimm-Breschkin et al., 2007; Meijer et al., 2009; Rameix-Welti et al., 2008; Sheu et al., 2008). Drug resistance to the known antivirals highlights the urgent need to optimize the effectiveness of current and novel antiviral treatments through development of new formulations, delivery routes or novel defense mechanisms. Due to the high mutation rate of influenza A virus, the threat of fast resistance formation against these compounds exists. In contrast, the human genome possesses a million fold lower mutation rate. The inhibition of host cell factors, which the virus is depending on during its replication cycle, offers an interesting alternative target for the development of new therapies. Here, the virus cannot replace the missing cellular component by mutations. It is well known that influenza A virus recruits host cell factors for efficient replication (Ehrhardt et al., 2010; Konig et al., 2010; Watanabe et al., 2010). Therefore, it is well traceable that targeting such host cell factors would be a promising approach for the development of new antiviral drugs. We previously demonstrated that influenza virus replication is dependent on the NF-κB pathway and on the Raf/MEK/ERK mitogenic kinase cascade. Inhibition of the IKK/NF-κB

by the use of acetylsalicylic acid (ASA), as well as inhibition of the Raf/MEK/ERK signaling pathways with the MEK inhibitor U0126, leads to strong reduction of influenza A virus infection (Ludwig and Planz, 2008; Ludwig et al., 2004; Mazur et al., 2007; Pleschka et al., 2001).

The 26S-proteasome – the central protolytic component of the ubiquitin-proteasome system (UPS) - can be selectively inhibited by proteasome inhibitors. The ability of such substances to inhibit the proteasome and thereby to prevent NF-κB activation is well known (Breccia and Alimena, 2010; Vink et al., 2006; Yu and Kem, 2010). During influenza virus infection NF-κB acts via induction of proapoptotic factors, such as TNF-related apoptosis-inducing ligand (TRAIL) or FasL followed by activation of caspases. This caspase-activation resulted in an enhanced nuclear export of viral RNPs, presumably by specific cleavage of nuclear pore proteins, resulting in an enhanced diffusion limit through the pores (Ludwig, 2009). This function appears to be relevant for viral replication since a nuclear retention of viral ribonucleoprotein (RNP) complexes can be observed in the presence of both, caspase- and NF-κB-inhibitors (Mazur et al., 2007; Wurzer et al., 2003).

An antiviral effect of proteasome inhibitors on different RNA viruses has previously been shown (Ma et al., 2010; Ott et al., 2003; Schubert et al., 2000). Widjaja and colleagues showed that inhibition of proteasome activity affects influenza A virus infection at a post-fusion step (Widjaja et al., 2010). Furthermore, proteasome inhibitors such as PS-341 (Velcade) are currently in clinical trails against cancer e.g. against relapsed and refractory multiple myeloma (Richardson et al., 2003; Richardson et al., 2005; San Miguel et al., 2008).

In the present study we wanted to investigate the antiviral effect of the proteasome inhibitor VL-01 (ViroLogik GmbH, Germany) in cell culture and in the mouse model. Delivery of the substance *via* the aerosol route led to reduction of progeny virus titer in lungs of mice after human influenza A virus infection. Furthermore, we demonstrated that inhibiting the proteasome activity leads to an increased survival after lethal influenza A virus infection. The proteasome inhibitor VL-01 also reduced cytokine release induced by LPS stimulation or by infection with highly pathogenic avian H5N1 influenza A virus. Aerosol application of VL-01 at the concentrations required for antiviral activity did not lead to any adverse effects. Thus, we conclude that efficient influenza virus replication is dependent on proteasome activity and that temporarily inhibition of proteasome activity might be effective for the development of novel treatment strategies.

2. Materials and Methods

2.1. Compound

The proteasome inhibitor VL-01 (ViroLogik GmbH, Germany) with a formula weight of 752.8 g/mol inhibits the 20S and 26S proteasome unit. The inhibitor was dissolved in 5% DMSO, 15% Cremophor in PBS before use in different concentrations.

2.2. Mice

Inbred BALB/c mice at the age of 6–8 weeks were obtained from the animal breeding facilities at the Friedrich-Loeffler-Institute, Federal Research Institute for Animal Health, Tuebingen, Germany and were used throughout all the experiments.

2.3. Virus

The human influenza virus A/Puerto Rico/8/34 (H1N1, PR8) and the pandemic influenza virus strain A/Regensburg/D6/09 (H1N1, RB1) were propagated in Madin-Darby canine kidney (MDCK) cells. Additionally, we used the highly pathogenic avian H5N1 influenza A virus strain A/Mallard/Bavaria/1/2006 (H5N1, MB1) grown in embryonated chicken eggs, which was originally obtained from the Bavarian Health and Food Safety Authority, Oberschleissheim, Germany.

2.4. Influenza virus titration (AVICEL® plaque assay)

To assess the number of infectious particles (plaque titers) in the samples, a plaque assay using AVICEL® was performed in 96-well plates (Vogel et al., 2010). Virus-infected cells were immunostained by incubating for 1h with a monoclonal antibody specific for the influenza A virus nucleoprotein (Serotec, Duesseldorf, Germany), followed by 30 min incubation with peroxidase-labeled anti-mouse antibody (DIANOVA, Hamburg, Germany) and 10 min incubation with True Blue™ peroxidase substrate (KPL, Gaithersburg, USA). Stained plates were scanned on a flat bed scanner and the data were acquired by Corel DRAW 9.0 software. To define the titer of progeny virus, the foci of infected cells for every sample in each well of the 96-well plates were counted and multiplied with the dilution factor. The

mean values were taken from the final number of foci in each well. The viral titers are shown as the logarithm to the base 10 of the mean values.

2.5. Measurement of pharmacological parameters in vitro

To determine the inhibitory effect (IC_{50}) of VL-01 *in vitro*, we treated human lung adenocarcinoma epithelial cells (A549) with different concentrations of VL-01 (0.1 – 50 µM) and measured the proteasome activity via P20-assay, based on the method of Adams and colloquies (Adams et al., 1999). For determination of the effective concentration 50% (EC_{50}) A549 cells were infected with PR8 (MOI of 0.001) and subsequently VL-01 treatment was started by adding culture medium with different concentrations of VL-01 (0 - 64 µM). Progeny virus in the supernatant of infected and treated cells was measured by plaque assay as described in 2.4. For calculation, each experiment was repeated three times independently with each comprising triplicates.

The cytotoxic concentration (CC_{50}) of VL-01 was determined in A549 and MDCK cells as well in primary hepatocytes, tonsils and peripheral blood mononuclear cells. All cell types were incubated with different VL-01 concentrations (0.1 – 50 µM) for 24h followed by a washing step and further incubation with VL-01 for 24, 48 or 72h. After 48, 72 or 96h of incubation with VL-01 in total, cytotoxic effects were measured. The effect in A549 cells and primary hepatocytes were examined by a water-soluble tetrazolium salt (WST-1) assay according to the manufactures protocol (Roche Diagnostics, Mannheim, Germany). MDCK cells were stained with crystal-violet as described by Lison and colleagues (Lison et al., 2008). For the evaluation of cytotoxic effects in tonsils and PBMCs over a time of 72h, cells were measured as apoptotic and necrotic cells by FACS analysis via annexin V / propidium iodide staining as described in the distributors protocol (Vybrant® Dead Cell Apoptosis Kit Invitrogen, Darmstadt, Germany). All experiments were done as triplicates. Results evaluated by GraphPad prism software showing a cytotoxic effect dependent on the VL-01 concentration (Nicole Studtrucker and Daniel Lüftenegger; unpublished data).

2.6. Virus inoculation of mice

Six to eight week-old BALB/c mice were obtained from the animal breeding facilities at the FLI. Before intranasal inoculation with MB1 (H5N1) or PR8 (H1N1), mice were anaesthetized by intraperitoneal injection of 150 µl of a ketamine (Sanofi)-rompun (Bayer)-

solution (equal amounts of a 2%-rompun-solution and a 10%-ketamin-solution were mixed at the rate of 1:10 with phosphate buffered saline (PBS)). All animal studies were approved by the Institutional Animal Care and Use Committee of Tuebingen.

2.7. VL-01-treatment of mice and virus infection

The aerosol-treatment of mice was performed in a self-made aerosol-application-device were four mice can be treated. For fumigation of dissolved VL-01 or solvent the PARI LC SPRINT® STAR nebulizer (PZN: 3870078 PARI GmbH, Starnberg, Germany) was used. The solutions were nebulized at 3 bar air pressure for 15 or 30 min. Discharged air was aspirated with 8 l/min via a vacuum-pump to ensure optimal air/aerosol flow. For prophylactic studies mice were treated via the aerosol route one hour prior to viral inoculation. For infection, mice were anaesthetized by intraperitoneal injection of ketamine/rompun and infected intranasally with the 5-fold MLD_{50} of different influenza A virus strains. After infection mice were treated at different time points, every 12h, either with VL-01 or solvent. According to the experimental setup, body weight and visual clinical symptoms of mice were monitored for a 21-day observation period or lungs of VL-01-treated and solvent-treated control mice were collected 24, 48, 72h after infection and viral titers were determined by plaque assay.

2.8. Cytokine analysis

All cytokine assays were performed using a multi Bio-Plex Protein Array System from BioRad (Bio-Rad Laboratories, Munich, Germany). To investigate the LPS induced cytokine response and the ability of VL-01 to modulate this response, four mice were 2h prior to LPS treatment (Lipopolysaccharides from Escherichia coli 055:B5, Sigma, Germany, 20 µg/mice) intravenously treated with 25 mg/kg VL-01 and four with diluent. At 1.5 and 3h after LPS treatment serum samples were taken and the cytokine profile was measured. In a second experiment the avian H5N1 virus A/mallard/Bavaria/1/2006 (MB1) was used as a cytokine inducer. A group of seven mice were i.v. treated with 25 mg/kg VL-01 2h prior to virus infection (MB1, 10-fold MLD_{50}), compared to seven mock-treated mice. Serum samples were collected at 0, 12, 30 and 72h after infection and cytokines were measured.

2.9. Immunofluorescence

A549 or MDCK cells were infected with RB1 (H1N1), PR8 (H1N1) or MB1 (H5N1) with a MOI of 1 in the absence or presence of 2 μM VL-01. After 4, 6, 8 and 12h p.i., cells were fixed for 30 min in 4% buffered paraformaldehyde at 4°C. The fixed cells were washed twice with PBS and permeabilized. Cells were fluorescently labelled using primary mouse anti-Influenza A nucleoprotein antibodies (AbD Serotec) and secondary Alexa Fluor® 555 F(ab')2 fragment of goat anti-mouse IgG (H+L) antibodies (Invitrogen). Nuclei were stained using DAPI (Fluka). Afterwards, cells were mounted with ProLong Gold Antifade Medium (Invitrogen, Darmstadt, Germany), and analyzed by the Apotome Care Invert Microscope Labovert FS (Leitz, Wetzlar, Germany) and the AxioVision Rel 4.5 (Carl Zeiss Imaging, Oberkochen, Germany).

2.10. Statistical analysis

Error bars are given as the SEM. For the calculation of the significance of differences, the paired t test ($p \leq 0.05$) or the logrank test was performed. All analyses were performed using GraphPad Prism version 5.00 for Windows (GraphPad Software, San Diego California USA).

3. Results

3.1. VL-01 inhibits proteasome activity and influenza virus replication in vitro

The pharmacological parameters, inhibition concentration 50% (IC_{50}), cytotoxic concentration (CC_{50}) and effective concentration 50% (EC_{50}) are most important to develop an antiviral drug. Therefore, we determined these parameters for the proteasome inhibitor VL-01. To examine the concentration of VL-01 to inhibit the proteasome activity up to 50% (IC_{50}), human lung adenocarcinoma epithelial cells (A549) were treated with different concentrations of VL-01 (0.1 – 50 µM). On different time points post infection (4, 8, 24 and 32h) the proteasome activity was measured using the P20-assay (measurement of chymotrypsin-like activity of the 20S subunit from the 26S proteasome). The proteasome inhibition by VL-01 showed a time-dependent effect. After 4 and 8h the IC_{50} values ranged between 2.7 and 1.8 µM, whereas after 24 and 32h the IC_{50} was approximately 1 µM (Fig. 1A). The cytotoxic effect (CC_{50}) of VL-01 treatment was assayed on A549 and MDCK cells with different concentrations of VL-01 (0.1 – 50 µM). After incubation periods of 24, 48, 72 and 96h the cell viability was measured by the WST-1 assay or crystal-violet staining. In terms of the IC_{50} value of proteasome inhibition of 1 µM after 24h, we could show that there was no cytotoxic effect of VL-01 after this treatment period. The CC_{50} was found at approximately 4 µM after 24h in A549 cells and there was no toxic effect on MDCK cells neither after 24 nor 48h (Fig. 1B, C). A longer incubation of 48, 72 or 96h shows a CC_{50} in A549 cells between 2.8 – 3.6 µM (Fig. 1B, C). In addition to these cell lines, different primary human cell lines, e.g. primary hepatocytes, tonsils and peripheral blood mononuclear cells reveals similar CC_{50} values (ViroLogik GmbH, unpublished data). Next, the effective concentration of 50% (EC_{50}), which demonstrates the ability to reduce influenza A virus titer up to 50%, was analyzed by measurement of progeny virus in presence of different VL-01 concentrations (0 – 64 µM) in infected A549 cells after 24h. VL-01 showed an EC_{50} value of approximately 1.7 µM in A/Puerto Rico/8/34 (H1N1, PR8) infected cells (Fig. 1D). The EC_{50} of A/Regensburg/D6/09 (H1N1v, RB1) infected cells is about 2.4 µM (Fig. 1E) and for the A/Mallard/Bavaria/1/2006 (H5N1, MB1) virus 0.82 µM (Fig. 1F). The IC_{50} and EC_{50} – i.e. the concentrations which are effective to inhibit the proteasome (1 µM) or virus replication (1.7 µM), respectively, were found below the concentration where VL-01 showed cytotoxic effects (4 µM). The window between antiviral activity and cytotoxic effects was not very broad in these studies. However, this may not be surprising, as the A549 adenocarcinoma cell

line represents highly proliferating tumor cells that are known to be inhibited by proteasome inhibitors.

3.2. Reduction of lung virus titer in mice after VL-01 treatment

To further analyze the anti influenza A virus potential, *in vivo* experiments were performed in the mouse model. In this context we wanted to investigate the VL-01 concentration that is most effective in reducing influenza virus replication *in vivo*. Therefore, mice were aerosol-treated one hour prior to human influenza A virus infection (PR8, H1N1, 5-fold MLD_{50}) with different concentrations of VL-01 (0 – 227.4 mg/kg). After 24h mice were sacrificed and viral titers in the lungs were measured by plaque assay. As shown in Figure 2A, an antiviral effect of VL-01 on progeny virus titer in the lung was found which increased with increasing VL-01 doses up to 113.7 mg/kg. No adverse effects were seen, even at the highest doses of VL-01 used for single aerosol treatment (data not shown). The calculated *in vivo* EC_{50} was 31.9 ± 7.5 mg/kg. Since a concentration of 14.1 mg/kg VL-01 was also sufficient to reproducible reduce progeny virus titer up to 1.1 ± 0.3 log_{10} pfu, this concentration was used for most of the further aerosol treatment experiments. It has to be noted that the aerosol device allows a drug deposition of approximately 1% of the evaporated drug in the lungs. Thus, the maximum amount of VL-01 that will reach the lung will be roughly 0.14 mg/kg (2.8µg per mouse).
After finding the optimal VL-01 concentration *in vivo* we addressed the question, whether this concentration was able to induce adverse effects after multiple treatments. Therefore, we treated mice either with 14.1 mg/kg VL-01 or solvent by daily aerosol-treatment over a period of 10 days. The physical parameters and the body weight of the animals were monitored daily (Fig. 2B). There were no evidences for toxic side effects during the whole observation period, neither change in body weight nor in any physical parameters. In a second study to investigate toxicity of VL-01 in mice, the animals were treated intraperitoneal (i.p.) for 14 days using two different mouse strains. With this assay mouse toxic doses (MTD) of 25 mg/kg (DmVk-mice) and 150 mg/kg (CD1 nu/nu mice) VL-01 were determined. Study of the acute toxicity in mice of VL-01 revealed that LD_{10}/ LD_{50} value following single intravenous administration equals to 57.2 (LD_{10}) and 135.5 mg/kg (LD_{50}). Furthermore, effective doses were tolerated in animal models with repeated i.p. doses of VL-01. A i.p. dose of 150 mg/kg appears to be the suitable dose for the mice model (data not shown).

3.3. Prolonged VL-01 aerosol-treatment leads to an increased antiviral effect

Optimization of frequency and duration of drug application is very important for efficient antiviral treatment. Thus, we raised the question whether multiple daily treatment or prolongation of drug-delivery time would improve antiviral activity. Therefore, we treated mice once with 14.1 mg/kg VL-01 one hour prior to infection (PR8, H1N1, 5-fold MLD_{50}) or twice (one prior and eleven hours past infection). After 24h mice were sacrificed and viral titers in the lungs were measured by plaque assay. A second treatment of mice with 14.1 mg/kg VL-01 resulted in an enhanced reduction of progeny virus titer in the lung (3.4 ± 0.06 $\log_{10}$ pfu) compared to single treatment (3.6 ± 0.13 $\log_{10}$ pfu). In comparison, in mock treated animals a viral titer of 4.6 ± 0.15 $\log_{10}$ pfu was measured (Fig. 3A, B).
The impact of the duration of aerosol-treatment was investigated by single treatment of mice for either 15 or 30 min resulting in a final VL-01 dose of 14.1 mg/kg or 28.2 mg/kg respectively. Less virus was found in the lung after 24h and 30 min treatment (2.3 ± 0.08 $\log_{10}$ pfu) compared to only 15 min treatment (2.8 ± 0.03 $\log_{10}$ pfu) (Fig. 3C, D). Mock treated animals showed viral titers of 3.5 ± 0.08 $\log_{10}$ pfu. Taken together, the deposition of increased amounts of VL-01 was found to lead to an increased antiviral effect in mice.

3.4. Increased survival of human influenza A virus infected mice after VL-01 treatment

To examine the antiviral effect of VL-01 on survival, we used the optimized parameters, dose, frequency and duration to perform a prophylactic survival experiment. Thus, we treated mice with 14.1mg/kg VL-01 or solvent one hour prior to infection (PR8, H1N1, 5-fold MLD_{50}) for 30 min. Mice were treated every 12 hours for four days. The physical parameters, body weight, onset of disease and survival were monitored daily for 21 days. The body weight-curve shows a nearly similar course for mock and VL-01 treated mice until day 6 (Fig. 4A). All mice developed the first disease symptoms by day 3 post infection. Within a few days, the symptoms in the mock-treated group became severe and resulted in high disease scores and finally in death. In contrast, VL-01-treated mice showed a delayed development of severe symptoms (Fig. 4B). At day 7, three out of four mock-treated mice died, whereas only one out of four VL-01-treated mice died. The last mock-treated mouse died at day 8 past infection. At day 9, a second VL-01-treated mouse died. The two remaining VL-01-treated mice raised their body weight constantly until day 19 where they accomplished again their starting weight (Fig. 4C). This experiment was performed several times with similar results (data not shown).

In summary, VL-01 treatment of mice starting prior to infection with human H1N1 influenza A virus leads to a survival rate of approximately 50% compared to 100% lethality found in mock-treated mice.

3.5. VL-01 treatment reduces cytokine release induced by LPS stimulation or by infection with highly pathogenic avian H5N1 influenza A virus

It is well known that highly pathogenic avian influenza A viruses induce release of a wide pattern of cytokines and chemokines called hypercytokinemia or cytokine storm. To investigate whether VL-01 treatment has an influence on the amount of cytokine and chemokine release, we used LPS as a positive control; a well-known cytokine- and chemokine inducer that acts as a common model to investigate anti-inflammatory effects (Carlsen et al., 2004; Errea et al., 2010). To examine the influence of VL-01 on influenza A virus mediated cytokine and chemokine release we used the highly pathogenic avian influenza A virus strain A/Mallard/Bavaria/1/2006 (MB1, H5N1). First, we investigated the LPS induced cytokine response and the ability of VL-01 to modulate this response. In order to test the effect of the proteasome inhibitor VL-01 on induced cytokine release, mice were treated intravenously (i.v.) 2h prior to LPS (20 µg/mice) application with 25 mg/kg VL-01. As mentioned in 3.2. this concentration is not toxic for mice. At 1.5 and 3h after LPS challenge serum samples were taken and the cytokine profile was measured. Mock-serum was taken 4h prior to any treatment.

In a second experiment infection with the highly pathogenic avian influenza A virus, MB1 (H5N1) was used as a cytokine inducer. Mice were treated i.v. with 25 mg/kg VL-01 2h prior to virus infection (MB1, 10-fold MLD_{50}). Serum samples were collected at 0, 12, 30 and 72h after infection and cytokines were measured by using multiplex assay (BioRad). VL-01 treatment significantly reduced LPS induced cytokines IL-1 beta, IL-6, MIP-1 beta, RANTES and TNF-alpha, either on both time points 1.5 and 3h (IL-1 beta, MIP-1 beta and RANTES) after induction or at one of the time point (1.5h, IL-6; 3h, TNF-alpha) by (Fig. 5A-E).

Similarly to LPS induction, the cytokines and chemokines induced by an avian H5N1 influenza A virus infection could also significantly be reduced by VL-01 treatment (Fig. 5 right panel, F-J). The IL-1 alpha and TNF-alpha serum levels in VL-01 treated mice showed a significant reduction at 12 and 30h after infection, compared to mock-treated mice. VL-01 treatment reduced the IL-6 serum level at 12 and 72h after infection. The level of MIP-1 beta

was only reduced at 72h after infection, compared to untreated control group. In contrast, the expression of RANTES was only marginally altered by VL-01 treatment.
In summary, this experiment demonstrated that VL-01 reduced the systemic cytokine and chemokine release induced by avian H5N1 influenza A virus infection in mice.

3.6. VL-01 treatment leads to a delayed nuclear export of viral RNPs in vitro

It is well known that NF-κB promotes influenza A virus production and enhances the nuclear export of viral RNPs (vRNP) via activation of caspase-3 (Planz, 2006; Wurzer et al., 2003). Next, we investigated whether the influenza virus vRNP-export is influenced by VL-01 treatment. Therefore, the nuclear export of the nucleoprotein (NP), the major part of the vRNP complexes, was analyzed by fluorescent microscopy in A549 and MDCK cells. Cells were infected with human influenza virus PR8 (H1N1), pandemic influenza virus RB1 (H1N1v) and highly pathogenic avian influenza virus MB1 (H5N1) in the absence or presence of 2 μM VL-01. After 6 hours, cells were fixed and stained against NP and visualized by fluorescent microscopy. VL-01 treatment of either RB1, PR8 or MB1 infected A549 cells shows that 6h after infection NP is detectable in the cytoplasm (Fig. 6A-C, upper panel) while in VL-01 treated cells NP is still located in the nucleus (Fig. 6A-C, lower panel). Similar results were found on MDCK cells (Supplemental Fig. 1). That demonstrates that vRNP export is efficiently impaired in the presence of VL-01 after influenza A virus infection.

4. Discussion

It is well known that influenza A virus recruits host cell factors for efficient replication (Ehrhardt et al., 2010; Konig et al., 2010; Ludwig et al., 1999; Watanabe et al., 2010). Therefore, it is traceable that targeting host cell factors could be a promising approach for new antiviral drugs. We were able to demonstrate that influenza virus infection of host cells leads to biphasic activation of the Raf/MEK/ERK signaling pathway and that inhibition of this pathway on the level of MEK leads to reduction in progeny virus (Ludwig et al., 2004; Pleschka et al., 2001). MEK inhibitors evaluated for cancer treatment in a phase I evaluation revealed that repeated treatment for 21 consecutive days was well tolerated (Lorusso et al., 2002). In another study we were able to demonstrate that acetylsalicylic acid (ASA) is highly effective against influenza virus (Mazur et al., 2007). ASA functions as an IKK/NF-κB inhibitor by interacting with IKK-beta to reduce ATP binding activity (Yin et al., 1998). Under normal conditions, NF-κB is held in an inactive state in a cytoplasmic complex with its inhibitory protein (IκB). Phosphorylation of IκBα targets IκB for ubiquitination and subsequent proteasomal degradation. NF-κB is released for nuclear translocation and transcriptional activation, which is also a prerequisite for efficient influenza virus replication.
Thus, targeting host cell factors with clinically established compounds might be a promising strategy for the development of new antivirals against influenza viruses.
In this context, we wanted to investigate whether inhibition of the proteasome might be such a strategy, since efficient degradation of IκB by the proteasome is needed to activate the NF-κB pathway (Karin and Ben-Neriah, 2000). Inhibition of the proteasome-mediated degradation leads to retention of NF-κB in the cytoplasm that should finally lead to reduced virus replication. Because of the vital function of UPS, the usage of proteasome inhibitors in humans is not trivial, in order to avoid adverse events. Nevertheless, proteasome inhibitors are being used against cancer. The proteasome inhibitor PS-341 (Velcade) has got the market approval by the FDA for relapsed and refractory multiple myeloma (Richardson et al., 2003; Richardson et al., 2005; San Miguel et al., 2008).
The goal of this study was to determine whether a newly designed proteasome inhibitor - VL-01 - would function as an antiviral agent against influenza A virus in mice. The EC_{50} value of VL-01 against H1N1 influenza virus on A549 cells revealed activity in the low µM range. For delivery of the substance *in vivo,* we decided to use an aerosol route for local delivery instead of systemic application. An *in vivo* dose-response experiment (Fig. 2A) showed that highest reduction of virus titer in the lung could be achieved when 14.1 mg/kg VL-01 or more were

administered to the animals. Interestingly, an increase of the amount of VL-01 did not lead to a significant further increase in reduction of viral titers in the lung. Therefore, a dose of 14.1 mg/kg VL-01 was used for further studies. This amount did not lead to any adverse side effects in the mouse. In this light, Ma and colleagues investigated the antiviral effect of proteasome inhibitors PS-341 and MG-132 in a murine model against SARS and described also no adverse effects (Ma et al., 2010). In various experiments we were able to show that delivery of VL-01 at a concentration of 14.1 mg/kg resulted in reduction of the viral titer in the mouse lung by more than one order of magnitude and a prolonged survival rate of 50%. Intriguingly, earlier studies have demonstrated that 1.2 μM of VL-01 is needed for inhibition of 50% of the NF-κB activity (data not shown). In this context, the amount of proinflammatory cytokines and chemokines were drastically reduced after i.v. VL-01 treatment of H5N1 infected mice or LPS treated mice (IL-1 alpha/beta, IL-6, MIP-1 beta, RANTES and TNF-alpha). Since the cytokine/chemokine gene expression is largely mediated and/or regulated by NF-κB (Homma et al., 2010; Lakshmanan and Porter, 2007; Pahl and Baeuerle, 1995), our data demonstrate that NF-κB function is impaired even when low concentrations of VL-01 were applied using i.v. application. However, fluorescent microscopy of the viral NP visualized that vRNP export is reduced in the presence of VL-01. This indicates a antiviral effect of VL-01 by inhibition of NF-κB via reduced proteasome-activity. In the study by Ma and colleagues, the authors also demonstrated a reduction of cytokine gene expression in mice after PS-341 treatment (Ma et al., 2010). This is in line with our observations. In this context, it has to be noted that VL-01 treatment of H5N1 infected mice led only to marginal reduction of virus titer in the lung and no differences regarding survival and severity of diseases. Since cytokines and chemokines were drastically reduced, this might be another example that the pathogenicity of HPAIV is more complex than currently known (Salomon et al., 2007). Using another model, i.e. H7N7 (FPV) infected mice, VL-01 induced a moderate reduction in viral titers in the lungs and a moderate increase in survival (25% in VL-01 treated mice vs. 0% in mock treated mice).

Expression of cytokines and chemokines (hypercytokinemia or cytokine storm) is a hallmark after influenza A virus infection, in particular with highly pathogenic avian influenza virus or pandemic strains. This cytokine and chemokine deregulation of the immune system leads to higher virus loads as well as higher lethality (Cheng et al., 2010; de Jong et al., 2006). Thus, in addition to controlling the virus replication it is also necessary to control the expression of proinflammatory cytokines, particularly in severe cases of influenza virus infection. Glucocorticoid-mediated suppression of cytokine expression might be beneficial to treat for

the development of influenza, but might also negatively influence the induction of the innate and adaptive immune response mediated by various cytokines and chemokines. Therefore, the use of glucocorticoids to treat severe influenza, accompanied with hypercytokinemia, is controversially discussed. VL-01 applied locally - directly into the lung - might have an advantage, since VL-01 has antiviral activity and anti inflammatory activity. Since the drug is given locally, accordingly the local inflammatory status at the application site, i.e. the lungs, rather than the systemic immune response will be affected.

In summary, this study presents evidence that proteasome inhibitors might be able to inhibit influenza virus replication *via* impaired vRNP export and induction of inflammatory cytokines. Nevertheless, the only marginal effect after H5N1 influenza A virus infection of mice indicate that a modification of the VL-01 formulation and/or of the application scheme may be required to assure a better up-take and deposition in the lung. Recently it was published that the proteasome inhibitor MG132 shows anti influenza virus activity by targeting a post-fusion step (Widjaja et al., 2010). In our study we demonstrate a new class of proteasome inhibitors (VL-01), which also might be used in combination with other antivirals in case of severe influenza A virus infection. In case of intensive care hospitalization due to influenza A virus infection, it might be of great advantage to counteract the disease pattern efficiency with antivirals having bivalent properties to fight against the virus and ameliorate the cytokine storm induced by influenza virus infection. These results suggest that proteasome inhibition by VL-01 is a novel therapeutic intervention that might be considered in case of severe influenza virus infection.

Acknowledgments

We thank Nicole Studtrucker and Daniel Lüftenegger for providing CC_{50}-values in primary hepatocytes, tonsils and PBMCs, and also Carmen Mueller for her excellent technical assistance. This work was supported by grants SFB 643-A1, SFB 796 A1, SCHU1125/3, and SCHU 1125/5, from the German Research Council to US. Furthermore, this research was partially supported by the Federal Government of Germany under the Influenza research program "FSI" and by the BMBF Zoonose Programm "FluResearchNet".

References

Adams, J., Palombella, V.J., Sausville, E.A., Johnson, J., Destree, A., Lazarus, D.D., Maas, J., Pien, C.S., Prakash, S., Elliott, P.J., 1999. Proteasome inhibitors: a novel class of potent and effective antitumor agents. Cancer Res 59, 2615-2622.

Breccia, M., Alimena, G., 2010. NF-kappaB as a potential therapeutic target in myelodysplastic syndromes and acute myeloid leukemia. Expert Opin Ther Targets 14, 1157-1176.

Carlsen, H., Alexander, G., Austenaa, L.M., Ebihara, K., Blomhoff, R., 2004. Molecular imaging of the transcription factor NF-kappaB, a primary regulator of stress response. Mutat Res 551, 199-211.

Chan, M.C., Cheung, C.Y., Chui, W.H., Tsao, S.W., Nicholls, J.M., Chan, Y.O., Chan, R.W., Long, H.T., Poon, L.L., Guan, Y., Peiris, J.S., 2005. Proinflammatory cytokine responses induced by influenza A (H5N1) viruses in primary human alveolar and bronchial epithelial cells. Respir.Res. 6, 135.

Cheng, X.W., Lu, J., Wu, C.L., Yi, L.N., Xie, X., Shi, X.D., Fang, S.S., Zan, H., Kung, H.F., He, M.L., 2010. Three fatal cases of pandemic 2009 influenza A virus infection in Shenzhen are associated with cytokine storm. Respir Physiol Neurobiol.

Cheung, C.Y., Poon, L.L., Lau, A.S., Luk, W., Lau, Y.L., Shortridge, K.F., Gordon, S., Guan, Y., Peiris, J.S., 2002. Induction of proinflammatory cytokines in human macrophages by influenza A (H5N1) viruses: a mechanism for the unusual severity of human disease? Lancet 360, 1831-1837.

Chotpitayasunondh, T., Ungchusak, K., Hanshaoworakul, W., Chunsuthiwat, S., Sawanpanyalert, P., Kijphati, R., Lochindarat, S., Srisan, P., Suwan, P., Osotthanakorn, Y., Anantasetagoon, T., Kanjanawasri, S., Tanupattarachai, S., Weerakul, J., Chaiwirattana, R., Maneerattanaporn, M., Poolsavathitikool, R., Chokephaibulkit, K., Apisarnthanarak, A., Dowell, S.F., 2005. Human disease from influenza A (H5N1), Thailand, 2004. Emerg.Infect.Dis. 11, 201-209.

de Jong, J.C., Claas, E.C., Osterhaus, A.D., Webster, R.G., Lim, W.L., 1997. A pandemic warning? Nature 389, 554.

de Jong, M.D., Simmons, C.P., Thanh, T.T., Hien, V.M., Smith, G.J., Chau, T.N., Hoang, D.M., Chau, N.V., Khanh, T.H., Dong, V.C., Qui, P.T., Cam, B.V., Ha, d.Q., Guan, Y., Peiris, J.S., Chinh, N.T., Hien, T.T., Farrar, J., 2006. Fatal outcome of human influenza A (H5N1) is associated with high viral load and hypercytokinemia. Nat.Med. 12, 1203-1207.

Droebner, K., Reiling, S.J., Planz, O., 2008. Role of hypercytokinemia in NF-kappaB p50-deficient mice after H5N1 influenza A virus infection. J Virol 82, 11461-11466.

Ehrhardt, C., Seyer, R., Hrincius, E.R., Eierhoff, T., Wolff, T., Ludwig, S., 2010. Interplay between influenza A virus and the innate immune signaling. Microbes Infect 12, 81-87.

Errea, A., Moreno, G., Sisti, F., Fernandez, J., Rumbo, M., Hozbor, D.F., 2010. Mucosal innate response stimulation induced by lipopolysaccharide protects against Bordetella pertussis colonization. Med Microbiol Immunol 199, 103-108.

Homma, T., Matsukura, S., Hirose, T., Ohnishi, T., Kimura, T., Kurokawa, M., Ieki, K., Odaka, M., Suzuki, S., Watanabe, S., Sato, M., Kawaguchi, M., Schleimer, R.P., Adachi, M., 2010. Cooperative activation of CCL5 expression by TLR3 and tumor necrosis factor-alpha or interferon-gamma through nuclear factor-kappaB or STAT-1 in airway epithelial cells. Int Arch Allergy Immunol 152 Suppl 1, 9-17.

Hurt, A.C., Ernest, J., Deng, Y.M., Iannello, P., Besselaar, T.G., Birch, C., Buchy, P., Chittaganpitch, M., Chiu, S.C., Dwyer, D., Guigon, A., Harrower, B., Kei, I.P., Kok, T., Lin, C., McPhie, K., Mohd, A., Olveda, R., Panayotou, T., Rawlinson, W., Scott, L., Smith, D., D'Souza, H., Komadina, N., Shaw, R., Kelso, A., Barr, I.G., 2009. Emergence and spread of oseltamivir-resistant A(H1N1) influenza viruses in Oceania, South East Asia and South Africa. Antiviral Res 83, 90-93.

Karin, M., Ben-Neriah, Y., 2000. Phosphorylation meets ubiquitination: the control of NF-[kappa]B activity. Annu Rev Immunol 18, 621-663.

Kobasa, D., Jones, S.M., Shinya, K., Kash, J.C., Copps, J., Ebihara, H., Hatta, Y., Kim, J.H., Halfmann, P., Hatta, M., Feldmann, F., Alimonti, J.B., Fernando, L., Li, Y., Katze, M.G., Feldmann, H., Kawaoka, Y., 2007. Aberrant innate immune response in lethal infection of macaques with the 1918 influenza virus. Nature 445, 319-323.

Konig, R., Stertz, S., Zhou, Y., Inoue, A., Hoffmann, H.H., Bhattacharyya, S., Alamares, J.G., Tscherne, D.M., Ortigoza, M.B., Liang, Y., Gao, Q., Andrews, S.E., Bandyopadhyay, S., De Jesus, P., Tu, B.P., Pache, L., Shih, C., Orth, A., Bonamy, G., Miraglia, L., Ideker, T., Garcia-Sastre, A., Young, J.A., Palese, P., Shaw, M.L., Chanda, S.K., 2010. Human host factors required for influenza virus replication. Nature 463, 813-817.

Lakshmanan, U., Porter, A.G., 2007. Caspase-4 interacts with TNF receptor-associated factor 6 and mediates lipopolysaccharide-induced NF-kappaB-dependent production of IL-8 and CC chemokine ligand 4 (macrophage-inflammatory protein-1). J Immunol 179, 8480-8490.

Le, Q.M., Kiso, M., Someya, K., Sakai, Y.T., Nguyen, T.H., Nguyen, K.H., Pham, N.D., Ngyen, H.H., Yamada, S., Muramoto, Y., Horimoto, T., Takada, A., Goto, H., Suzuki, T., Suzuki, Y., Kawaoka, Y., 2005. Avian flu: isolation of drug-resistant H5N1 virus. Nature 437, 1108.

Lison, D., Thomassen, L.C., Rabolli, V., Gonzalez, L., Napierska, D., Seo, J.W., Kirsch-Volders, M., Hoet, P., Kirschhock, C.E., Martens, J.A., 2008. Nominal and effective dosimetry of silica nanoparticles in cytotoxicity assays. Toxicol Sci 104, 155-162.

Lorusso, V., Crucitta, E., Panza, N., Silvestris, N., Guida, M., Carpagnano, F., Mancarella, S., Sambiasi, D., De Lena, M., 2002. Phase I/II study of paclitaxel, gemcitabine and vinorelbine as first-line chemotherapy of non-small-cell lung cancer. Ann Oncol 13, 1862-1867.

Ludwig, S., 2009. Targeting cell signalling pathways to fight the flu: towards a paradigm change in anti-influenza therapy. J Antimicrob Chemother 64, 1-4.

Ludwig, S., Planz, O., 2008. Influenza viruses and the NF-kappaB signaling pathway - towards a novel concept of antiviral therapy. Biol Chem 389, 1307-1312.

Ludwig, S., Pleschka, S., Wolff, T., 1999. A fatal relationship--influenza virus interactions with the host cell. Viral Immunol 12, 175-196.

Ludwig, S., Wolff, T., Ehrhardt, C., Wurzer, W.J., Reinhardt, J., Planz, O., Pleschka, S., 2004. MEK inhibition impairs influenza B virus propagation without emergence of resistant variants. FEBS Lett 561, 37-43.

Ma, X.Z., Bartczak, A., Zhang, J., Khattar, R., Chen, L., Liu, M.F., Edwards, A., Levy, G., McGilvray, I.D., 2010. Proteasome inhibition in vivo promotes survival in a lethal murine model of severe acute respiratory syndrome. J Virol 84, 12419-12428.

Mazur, I., Wurzer, W.J., Ehrhardt, C., Pleschka, S., Puthavathana, P., Silberzahn, T., Wolff, T., Planz, O., Ludwig, S., 2007. Acetylsalicylic acid (ASA) blocks influenza virus propagation via its NF-kappaB-inhibiting activity. Cell Microbiol. 9, 1683-1694.

McKimm-Breschkin, J.L., Selleck, P.W., Usman, T.B., Johnson, M.A., 2007. Reduced sensitivity of influenza A (H5N1) to oseltamivir. Emerg.Infect.Dis. 13, 1354-1357.

Meijer, A., Lackenby, A., Hungnes, O., Lina, B., van-der-Werf, S., Schweiger, B., Opp, M., Paget, J., van-de-Kassteele, J., Hay, A., Zambon, M., 2009. Oseltamivir-resistant influenza virus A (H1N1), Europe, 2007-08 season. Emerg Infect Dis 15, 552-560.

Ott, D.E., Coren, L.V., Chertova, E.N., Gagliardi, T.D., Nagashima, K., Sowder, R.C., 2nd, Poon, D.T., Gorelick, R.J., 2003. Elimination of protease activity restores efficient virion production to a human immunodeficiency virus type 1 nucleocapsid deletion mutant. J Virol 77, 5547-5556.

Pahl, H.L., Baeuerle, P.A., 1995. Expression of influenza virus hemagglutinin activates transcription factor NF-kappa B. J Virol 69, 1480-1484.

Planz, O., 2006. [Influenza viruses and intracellular signalling pathways]. Berl Munch Tierarztl Wochenschr 119, 101-111.

Pleschka, S., Wolff, T., Ehrhardt, C., Hobom, G., Planz, O., Rapp, U.R., Ludwig, S., 2001. Influenza virus propagation is impaired by inhibition of the Raf/MEK/ERK signalling cascade. Nat.Cell Biol. 3, 301-305.

Rameix-Welti, M.A., Enouf, V., Cuvelier, F., Jeannin, P., van der, W.S., 2008. Enzymatic properties of the neuraminidase of seasonal H1N1 influenza viruses provide insights for the emergence of natural resistance to oseltamivir. PLoS.Pathog. 4, e1000103.

Richardson, P.G., Barlogie, B., Berenson, J., Singhal, S., Jagannath, S., Irwin, D., Rajkumar, S.V., Srkalovic, G., Alsina, M., Alexanian, R., Siegel, D., Orlowski, R.Z., Kuter, D., Limentani, S.A., Lee, S., Hideshima, T., Esseltine, D.L., Kauffman, M., Adams, J.,

Schenkein, D.P., Anderson, K.C., 2003. A phase 2 study of bortezomib in relapsed, refractory myeloma. N Engl J Med 348, 2609-2617.

Richardson, P.G., Sonneveld, P., Schuster, M.W., Irwin, D., Stadtmauer, E.A., Facon, T., Harousseau, J.L., Ben-Yehuda, D., Lonial, S., Goldschmidt, H., Reece, D., San-Miguel, J.F., Blade, J., Boccadoro, M., Cavenagh, J., Dalton, W.S., Boral, A.L., Esseltine, D.L., Porter, J.B., Schenkein, D., Anderson, K.C., 2005. Bortezomib or high-dose dexamethasone for relapsed multiple myeloma. N Engl J Med 352, 2487-2498.

Salomon, R., Hoffmann, E., Webster, R.G., 2007. Inhibition of the cytokine response does not protect against lethal H5N1 influenza infection. Proc.Natl.Acad.Sci.U.S.A 104, 12479-12481.

San Miguel, J.F., Schlag, R., Khuageva, N.K., Dimopoulos, M.A., Shpilberg, O., Kropff, M., Spicka, I., Petrucci, M.T., Palumbo, A., Samoilova, O.S., Dmoszynska, A., Abdulkadyrov, K.M., Schots, R., Jiang, B., Mateos, M.V., Anderson, K.C., Esseltine, D.L., Liu, K., Cakana, A., van de Velde, H., Richardson, P.G., 2008. Bortezomib plus melphalan and prednisone for initial treatment of multiple myeloma. N Engl J Med 359, 906-917.

Schubert, U., Ott, D.E., Chertova, E.N., Welker, R., Tessmer, U., Princiotta, M.F., Bennink, J.R., Krausslich, H.G., Yewdell, J.W., 2000. Proteasome inhibition interferes with gag polyprotein processing, release, and maturation of HIV-1 and HIV-2. Proc Natl Acad Sci U S A 97, 13057-13062.

Sheu, T.G., Deyde, V.M., Okomo-Adhiambo, M., Garten, R.J., Xu, X., Bright, R.A., Butler, E.N., Wallis, T.R., Klimov, A.I., Gubareva, L.V., 2008. Surveillance for neuraminidase inhibitor resistance among human influenza A and B viruses circulating worldwide from 2004 to 2008. Antimicrob.Agents Chemother. 52, 3284-3292.

Tumpey, T.M., Lu, X., Morken, T., Zaki, S.R., Katz, J.M., 2000. Depletion of lymphocytes and diminished cytokine production in mice infected with a highly virulent influenza A (H5N1) virus isolated from humans. J.Virol. 74, 6105-6116.

Vink, J., Cloos, J., Kaspers, G.J., 2006. Proteasome inhibition as novel treatment strategy in leukaemia. Br J Haematol 134, 253-262.

Vogel, A.B., Haasbach, E., Reiling, S.J., Droebner, K., Klingel, K., Planz, O., 2010. Highly pathogenic influenza virus infection of the thymus interferes with T lymphocyte development. J Immunol 185, 4824-4834.

Watanabe, T., Watanabe, S., Kawaoka, Y., 2010. Cellular networks involved in the influenza virus life cycle. Cell Host Microbe 7, 427-439.

Widjaja, I., de Vries, E., Tscherne, D.M., Garcia-Sastre, A., Rottier, P.J., de Haan, C.A., 2010. Inhibition of the ubiquitin-proteasome system affects influenza A virus infection at a postfusion step. J Virol 84, 9625-9631.

Wong, S.S., Yuen, K.Y., 2006. Avian influenza virus infections in humans. Chest 129, 156-168.

Wurzer, W.J., Planz, O., Ehrhardt, C., Giner, M., Silberzahn, T., Pleschka, S., Ludwig, S., 2003. Caspase 3 activation is essential for efficient influenza virus propagation. EMBO J. 22, 2717-2728.

Yin, M.J., Yamamoto, Y., Gaynor, R.B., 1998. The anti-inflammatory agents aspirin and salicylate inhibit the activity of I(kappa)B kinase-beta. Nature 396, 77-80.

Yu, X., Kem, D.C., 2010. Proteasome inhibition during myocardial infarction. Cardiovasc Res 85, 312-320.

WHO, Influenza A(H1N1) virus resistance to oseltamivir - 2008/2009 influenza season, northern hemisphere 18. März 2009.
http://www.who.int/csr/disease/influenza/H1N1webupdate20090318%20ed_ns.pdf

Figure legends

Fig. 1. Determination of the inhibition concentration 50% (IC_{50}) (A), cytotoxic concentration (CC_{50}) (B, C) and effective concentration 50% (EC_{50}) (D-F) of VL-01. A549 cells were treated with different concentrations of VL-01 (0.1 – 50 µM) and at different time points (4, 8, 24 and 32h) the proteasome activity was measured by P20-assay (measurement of chymotrypsinactivity of the 20S subunit from the 26S proteasome). Cytotoxic effects of VL-01 treatment were assayed on A549 and MDCK cells with different concentrations of VL-01 (0.1 – 50 µM). After the incubation period of 24, 48, 72 and 96h the cell viability was measured by WST-1 assay or crystal-violet staining. The EC_{50} was analyzed 24h past infection by plaque assay. Therefore, A549 cells were infected with PR8 (D), RB1 (E) or MB1 (F) (MOI of 0.001) and subsequently VL-01 treatment was started by adding infection medium with different concentrations of VL-01 (0 - 64 µM). For calculation, each experiment was repeated three times independently with each comprising triplicates.

Fig. 2. Determination of the optimal VL-01 concentration for aerosol application *in vivo*. Four BALB/c mice were aerosol-treated one hour prior to infection (PR8, H1N1, 5-fold MLD_{50}) with different concentrations of VL-01 (0 – 227.4 mg/kg). After 24h mice were sacrificed and the viral lung titers were measured by plaque assay. (A) (n = 4, * $p<0.05$) Investigation of toxic side effects after 10-day VL-01 treatment. Two groups of 4 BALB/c mice were treated either with 14.1 mg/kg VL-01 or solvent alone. The aerosol-treatment was applied once a day over a period of 10 days. The physical parameters and body weight of the animals were monitored daily. (B) (n = 4)

Fig. 3. Optimal frequency and duration of VL-01 treatment. BALB/c mice were either treated once with 14.1 mg/kg VL-01 for one hour prior to infection (PR8, H1N1, 5-fold MLD_{50}) or twice (one prior and eleven hours after infection). After 24h mice were sacrificed and viral lung titers were measured by plaque assay. (A in pfu/ml, B in %, n = 4, * $p<0.05$) Mice were treated once for 15 or 30 min with VL-01 resulting in a final dose of 14.1 mg/kg or 28.2 mg/kg, respectively. After 24h mice were sacrificed and viral lung titers were measured by plaque assay. (C in pfu/ml, D in %, n = 4, * $p<0.05$)

Fig. 4. BALB/c mice were treated with 14.1 mg/kg VL-01 or solvent one hour prior to infection (PR8, H1N1, 5-fold MLD_{50}) for 30 min. The mice were treated every 12 hours for

four days. The physical parameters, body weight (A), onset of disease (B) and survival of animals (C) were monitored daily. Several experiments show similar results. (n = 4, * $p<0.05$, Logrank-Test)

Fig. 5. Cytokine and chemokine expression after LPS treatment or avian H5N1 influenza A virus infection. 2h prior to LPS treatment (20 µg/mice) mice were i.v. treated with 25 mg/kg VL-01. Serum samples were taken 4h before (control serum) and 1.5 and 3h after LPS application and cytokine profile was measured by multiplex assay (left panel, A-E). In a second experiment, the avian H5N1 virus A/mallard/Bavaria/1/2006 (MB1) was used as a cytokine inducer. Mice were i.v. treated with 25 mg/kg VL-01 2h prior to virus infection (MB1, 10-fold MLD_{50}). Serum samples were collected at 0, 12, 30 and 72h after infection and cytokines were measured by multiplex assay (right panel, F-J). (n = 4-7, * $p<0.05$) Note, IL-1α was not reduced after LPS induction, as well as no reduction for IL-1β by influenza infection.

Fig. 6. VL-01 treatment of influenza A virus infected A549 cells results in nuclear retention of viral NP in the nucleus. A549 cells were infected with RB1 (H1N1) (A), PR8 (H1N1) (B) or MB1 (H5N1) (C) (MOI 1) in the absence or presence of 2 µM VL-01. Six hours p.i. cells were subjected to immunofluorescence analyses using an anti-NP antibody to stain for viral RNP complexes; cell nuclei were counterstained with DAPI.

Supplemental Fig. 1. VL-01 treatment of influenza A virus infected MDCK cells results in nuclear retention of viral NP in the nucleus. MDCK cells were infected with RB1 (H1N1) (A), PR8 (H1N1) (B) or MB1 (H5N1) (C) (MOI of 1) in the absence or presence of 2µM VL-01. Six hours p.i. cells were subjected to immunofluorescence analyses using an anti-NP antibody to stain for viral RNP complexes, cell nuclei were counterstained with DAPI.

Figures

Figure 1

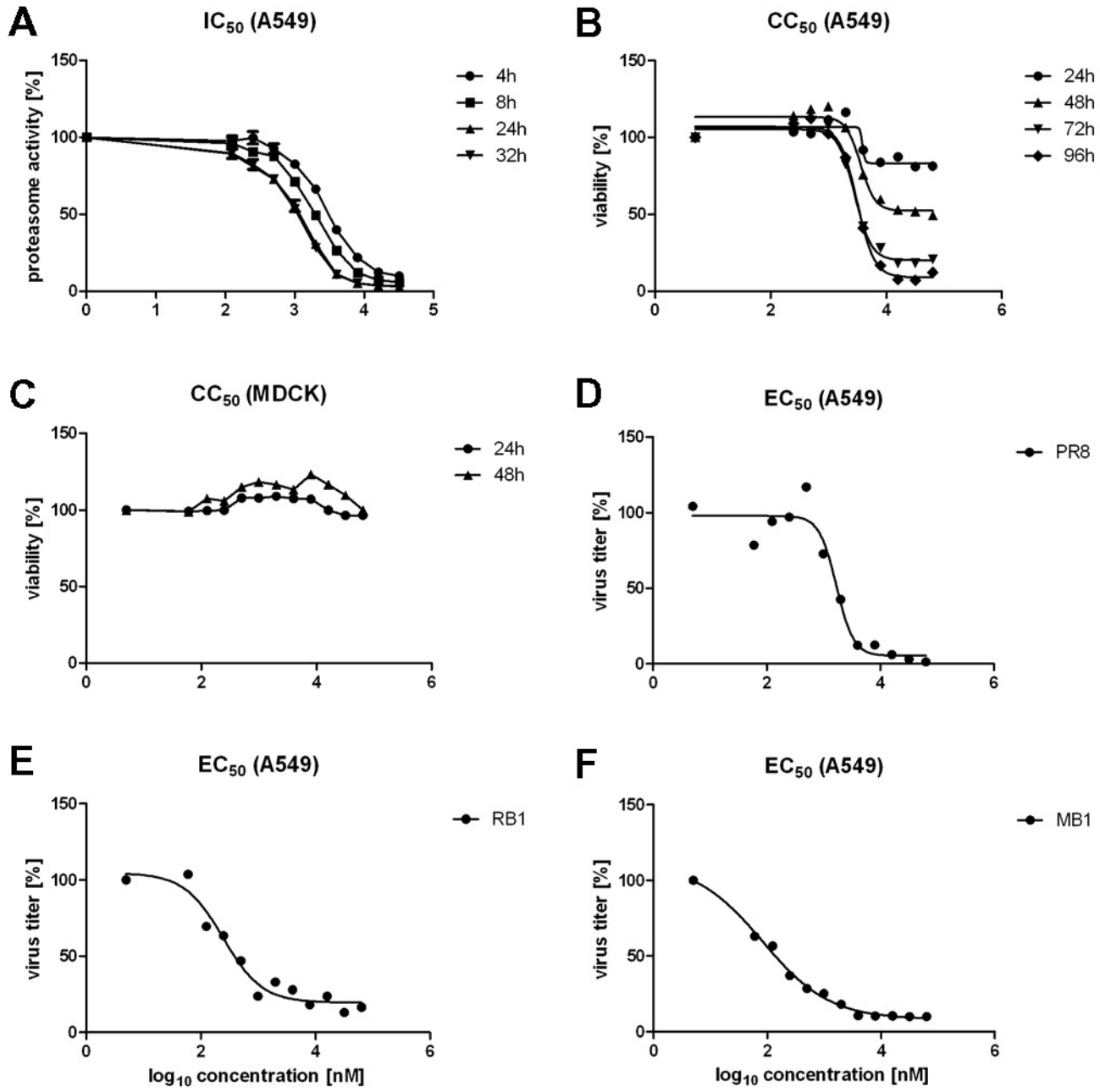

Figure 2

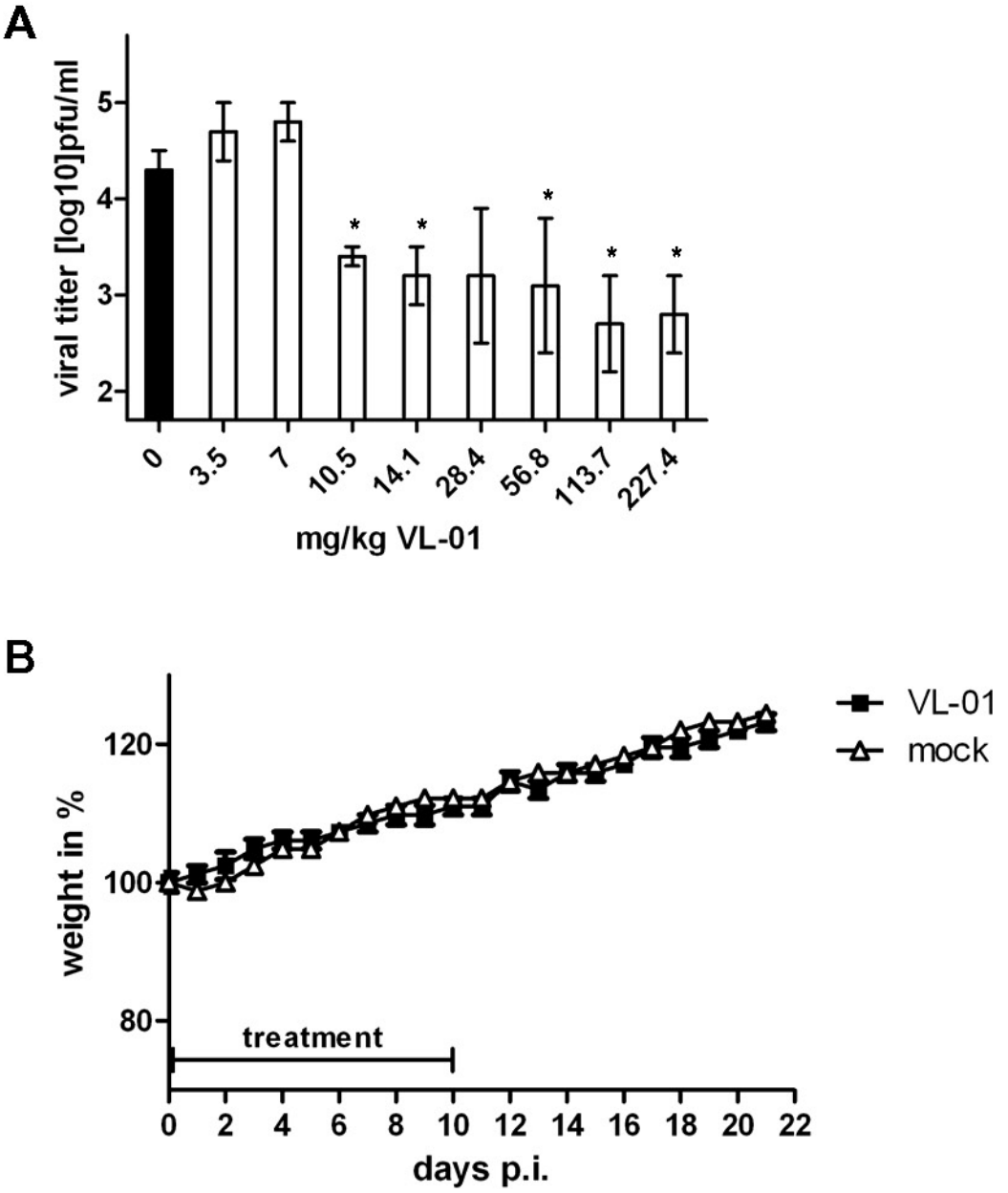
A
viral titer [log10]pfu/ml
5
4
3
2
0
3.5
7
10.5
14.1
28.4
56.8
113.7
227.4
mg/kg VL-01
B
weight in %
120
100
80
treatment
0
2
4
6
8
10
12
14
16
18
20
22
days p.i.
VL-01
mock

Figure 3

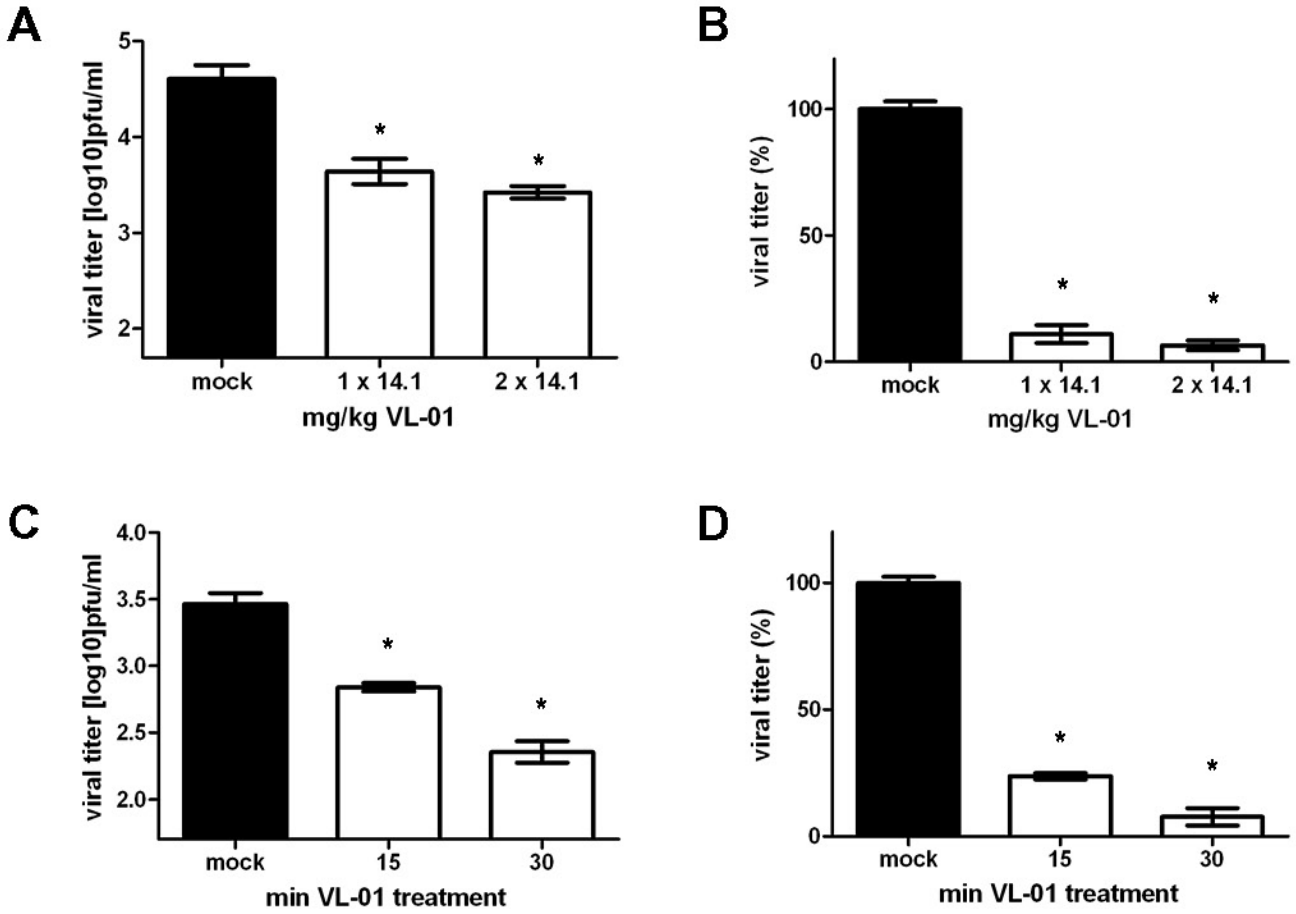
A
viral titer [log10]pfu/ml
5
4
3
2
*
*
mock
1 x 14.1
2 x 14.1
mg/kg VL-01
B
viral titer (%)
100
50
0
*
*
mock
1 x 14.1
2 x 14.1
mg/kg VL-01
C
viral titer [log10]pfu/ml
4.0
3.5
3.0
2.5
2.0
*
*
mock
15
30
min VL-01 treatment
D
viral titer (%)
100
50
0
*
*
mock
15
30
min VL-01 treatment

Figure 4

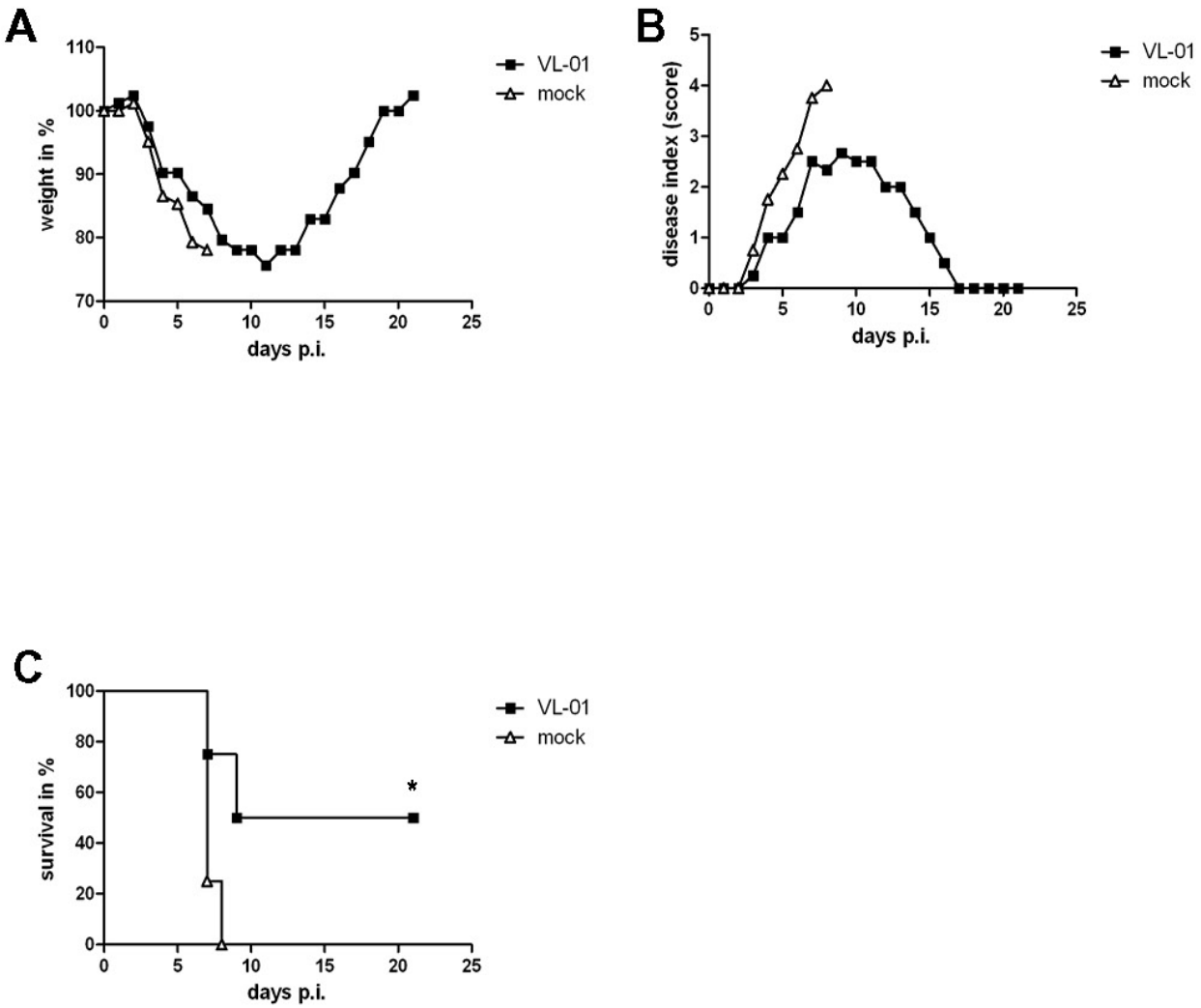
A
weight in %
110
100
90
80
70
0
5
10
15
20
25
days p.i.
VL-01
mock
B
disease index (score)
5
4
3
2
1
0
0
5
10
15
20
25
days p.i.
VL-01
mock
C
survival in %
100
80
60
40
20
0
0
5
10
15
20
25
days p.i.
*
VL-01
mock

Figure 5

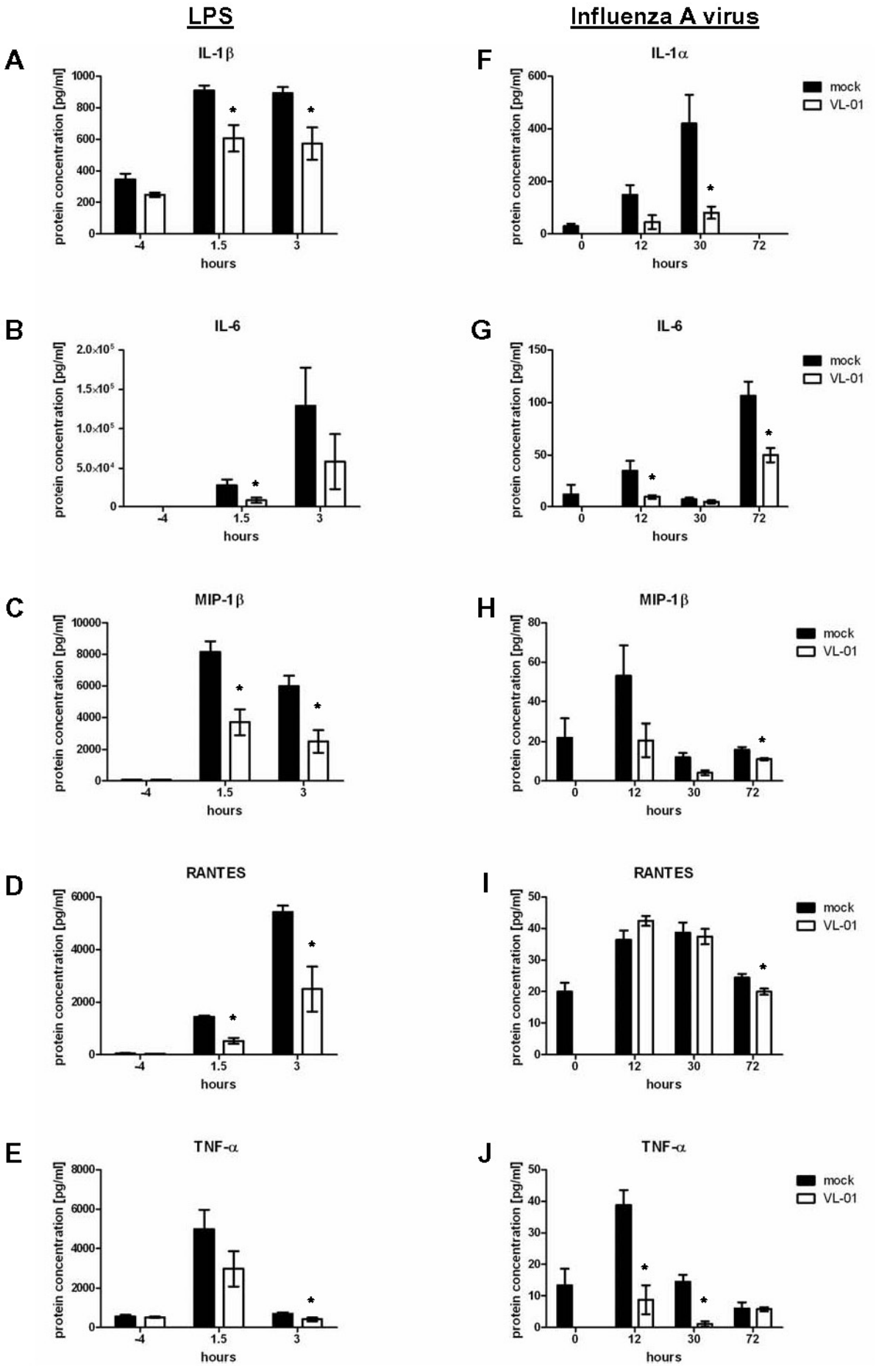
LPS
Influenza A virus
A
IL-1β
protein concentration [pg/ml]
hours
F
IL-1α
mock
VL-01
B
IL-6
G
IL-6
C
MIP-1β
H
MIP-1β
D
RANTES
I
RANTES
E
TNF-α
J
TNF-α

Figure 6

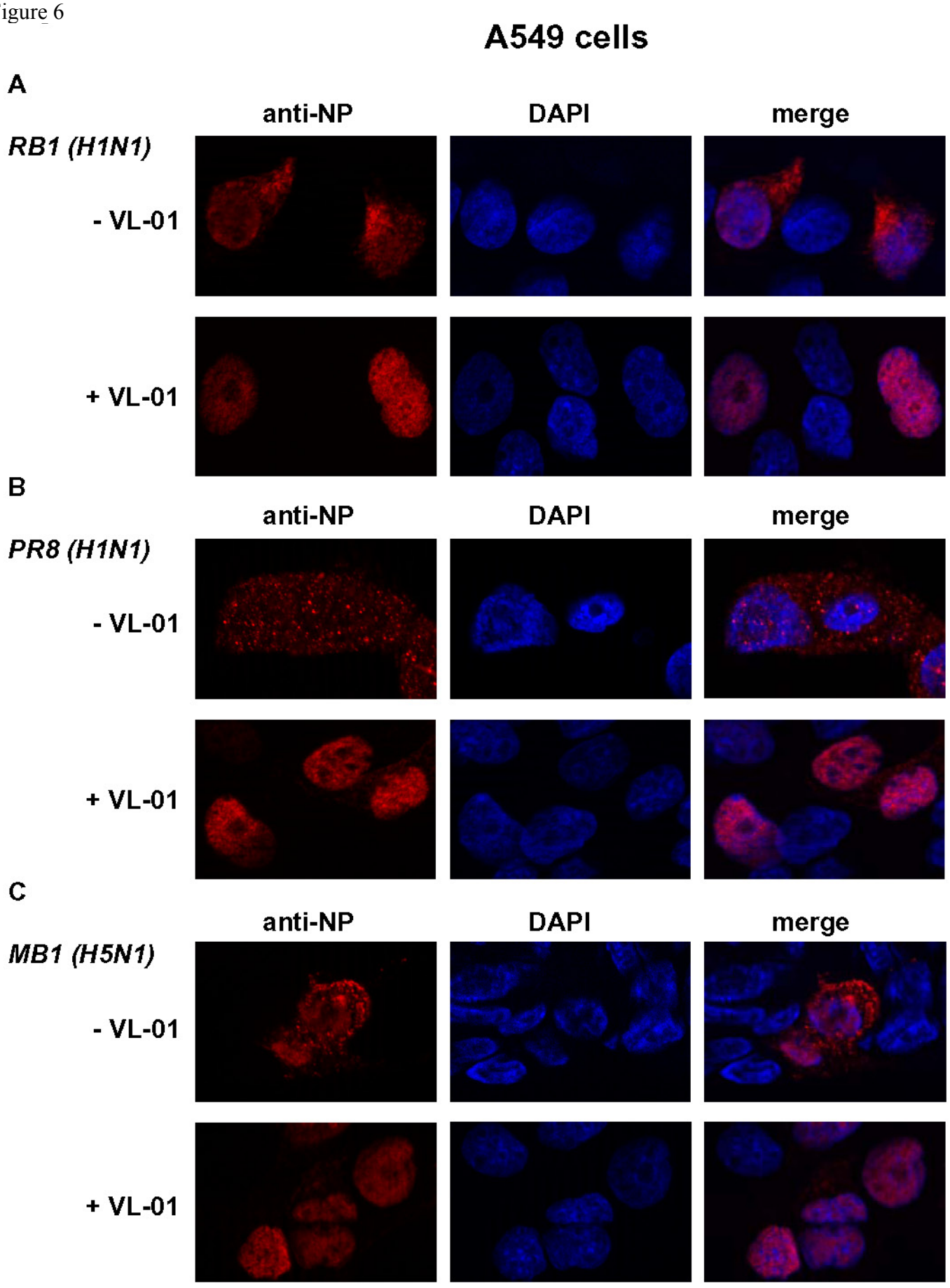
A549 cells
A
anti-NP
DAPI
merge
RB1 (H1N1)
- VL-01
+ VL-01
B
anti-NP
DAPI
merge
PR8 (H1N1)
- VL-01
+ VL-01
C
anti-NP
DAPI
merge
MB1 (H5N1)
- VL-01
+ VL-01

Supplementary figure 1

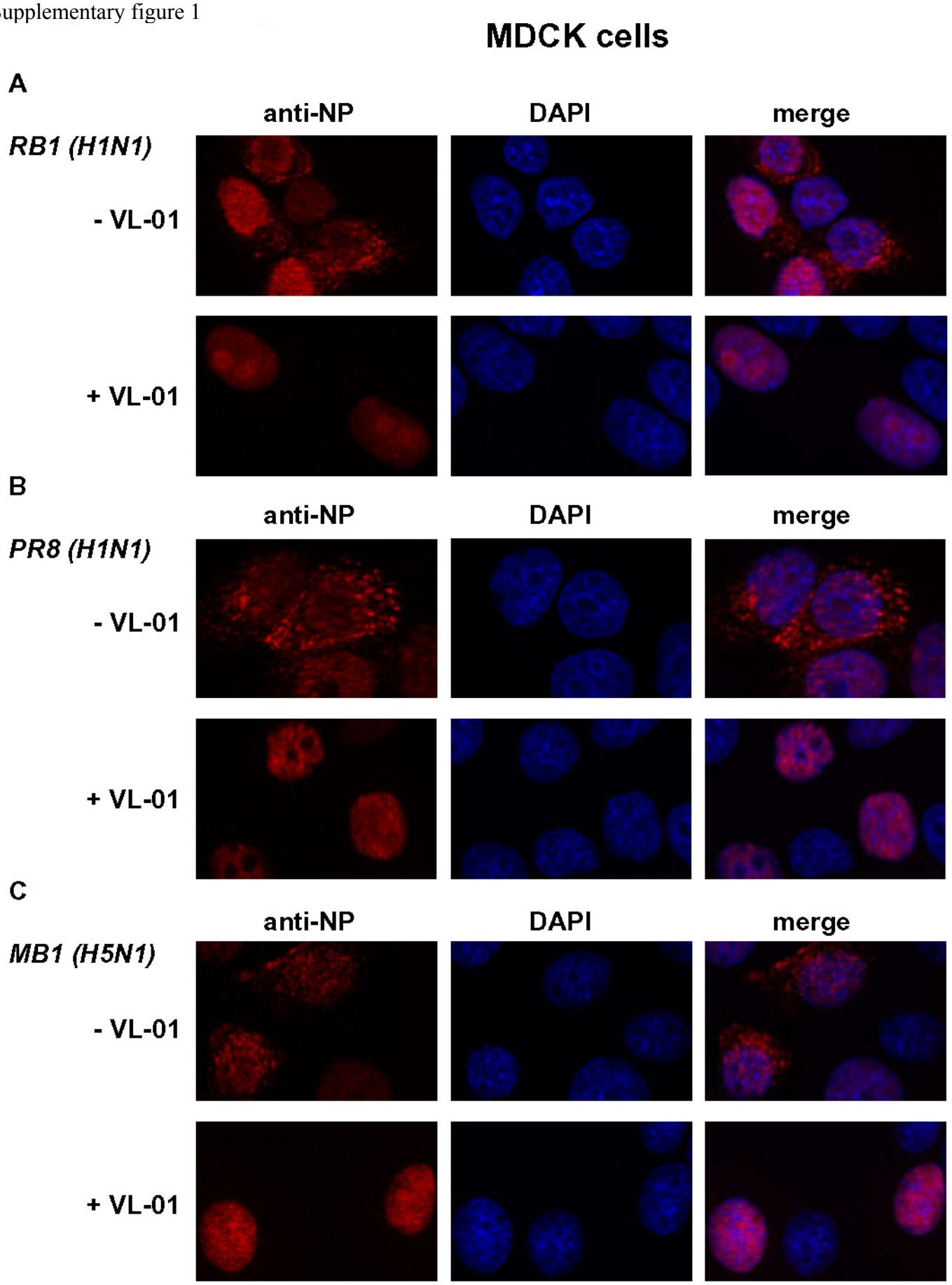

PUBLICATION #2:

Low-dose interferon type I treatment is effective against H5N1 and swine-origin H1N1 influenza A viruses *in vitro* and *in vivo*

Emanuel Haasbach, Karoline Droebner, Annette B. Vogel, and Oliver Planz*

Friedrich-Loeffler-Institut, Institute of Immunology, Paul-Ehrlich Str. 28, 72076 Tuebingen, Germany

*Corresponding author: Prof. Dr. Oliver Planz
Friedrich-Loeffler-Institut; Institute of Immunology,
Federal Research Institute for Animal Health,
Paul-Ehrlich Str. 28
72076 Tuebingen, Germany
Tel: +49 7071 967 254
Fax: +49 7071 967 105
E-mail: oliver.planz@fli.bund.de

Keywords: Influenza A virus; low-dose interferon alpha; cytokines; drug-resistance

Abstract

The recent emergence of pandemic swine-origin influenza virus (H1N1) and the severe outbreaks of highly pathogenic avian influenza virus of the H5N1 subtype leading to death in humans is a reminder that influenza remains a frightening foe throughout the world. Beside vaccination, there is an urgent need for new antiviral strategies to protect against influenza. The innate immune response to influenza viruses involves production of interferon alpha and beta (IFN-α/β) which plays a crucial role in virus clearance during the initial stage of infection. We examined the effect of IFN-α on the replication of H5N1 and H1N1 *in vitro* and *in vivo*. A single pretreatment with low-dose IFN-α reduced lung virus titers up to 1.4 $\log_{10}$ pfu. The antiviral effect increased after multiple pretreatments. Low-dose IFN-α protected mice against lethal H5N1 viral infection. Furthermore, IFN-α was also effective against H1N1 *in vitro* and in the mouse model. These results indicate that low-dose IFN-α treatment leads to the induction of antiviral cytokines that are involved in the reduction of influenza virus titers in the lung. Moreover, it might be possible that a medical application during pandemic outbreak could help contain fulminant infections.

Introduction

Since 2003, highly pathogenic avian influenza virus (HPAIV) H5N1 has caused roughly 500 human cases in Asia, Africa and Europe with a case fatality rate of nearly 60% according to WHO. The long endemic scenario and the high genetic diversity of H5N1 viruses indicate that H5N1 virus strains remain a severe pandemic threat for humans. The pandemic situation of the newly emerging A/H1N1 swine-origin influenza virus (SOIV) places a burden on human health care and gives rise to fears that this virus could reassort with H5N1 to become a highly contagious pathogenic pandemic virus. Human influenza A virus is highly transmissible and replicates in the upper respiratory tract (Thompson and others 2006). The most severe complication is primary viral pneumonia resulting in respiratory failure and death. Patients suffering from chronic bronchitis, asthma or obstructive pulmonary disease have a higher risk of developing influenza-associated secondary bacterial infections (Cox and Subbarao 1999). Even though antiviral compounds are available against influenza virus infection, their efficacy is often limited because of the emergence of drug-resistant virus mutants (Gubareva and others 2001; Gubareva and others 1998; Le and others 2005). Additionally, the long term usage of antiviral drugs sometimes causes adverse effects (Jefferson and others 2009). Consequently, there is an urgent need for new antiviral strategies for protection and treatment against influenza.

In the first stage of influenza infection, it is essential to protect the airway epithelium against infection. There are two major pathways that activate the host innate immune response against viral infection, namely the RNA helicase RIG-I as a receptor for intracellular viral double-stranded RNA and the Toll-like receptor (TLR) family. TLRs induce interferons (IFNs) to activate the transcription factors NF-κB, IRF3 and IRF7 (Ludwig and others 2006; Seth and others 2006). These IFNs are one of the most potent known antiviral mechanisms of the host response that can limit virus replication and spread (Goodbourn and others 2000; Randall and Goodbourn 2008). The importance of this innate immune response against pathogens is highlighted by the fact that several viruses such as influenza virus, measles virus, Newcastle disease virus and respiratory syncytial virus inhibit the synthesis of IFNs by interacting with the host IFN response (Huang and others 2003; Kochs and others 2007a; Lo and others 2005; Palosaari and others 2003). Type I IFNs, namely IFN-α and IFN-β are synthesized and secreted by cells in response to viral infection. They act in an autocrine as well as a paracrine manner to up-regulate the expression of hundreds of IFN stimulated antiviral genes (ISG). These ISG are involved in the up-regulation of the double-stranded RNA-activated protein

kinase R (PKR), 2',5'-oligoadenylate synthetase and Mx proteins, which are all known to mediate resistance to viral infections (Silverman 2007). The MxA protein has been shown to directly interfere with influenza A virus replication (Haller and others 2009). In addition to the direct antiviral properties, IFNs-α/β modify the host immune response in different ways. IFNs-α/β up-regulate MCP-1, MCP-3 and IP-10 gene expression which results in additive recruitment of monocytes/macrophages to the site of infection. IFNs-α/β also enhance the antigen presentation of macrophages and dendritic cells by up-regulating MHC gene expression (Stark and others 1998). Moreover, IFNs-α/β are important cofactors in the development of Th1-type immune response. IFNs-α/β are involved in T lymphocyte survival, enhancement of IL-12 receptor and IFN-γ gene expression in human natural killer cells (NK) and T lymphocytes (Matikainen and others 1999; Rogge and others 1997). These data underline an essential role of IFNs-α/β in both innate and adaptive immunity against influenza A and other viral infections. During influenza A virus infection the non-structural protein (NS1) of the virus is one of the most important antagonist for this antiviral state (Haye and others 2009). Influenza viruses that are unable to express NS1 (delNS1) induce large amounts of IFN in infected cells. (Garcia-Sastre and others 1998; Kochs and others 2007b). These findings demonstrate that type I IFNs play an important role in inducing the antiviral state in the first line of defense and to help protect the tissue against a fatal infection.

Treatments of high-dose interferon ($3x10^6$ to $9x10^6$ units) are actually applied in a wide spectrum of diseases like hepatitis B and C, multiple sclerosis and autoimmune disorders (Cooksley 2004; Pereira and Jacobson 2009; Sottini and others 2009). These long term high-dose treatments are often accompanied by various severe adverse events such as depression, fever, chills, muscle aches, headache, and a general feeling of discomfort. The short-term intranasal administration of IFN-α treatment for human viral respiratory diseases has been shown in Eastern Europe and Russia to have promising antiviral effects (Imanishi and others 1980; Isomura and others 1982; Saito and others 1985). The question arises whether low-dose IFN-α is effective *in vitro* and *in vivo* to protect against highly pathogenic and seasonal influenza A virus infections.

In the present study, we examined the antiviral effect of low-dose IFN-α treatment on influenza A virus infection of cell cultures and in the mouse model. IFN treatment of human and mouse cell lines resulted in a reduction of progeny viral titers. Decreased lung viral titers of H5N1 and H1N1v were observed after intranasal IFN-α treatment of infected mice. The decrease of virus in the lung apparently resulted in prolonged survival of mice that were infected with an otherwise lethal dose of influenza H5N1 virus.

Material and Methods

Virus strains

The highly pathogenic avian influenza A H5N1 virus strains A/mute swan/Germany/R1349/07 (SN1) and A/goosander/Bavaria/20/2006 (GSB1) were grown in embryonated chicken eggs. This isolate was originally obtained from the Bavarian Health and Food Safety Authority, Oberschleissheim, Germany. The H1N1 swine-origin influenza A virus A/Hamburg/4/2009 (SH4) isolated from a patient in Hamburg was originally obtained from Robert-Koch-Institute Berlin, Germany and further propagated on MDCK cells at the Friedrich-Loeffler-Institut, Federal Research Institute for Animal Health, Tuebingen, Germany (FLI).

Virus inoculation of mice

Six to eight week-old BALB/c mice were obtained from the animal breeding facilities at the FLI. Before intranasal inoculation with H5N1 or H1N1, mice were anaesthetized by intraperitoneal injection of 150 µl of a ketamine (Sanofi)-rompun (Bayer)-solution (equal amounts of a 2%-rompun-solution and a 10%-ketamin-solution were mixed at the rate of 1:10 with phosphate buffered saline (PBS)). All animal studies were approved by the Institutional Animal Care and Use Committee of Tuebingen.

IFN-α treatment of cell cultures and experimental design of in vivo studies

Mouse fibroblast cells (MC57) or human lung adenocarcinoma epithelial cells (A549) were grown in minimal-essential medium (MEM) supplemented with 10% heat-inactivated fetal calf serum (FCS) and antibiotics (penicillin and streptomycin). Prior to infection, cells were grown overnight in 24-well plates. Immediately before IFN treatment, the cells were washed with PBS and subsequently incubated for 8h with 100, 1000 or 5000 units of IFN-α (mu-IFN-α or hu-IFN-α, PBL, NJ, USA) in MEM containing 0.2% bovine albumin (BA) and antibiotics. After incubation IFN-α was aspirated and cells were washed with PBS. Thereafter cells were inoculated with the H5N1 virus strain or with the H1N1 strain at a multiplicity of infection (MOI) of 0.001 diluted in PBS/BA (0.2 % BA), 1 mM $MgCl_2$, 0.9 mM $CaCl_2$, penicillin and streptomycin for 30 min at 37°C. After the 30-min incubation time, the inoculum was aspirated and cells were incubated with 1ml MEM containing 0.2% BA and antibiotics. Supernatants from MC57 and A549 cells were collected at 24, 48 or 72h post inoculation (p.i.) and virus was titrated on MDCK cells by AVICEL® plaque assay.

The *in vivo* studies were performed in 6-8 week old BALB/c mice. At 8, 32 and 56h prior to viral inoculation, mice were anaesthetized by intraperitoneal injection of ketamine/rompun and treated intranasally with 1000 units murine IFN-α (PBL, NJ, USA) in 50 µl PBS, 0.1% BSA. Five BALB/c mice were treated with murine IFN-α and inoculated with H5N1 virus. A single intranasal treatment of mice was performed with 1000 units mouse IFN-α at 8, 24, 48 or 72h prior to H5N1 inoculation. The lungs of IFN-α treated and solvent-treated control mice were collected 48h p.i. and viral titers were determined by plaque assay.

To examine the effect of an additive IFN-α treatment on the virus replication, experiments were conducted using a multiple pre-treatment protocol. Eight mice per group were treated with 1000 units IFN-α or solvent 56, 32 and 8h prior to H5N1 inoculation and one group of mice was treated only once with 1000 units of IFN-α 8h prior to inoculation with H5N1 virus. After IFN-α administration, animals from both groups were inoculated with a 10-fold MLD_{50} of the H5N1 influenza virus ($2x10^2$ pfu). Lungs were collected 48h p.i. and the virus titers were determined by plaque assay. After mice were inoculated with $1x10^5$ pfu of H1N1, the lung viral titers were analyzed 48h p.i. by plaque assay.

To determine survival after IFN treatment, 8 BALB/c mice per group were given 1000 units IFN-α or solvent. IFN-α was administrated 56, 32 and 8h prior inoculation of 10-fold mouse lethal dose 50% (MLD_{50}) of H5N1. Treatment was extended to 24 and 48h post infection. In addition, to determine the blood level of IFN-α in treated mice, sera of individual animals were collected between treatments and the amounts of IFN-α were analyzed by ELISA. Four mice out of each group were killed 84h p.i. The weights of livers and spleens after multiple IFN-α treatment were compared to solvent-treated controls. The bodyweight and visual clinical symptoms of the remaining four mice per group were monitored for a 14-day observation period. Clinical symptoms were scored as described earlier (Droebner and others 2008). To determine whether IFN-α given intranasally caused adverse events, five mice were treated once with 1000 units of IFN-α. After 48h, the spleens and livers of each mouse were weighed and compared to weights of control mice.

Influenza virus titration (AVICEL® plaque assay)

To assess the number of infectious particles (plaque titers) in the samples, a plaque assay using AVICEL® was performed in 96-well plates as described by Droebner et al. (Droebner and others 2008). Virus-infected cells were immunostained by incubating for 1h with a monoclonal antibody specific for the influenza A virus nucleoprotein (Serotec) followed by 30-min incubation with peroxidase-labeled anti-mouse antibody (DIANOVA) and 10-min

incubation with True Blue™ peroxidase substrate (KPL). Stained plates were scanned on a flat bed scanner and the data were acquired by Corel DRAW 9.0 software. To define the titer of progeny virus, the foci of infected cells for every sample in each well of the 96-well plates were counted and multiplied with the dilution factor. From the final number of foci in each well, the mean values were taken. The viral titers are shown as the logarithm to the base 10 of the mean values.

IC50 determination of IFN-α and Oseltamivir

Oseltamivir carboxylate was obtained from Toronto Research Chemicals Inc. (TCR, North York, Canada) and dissolved in sterile PBS and IFN-α as previously described. For the determination of the $IC_{50,}$ cells were infected and treated with different concentrations of oseltamivir (0.01 nM to 1 mM) or IFN-α (0 to 5000 units). The viral titers of cell culture supernatants were calculated in percent. The number of pfu of untreated virus-infected control was set as 100% and the titers of IFN-α treated sample were calculated as follows:

Percent inhibition =100/(pfu virus-infected sample x IFN-α treated sample). The IC_{50} value (i.e. the concentration of IFN-α required to reduce the virus titer to 50%) was determined with the GraphPad Prism 5 Software by plotting the percent virus titer as a function of IFN-α concentration.

Enzyme Kinetics and neuraminidase (NA) inhibition assay

For determination of Km and V_{max} for every virus a standardize enzyme activity (0.5 OD units at λ = 540 nM) was incubated with five different fetuin substrate concentration for different time points. Both values were determined with the GraphPad Prism 5 Software by plotting the enzyme velocity against substrate concentration. Kinetic assays were performed in triplicates. NA activity was measured by a colorimetric assay (Aymard-Henry and others 1973) with fetuin (Sigma-Aldrich, Germany) as a substrate. The inhibitory effect of oseltamivir on neuraminidase activity was determined by assaying for enzyme activity in the presence of a range of concentrations.

Measurement of type I Interferon with enzyme-linked immunosorbent assay (ELISA)

Sera of IFN-α treated mice were collected at 57, 44 and 20h prior to inoculation as well as 16, 36, 60 and 84h post inoculation. The sera were stored at -70°C until the analysis of IFN-α. The IFN-α level in sera was measured using sandwich enzyme-linked immunosorbent assay (ELISA) (IFN-α ELISA test kits were purchased from PBL, NJ, USA). IFN-α was quantified

on the basis of a standard curve obtained with recombinant IFN-α. The protein concentrations were given in x-fold secretion, compared to sera of untreated mice. ELISA was performed according to the manufacturer's instructions.

Quantitative real-time RT-PCR

Total RNA was isolated from the lungs of IFN-α or solvent treated mice using TRIzol reagent (Invitrogen). Mice were treated 56, 32 and 8h prior RNA isolation either with 1000 units IFN-α or solvent. The quantitative real-time RT-PCR (qRT-PCR) was performed as described previously (Vogel and others 2010). Briefly, a total of 50 ng RNA was used for qRT-PCR to determine the expression of IFN-α, OAS, RNaseL and GAPDH using the QuantiFast SYBR Green RT-PCR Kit (Qiagen, Hilden, Germany), and the SmartCycler System and software (Cepheid, Sunnyvale, CA). The following specific primers for qRT-PCR were used: Mm_Ifna2_1_SG, Mm_Oas1a_1_SG, Mm_Rnasel_2_SG and Mm_Gapdh_2_SG (Qiagen). The relative expression values (ratio) were normalized to the expression value of the housekeeping gene GAPDH.

Statistical analysis

Statistical analysis was performed using GraphPad Prism software v5.02. For the investigation of significant differences between two groups Mann-Whitney-Test as well as paired t test (p-value <0.05) was performed, for more groups ANOVA Newman-Keuls-Test (p-value <0.01) was performed. Error bars are given as the standard error of the mean.

Results

Interferon alpha treatment reduces progeny influenza virus titer in vitro

To investigate the antiviral potential of interferon alpha (IFN-α) against influenza A virus infection *in vitro*, MC57 cells were treated 8h prior to infection with 100, 1000 or 5000 units mouse IFN-α. After removal of IFN-α, cells were infected with H5N1 influenza virus at a MOI of 0.001. The progeny virus titers were determined by plaque assay 24 or 48h past infection (p.i.). H5N1 virus replicated 24h p.i. in mock-treated cells to 3.1 ± 0.24 $\log_{10}$ pfu/ml (Fig. 1A; white bar). Reduced virus titers were found in cell cultures treated with IFN-α. Treatment with 100 or 1000 units of IFN lead to a virus titer reduction of 0.7 ± 0.1 $\log_{10}$ pfu; treatment with 5000 units of IFN resulted in viral titer reduction up to 1.0 ± 0.1 $\log_{10}$ pfu (Fig. 1A). An enhanced reduction of viral titer after IFN-α treatment was observed 48h post infection depending on the dose of IFN-α used (Fig. 1B). The use of 5000 units of IFN-α resulted in a 1.4 ± 0.11 $\log_{10}$ pfu reduction, while treatment of infected cells with 1000 and 100 units IFN-α led to virus titer reductions of 1.2 ± 0.08 and 1.0 ± 0.05 $\log_{10}$ pfu, respectively, compared to control cells.

In addition to infection with the H5N1 influenza virus strain, experiments were performed with the pandemic H1N1 virus. Human lung adenocarcinoma epithelial cells A549 and human IFN-α was used for these experiments. Cells were treated 8h prior to H1N1 infection with 100, 1000 or 5000 units human IFN-α. The progeny virus titer was determined 48 or 72h past infection, because of the slow replication rate of the virus. In control cells H1N1 replicated 48h p.i. to a titer of 3.77 ± 0.44 $\log_{10}$ pfu/ml and 4.10 ± 0.22 $\log_{10}$ pfu/ml after 72h. After IFN-α treatment hardly any virus was detectable in the cell culture supernatants 48 and 72h p.i. (Fig. 1C, D). These results demonstrated the potent antiviral effect of hu-IFN-α against the pandemic H1N1 influenza A virus strain. The IFN-α concentrations used in these experiments showed on both cell lines no toxic effects assayed by crystal violet toxicity assay (data not shown).

IFN-α is effective against oseltamivir-resistant H5N1 influenza A virus

In order to investigate the antiviral potential of IFN-α in contrast to oseltamivir, IC_{50} values based on reduction of either virus titer (IFN-α) or neuraminidase activity (oseltamivir) to 50% were determined for three different influenza A virus strains. The IC_{50} values for IFN-α ranged from 1.49 ± 1.37 to 250.3 ± 1.26 units (Table 1). IFN-α demonstrated the highest sensitivity against the H1N1 isolate with IC_{50} value of 1.49 ± 1.37 units. The IC_{50} values

evaluated for oseltamivir ranged from 0.23 ± 0.15 to 346.20 ± 1.89 nM indicating that the influenza A H5N1 virus isolate, GSB1 (346.20 ± 1.89 nM) can be considered resistant against oseltamivir (Gubareva and others 2002). In contrast to the ineffective antiviral properties of oseltamivir, the IC_{50} of IFN-α against this oseltamivir-resistant H5N1 isolate is 23.43 ± 1.20 units. Because of the differences in the responsiveness to oseltamivir, we also determined enzymatic parameters for the sialidase activities of the neuraminidases. The Michaelis-Menten constant (Km), which reflects the affinity for the substrate, ranged from 146.64 ± 11.87 to 603.58 ± 102.06 μM of fetuin. V_{max} values, reflecting the activity of the enzyme were for the H1N1 and H5N1 (SN1) isolates similar ranging from 2.77 ± 0.35 to 2.75 ± 0.11 x 10^{-3}, except for the oseltamivir-resistant H5N1 isolate GSB1 with an V_{max} of 40.01 x 10^3 (Table 1). The mean inhibition constant (Ki) values for oseltamivir ranged from 0.23 ± 0.17 to 346.12 ± 1.97 nM and were higher for less susceptible isolates. Taken together, the in vitro date concerning the progeny virus titer after IFN-α treatment correlated well with the determined IC_{50} values of IFN-α as well as the oseltamivir-resistance of one H5N1 isolate.

Swine-origin H1N1 influenza A virus is susceptible to low-dose IFN-α treatment

Because of the strong antiviral effects of IFN-α even at low concentrations against influenza virus *in vitro,* we raised the question whether low-dose IFN-treatment was also effective *in vivo* against the pandemic H1N1 strain. Therefore, 1000 units murine IFN-α were given three times (8, 32 and 56h) prior to infection of five BALB/c mice. The animals were infected with $1x10^5$ pfu of H1N1. Lung virus titers were analyzed 48h p.i. by plaque assay. The administration of IFN-α was able to reduce the virus titers in lungs of infected mice up 1 log unit (mock 7.18 ± 0.28 vs. IFN-α 6.19 ± 0.42 log_{10} pfu/ml) compared to solvent-treated animals (Fig. 2A). In percent, there was a 77% reduction of viral lung titer after low-dose IFN-treatment in pandemic H1N1 virus infected mice (Fig. 2B).

Single low-dose IFN-α administration reduces progeny virus titer in the lungs of H5N1 infected mice

Next, we were interested in the antiviral activity of IFN-α against the H5N1 influenza virus. Therefore, five BALB/c mice were treated with murine IFN-α and infected with the avian H5N1 influenza A virus. A single intranasal treatment of mice was performed with 1000 units mouse IFN-α at different time points prior H5N1 infection. The IFN-α application was carried out either 8 or 24 or 48 or 72h prior to infection. The lungs of IFN-α treated and mock-treated control mice were collected 48h p.i. and virus titers were determined by plaque assay. In the

lungs of mock-treated mice a virus titer of 3.22 ± 0.17 log_{10} pfu/ml was noted (Fig. 3A, white bar). Mice treated with IFN-α once 72h prior to infection showed a titer reduction of 0.8 ± 0.38 log_{10} pfu/ml in the lung to 2.41 ± 0.23 log_{10} pfu/ml. An even higher reduction in virus concentration resulted when IFN-α was applied 48h (reduction of 1.1 ± 0.3 log_{10} pfu), 24h (1.3 ± 0.36 log_{10} pfu) and 8h (1.4 ± 0.04 log_{10} pfu) prior to inoculation (Fig. 3A). To investigate whether 1000 unit IFN-α shows adverse events, five mice were once treated with 1000 units IFN-α. Spleens (Fig. 3B) and livers (Fig. 3C) of processed animals showed no significant differences in weight or appearance when compared to organs of mock-treated animals. Thus, the administration of a single dose of 1000 U IFN-α did not appear to be toxic in mice.

Repeated low-dose IFN-α pre-treatment of H5N1 infected mice increased the antiviral effect

As demonstrated in Fig. 3, a single low-dose treatment of mice with 1000 units IFN-α resulted in a reduction of virus in lungs after H5N1 influenza A virus infection. Next, we asked whether a repeated IFN-α application would enhance the antiviral effect. Therefore, mice were treated with 1000 units IFN-α or solvent 56, 32 and 8h prior to H5N1 infection. To investigate whether multiple prophylactic treatment is beneficial compared to a single treatment, one group of mice was treated only once 8h prior to infection with 1000 units IFN-α. Additionally, the distribution of viral load in mice after multiple IFN-α or solvent treatment was examined by titrating lung, heart, spleen, kidney, liver, brain and blood 2, 4 and 6 days past infection.

In the lungs of mock-treated mice, progeny virus replicated to a titer of 4.04 ± 0.05 log_{10} pfu/ml (Fig. 4, white bars) 48h past infection. The viral titer was reduced to 2.86 ± 0.35 log_{10} pfu/ml in the lungs of mice that were treated only once with low-dose IFN-α (1000 U). In contrast the viral titer in lungs of mice that were treated multiple times with 1000 U IFN-α was reduced to 2.00 ± 0.12 log_{10} pfu/ml (Fig. 4). Thus, the single low-dose IFN-α treatment resulted in a viral titer reduction of 1.18 ± 0.61 log_{10} pfu/ml, while the multiple administrations IFN-α led to a titer reduction of 2.04 log_{10} ± 0.15 pfu/ml compared to mock-treated animals (Fig. 4). Table 2 shows the distribution of viral load 2, 4 and 6 days after multiple IFN-α or solvent treatment and H5N1 virus infection in mice. Progeny virus was only measurable in the lung, heart and spleen. There was no virus detectable in kidney, liver, brain or blood (data not shown). At every time point and in all tissues were progeny virus was detectable IFN-α treated mice shows a reduced virus titer compared to control mice.

Low-dose IFN-α treatment protected mice against a lethal H5N1 influenza A virus infection

From the reduction of progeny virus in IFN-α treated mammalian cell cultures and the decreased viral loads in mouse lungs after intranasal low-dose (1000 U) IFN-α application we concluded that the antiviral effect of IFN-α is sufficient to prolong the survival of mice infected with influenza A virus. Mice were either treated with 1000 units IFN-α or solvent. IFN-α was administered 56, 32 and 8h prior infection with 10-fold MLD_{50} of H5N1 influenza A virus. Furthermore, treatment was performed 24 and 48h past infection. In addition, to investigate the level of IFN-α in treated mice, sera of individual animals were collected between treatments and ELISA analyzed the amounts of IFN-α. We also measured RNA level of IFN-α, OAS and RNaseL after triple IFN-α treatment (-56, -32 and -8h) in lungs of uninfected mice. To answer the question whether multiple treatments would lead to adverse effects four mice out of each group were sacrificed 84h p.i. to define the weight of liver and spleen after multiple IFN-α treatment compared to mock-treated controls. The bodyweight and visual clinical symptoms of the other four mice per group were monitored for 14 days.

Six days after inoculation, the control mice started to lose weight (Fig. 5A) and developed first clinical symptoms like ruffled fur or the reduction of their normal activity rate. Within the next three days all control mice died (Fig. 5B, black squares). Interestingly, only one out of four mice of the IFN-α treated group showed clinical symptoms comparable to the control group; this one mouse died at day eleven p.i. (Fig. 5C). The other three IFN-treated mice did not lose weight (Fig. 5A, white squares), remained normal and survived the otherwise lethal challenge infection (Fig. 5B, white squares).

No statistically significant differences in the weights of spleens and livers were found when comparing treated animals to untreated controls. The multiple IFN-α treatments did not provoke noticeable toxic side effects (Fig. 5D, E). When the IFN-α level in sera of treated mice was compared to untreated mice, an additive effect of IFN-α induction was observed (Fig. 6A). After the first two treatments at 56 and 32h prior to infection, an increased amount of IFN-α (4.86 ± 0.3 fold) was detected in treated mice compared to untreated controls. After inoculation of H5N1 virus, the level of IFN-α was reduced until 24h post inoculation. Nevertheless, the next two IFN-α treatments (24 and 48h p.i.) increased the level up to 1.6 ± 0.01 fold (36h), 2.0 ± 0.01 fold (60h) and 2.7 ± 0.14 fold (84h) post infection, compared to IFN-α levels in untreated mice. The relative quantification of IFN-α, OAS and RNaseL RNA after triple IFN-α treatment in the lung shows for all gens an enhanced amount in IFN-α treated mice compared to untreated controls. IFN-α treatment leads to more then 1.5-fold higher IFN-α, 3-fold OAS and 6.5-fold RNaseL RNA level in contrast to solvent treated mice.

From these results one might speculate that the antiviral effect of intranasal administration of low-dose IFN-α enhances endogenous IFN production *in vivo*.

Discussion

Infections with human and avian influenza A viruses are a major burden in human health care and the options for control and treatment of the disease are limited. Viral resistance against the common influenza antivirals, amantadine and oseltamivir underlines the urgent need for new antiviral drugs (Bai and others 2009; McKimm-Breschkin and others 2007; Sheu and others 2008). The continuous circulation and reassortment of influenza viruses represents a chronic public health threat. In this study, we demonstrated that treatment with low-dose IFN-α reduced progeny virus replication in cell culture. Reduction of highly pathogenic influenza H5N1 and the pandemic H1N1 influenza virus was also observed in mice treated with intranasal low-dose (1000 units) IFN-α. Increased survival from IFN treatment was observed without any adverse effects. Moreover, we are able to induce interferon stimulated genes (ISG) in the lung after low-dose IFN-α treatment.

After entry of a pathogen into the host, IFNs form the first line of defense and establish an "antiviral state". This results in the induction of a large number of ISG. These genes are involved in expression of cytokines/chemokines and enzymes that interact with cellular and viral processes to avoid viral replication and spread (Goodbourn and others 2000; Randall and Goodbourn 2008; Stark and others 1998). IFN-α mediated antiviral status in the innate immune response involves three mechanisms. All three mechanisms are important for the development of an efficient foreign pathogen clearance. First, activated double stranded RNA (dsRNA)-dependent protein kinase R (PKR) which detects dsRNA, inhibits protein synthesis by phosphorylating the eukaryotic initiation factor 2 (eIF2a) (Garcia and others 2006). Secondly, the 2',5'-oligoadenylate synthetase (OAS) triggered by dsRNA activates the cellular endoribonuclease, RNaseL, which degrades cellular but also viral single-stranded RNA, resulting in inhibition of protein synthesis (Silverman 2007). The third mechanism by which IFN-α induces an antiviral state is the induction of the transcription of the Mx protein that interacts in a direct way with viral components to trap and sort them to cellular compartments where they become unavailable for the production of new virus particles (Haller and others 2007). In the present study wild-type mice were used that lack the Mx protein. Thus our present results demonstrate that Mx protein is not a prerequisite to assure the antiviral effect mediated by IFN-α treatment. Furthermore, the results give rise to the assumption that the IFN-α mediated antiviral effect is even more pronounced when Mx protein is present.

The question then arises as to how intranasal delivery of IFN-α contributes to protection against highly pathogenic influenza virus infection. The molecular basis of IFN-α mediated

action after oral administration is not fully understood. It is well accepted that oral IFN-α treatment leads to the induction of 2',5'-oligoadenylate synthetase (OAS) that functions as a molecular marker for IFN-induced cellular activation (Cummins and others 2005). In this concern, it is of interest that influenza A virus developed several ways to evade the host immune response and virus clearance. One way is the interaction of viral NS1 protein with several cellular factors. NS1 can directly block the function of 2',5'-oligoadenylate synthetase (OAS) and the dsRNA- dependent protein kinase R (PKR) (Min and Krug 2006; Min and others 2007; Wolff and Ludwig 2009). Besides OAS activation, orally administered IFN also leads to a local increase of MHC class I expression which is a prerequisite for $CD8^+$ T-cell effector function. Oropharyngeal delivery of IFN-α leads to activation of the interferon-activated natural killer cells, B-cells and subpopulations of the cellular immune response (Cummins and others 2005). Investigations in animals and humans using radiolabeled IFN-α demonstrated a mucosal binding of IFN-α after oropharyngeal delivery in the salvia, oral cavity, nose and in the paranasal sinuses (Diez and others 1987; Schellekens and others 2001). Taken together, these data suggest that the Type I IFN detected in the blood of our mice treated via the intranasally route was of endogenous origin since the low dose IFN would not be detectable systemically in the amounts shown in Figure 6A. In addition, the enhanced RNA levels of ISG (IFN-α, OAS and RNaseL) after IFN-α treatment underline the endogenous origin (Fig. 6B). IFN-α treatment did not provoke noticeable toxic side effects since there were no significant differences in the weights of spleens and livers (Meng and others 2008; Van Loveren and others 1994). Moreover, the data also demonstrate that orally administered IFN-α leads to an induction of an “antiviral state” in the region of the body where influenza virus replication takes place first.

Pre-treatment with low-dose IFN-α reduced influenza virus in the lung of mice and protected these animals against a lethal infection. Beilharz et al already demonstrated the potential of low-dose IFN-α prophylactic treatment of mice infected with mouse adapted human influenza virus A/Puerto Rico/8/34 (Beilharz and others 2007). In addition, oromucosal administration including low-dose IFN treatment was demonstrated to be protective against various virus infections including vesicular stomatitis virus, encephalomyelitis virus, vaccinia virus and cytomegalovirus (Bosio and others 1999; Lawson and Beilharz 1999; Sonnenfeld and others 2001; Tovey and Maury 1999).

Low-dose IFN-α treatment is a novel way to deal with potential pandemic outbreaks of new emerging influenza A viruses. The importance for new antiviral drugs especially after development of partial viral resistance to the available antiviral drugs against influenza virus

is a prerequisite to assure human health. Related to develop resistance we could show that the oseltamivir-resistant H5N1 virus strain A/goosander/Bavaria/20/2006 (GSB1) is susceptible for low-dose IFN-α treatment. Therefore, low-dose IFN-α could maybe an effective antiviral drug by oseltamivir or other resistance viruses. In contrast to hepatitis B and C long-term therapy with high concentrations of IFN-α which leads to serious adverse effects, tissue specific intranasal treatment with low-dose IFN does not cause adverse events. Thus, our findings demonstrate that low-dose IFN-α is a potential antiviral drug to induce the antiviral state as part of the first line of defense to protect against a fatal influenza virus infection.

Acknowledgments

We thank Carmen Mueller for her excellent technical assistance. We also thank Martin and Joseph Cummins for their editorial support and for providing some interferon for the studies. This work is part of the EUROFLU consortium activities and of the VIRGIL European Network of Excellence on Antiviral Drug Resistance supported by a grant (LSHMCT-2004-503359) from the Priority 1 “Life Sciences, Genomics and Biotechnology for Health” program in the 6th Framework Program of the EU. Furthermore, this research was partially supported by the Federal Government of Germany under the Influenza Research Program “FSI” and by the BMBF Zoonose program “FluResearchNet”.

References

Aymard-Henry M, Coleman MT, Dowdle WR, Laver WG, Schild GC, Webster RG. 1973. Influenzavirus neuraminidase and neuraminidase-inhibition test procedures. Bull World Health Organ 48(2):199-202.

Bai GR, Chittaganpitch M, Kanai Y, Li YG, Auwanit W, Ikuta K, Sawanpanyalert P. 2009. Amantadine- and oseltamivir-resistant variants of influenza A viruses in Thailand. Biochem Biophys Res Commun 390(3):897-901.

Beilharz MW, Cummins JM, Bennett AL. 2007. Protection from lethal influenza virus challenge by oral type 1 interferon. Biochem Biophys Res Commun 355(3):740-4.

Bosio E, Beilharz MW, Watson MW, Lawson CM. 1999. Efficacy of low-dose oral use of type I interferon in cytomegalovirus infections in vivo. J Interferon Cytokine Res 19(8):869-76.

Cooksley WG. 2004. The role of interferon therapy in hepatitis B. MedGenMed 6(1):16.

Cox NJ, Subbarao K. 1999. Influenza. Lancet 354(9186):1277-82.

Cummins JM, Krakowka GS, Thompson CG. 2005. Systemic effects of interferons after oral administration in animals and humans. Am J Vet Res 66(1):164-76.

Diez RA, Perdereau B, Falcoff E. 1987. From old results to new perspectives: a look at interferon's fate in the body. J Interferon Res 7(5):553-7.

Droebner K, Haasbach E, Fuchs C, Weinzierl AO, Stevanovic S, Buttner M, Planz O. 2008. Antibodies and CD4(+) T-cells mediate cross-protection against H5N1 influenza virus infection in mice after vaccination with a low pathogenic H5N2 strain. Vaccine 26(52):6965-74.

Garcia-Sastre A, Egorov A, Matassov D, Brandt S, Levy DE, Durbin JE, Palese P, Muster T. 1998. Influenza A virus lacking the NS1 gene replicates in interferon-deficient systems. Virology 252(2):324-30.

Garcia MA, Gil J, Ventoso I, Guerra S, Domingo E, Rivas C, Esteban M. 2006. Impact of protein kinase PKR in cell biology: from antiviral to antiproliferative action. Microbiol Mol Biol Rev 70(4):1032-60.

Goodbourn S, Didcock L, Randall RE. 2000. Interferons: cell signalling, immune modulation, antiviral response and virus countermeasures. J Gen Virol 81(Pt 10):2341-64.

Gubareva LV, Kaiser L, Matrosovich MN, Soo-Hoo Y, Hayden FG. 2001. Selection of influenza virus mutants in experimentally infected volunteers treated with oseltamivir. J.Infect.Dis. 183(4):523-531.

Gubareva LV, McCullers JA, Bethell RC, Webster RG. 1998. Characterization of influenza A/HongKong/156/97 (H5N1) virus in a mouse model and protective effect of zanamivir on H5N1 infection in mice. J.Infect.Dis. 178(6):1592-1596.

Gubareva LV, Webster RG, Hayden FG. 2002. Detection of influenza virus resistance to neuraminidase inhibitors by an enzyme inhibition assay. Antiviral Res 53(1):47-61.

Haller O, Staeheli P, Kochs G. 2007. Interferon-induced Mx proteins in antiviral host defense. Biochimie 89(6-7):812-8.

Haller O, Staeheli P, Kochs G. 2009. Protective role of interferon-induced Mx GTPases against influenza viruses. Rev Sci Tech 28(1):219-31.

Haye K, Burmakina S, Moran T, Garcia-Sastre A, Fernandez-Sesma A. 2009. The NS1 protein of a human influenza virus inhibits type I interferon production and the induction of antiviral responses in primary human dendritic and respiratory epithelial cells. J Virol 83(13):6849-62.

Huang Z, Krishnamurthy S, Panda A, Samal SK. 2003. Newcastle disease virus V protein is associated with viral pathogenesis and functions as an alpha interferon antagonist. J Virol 77(16):8676-85.

Imanishi J, Karaki T, Sasaki O, Matsuo A, Oishi K, Pak CB, Kishida T, Toda S, Nagata H. 1980. The preventive effect of human interferon-alpha preparation on upper respiratory disease. J Interferon Res 1(1):169-78.

Isomura S, Ichikawa T, Miyazu M, Naruse H, Shibata M, Imanishi J, Matsuo A, Kishida T, Karaki T. 1982. The preventive effect of human interferon-alpha on influenza infection; modification of clinical manifestations of influenza in children in a closed community. Biken J 25(3):131-7.

Jefferson T, Jones M, Doshi P, Del Mar C. 2009. Possible harms of oseltamivir--a call for urgent action. Lancet 374(9698):1312-3.

Kochs G, Garcia-Sastre A, Martinez-Sobrido L. 2007a. Multiple anti-interferon actions of the influenza A virus NS1 protein. J Virol 81(13):7011-21.

Kochs G, Koerner I, Thiel L, Kothlow S, Kaspers B, Ruggli N, Summerfield A, Pavlovic J, Stech J, Staeheli P. 2007b. Properties of H7N7 influenza A virus strain SC35M lacking interferon antagonist NS1 in mice and chickens. J Gen Virol 88(Pt 5):1403-9.

Lawson CM, Beilharz MW. 1999. Low-dose oral use of interferon inhibits virally induced myocarditis. J Interferon Cytokine Res 19(8):863-7.

Le QM, Kiso M, Someya K, Sakai YT, Nguyen TH, Nguyen KH, Pham ND, Ngyen HH, Yamada S, Muramoto Y, Horimoto T, Takada A, Goto H, Suzuki T, Suzuki Y,

Kawaoka Y. 2005. Avian flu: isolation of drug-resistant H5N1 virus. Nature 437(7062):1108.

Lo MS, Brazas RM, Holtzman MJ. 2005. Respiratory syncytial virus nonstructural proteins NS1 and NS2 mediate inhibition of Stat2 expression and alpha/beta interferon responsiveness. J Virol 79(14):9315-9.

Ludwig S, Pleschka S, Planz O, Wolff T. 2006. Ringing the alarm bells: signalling and apoptosis in influenza virus infected cells. Cell Microbiol. 8(3):375-386.

Matikainen S, Sareneva T, Ronni T, Lehtonen A, Koskinen PJ, Julkunen I. 1999. Interferon-alpha activates multiple STAT proteins and upregulates proliferation-associated IL-2Ralpha, c-myc, and pim-1 genes in human T cells. Blood 93(6):1980-91.

McKimm-Breschkin JL, Selleck PW, Usman TB, Johnson MA. 2007. Reduced sensitivity of influenza A (H5N1) to oseltamivir. Emerg Infect Dis 13(9):1354-7.

Meng J, Yan Z, Wu Y, Gao M, Li W, Gao F, Wang H, Han W, Zhang Y. 2008. Preclinical safety evaluation of IFNalpha2a-NGR. Regul Toxicol Pharmacol 50(3):294-302.

Min JY, Krug RM. 2006. The primary function of RNA binding by the influenza A virus NS1 protein in infected cells: Inhibiting the 2'-5' oligo (A) synthetase/RNase L pathway. Proc Natl Acad Sci U S A 103(18):7100-5.

Min JY, Li S, Sen GC, Krug RM. 2007. A site on the influenza A virus NS1 protein mediates both inhibition of PKR activation and temporal regulation of viral RNA synthesis. Virology 363(1):236-43.

Palosaari H, Parisien JP, Rodriguez JJ, Ulane CM, Horvath CM. 2003. STAT protein interference and suppression of cytokine signal transduction by measles virus V protein. J Virol 77(13):7635-44.

Pereira AA, Jacobson IM. 2009. New and experimental therapies for HCV. Nat Rev Gastroenterol Hepatol 6(7):403-11.

Randall RE, Goodbourn S. 2008. Interferons and viruses: an interplay between induction, signalling, antiviral responses and virus countermeasures. J Gen Virol 89(Pt 1):1-47.

Rogge L, Barberis-Maino L, Biffi M, Passini N, Presky DH, Gubler U, Sinigaglia F. 1997. Selective expression of an interleukin-12 receptor component by human T helper 1 cells. J Exp Med 185(5):825-31.

Saito H, Takenaka H, Yoshida S, Tsubokawa T, Ogata A, Imanishi F, Imanishi J. 1985. Prevention from naturally acquired viral respiratory infection by interferon nasal spray. Rhinology 23(4):291-5.

Schellekens H, Geelen G, Meritet JF, Maury C, Tovey MG. 2001. Oromucosal interferon therapy: relationship between antiviral activity and viral load. J Interferon Cytokine Res 21(8):575-81.

Seth RB, Sun L, Chen ZJ. 2006. Antiviral innate immunity pathways. Cell Res 16(2):141-7.

Sheu TG, Deyde VM, Okomo-Adhiambo M, Garten RJ, Xu X, Bright RA, Butler EN, Wallis TR, Klimov AI, Gubareva LV. 2008. Surveillance for neuraminidase inhibitor resistance among human influenza A and B viruses circulating worldwide from 2004 to 2008. Antimicrob Agents Chemother 52(9):3284-92.

Silverman RH. 2007. Viral encounters with 2',5'-oligoadenylate synthetase and RNase L during the interferon antiviral response. J Virol 81(23):12720-9.

Sonnenfeld G, Tovey M, Schellekens H, Kinney KS, Belay T, Morton DS, Austin CE, Reitman M, Fong TA, Vaughan HS. 2001. Efficacy and safety of orally/sublingually, intranasally, and intraperitoneally administered recombinant murine interferon in the treatment of murine encephalomyocarditis virus. J Interferon Cytokine Res 21(7):539-45.

Sottini A, Capra R, Serana F, Chiarini M, Caimi L, Imberti L. 2009. Interferon-beta therapy monitoring in multiple sclerosis patients. Endocr Metab Immune Disord Drug Targets 9(1):14-28.

Stark GR, Kerr IM, Williams BR, Silverman RH, Schreiber RD. 1998. How cells respond to interferons. Annu Rev Biochem 67:227-64.

Thompson CI, Barclay WS, Zambon MC, Pickles RJ. 2006. Infection of human airway epithelium by human and avian strains of influenza a virus. J Virol 80(16):8060-8.

Tovey MG, Maury C. 1999. Oromucosal interferon therapy: marked antiviral and antitumor activity. J Interferon Cytokine Res 19(2):145-55.

Van Loveren H, Gianotten N, Hendriksen CF, Schuurman HJ, Van der Laan JW. 1994. Assessment of immunotoxicity of buprenorphine. Lab Anim 28(4):355-63.

Vogel AB, Haasbach E, Reiling SJ, Droebner K, Klingel K, Planz O. 2010. Highly pathogenic influenza virus infection of the thymus interferes with T lymphocyte development. J Immunol 185(8):4824-34.

Wolff T, Ludwig S. 2009. Influenza viruses control the vertebrate type I interferon system: factors, mechanisms, and consequences. J Interferon Cytokine Res 29(9):549-57.

Figure legends

FIG. 1. The titer of H5N1 and H1N1 virus was reduced by IFN-α treatment. Cells were treated with 0, 100, 1000 or 5000 units of IFN-α for 8h prior to virus inoculation. (A, B) After aspiration of IFN-α, cells were inoculated with highly pathogenic avian influenza A H5N1 virus A/mute swan/Germany/R1349/07 (SN1). After 24h (**A**) and 48h (**B**) progeny virus titers in the supernatant were determined by plaque assay. *$P < 0.01$ (Newmann-Keuls-Test). (C, D) After aspiration of IFN-α, cells were inoculated with the H1N1 swine-origin influenza A virus A/Hamburg/4/2009 (SH4). After 48h (**C**) and 72h (**D**) progeny virus titers in the supernatant were determined by plaque assay. *$P < 0.01$ (Newmann-Keuls-Test).

FIG. 2. Intranasal IFN-α treatment reduced viral titers in the lungs of H1N1 inoculated mice. Five BALB/c mice were treated intranasally with 1000 units of mu-IFN-α 56, 32 and 8h prior to inoculation with $1x10^5$ pfu H1N1. After an incubation period of 48h, viral lung titers were determined by plaque assay. Viral titer in log10 pfu/ml (**A**) and in percent (**B**). *$P < 0.05$ (Mann-Whitney-Test).

FIG. 3. Reduction of viral titers in the lungs depended on the time point of IFN-α treatment. (**A**) Five BALB/c mice per group were given 1000 units mu-IFN-α or solvent at 72, 48, 24 and 8h prior to $2x10^2$ pfu H5N1 inoculation. At 48h p.i. spleens (**B**) and livers (**C**) were weighted and viral titers in the lungs were determined by plaque assay. *$P < 0.01$ (Newmann-Keuls-Test).

FIG. 4. IFN-α treatment reduced viral titers in the lungs. Mice were intranasally treated with 1000 units mu-IFN-α once (8h) or three times (8, 32 and 56h) prior to inoculation with 10-fold MLD_{50} ($2x10^2$ pfu) of the H5N1 strain SN1. Progeny virus titers in the lungs were determined 48h post infection. *$P < 0.01$ (Newmann-Keuls-Test).

FIG. 5. Multiple IFN-α treatment protected mice against lethal H5N1 influenza A virus infection. Eight mice from each group were treated with 1000 units mu-IFN-α three times (56, 32 and 8h) prior to, and 24 and 48h, after inoculation with $2x10^2$ pfu H5N1. (**A**) Average body weights of solvent (black squares) and IFN-α treated (white squares) animals. (**B**) Survival rates of solvent (black squares) and IFN-α treated (white squares) mice (*$P < 0.01$).

(C) Clinical score of solvent (black squares) and IFN-α treated (white squares) mice. Four out of eight mice were sacrificed to define the weight of spleen (**D**) and liver (**E**).

FIG. 6. IFN-α level in sera of mice treated with IFN-α was measured by ELISA and is given as x-fold expression relative to solvent treated mice (*$P < 0.01$ (Newmann-Keuls-Test)) (**A**). Quantitative real-time RT-PCR of interferon stimulated genes (IFN-α, OAS and RNaseL) (**B**). Total RNA was isolated from the lungs of mice which were treated 56, 32 and 8h prior RNA isolation either with 1000 units IFN-α or solvent. The relative expression values (ratio) were normalized to the expression value of the housekeeping gene GAPDH. *$P < 0.05$ (paired t test)

Tables

Table 1: In vitro effect of IFN-α and oseltamivir on influenza A virus strains.

	IFN-α	Oseltamivir			
isolate	**IC_{50} (units)[a]**	**IC_{50} (nM)[b]**	**V_{max} ($x10^{-3}$)[c]**	**Km (µM) of fetuin[c]**	**Ki (nM)[d]**
H1N1	1.49 ± 1.37	0.23 ± 0.15	2.77 ± 0.35	603.58 ± 102.06	0.23 ± 0.17
H5N1 (SN1)	250.3 ± 1.26	1.60 ± 1.35	2.75 ± 0.11	146.64 ± 11.87	1.60 ± 1.57
H5N1 (GSB1)	23.43 ± 1.20	346.20 ± 1.89	40.01 ± 3.45	563.50 ± 65.04	346.12 ± 1.97

[a] determined by in vitro screening and represents the IFN-α units required to reduce the virus titer to 50%. IC_{50} values were determined for a 24h infection period (MOI 0.001) for each virus with the GraphPad Prism 5 software by plotting the percent virus titer as a function of compound concentration. The experiment was performed in triplicates.

[b] The IC_{50} value (i.e. the concentration of compound required to reduce the viral NA activity to 50%) was determined for each virus with the GraphPad Prism 5 Software by plotting the percent NA activity as a function of compound concentration. The inhibition assays were performed in triplicates. The IC_{50} values were determined for each virus with the GraphPad Prism 5 Software by plotting the percent neuraminidase activity as a function of compound concentration.

[c] For the determination of Km and V_{max} for every virus a standardize enzyme activity (0.5 OD units at λ = 540 nM) was incubated with five different fetuin substrate concentration for different time points. Both values were determined with the GraphPad Prism 5 Software by plotting the enzyme velocity against substrate concentration.

[d] Ki values were obtained using the fallowing equation: Ki = IC_{50}/ 1+ (substrate concentration/Km)

Table 2: Distribution of viral load 2, 4 and 6 days after multiple IFN-α treatment and influenza virus infection in BALB/c mice[a].

	Lung			Heart			Spleen		
	mock	IFN-α	Δ virus titer	mock	IFN-α	Δ virus titer	mock	IFN-α	Δ virus titer
day 2	4.04 ± 0.05	2.00 ± 0.12	2.04	< 1.7	< 1.7	-	2.74 ± 0.36	2.21 ± 0.50	0.53
day 4	4.63 ± 0.23	4.09 ± 0.50	0.54	1.96 ± 0.25	< 1.7	0.26	2.73 ± 0.32	2.15 ± 0.43	0.58
day 6	5.43 ± 0.42	4.92 ± 0.66	0.51	2.34 ± 0.74	1.94 ± 0.53	0.40	3.22 ± 0.14	< 1.7	1.52

[a] Virus titers are given as the logarithm in pfu per 1ml organ-homogenate.

.

Figures

Figure 1

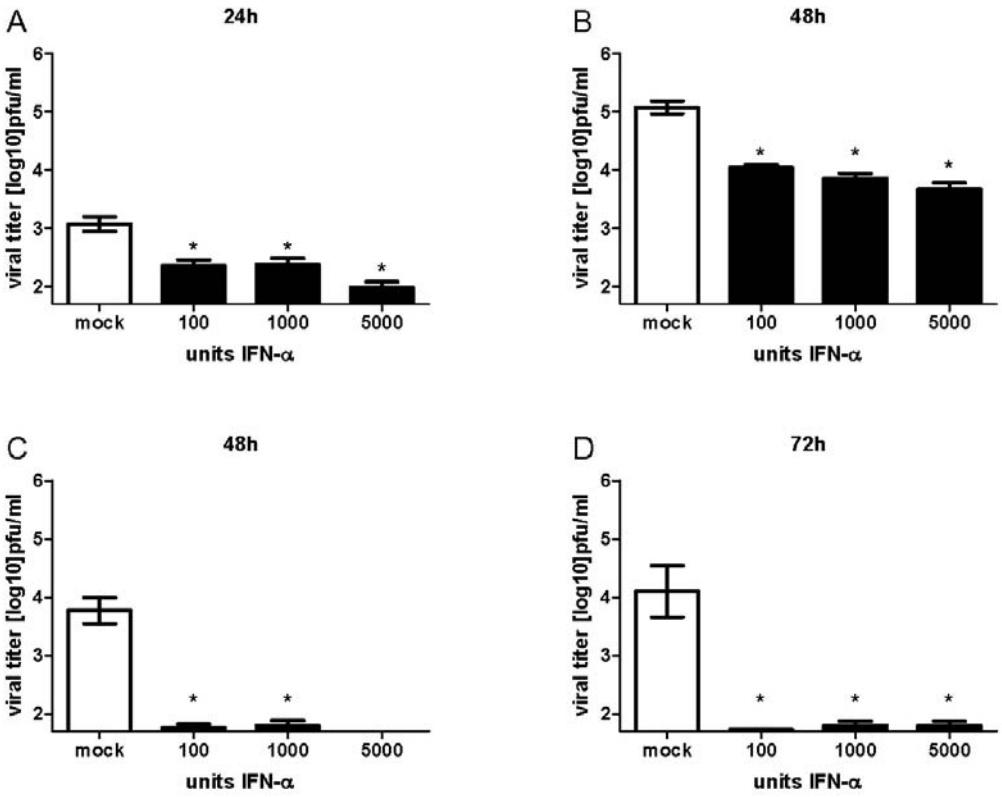

Figure 2

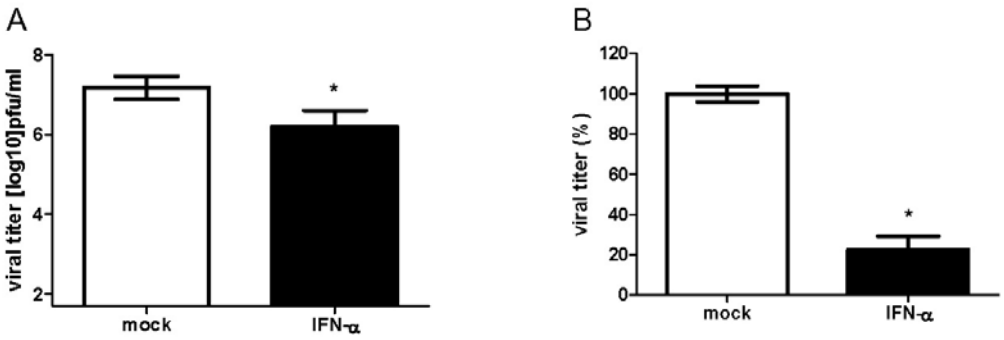

Figure 3

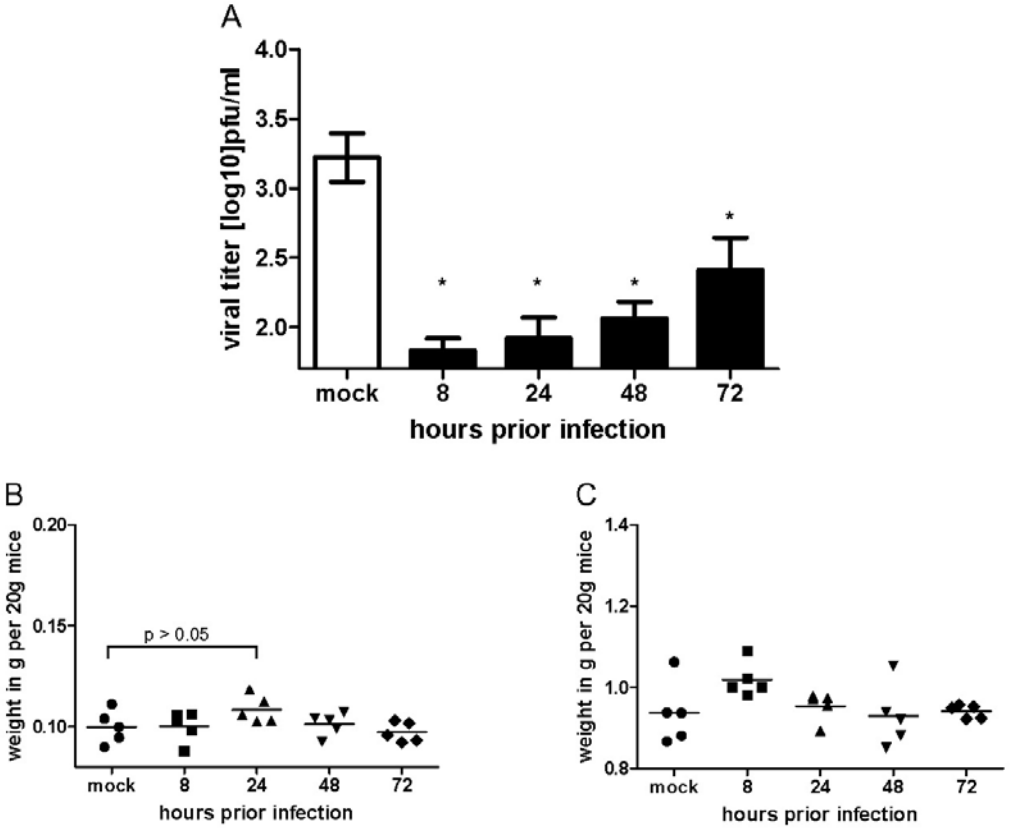

Figure 4

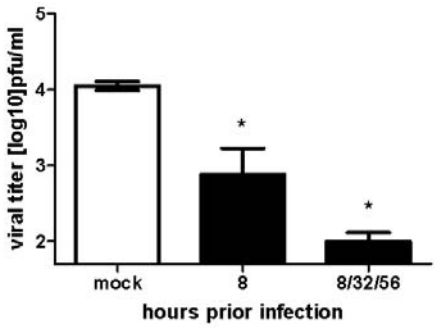

Figure 5

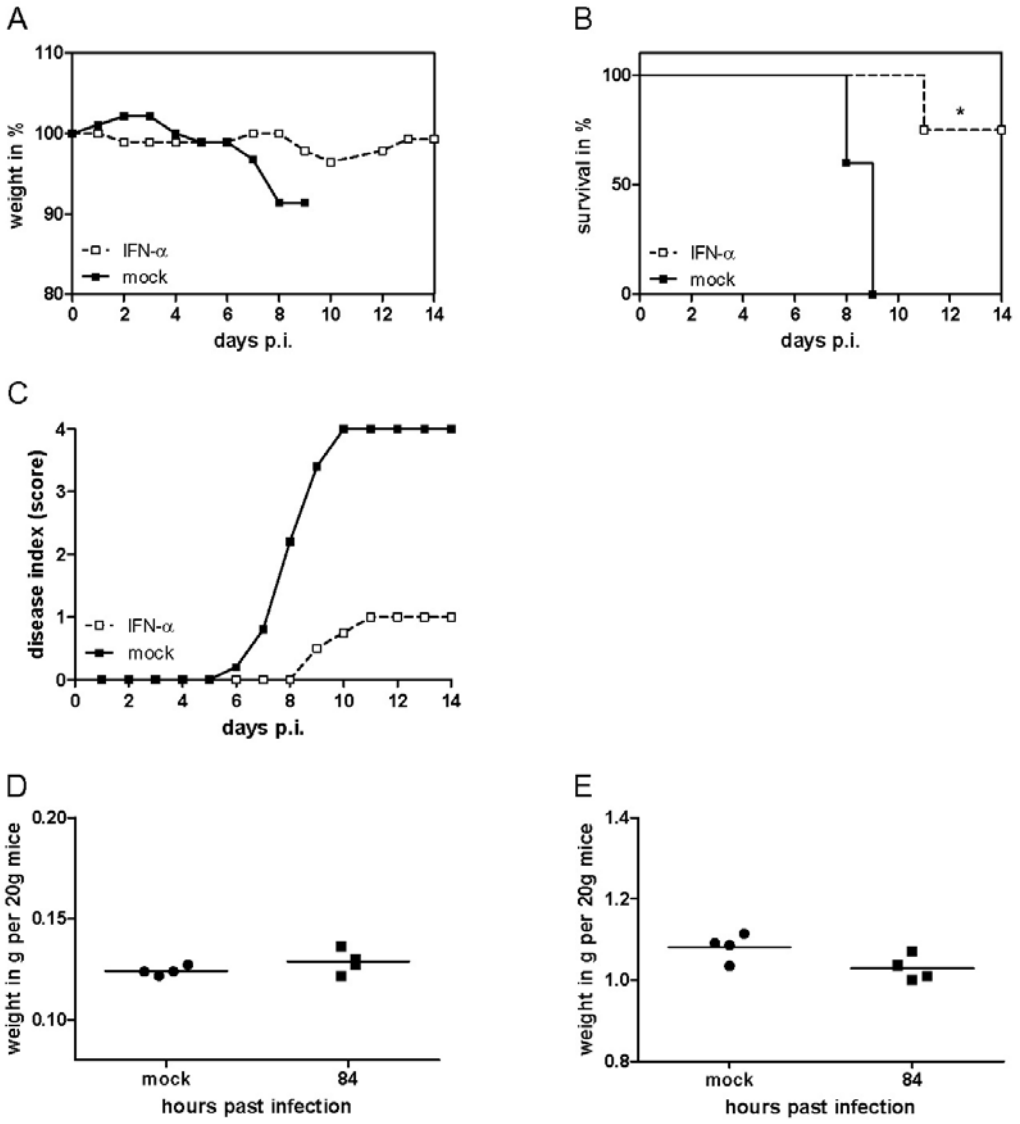
A
weight in %
110
100
90
80
IFN-α
mock
0 2 4 6 8 10 12 14
days p.i.
B
survival in %
100
50
0
*
IFN-α
mock
0 2 4 6 8 10 12 14
days p.i.
C
disease index (score)
4
3
2
1
0
IFN-α
mock
0 2 4 6 8 10 12 14
days p.i.
D
weight in g per 20g mice
0.20
0.15
0.10
mock
84
hours past infection
E
weight in g per 20g mice
1.4
1.2
1.0
0.8
mock
84
hours past infection

Figure 6

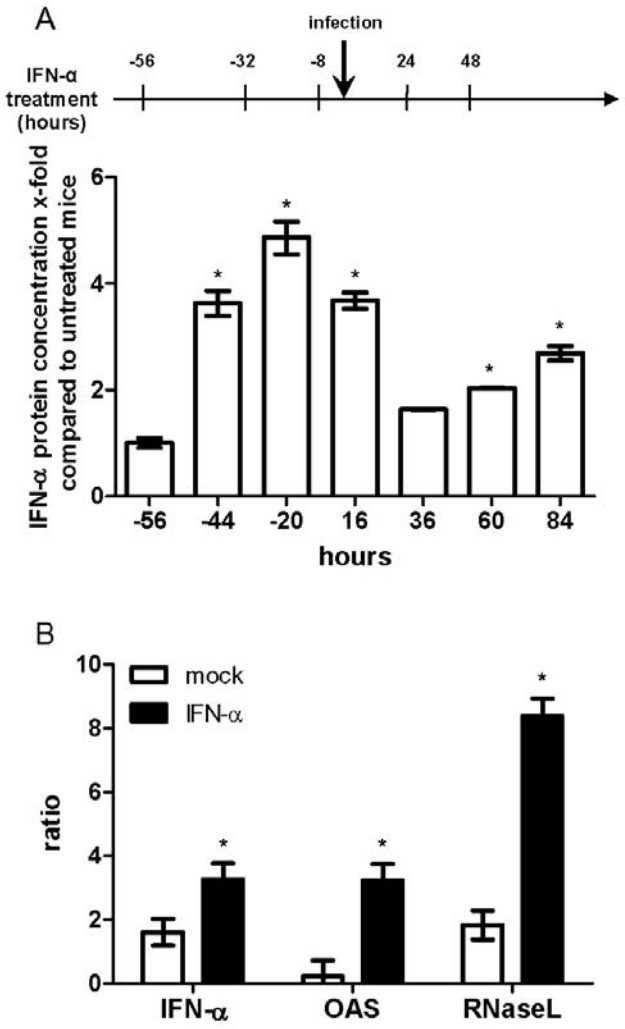
A
infection
-56
-32
-8
24
48
IFN-α treatment (hours)
IFN-α protein concentration x-fold compared to untreated mice
0
2
4
6
-56
-44
-20
16
36
60
84
hours
B
mock
IFN-α
ratio
0
2
4
6
8
10
IFN-α
OAS
RNaseL

PUBLICATION #3:

Influenza virus infection aggravates stroke outcome

Sajjad Muhammad, MD,[1*] Emanuel Haasbach,[2*] Maria Kotchourko,[1] Anne Strigli,[1] Antje Krenz, PhD,[1] Dirk A. Ridder, MD,[1] Annette B. Vogel,[2] Hugo H. Marti, MD,[3] Yousef Al-Abed, PhD,[4] Oliver Planz, PhD,[2+] Markus Schwaninger, MD[1+]

[1] Department of Pharmacology, University of Heidelberg, Germany.

[2] Friedrich-Loeffler-Institut, Institute of Immunology, Tübingen, Germany.

[3] Department of Physiology, University of Heidelberg, Germany.

[4] Department of Medicinal Chemistry, The Feinstein Institute for Medical Research, USA.

*,[+] contributed equally to this work

Address correspondence concerning stroke to: Markus Schwaninger, Department of Pharmacology, University of Heidelberg, Im Neuenheimer Feld 366, 69120 Heidelberg, Germany, Phone: +49-6221-548691, Fax: +49-6221-548549, email: markus.schwaninger@pharma.uni-heidelberg.de

Address correspondence concerning influenza to: Oliver Planz, Friedrich-Loeffler-Institut, Institute of Immunology, Paul-Ehrlich-Str. 28, 72076 Tübingen, Germany, Phone: +49-7071-967254, email: oliver.planz@fli.bund.de

Keywords: Influenza, Stroke, Cytokines, RANTES, α7 nicotinic acetylcholine receptor

Abstract

BACKGROUND AND PURPOSE: Stroke is triggered by several risk factors, including influenza and other respiratory tract infections. However, it is unknown how and in which way influenza infection affects stroke outcome.

METHODS: We infected mice intranasally with human influenza A (H1N1) virus and occluded the middle cerebral artery to induce ischemic strokes. Infarct volume and intracerebral hemorrhage were determined by histology. To evaluate the integrity of the blood-brain barrier and inflammation, we measured various cytokines in vivo and in vitro and performed immunohistochemistry of leukocyte markers, collagen IV, immunoglobulins, and matrix metalloproteinase-9.

RESULTS: Influenza virus infection increased infarct size. Whereas changes in cardiovascular parameters did not explain this effect, we found evidence for an inflammatory mechanism. In influenza virus infection, the respiratory tract released cytokines into the blood, such as RANTES that induced macrophage inflammatory protein-2 and other inflammatory mediators in the ischemic brain. In infected mice, there was an increased number of neutrophils expressing the matrix metalloproteinase-9 in the ischemic brain. This was accompanied by severe disruption of the blood-brain barrier and an increased rate of intracerebral hemorrhages after tissue plasminogen activator treatment. To investigate the role of cytokines, we blocked cytokine release by using GTS-21, a selective agonist of the α7 nicotinic acetylcholine receptor. GTS-21 ameliorated ischemic brain damage and improved survival.

CONCLUSIONS: Influenza virus infection triggers a cytokine cascade that aggravates ischemic brain damage and increases the risk of intracerebral hemorrhage after tissue plasminogen activator treatment. Blockade of cytokine production by α7 nicotinic acetylcholine receptor agonists is a novel therapeutic option to treat stroke in a proinflammatory context.

Non-standard Abbreviations and Acronyms:

α7nAchR, α7 nicotinic acetylcholine receptor; BBB, blood-brain barrier; G-CSF, granulocyte colony stimulating factor; MCA, middle cerebral artery; MCP-1, monocyte chemoattractant protein-1; MIP, macrophage inflammatory protein; MMP-9, matrix metalloproteinase-9; OGD, oxygen glucose deprivation; pMCAO, permanent middle cerebral artery occlusion; RANTES, regulated upon activation normal T cell expressed and secreted; tMCAO, transient middle cerebral artery occlusion; tPA, tissue plasminogen activator

Introduction

Seasonal influenza is a serious health problem. Estimates suggest that influenza virus infection caused about 36,000 deaths per year in the USA between 1993 and 2003.[1] During pandemic influenza the mortality rate is even higher. The excess mortality from influenza is only to a small extent due to viral pneumonia, the majority being attributed to secondary respiratory infections or circulatory deaths.[2] Indeed, influenza virus infection triggers several other diseases including myocardial infarction and stroke. In the case of stroke, the link to influenza is supported by several lines of evidence. First, the seasonal variation in stroke incidence closely resembles the occurrence of respiratory tract and influenza virus infections.[3] It has been shown that stroke patients have an increased rate of preceding respiratory tract infections,[4-5] and that respiratory tract infections are followed by an increased stroke risk.[6] The interval between symptoms of respiratory tract infection and stroke is often about 3 days.[6] Moreover, influenza vaccination has been shown to reduce stroke risk,[7-8] and stroke mortality.[9]

If influenza can trigger stroke, what is the effect of concomitant influenza on the pathogenic cascade leading from cerebral ischemia to tissue demise? Though hard to answer from clinical data this question is of great importance for the treatment of both influenza and stroke. Experimental studies have shown that systemic inflammation due to lipopolysaccharides may aggravate neuroinflammation in cerebral ischemia,[10] but the effect of more naturalistic infections is unknown. The interplay between systemic inflammation and stroke pathophysiology is also highly relevant because stroke often occurs in a preexisting state of inflammation due to atherosclerosis, obesity, or infection.[11] Previous preclinical stroke research has mostly neglected this fact by investigating healthy young animals. Here, we show that a concomitant influenza virus infection increases ischemic brain damage and may affect the safety and efficacy of stroke treatment. In influenza-infected mice the blood-brain barrier (BBB) was severely disrupted after stroke and thrombolysis led to more hemorrhages. Our data suggest that RANTES and possibly other cytokines mediate the effect of the respiratory infection on ischemic brain damage. Activation of the cholinergic control of immunity blocked cytokine release and reversed the effect of influenza virus infection on ischemic brain damage.

Methods

Influenza virus and infection

Human influenza virus A/Puerto Rico/8/34 (H1N1; PR8) was propagated on Madin-Darby canine kidney (MDCK) cells as described earlier.[59] Male C57BL/6 mice at an age of 3–4 months if not indicated otherwise were anesthetized by i.p. injection of xylazine (50 µl per 10 g body weight, 0.1%) and ketamine (50 µl per 10 g body weight, 0.5%) and kept in a supine position. We administered the H1N1 virus (1 x 10^5 PFU) or the control inoculum (PBS) in a final volume of 50 µl (25 µl in each nasal opening) and monitored breathing to assure complete inhalation of virus. Successful infection was controlled by virus titration of lungs. To investigate survival we used C57BL/6 mice at an age of 7–9 weeks since the LD_{50} of PR8 (2 x 10^3 PFU) was evaluated in this age group of C57BL/6 mice. All animal experiments were approved by the local animal welfare committee.

Permanent middle cerebral artery occlusion (pMCAO)

Male mice were anesthetized at the age of 3–4 months by i.p. injection of 2.5% tribromoethanol (150 µl per 10 g body weight). A skin incision was made between the ear and the orbit on the left side. The temporal muscle was removed by electrical coagulation. The stem of the middle cerebral artery (MCA) was exposed through a burr hole and occluded by microbipolar coagulation (Erbe, Tübingen, Germany). Surgery was performed under a microscope (Hund, Wetzlar, Germany). A body temperature of 37°C was maintained in the mice by using a heating pad. For sham surgery, mice were anesthetized and the temporal muscle was removed but the MCA was not occluded. In some groups, mice were treated with GTS-21 (10 mg/kg i.p.) or saline injection before surgery, 6 h, 24 h, and 36 h after surgery. If not indicated otherwise, mice were deeply reanesthetized with tribromoethanol 48 h after pMCAO and perfused intracardially with 4% paraformaldehyde (PFA). The brains were kept in 4% PFA for 3–4 h and then transferred to 30% sucrose solution for 24 h. Finally, the brains were frozen on dry ice. Coronal cryosections of the brains (20 µm in thickness) were cut every 400 µm and stained with the Nissl technique. Infarct volumes were corrected for brain edema as previously described.[60] Surgery was performed and ischemic damage was measured without knowledge of treatment. To evaluate the effects of hypoxemia, mice were exposed to normobaric hypoxia at 16% oxygen during surgery and for a period of 48 h after surgery.[61]

Transient middle cerebral artery occlusion (tMCAO)

Male mice were anesthetized at the age of 3–4 months by i.p. injection of xylazine (50 µl per 10g body weight, 0.1%) and ketamine (50 µl per 10 g body weight, 0.5%). For tMCAO, a median neck incision was performed and the left common carotid artery was exposed. A silicon rubber-coated 7-0 monofilament of 20-mm length (Doccol Corporation, Cat. No. 7019PK5Re) was inserted into the common carotid artery on the left side. The filament was advanced into the internal carotid artery about 11 mm from the bifurcation until the coated part of filament was no longer visible. The filament was reversibly fixed during the whole time of ischemia. Surgery was performed under a microscope (Hund, Wetzlar, Germany) and a body temperature of 37°C was maintained by using a heating pad during the time of occlusion. After 45 min of occlusion, the filament was removed to establish reperfusion. During the time of occlusion, the femoral vein was exposed and cannulated with a 20-cm long catheter (Polyethylene [PE]-10). Human tissue plasminogen activator (tPA, 10 mg/kg in a volume of 300 µl, Boehringer Ingelheim, Germany) was administered starting 30 min after MCAO with a bolus (1 mg/kg). The remaining dose (9 mg/kg) was infused over 20 min with a pump (PHD2000 Programmable, Harvard Apparatus). At 24 h after tMCAO the animals were reanesthetized and perfused intracardially with 4% PFA.

Measurement of physiological parameters

To determine physiological parameters that could affect stroke pathophysiology, the femoral artery was cannulated after anesthesia with Rompun and Ketamine (see above) in a separate cohort of animals. Arterial blood gases and glucose were measured 10 min before and 10 min into pMCAO in a blood sample of 100 µl. For laser Doppler measurements, the probe (P415-205; Perimed, Järfälla, Sweden) was placed 3 mm lateral and 6 mm posterior to the bregma. Relative perfusion units were determined (Periflux 4001; Perimed). For the measurement of body temperature after infection we used a telemetry monitoring system (VitalView®, Minimiter, USA) as described previously.[17] Oxygen saturation was measured in awake mice using the MouseOx® (Starr Life Sciences Corp).

Influenza virus titration

To assess the number of infectious particles (plaque titers) in lung, blood, brain, and cell culture supernatants a plaque assay using Avicel® was performed in 96-well plates as described previously.[27] Organs were homogenized in saline buffer. A 10% homogenate was titrated and used for infection of MDCK target cells. After a 48-h incubation period the virus-infected MDCK cells were immunostained by incubating for 1 h with a monoclonal antibody

specific for the influenza A virus nucleoprotein (Serotec) followed by 30-min incubation with peroxidase-labeled anti-mouse antibody (DIANOVA) and 10-min incubation with True Blue™ peroxidase substrate (KPL). Stained plates were scanned on a flat bed scanner and the data were acquired by Microsoft® Paint software. The virus titer is given as the logarithm to the base 10 of the mean value. The detection limit for this test was <1.7 log 10 PFU/ml.

Immunohistochemistry

For fluorescent immunohistochemistry, cryosections of 20-µm thickness were fixed in 4% PFA for 30 min. Sections were then permeabilized with 0.25% Triton X-100 in PBS for 5 min and blocked in 5% normal horse serum or 5% bovine serum albumin for 90 min except for collagen staining, for which sections were permeabilized by 0.25% Triton X-100 for 2.5 h. The following primary antibodies were used: rabbit anti-mouse collagen IV (1:500; Abcam, Cambridge, UK; Cat. No. ab19808), rabbit anti-mouse polymorphonuclear leukocyte (1:100; Accurate Chemical & Scientific, Westbury, NY, USA; Cat. No. AIAG31140), goat anti-mouse MMP-9 (1:50; R&D-Systems, Wiesbaden-Nordenstadt, Germany; Cat. No. AF909), and rat anti-mouse CD11b (1:100 AbD, Serotec, Düsseldorf, Germany Cat. No. MCA 711G). The primary antibodies were applied overnight at room temperature with the exception of the anti-PMN antibody, which was applied for 2 h. After washing, the following secondary antibodies were added: Cy3-conjugated donkey anti-goat (1:200; Dianova, Hamburg, Germany; Cat. No. 705-165-147), Cy3-conjugated donkey anti-rabbit (1:200; Dianova; Cat. No. 711-165-152), Alexa-Fluor-488 donkey anti-goat (1:200; Invitrogen, Karlsruhe, Germany; Cat. No. A11055), Alexa-Fluor-488 donkey anti-rabbit (1:100; Invitrogen; Cat. No. A212065), Alexa-Fluor-488 donkey anti-rat (1:200; Invitrogen; Cat. No. A21208), and HRP-conjugated goat anti-mouse IgG (1:100; Dianova; Cat. No. 115-035-003). Finally, sections were mounted with Mowiol 4-88-mounting medium with DABCO (Roth, Karlsruhe, Germany; Cat. No. 0713). To exclude unspecific staining we repeated the procedure without the primary antibodies.

To stain the viral nucleoprotein and sialic acid-containing influenza receptors, cryosections were used. The sections were fixed in 4% PFA for 30 min. Endogenous peroxidase activity was then blocked by incubation in PBS containing 3.0% H_2O_2 for 10 min. After incubation with 2.5% normal horse serum or 3% bovine albumin serum for 20 min, goat anti-nucleoprotein (AbD Serotec; 1:4000), biotinylated Sambucus nigra lectin (α 2,6; Vector Laboratories, Burlingame, CA;10 µg/ml), or biotinylated Maackia amurensis II lectin (α 2,3; Vector laboratories; 10 µg/ml) were applied overnight. After adding ImmPRESS REAGENT

(anti-goat IgG; Vector Laboratories Cat. No. MP-7405) or ABC reagent for 30 min, sections were stained with 3,3'-diaminobenzidine (Vector laboratories) according to the manufacturer's protocol. Finally, the sections were counterstained with hematoxylin, dehydrated with ascending alcohol row and incubated in Roti Histoclear solution for 10 min. The sections were covered in ENTELLAN (Merck) and dried for 30 min.

MMP-9 and collagen IV staining were quantified in predefined areas (Figure 3C) on coronal sections containing the anterior commissure without knowledge of treatment using Leica DM4000B (Leica Microsystems) and PictureFrame Application 2.3 (Camera Type: MICROFIRE_C). Neutrophils were counted in the infarct area on a section containing the anterior commissure. For quantification of integrated density we used Image J (Wayne Rasband, National Institute of Mental Health, Maryland, USA). For confocal microscopy a Nikon A1R 4 laser line confocal microscope with hybrid scanner and 32 channel spectral detector was used.

Quantification of hemorrhagic transformations

To quantify hemorrhagic transformation, mice were perfused 24 h after tMCAO as described above. We scored hemorrhages at 20-21 levels throughout the brain without knowledge of the treatment as described previously.[62] Briefly, microscopic hemorrhage (evident to the eye aided by a 10 x magnifying glass) was scored 1 and macroscopic hemorrhage (evident to the unaided eye) was scored 3, 4, or 5 according to its size. To visualize the hemorrhage (Fig 5D) we stained the sections with hematoxylin and eosin and diaminobenzidine (DAB). DAB is known to react with peroxidases in the red blood cells, facilitating precise identification of intracranial hemorrhage.

Hemoglobin assay

To measure the hemoglobin content in the brain we performed a spectrophotometric assay using Drabkin's solution. Briefly, the animals were perfused transcardially 24 h after tMCAO with PFA (4%, 20 ml with a perfusion speed of 1.5 ml/min). To prepare the standards, fresh blood was injected into the cortex immediately before perfusion. The brains were homogenized by sonication in 1 ml PBS per hemisphere. After centrifugation 120 µl of Drabkin's solution containing Drabkin's reagent (Sigma, Cat. No.: D5941) and Brij 35 solution (0.015%, Sigma, Cat. No. B 4184) was added to 30 µl of supernatant and the absorption was measured at 540 mm (Spectra MAX 250, Molecular Devices Corp).

Measurement of cytokines

On day 3 after influenza virus infection male C57BL/6 mice were subjected to pMCAO as described above. At 15 h after occlusion mice were deeply reanesthetized with tribromoethanol. Blood was drawn from the caval vein and plasma was stored at -20°C until analysis by Bioplex.

Cell culture

Glial cells were prepared from the brains of neonatal (postnatal day 2) mice as has been described.[63] Cells were cultured in DMEM (Invitrogen) containing glucose (4.5 g/l), L-glutamine (0.5 mM), fetal calf serum (FCS, 10%, Invitrogen), penicillin (100 IU/ml), and streptomycin (100 µg/ml). The mouse brain endothelial cell line bEnd.3 was obtained from American Type Culture Collection (Manass, VA, USA) and grown in DMEM containing glucose (4.5 g/l), FCS (10%), penicillin (100 IU/ml), streptomycin (100 µg/ml), and L-glutamine (2 mM). Oxygen glucose deprivation (OGD) was used as an *in vitro* model of ischemia. At 1 h before oxygen deprivation, recombinant mouse RANTES (100 ng/ml, Peprotech, Hamburg, Germany) and 2-deoxy-D-glucose (5 mM) were added to medium. Cells were placed in an anaerobic chamber flushed with 5% CO_2 in 95% N_2 for 15 min before the chamber was sealed and incubated for 3 h at 37°C. Control cells were kept under normoxic conditions without 2-deoxy-D-glucsoe for 3 h. The medium was then replaced and the cells were allowed to recover for 24 h under normal conditions. MIP-2 release in the medium was measured using the mouse MIP-2 Quantikine ELISA (R&D).

The human lung epithelial cell line A549 was grown in minimal-essential medium (MEM) supplemented with 10% heat-inactivated FCS, penicillin (100 U/ml), and streptomycin (100 µg/ml). Cells were infected with PR8 (MOI = 1) and treated with GTS-21 for 48 h after infection. RANTES was measured in the medium with the human RANTES direct ELISA kit (Invitrogen).

For the cell viability assay, A549 cells were infected with PR8 virus at MOI of 1.[64] At 48 h after addition of GTS-21, cells were fixed and viable cells were stained with crystal violet (Sigma-Aldrich, Steinheim, Germany). After extraction of crystal violet from viable cells with 100% methanol (Carl Roth, Karlsruhe, Germany), the extinction was measured by 450 nm with a microplate absorbance reader (Sunrise, Tecan).

Statistics

Student's t-test was used to compare two groups and one-way ANOVA (analysis of variance) to compare more than two groups, followed by the Newman-Keuls multiple comparison test. Data are expressed as means ± sem.

Results

Influenza aggravates concomitant stroke

Mice were infected intranasally with the human H1N1 influenza A virus PR8. To induce an ischemic stroke we permanently occluded the middle cerebral artery (pMCAO) 3, 4, or 5 days after infection. These time points were chosen because symptoms of respiratory tract infections often precede stroke by 3–5 days.[6] Influenza virus infection increased the infarct size at all three time points (Figure 1A). Infarcts were mostly limited to the cortex in the pMCAO stroke model (Figure 1B). Influenza virus infection enlarged the infarct size in the full rostro-caudal extension of the lesion (Figure 1C). However, the infection had no effect on the mortality of mice after stroke (pMCAO) (Table 1).

The human influenza virus infects cells of the respiratory tract and has only rarely been detected in the brain.[12] However, there is a short-lasting influenza viremia in humans and mice.[13-14] Furthermore, neural cells express the influenza receptors Siaα2-3gal and Siaα2-6gal (Figure 2A).[15] Therefore, we investigated whether infection of ischemic brain tissue could underlie the increased infarct size. At 5 days after infection we detected the viral nucleoprotein (NP), a marker of ongoing viral replication, in lung tissue but not in ischemic brain (Figure 2A). In addition, we could recover PR8 virus from lung tissue but not from blood or brain (Figure 2B). These data argue against a role of direct brain infection in the aggravation of stroke.

As influenza virus pneumonia may lead to hypoxemia, we considered the possibility that hypoxemia is responsible for the enlarged infarct size during influenza. Oxygen saturation in awake mice was not reduced 3, 4, and 5 days after influenza virus infection (Figure 2C). However, the arterial pO_2 measured in anesthetized mice dropped after influenza virus infection (Figure 2D). A significant decrease of pO_2 was observed 4 and 5 days after infection. A similar drop of pO_2 levels was measured in uninfected mice if the O_2 concentration of the air was reduced to 16% corresponding to an altitude of about 2,400 m (Fig 2E, left panel). Exposure of mice to 16% O_2 during and after pMCAO had no effect on the infarct size (Figure 2E, right panel). This indicates that the enlarged infarct size after influenza virus infection cannot be explained by hypoxemia. Since it has been reported previously that body temperature decreases in mice after influenza virus infection,[16-17] we measured body temperature after stroke. There was no difference between the sham and stroke group (Figure 2F). As hypothermia is neuroprotective,[18] the lower body temperature in influenza virus infected mice would clearly not enlarge the infarct size. Other physiological

parameters that are known to influence the infarct size were not altered after influenza infection (Table 2).

Respiratory influenza virus infection augments neuroinflammation in stroke

Influenza virus infection leads to a profound inflammatory response in the lung that may have distant effects on the ischemic brain. In accordance with previous reports, we found elevated concentrations of MIP1α, IL-6, IL-1β, MCP-1, RANTES, and MIP-2 in lung tissue of influenza virus infected mice (Figure 3A–F, left panel). In plasma, RANTES levels were higher after influenza virus infection both in sham and stroke mice (Figure 3E). In contrast, plasma levels of other cytokines were not affected by influenza infection in stroke mice (Figure 3A–D, 3F, Suppl. Fig 1A–D, 2C). In the brain influenza virus infection alone had no effect on cytokine expression. However, it significantly increased the expression of IL-1β, MCP-1, and MIP-2 in concomitant stroke (Figure 3C, D, F). Also, G-CSF, MIP-1β, and TNF were increased (Suppl. Figure 1A, C, D). However, IL-17, GM-CSF, INFγ were not affected (Suppl. Figure 1B, 2A, B,).

Because RANTES plasma levels were elevated after influenza virus infection we wondered whether RANTES would induce cytokine expression in neural cells. In primary glial cells RANTES stimulated MIP-2 release into the medium (Figure 3G). Likewise, oxygen glucose deprivation (OGD), an *in vitro* model of cerebral ischemia, raised MIP-2 release but the combination of RANTES and OGD had no further effect on MIP-2 secretion (Figure 3G). In brain endothelial bEnd.3 cells RANTES and OGD alone had no effect on MIP-2 release but the combination increased MIP-2 release (Figure 3H). The stimulation of MIP-2 release by the combination of OGD and RANTES may explain the synergistic effect of stroke and influenza on MIP-2 levels in the brain (Figure 3F, right panel).

The cytokines MIP-2, IL-1β, and MCP-1, which were up-regulated in the ischemic brain after influenza virus infection, are involved in the recruitment of neutrophils.[19-20] Indeed, we found an elevated number of neutrophils in the ischemic brain after influenza virus infection (Figure 4A), but no change in the number of CD11b-positive macrophages and microglia (data not shown). At the same time, levels of matrix metalloproteinase-9 (MMP-9), a neutrophilic enzyme, increased in the ischemic brain of influenza virus infected mice as compared to uninfected controls (Figure 4B). Double staining confirmed that MMP-9 was expressed by neutrophils but also revealed a vascular staining pattern for MMP-9 (Figure 4C). This supports the notion that MIP-2 attracted neutrophils expressing MMP-9 in the ischemic brain after influenza virus infection.

Disruption of the blood-brain barrier increases hemorrhagic risk in thrombolysis

MMP-9 is known to degrade the extracellular matrix of the BBB. Therefore, we investigated protein levels of collagen IV, a component of the basal membrane, in the ischemic brain by immunohistochemistry. After influenza virus infection we found reduced collagen IV staining in the ischemic area (Figure 4D). The extravasation of IgG was increased in stroked mice after influenza virus infection as compared to uninfected animals (Figure 4E), indicating that a concomitant influenza virus infection aggravates the disruption of the BBB in cerebral ischemia.

Disruption of the BBB is an important cause of hemorrhage in thrombolytic treatment, which is the only effective therapeutic option in stroke. To evaluate the consequences of influenza virus infection for thrombolysis we employed a stroke model (transient middle cerebral artery occlusion, tMCAO) that has been used previously to investigate complications of tPA treatment.[21] We administered tPA already 30 min after occlusion to minimize intracerebral hemorrhages in uninfected mice (Figure 5A, B). However, after influenza virus infection tPA treatment significantly increased the hemorrhage volume that was assessed by the hemoglobin concentration in the brain (Figure 5A). A similar result was obtained when the number of macroscopic and microscopic hemorrhages on the side of the lesion was scored (Figure 5B). In this stroke model plasma levels of MMP-9 were elevated in influenza virus infected mice suggesting a possible cause for the increased rate of hemorrhages (Suppl. Figure 3A). However, the effect of MMP-9 may be dampened by a similar increase in the MMP-9 inhibitor TIMP-1 (Suppl. Figure 3B). Surprisingly, in the tMCAO stroke model the infarct size was not larger in influenza virus infected mice (Figure 5C). Still, mortality increased significantly after influenza virus infection in tMCAO (Table 1). As only surviving mice were included in the analysis of infarct size, it is possible that death due to a large infarct concealed an effect of influenza on infarct size.

Activation of α7 nicotinic acetylcholine receptor (α7nAchR) to combat neuroinflammation in influenza-associated stroke

If inflammatory mediators are the link between influenza virus infection of the respiratory tract and aggravated ischemic brain damage, anti-inflammatory treatment should be beneficial. In influenza virus infection, lung epithelial cells and macrophages produce cytokines.[22] Both cell types express the α7 nicotinic acetylcholine receptor (α7nAchR) that limits cytokine release in the reflex control of immunity.[23-24] Therefore, we investigated whether the α7nAchR agonist GTS-21 interferes with the effects of influenza virus infection.

GTS-21 increased the viability of A549 lung epithelial cells infected by influenza virus (Figure 6A), but had no effect on viral replication (Suppl. Figure 4). Interestingly, GTS-21 blocked the release of RANTES from A549 cells after influenza virus infection (Figure 6B). To exploit this mechanism we administered GTS-21 to mice (10 mg/kg i.p., before and 6 h after surgery). Also *in vivo*, GTS-21 lowered RANTES plasma concentrations in infected mice (Figure 6C). In contrast, GTS-21 had no effect on plasma levels of MIP-1α and IL-6 (Suppl. Figure 5). In the brain, GTS-21 reduced levels of IL-1β, MCP-1, and MIP-2 that were elevated by influenza virus infection in the ischemic brain (Figure 6D, 6E, 6F). In contrast, GTS-21 had no effect on the expression of MIP-1α and RANTES in the ischemic brain (Suppl. Figure 5). Importantly, GTS-21 significantly reduced the infarct size of influenza-infected mice but had no effect on the infarct size in non-infected animals (Figure 6G), suggesting that GTS-21 specifically interferes with influenza-triggered aggravation of ischemic brain death. These data are in line with the notion that GTS-21 is neuroprotective by interrupting a cytokine cascade that is initiated in the infected lung and extends to the ischemic brain. GTS-21 treatment did not affect viral titers in the lung 4 days after infection (vehicle-treated group, 5.53 ± 0.05 $\log_{10}$ PFU/ml; GTS-21-treated group, 5.61 ± 0.12 $\log_{10}$ PFU/ml, n=3). Furthermore, the effect of GTS-21 treatment on survival after influenza infection and stroke was investigated. GTS-21 treatment prolonged survival for 1 day (Figure 6H). These data exclude an aggravation of the influenza infection due to GTS-21 treatment.

Discussion

Influenza causes a major mortality burden worldwide. Death is not solely due to the respiratory tract infection but often due to aggravation of cardiovascular and other diseases. Therefore, a way to lessen the mortality burden of influenza could lie in a reduction of secondary diseases. Epidemiological data establish influenza as a stroke trigger.[4-9] Here, we show in a mouse model that influenza aggravates stroke pathophysiology. The detrimental effect could not be explained by an infection of the brain, fever, or hypoxemia, but rather, cytokines likely mediate the effect of influenza virus infection on stroke pathophysiology.

Hypercytokinemia has been linked to highly virulent forms of influenza viruses.[25-27] However, elevated cytokine levels have also been observed with less virulent viral strains,[28] and mediate key symptoms of influenza in the hypothalamus, such as changes in body temperature, malaise, and anorexia.[29-33] Our data suggest a mechanism through which cytokines could contribute to ischemic brain damage. Influenza virus infection of epithelial cells and alveolar macrophages in the respiratory tract elicits the release of cytokines into the blood, such as RANTES. Circulating RANTES induces the expression of MIP-2 and possibly other cytokines in cells of the BBB. Consequently, MIP-2 recruits neutrophils to the ischemic brain of influenza virus infected mice. As neutrophils mediate ischemic brain damage,[10, 34-38] this mechanism may contribute to the aggravation of stroke by influenza. In addition, neutrophils release MMP-9, a protease that degrades collagen IV and other components of the extracellular matrix of the BBB.[39] In line with this notion, we found evidence that influenza virus infection elevates MMP-9 levels in the brain and enhances the ischemia-induced degradation of collagen IV and the disruption of the BBB, even though the brain is not a direct target of the virus. Disruption of the BBB by MMP-9 has been implicated in tPA-induced brain hemorrhages.[40-42] Indeed, a concomitant influenza virus infection increased brain hemorrhage after tPA treatment in our mouse model. Thus, standard stroke treatment may be risky in the case of concomitant influenza. Our data suggest neutralization of RANTES as a strategy to interfere with the pathogenic cascade that worsens ischemic brain damage and disrupts the BBB. However, selective antagonism of RANTES has been reported to weaken antiviral defense and to prolong infection of the lung.[43] Furthermore, other cytokines probably contribute to the interaction between influenza and stroke. In this situation, activation of the cholinergic anti-inflammatory pathway seems to be a better choice.

The autonomic nervous system regulates immunity.[24] In influenza or stroke, the sympathetic nervous system influences immune response and outcome,[44-45] but the role of the

parasympathetic cholinergic nervous system has not been studied in detail. Cholinergic control of immunity converges on the α7nAchR.[24] Interestingly, this receptor is expressed by alveolar macrophages and epithelial cells in the respiratory tract, which are the main sources of cytokine production in influenza. Our study demonstrates that activation of α7nAchR by the selective agonist GTS-21 inhibited the release of RANTES from influenza virus infected lung epithelial cells. Upon GTS-21 treatment lower levels of circulating RANTES were associated with decreased levels of inflammatory mediators in the brain and smaller infarct size. In addition, GTS-21 may activate α7nAchR in glial and endothelial cells,[46-47] and thereby inhibit cytokine expression in the ischemic brain. However, it is noteworthy that GTS-21 only reduced the infarct size in influenza virus infected mice suggesting that GTS-21 specifically targets the aggravation of ischemic brain damage by influenza. α7nAchR activation is known to reduce cytokine release in sepsis models.[48] Our data show that this strategy may also be successful to dampen the hypercytokinemia in influenza without any direct effect on viral replication. This effect may help to reduce influenza-associated mortality, which is largely due to cardiovascular diseases in both the common seasonal form of influenza and during pandemics.[49]

Systemic inflammation in influenza virus infection promotes vascular diseases in several ways. First, influenza leads to inflammation, smooth muscle cell proliferation, and fibrin deposition in atherosclerotic plaques.[50] Second, the systemic inflammation elicits a prothrombotic state that is able to trigger myocardial infarction and stroke.[51] In addition, we provide evidence that influenza is able to enhance the inflammatory response to tissue ischemia. Similar mechanisms are likely to occur in myocardial ischemia because systemic inflammation is able to influence tissue damage after coronary artery ligation.[52] If systemic inflammation also plays a role in human influenza, an anti-inflammatory strategy, such as α7nAchR agonists, would have enormous potential to reduce complications and mortality in influenza beyond anti-viral treatment. Notably, GTS-21 was still effective when administered 3 days after infection, suggesting a wider therapeutic window than for anti-viral treatment.

In stroke research, preclinical studies have had a notoriously low predictive value for the clinical efficacy of compounds. An important reason for the disparity between preclinical and clinical data is probably the fact that preclinical studies relied largely on healthy young rodents, whereas clinical stroke often occurs in the context of preexisting diseases.[53] Many of the disorders that predispose to stroke such as atherosclerosis, obesity, and infection are associated with systemic inflammation.[54] Our study demonstrates that concomitant inflammatory disease has an important impact on the safety of thrombolysis, the only

approved stroke treatment. An increased bleeding risk of thrombolysis in influenza virus infected patients has been indirectly suggested by clinical data showing that MMP-9 blood levels, which correlate with an increased risk of hemorrhage after tPA, rise in influenza.[55-57] A recent study reporting an increased rate of hemorrhagic transformation of infarcts in obese mice suggests that the chronic low-grade inflammation of obesity also weakens the BBB.[58] However, the impact of this finding for thrombolysis is still unclear. Whereas the risk of thrombolysis in influenza may be greater, an α7nAchR agonist is only efficacious in association with an inflammatory condition. Thus, our study suggests that stroke treatment should be stratified according to concomitant diseases.

Acknowledgments

We acknowledge the Nikon Imaging Center at the University of Heidelberg. MS is a member of the Excellence Cluster *CellNetworks* at Heidelberg University.

Sources of Funding

The research leading to these results has received funding from the European Union's Seventh Framework Program FP7/2007–2013) under grant agreements 201024 and 202213 (European Stroke Network), from the Federal Government of Germany under the Influenza Research Program "FSI", from the Postdoc program of the Medical Faculty, University of Heidelberg, and from the BMBF Zoonose program "FluResearchNet" (01KI07141).

Disclosures

The authors have no conflicting financial interest.

References

1. Thompson WW, Weintraub E, Dhankhar P, Cheng PY, Brammer L, Meltzer MI, Bresee JS, Shay DK. Estimates of US influenza-associated deaths made using four different methods. *Influenza Other Respi. Viruses.* 2009;3(1):37-49.

2. Nicholson KG, Wood JM, Zambon M. Influenza. *Lancet.* 2003;362(9397):1733-1745.

3. Lanska DJ, Hoffmann RG. Seasonal variation in stroke mortality rates. *Neurology.* 1999;52(5):984-990.

4. Grau AJ, Buggle F, Heindl S, Steichen-Wiehn C, Banerjee T, Maiwald M, Rohlfs M, Suhr H, Fiehn W, Becher H, et al. Recent infection as a risk factor for cerebrovascular ischemia. *Stroke.* 1995;26(3):373-379.

5. Grau AJ, Buggle F, Becher H, Zimmermann E, Spiel M, Fent T, Maiwald M, Werle E, Zorn M, Hengel H, Hacke W. Recent bacterial and viral infection is a risk factor for cerebrovascular ischemia: clinical and biochemical studies. *Neurology.* 1998;50(1):196-203.

6. Smeeth L, Thomas SL, Hall AJ, Hubbard R, Farrington P, Vallance P. Risk of Myocardial Infarction and Stroke after Acute Infection or Vaccination. *N. Engl. J. Med.* . 2004;351(25):2611-2618.

7. Nichol KL, Nordin J, Mullooly J, Lask R, Fillbrandt K, Iwane M. Influenza Vaccination and Reduction in Hospitalizations for Cardiac Disease and Stroke among the Elderly. *N. Engl. J. Med.* 2003;348(14):1322-1332.

8. Grau AJ, Fischer B, Barth C, Ling P, Lichy C, Buggle F. Influenza vaccination is associated with a reduced risk of stroke. *Stroke.* 2005;36(7):1501-1506.

9. Wang C-S, Wang S-T, Lai C-T, Lin L-J, Chou P. Impact of influenza vaccination on major cause-specific mortality. *Vaccine.* 2007;25(7):1196-1203.

10. McColl BW, Rothwell NJ, Allan SM. Systemic Inflammatory Stimulus Potentiates the Acute Phase and CXC Chemokine Responses to Experimental Stroke and Exacerbates Brain Damage via Interleukin-1- and Neutrophil-Dependent Mechanisms. *J. Neurosci.* 2007;27(16):4403-4412.

11. Emsley HCA, Hopkins SJ. Acute ischaemic stroke and infection: recent and emerging concepts. *Lancet Neurol.* 2008;7(4):341-353.

12. Steininger C, Popow-Kraupp T, Laferl H, Seiser A, Godl I, Djamshidian S, Puchhammer-Stockl E. Acute encephalopathy associated with influenza A virus infection. *Clin. Infect. Dis.* 2003;36(5):567-574.

13. Stanley ED, Jackson GG. Viremia in Asian influenza. *Trans. Assoc. Am. Physicians.* 1966;79:376-387.

14. Mori I, Komatsu T, Takeuchi K, Nakakuki K, Sudo M, Kimura Y. Viremia induced by influenza virus. *Microb. Pathog.* 1995;19(4):237-244.

15. Wang G, Zhang J, Li W, Xin G, Su Y, Gao Y, Zhang H, Lin G, Jiao X, Li K. Apoptosis and proinflammatory cytokine responses of primary mouse microglia and astrocytes induced by human H1N1 and avian H5N1 influenza viruses. *Cell. Mol. Immunol.* 2008;5(2):113-120.

16. Conn CA, McClellan JL, Maassab HF, Smitka CW, Majde JA, Kluger MJ. Cytokines and the acute phase response to influenza virus in mice. *Am. J. Physiol.* 1995;268(1 Pt 2):R78-84.

17. Droebner K, Ehrhardt C, Poetter A, Ludwig S, Planz O. CYSTUS052, a polyphenol-rich plant extract, exerts anti-influenza virus activity in mice. *Antiviral Res.* 2007;76(1):1-10.

18. Polderman KH. Induced hypothermia and fever control for prevention and treatment of neurological injuries. *Lancet.* 2008;371(9628):1955-1969.

19. Kobayashi Y. The role of chemokines in neutrophil biology. *Front. Biosci.* 2008;13:2400-2407.

20. Johnston B, Burns AR, Suematsu M, Issekutz TB, Woodman RC, Kubes P. Chronic inflammation upregulates chemokine receptors and induces neutrophil migration to monocyte chemoattractant protein-1. *J. Clin. Invest.* 1999;103(9):1269-1276.

21. Cheng T, Petraglia AL, Li Z, Thiyagarajan M, Zhong Z, Wu Z, Liu D, Maggirwar SB, Deane R, Fernandez JA, LaRue B, Griffin JH, Chopp M, Zlokovic BV. Activated protein C inhibits tissue plasminogen activator-induced brain hemorrhage. *Nat. Med.* 2006;12(11):1278-1285.

22. Julkunen I, Melén K, Nyqvist M, Pirhonen J, Sareneva T, Matikainen S. Inflammatory responses in influenza A virus infection. *Vaccine.* 2000;19(Supplement 1):S32-S37.

23. Paleari L, Sessa F, Catassi A, Servent D, Mourier G, Doria-Miglietta G, Ognio E, Cilli M, Dominioni L, Paolucci M, Calcaterra A, Cesario A, Margaritora S, Granone P, Russo P. Inhibition of non-neuronal alpha7-nicotinic receptor reduces tumorigenicity in A549 NSCLC xenografts. *Int J Cancer.* 2009;125(1):199-211.

24. Tracey KJ. Reflex control of immunity. *Nat. Rev. Immunol.* 2009;9(6):418-428.

25. Kobasa D, Jones SM, Shinya K, Kash JC, Copps J, Ebihara H, Hatta Y, Kim JH, Halfmann P, Hatta M, Feldmann F, Alimonti JB, Fernando L, Li Y, Katze MG,

Feldmann H, Kawaoka Y. Aberrant innate immune response in lethal infection of macaques with the 1918 influenza virus. *Nature.* 2007;445(7125):319-323.

26. de Jong MD, Simmons CP, Thanh TT, Hien VM, Smith GJD, Chau TNB, Hoang DM, Van Vinh Chau N, Khanh TH, Dong VC, Qui PT, Van Cam B, Ha DQ, Guan Y, Peiris JSM, Chinh NT, Hien TT, Farrar J. Fatal outcome of human influenza A (H5N1) is associated with high viral load and hypercytokinemia. *Nat. Med.* 2006;12(10):1203-1207.

27. Droebner K, Reiling SJ, Planz O. Role of Hypercytokinemia in NF-kB p50-Deficient Mice after H5N1 Influenza A Virus Infection. *J. Virol.* 2008;82(22):11461-11466.

28. Hayden FG, Fritz R, Lobo MC, Alvord W, Strober W, Straus SE. Local and systemic cytokine responses during experimental human influenza A virus infection. Relation to symptom formation and host defense. *J. Clin. Invest.* 1998;101(3):643-649.

29. Swiergiel AH, Dunn AJ. The roles of IL-1, IL-6, and TNFalpha in the feeding responses to endotoxin and influenza virus infection in mice. *Brain Behav. Immun.* 1999;13(3):252-265.

30. Kozak W, Zheng H, Conn CA, Soszynski D, van der Ploeg LH, Kluger MJ. Thermal and behavioral effects of lipopolysaccharide and influenza in interleukin-1 beta-deficient mice. *Am. J. Physiol.* 1995;269(5 Pt 2):R969-977.

31. Traynor TR, Majde JA, Bohnet SG, Krueger JM. Interferon type I receptor-deficient mice have altered disease symptoms in response to influenza virus. *Brain Behav. Immun.* 2007;21(3):311-322.

32. Kozak W, Poli V, Soszynski D, Conn CA, Leon LR, Kluger MJ. Sickness behavior in mice deficient in interleukin-6 during turpentine abscess and influenza pneumonitis. *Am. J. Physiol.* 1997;272(2 Pt 2):R621-630.

33. Kurokawa M, Imakita M, Kumeda CA, Shiraki K. Cascade of fever production in mice infected with influenza virus. *J. Med. Virol.* 1996;50(2):152-158.

34. Chen H, Chopp M, Zhang RL, Bodzin G, Chen Q, Rusche JR, Todd RF, 3rd. Anti-CD11b monoclonal antibody reduces ischemic cell damage after transient focal cerebral ischemia in rat. *Ann. Neurol.* 1994;35(4):458-463.

35. Murikinati S, Jüttler E, Keinert T, Ridder DA, Muhammad S, Waibler Z, Ledent C, Zimmer A, Kalinke U, Schwaninger M. Activation of cannabinoid 2 receptors protects against cerebral ischemia by inhibiting neutrophil recruitment. *Faseb J.* 2010;24:788-798.

36. Connolly ES, Jr., Winfree CJ, Springer TA, Naka Y, Liao H, Yan SD, Stern DM, Solomon RA, Gutierrez-Ramos JC, Pinsky DJ. Cerebral protection in homozygous null ICAM-1 mice after middle cerebral artery occlusion. Role of neutrophil adhesion in the pathogenesis of stroke. *J. Clin. Invest.* 1996;97(1):209-216.

37. Dawson DA, Ruetzler CA, Carlos TM, Kochanek PM, Hallenbeck JM. Polymorphonuclear leukocytes and microcirculatory perfusion in acute stroke in the SHR. *Keio J. Med.* 1996;45(3):248-252; discussion 252-243.

38. Arumugam TV, Salter JW, Chidlow JH, Ballantyne CM, Kevil CG, Granger DN. Contributions of LFA-1 and Mac-1 to brain injury and microvascular dysfunction induced by transient middle cerebral artery occlusion. *Am. J. Physiol. Heart Circ. Physiol.* 2004;287(6):H2555-2560.

39. McColl BW, Rothwell NJ, Allan SM. Systemic Inflammation Alters the Kinetics of Cerebrovascular Tight Junction Disruption after Experimental Stroke in Mice. *J. Neurosci.* 2008;28(38):9451-9462.

40. Sumii T, Lo EH. Involvement of Matrix Metalloproteinase in Thrombolysis-Associated Hemorrhagic Transformation After Embolic Focal Ischemia in Rats. *Stroke.* 2002;33(3):831-836.

41. Pfefferkorn T, Rosenberg GA. Closure of the blood-brain barrier by matrix metalloproteinase inhibition reduces rtPA-mediated mortality in cerebral ischemia with delayed reperfusion. *Stroke.* 2003;34(8):2025-2030.

42. Murata Y, Rosell A, Scannevin RH, Rhodes KJ, Wang X, Lo EH. Extension of the Thrombolytic Time Window With Minocycline in Experimental Stroke. *Stroke.* 2008;39(12):3372-3377.

43. Tyner JW, Uchida O, Kajiwara N, Kim EY, Patel AC, O'Sullivan MP, Walter MJ, Schwendener RA, Cook DN, Danoff TM, Holtzman MJ. CCL5-CCR5 interaction provides antiapoptotic signals for macrophage survival during viral infection. *Nat. Med.* 2005;11(11):1180-1187.

44. Prass K, Meisel C, Hoflich C, Braun J, Halle E, Wolf T, Ruscher K, Victorov IV, Priller J, Dirnagl U, Volk H-D, Meisel A. Stroke-induced Immunodeficiency Promotes Spontaneous Bacterial Infections and Is Mediated by Sympathetic Activation Reversal by Poststroke T Helper Cell Type 1-like Immunostimulation. *J. Exp. Med.* 2003;198(5):725-736.

45. Grebe KM, Takeda K, Hickman HD, Bailey AM, Embry AC, Bennink JR, Yewdell JW. Cutting Edge: Sympathetic Nervous System Increases Proinflammatory

Cytokines and Exacerbates Influenza A Virus Pathogenesis. *J. Immunol.* 2010;184(2):540-544.

46. Shytle RD, Takashi M, Kirk T, Martina V, Nan S, Jin Z, Jared E, Archie AS, Paul RS, Jun T. Cholinergic modulation of microglial activation by a7 nicotinic receptors. *J. Neurochem.* 2004;89(2):337-343.

47. Saeed RW, Varma S, Peng-Nemeroff T, Sherry B, Balakhaneh D, Huston J, Tracey KJ, Al-Abed Y, Metz CN. Cholinergic stimulation blocks endothelial cell activation and leukocyte recruitment during inflammation. *J Exp Med.* 2005;201(7):1113-1123.

48. Pavlov VA, Ochani M, Yang LH, Gallowitsch-Puerta M, Ochani K, Lin X, Levi J, Parrish WR, Rosas-Ballina M, Czura CJ, Larosa GJ, Miller EJ, Tracey KJ, Al-Abed Y. Selective alpha7-nicotinic acetylcholine receptor agonist GTS-21 improves survival in murine endotoxemia and severe sepsis. *Crit. Care Med.* 2007;35(4):1139-1144.

49. Collins S. Excess mortality from causes other than influenza and pneumonia during influenza epidemics. *Public Health Rep.* 1932;47:2159-2180.

50. Naghavi M, Wyde P, Litovsky S, Madjid M, Akhtar A, Naguib S, Siadaty MS, Sanati S, Casscells W. Influenza Infection Exerts Prominent Inflammatory and Thrombotic Effects on the Atherosclerotic Plaques of Apolipoprotein E-Deficient Mice. *Circulation.* 2003;107(5):762-768.

51. Keller TT, van der Sluijs KF, de Kruif MD, Gerdes VEA, Meijers JCM, Florquin S, van der Poll T, van Gorp ECM, Brandjes DPM, Buller HR, Levi M. Effects on Coagulation and Fibrinolysis Induced by Influenza in Mice With a Reduced Capacity to Generate Activated Protein C and a Deficiency in Plasminogen Activator Inhibitor Type 1. *Circ. Res.* . 2006;99(11):1261-1269.

52. Shimamoto A, Chong AJ, Yada M, Shomura S, Takayama H, Fleisig AJ, Agnew ML, Hampton CR, Rothnie CL, Spring DJ, Pohlman TH, Shimpo H, Verrier ED. Inhibition of Toll-like Receptor 4 With Eritoran Attenuates Myocardial Ischemia-Reperfusion Injury. *Circulation.* 2006;114(1_suppl):I-270-274.

53. Endres M, Engelhardt B, Koistinaho J, Lindvall O, Meiairs S, Mohr JP, Planas A, Rothwell N, Schwaninger M, Schwab ME, Vivien D, Wieloch T, Dirnagl U. Improving outcome after stroke: overcoming the translational roadblock. *Cerebrovasc. Dis.* 2008;25(3):268-278.

54. Emsley HC, Tyrrell PJ. Inflammation and infection in clinical stroke. *J. Cereb. Blood Flow Metab.* 2002;22(12):1399-1419.

55. Ichiyama TMD, Morishima TMD, Kajimoto MMD, Matsushige TMD, Matsubara TMD, Furukawa SMD. Matrix metalloproteinase-9 and tissue inhibitors of metalloproteinases 1 in influenza-associated encephalopathy. *Pediatr. Infect. Dis. J.* 2007;26(6):542-544.

56. Lansberg MG, Albers GW, Wijman CAC. Symptomatic Intracerebral Hemorrhage following Thrombolytic Therapy for Acute Ischemic Stroke: A Review of the Risk Factors. *Cerebrovas. Dis.* 2007;24(1):1-10.

57. Montaner J, Molina CA, Monasterio J, Abilleira S, Arenillas JF, Ribo M, Quintana M, Alvarez-Sabin J. Matrix metalloproteinase-9 pretreatment level predicts intracranial hemorrhagic complications after thrombolysis in human stroke. *Circulation.* 2003;107(4):598-603.

58. McColl BW, Rose N, Robson FH, Rothwell NJ, Lawrence CB. Increased brain microvascular MMP-9 and incidence of haemorrhagic transformation in obese mice after experimental stroke. *J. Cereb. Blood Flow Metab.* 2010;30:267-272.

59. Ehrhardt C, Wolff T, Pleschka S, Planz O, Beermann W, Bode JG, Schmolke M, Ludwig S. Influenza A Virus NS1 Protein Activates the PI3K/Akt Pathway To Mediate Antiapoptotic Signaling Responses. *J. Virol.* 2007;81(7):3058-3067.

60. Lin TN, He YY, Wu G, Khan M, Hsu CY. Effect of brain edema on infarct volume in a focal cerebral ischemia model in rats. *Stroke.* 1993;24(1):117-121.

61. Bauer AT, Bürgers HF, Rabie T, Marti HH. Matrix metalloproteinase-9 mediates hypoxia-induced vascular leakage in the brain via tight junction rearrangement. *J. Cereb. Blood Flow Metab.* 2010;30:837-848.

62. Haddad M, Beray-Berthat V, Coqueran B, Palmier B, Szabo C, Plotkine M, Margaill I. Reduction of hemorrhagic transformation by PJ34, a poly(ADP-ribose)polymerase inhibitor, after permanent focal cerebral ischemia in mice. *Eur. J. Pharmacol.* 2008;588(1):52-57.

63. Muhammad S, Barakat W, Stoyanov S, Murikinati S, Yang H, Tracey KJ, Bendszus M, Rossetti G, Nawroth P, Bierhaus A, Schwaninger M. The HMGB1 receptor RAGE mediates ischemic brain damage. *J. Neurosci.* 2008;28:12023-12031.

64. Gillies RJ, Didier N, Denton M. Determination of cell number in monolayer cultures. *Anal Biochem.* 1986;159(1):109-113.

Figure legends

Figure 1. Influenza virus infection increases the infarct volume after stroke (pMCAO).
A, The infarct volume was increased when stroke was induced 3, 4, or 5 days after influenza virus infection (Flu). *$p<0.05$ (t-test, n=8–14).
B, Nissl-stained coronal sections showing the increased infarct area when stroke (pMCAO) was induced 3 days after influenza virus infection.
C, Infarct distribution on coronal sections in mice that were subjected to stroke 4 days after influenza virus infection; n=9.

Figure 2. Infection of the brain and altered physiological parameters do not explain the increased infarct volumes after influenza virus infection.
A, Immunohistochemistry showed that influenza receptors Siaα2-3gal and Siaα2-6gal were expressed in lung and brain tissue. However, the viral nucleoprotein (NP) was only detected in lungs of infected mice but not in the ischemic brain area. Scale bar, 50 μm.
B, Virus titration showed that influenza viruses could be detected in the lung of infected mice but not in blood or brain; n=5.
C, The oxygen saturation in awake mice was normal on day 3, 4, and 5 after influenza virus infection (n=3–4).
D, The arterial pO_2 dropped in anesthetized mice on days 4 and 5 after influenza virus infection. ANOVA, $F(3/28)=10.546$, $p<0.001$. *$p<0.005$ (Newman-Keuls post-hoc test).
E, An O_2 concentration of 16% in the air decreased the arterial pO_2 to the level that was observed 5 days after influenza virus infection but had no effect on the infarct volume (n=8–9). *$p<0.05$ (t-test, n=4).
F, Telemetric measurement showed a slight drop in body temperature after influenza virus infection in mice with or without stroke (pMCAO). Mean temperatures are shown (n=5–7).

Figure 3. Influenza virus infection leads to an induction of cytokines in the ischemic brain.
A–F, Cytokine levels in lung, plasma, and brain after influenza virus infection and stroke. At 3 days after influenza virus infection pMCAO or sham surgery were performed and cytokine levels were determined 15 h later. *$p<0.05$ (Newman-Keuls post-hoc test, if ANOVA showed a significant difference between groups). We have only indicated significant differences between influenza virus infected and uninfected mice.

G, In primary mouse astrocytes OGD and RANTES (100 ng/ml) stimulated the release of MIP-2. ANOVA, $F(3/20)=5.960$, $p<0.005$. *$p<0.05$ (Newman-Keuls post-hoc test).
H, In brain endothelial bEnd.3 cells oxygen glucose deprivation (OGD) and RANTES (100 ng/ml) stimulated the release of MIP-2. ANOVA, $F(3/44)=5.513$, $p<0.005$. *$p<0.05$ (Newman-Keuls post-hoc test).

Figure 4. Influenza virus infection increases the infiltration of neutrophils, MMP-9 expression and the disruption of the blood-brain barrier in the ischemic area.
A, Immunohistochemistry showing increased neutrophil count in the ischemic area after influenza virus infection. *$p<0.05$ (t-test, n=4-5). Scale bar, 20 µm.
B, Increased MMP-9 expression in the ischemic area after influenza virus infection. *$p<0.05$ (t-test, n=5–6). Scale bar, 20 µm.
C, MMP-9 staining (red) is localized in neutrophils (green) and in vessel-like structures in the ischemic area after influenza virus infection. Right panel, scheme illustrating the localization of areas in which collagen IV and MMP-9 staining was quantified. Scale bar, 50 µm.
D, Reduced staining of collagen IV in the ischemic area after influenza virus infection. *$p<0.05$ (t-test, n=8-9). Scale bar, 20 µm.
E, Increased IgG extravasation in the ischemic area after influenza virus infection. *$p<0.05$ (t-test, n=8-12).

Figure 5. In influenza virus infected mice tPA treatment of stroke is afflicted with more hemorrhages. At 3 days after influenza virus infection stroke was induced with the tMCAO model.
A, The hemorrhage volume in the ischemic brain was elevated by tPA treatment in influenza virus infected mice. Hemoglobin content of the brain was measured by a spectrophotometric assay. ANOVA, $F(3/28)=5.797$, $p=0.003$. *$p<0.01$ (Newman-Keuls post-hoc test).
B, In influenza virus infected mice tPA treatment increased the size of hemorrhages into the ischemic brain. Upper panel, DAB-stained cryosections of intracerebral hemorrhages. Scale bar, 50 µm. Lower panel, hemorrhagic score. ANOVA, $F(3/28)=5.710$, $p=0.004$. *$p<0.05$ (Newman-Keuls post-hoc test).
C, Infarct volume in tPA-treated mice. ANOVA, $F(3/27)=6.890$, $p=0.001$. *$p<0.05$ (Newman-Keuls post-hoc test).

Figure 6. The α7nAchR agonist GTS-21 reduced cytokine expression and stroke volume after influenza virus infection.

A, GTS-21 improved cell viability in A549 cells after influenza infection. ANOVA, $F(3/44)=35.15$, $p<0.0001$. *$p<0.0001$ (Newman-Keuls post-hoc test).

B, GTS-21 blocked the RANTES release from influenza virus infected lung epithelial A549 cells. ANOVA, $F(3/16)=1354$, $p<0.0001$. *$p<0.0001$ compared to other influenza virus infected groups (Newman-Keuls post-hoc test).

C-F, Cytokine levels in plasma and brain after GTS-21 treatment (10 mg/kg i.p., immediately before and 6 h after surgery). At 3 days after influenza virus infection stroke was induced (pMCAO). Cytokine levels were measured 15 h after pMCAO. Cytokine levels are expressed relative to the value measured in vehicle-treated groups with the same infection and stroke status. *$p<0.05$ (t-test with Bonferroni correction for multiple testing).

G, Infarct volume in GTS-21 treated mice. GTS-21 (10 mg/kg) was administered before surgery and 6 h, 24 h, and 36 h after surgery. The infarct size was determined 48 h after pMCAO. ANOVA, $F(3/30)=19.18$, $p<0.0001$. *$p<0.0001$ (Newman-Keuls post-hoc test).

H, Survival in mice subjected to influenza virus infection and stroke was improved by GTS-21 treatment. GTS-21 (10 mg/kg) was administered before surgery and 6 h, 24 h, and 36 h after surgery. Chi square 15.18, $p<0.0001$ (log-rank test, 10 mice per group).

Supplementary Methods

Measurement of MMP-9 and TIMP-1

For the quantification of MMP-9 and TIMP-1 plasma levels, blood samples were obtained 24 h after tMCAO. ELISA was performed according to the manufacturers' instructions (MMP-9, Uscn Life Science Inc., Wuhan, Cat. No.: E0553Mu; TIMP-1, RayBiotech, Inc.; Cat. No.: ELM-TIMP1-001). To quantify TIMP-1 in the plasma, the samples were diluted 1:50.

Figure 1. Levels of G-CSF, IL-17, MIP-1β, and TNF in plasma, and brain after influenza virus infection and stroke. At 3 days after influenza virus infection pMCAO or sham surgery were performed and cytokine levels were determined 15 h later. *$p<0.05$ (Newman-Keuls post-hoc test, if ANOVA showed a significant difference between groups). Only significant differences between influenza virus infected and uninfected mice were indicated.

Figure 2. Levels of GM-CSF and INFγ in brain and HMGB1 in plasma after influenza virus infection and stroke. At 3 days after influenza virus infection pMCAO or sham surgery were performed and cytokine levels were determined 15 h later.

Figure 3. Plasma concentrations of MMP-9 and TIMP-1 in tPA-treated mice. At 3 days after influenza virus infection mice were subjected to tMCAO or sham surgery and were treated with tPA or vehicle. Plasma was sampled 24 h after tMCAO.

A, Plasma MMP-9 concentrations after tMCAO and tPA treatment were elevated in influenza-infected mice. ANOVA, $F(3/26)=15.082$, $p<0.001$, $^{*}p<0.001$. (Newman-Keuls post-hoc test).

B, Plasma TIMP-1 concentrations after tMCAO and tPA treatment were elevated in influenza-infected mice. ANOVA, $F(3/26)=6.071$, $p=0.003$. $^{*}p<0.01$ (Newman-Keuls post-hoc test).

Figure 4. Effect of GTS-21 on virus titer in A549 cells after influenza virus infection. Virus titers were not significantly affected by GTS-21. ANOVA, $F(3/16)=3.061$, $p=0.06$.

Figure 5. Cytokine levels in plasma and brain after GTS-21 treatment (10 mg/kg i.p., immediately before and 6 h after surgery). At 3 days after influenza virus infection stroke was induced (pMCAO). Cytokine levels were measured 15 h after pMCAO. Cytokine levels are expressed relative to the value measured in vehicle-treated groups with the same infection and stroke status.

Table

Table 1. Survival of mice after permanent MCAO (pMCAO) and transient MCAO (tMCAO).

*p<0.005 in comparison to uninfected mice (Fisher's exact test).

Survival after pMCAO (48 h)

Groups	**Number of mice [n]**	**Surviving mice [% (n)]**
Uninfected – pMCAO	40	87.5% (35)
Infected – pMCAO	50	78.0% (39)
Uninfected – GTS-21 – pMCAO	10	90.0% (9)
Infected – GTS-21 – pMCAO	10	90.0% (9)

Survival after pMCAO (15 h)

Groups	**Number of mice [n]**	**Surviving mice [% (n)]**
Uninfected - Sham	23	100.0% (23)
Infected - Sham	23	95.6% (22)
Uninfected - pMCAO	25	100.0% (25)
Infected - pMCAO	25	100.0% (25)
Uninfected – GTS-21 - Sham	6	100.0% (6)
Infected – GTS-21 - Sham	6	100.0% (6)
Uninfected – GTS-21 - pMCAO	6	100.0% (6)
Infected – GTS-21 - pMCAO	6	100.0% (6)

Survival after tMCAO (24 h)

Groups	Number of mice [n]	Surviving mice [% (n)]
Uninfected - tMCAO	20	80.0% (16)
- Vehicle	- 10	- 80% (8)
- tPA	- 10	- 80% (8)
Infected - tMCAO	41	39.0%* (16)
- Vehicle	- 18	- 44.4% (8)
- tPA	- 23	- 34.8% (8)

Table 2. Physiological parameters in influenza-infected mice and controls. There were no statistically significant differences between infected and control mice (n=7-8).

Parameter	Control mice		Influenza infected mice (day 3 post infection)		Influenza infected mice (day 4 post infection)		Influenza infected mice (day 5 post infection)	
	Before MCAO	After MCAO	Before MCAO	After MCAO	Before MCAO	After MCAO	Before MCAO	After MCAO
MABP (mm Hg)	75.9 ± 2.2	65.1 ± 2.6	76.5 ± 1.7	63.1 ± 2.1	76.1 ± 1.5	67.6 ± 2.3	74.9 ± 1.9	66.7 ± 3.6
pCO_2 (mm Hg)	58.1 ± 2.7	59.1 ± 2.5	57.9 ± 2.6	64.5 ± 2.2	58.0 ± 2.8	59.3 ± 4.2	55.8 ± 3.9	60.9 ± 3.2
pH	7.20 ± 0.00	7.16 ± 0.01	7.25 ± 0.02	7.19 ± 0.02	7.24 ± 0.01	7.18 ± 0.03	7.30 ± 0.01	7.22 ± 0.02
Drop in Doppler signal (%)		72.9 ± 1.7		74.4 ± 2.8		72.8 ± 4.8		74.1 ± 3.4

Figures

Figure 1

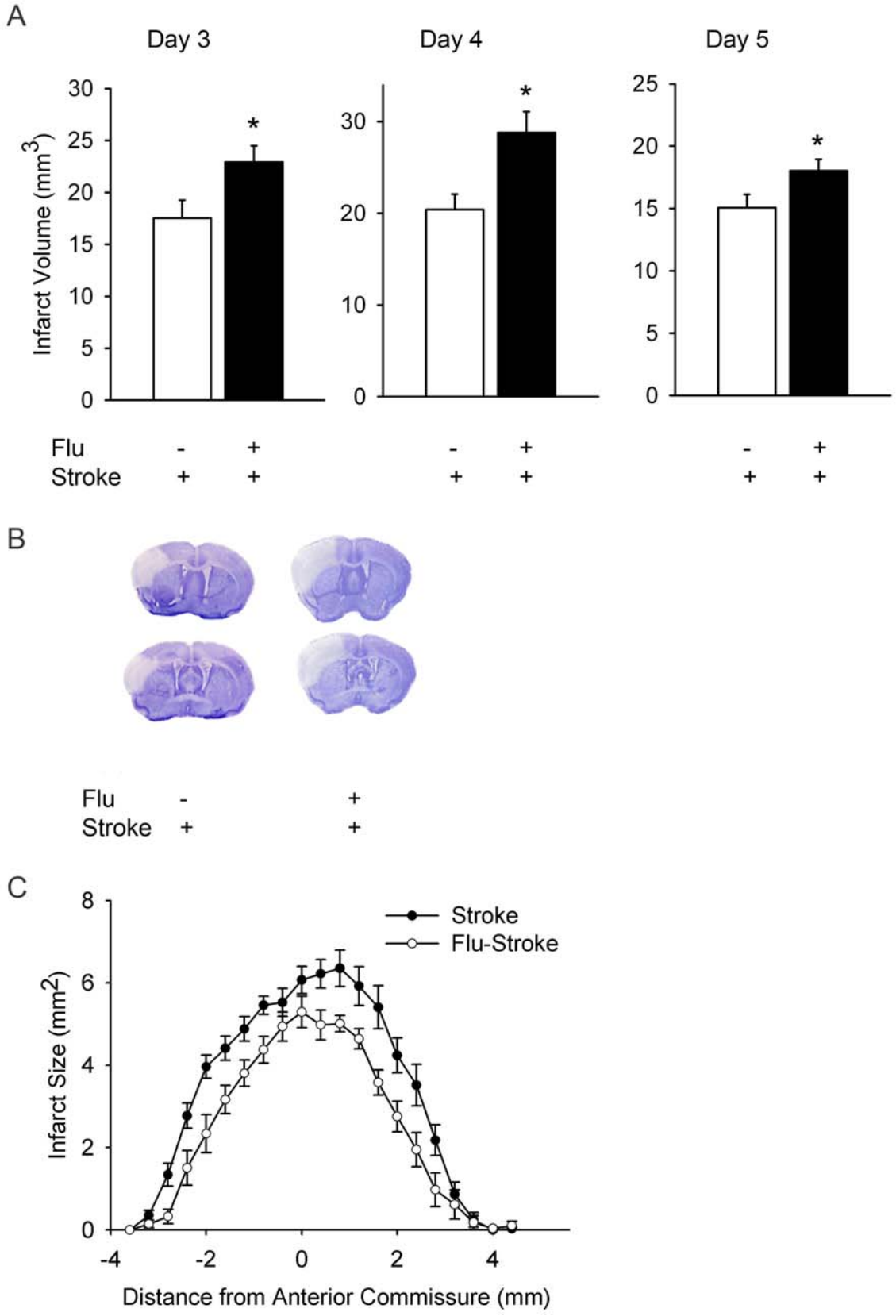

Figure 2

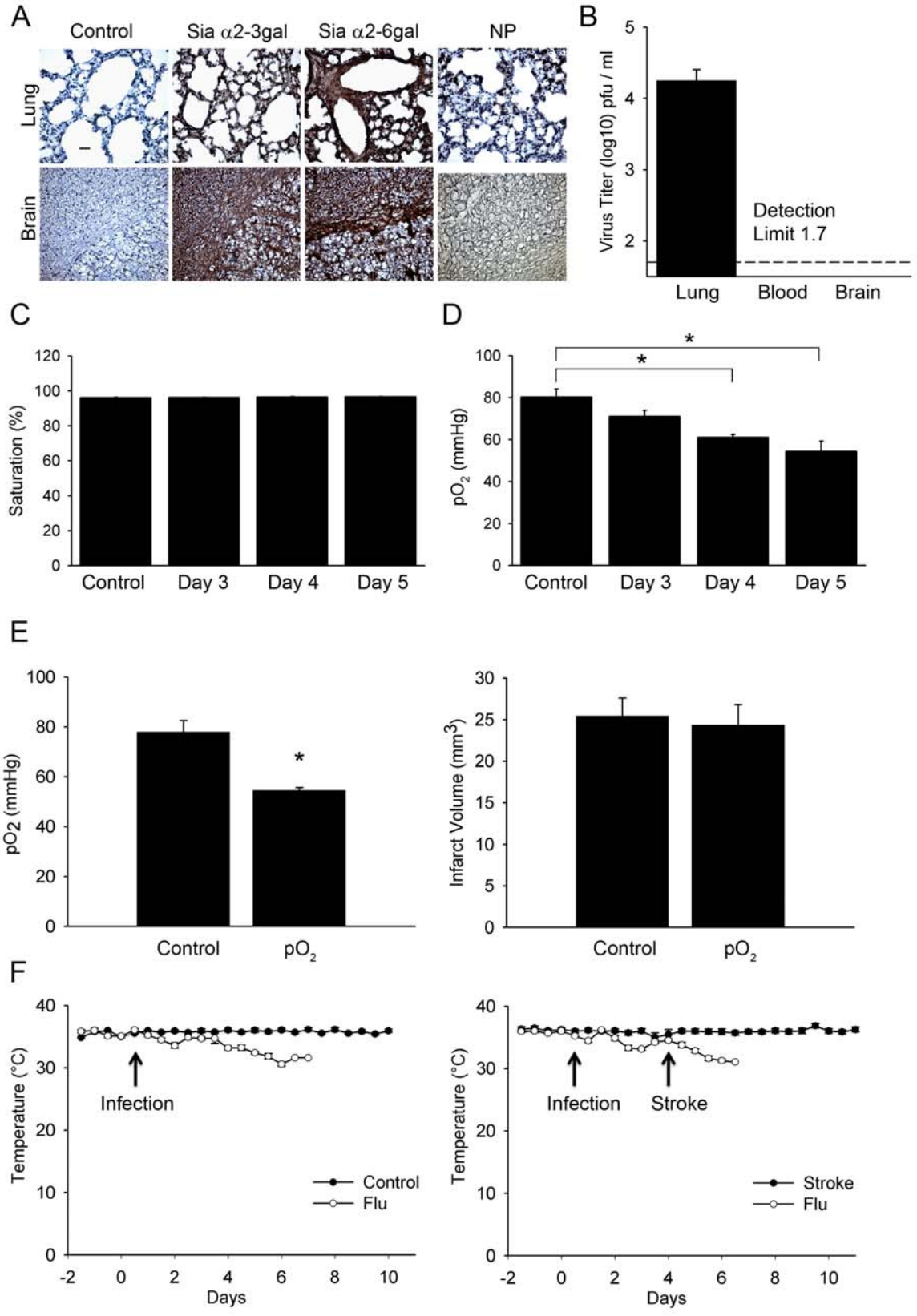
A
Control
Sia α2-3gal
Sia α2-6gal
NP
Lung
Brain
B
Virus Titer (log10) pfu / ml
Detection Limit 1.7
Lung
Blood
Brain
C
Saturation (%)
Control
Day 3
Day 4
Day 5
D
pO2 (mmHg)
Control
Day 3
Day 4
Day 5
E
pO2 (mmHg)
Control
pO2
Infarct Volume (mm3)
Control
pO2
F
Temperature (°C)
Infection
Control
Flu
Days
Temperature (°C)
Infection
Stroke
Stroke
Flu
Days

Figure 3

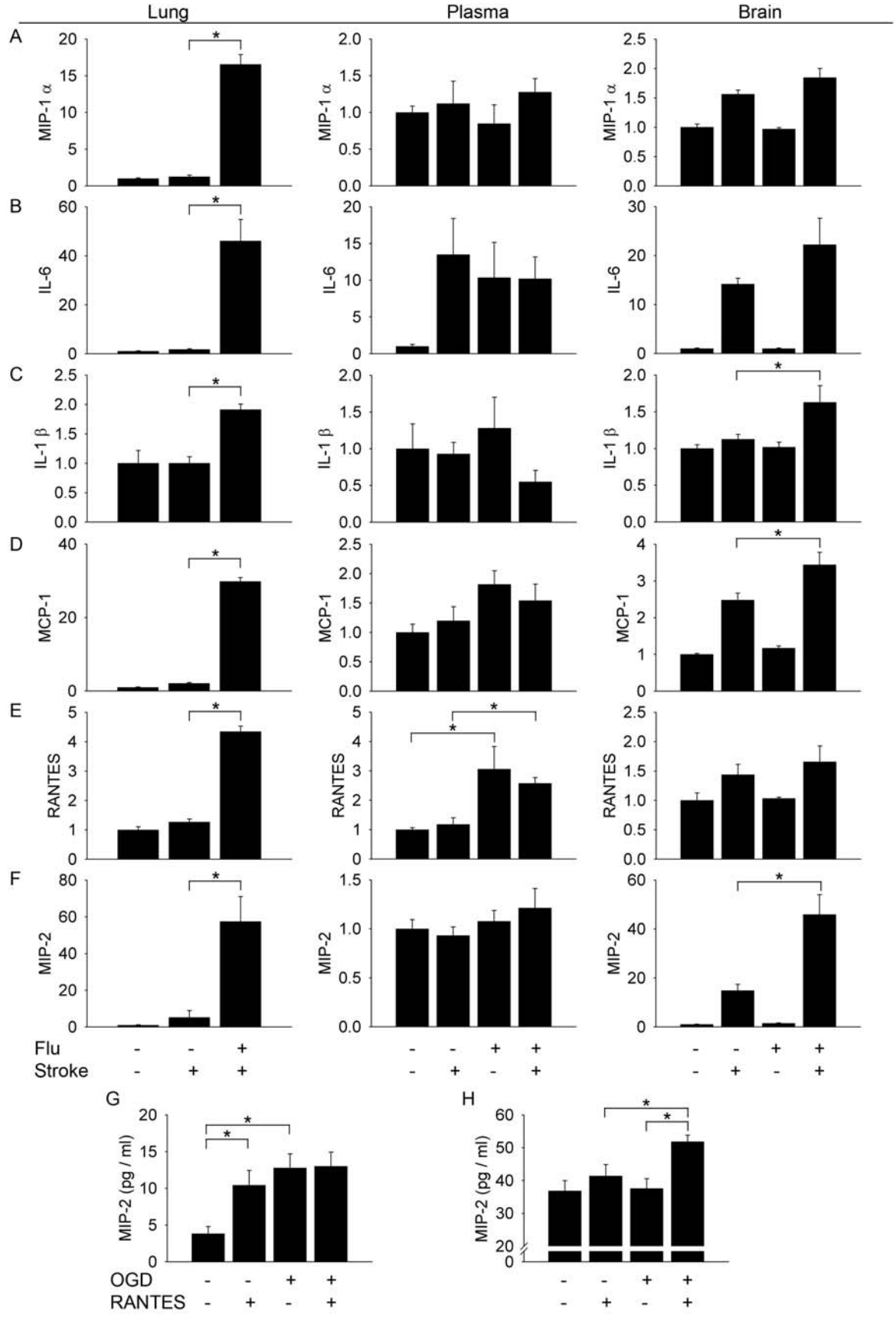
Lung
Plasma
Brain
A
MIP-1 α
B
IL-6
C
IL-1 β
D
MCP-1
E
RANTES
F
MIP-2
Flu
Stroke
G
MIP-2 (pg / ml)
OGD
RANTES
H
MIP-2 (pg / ml)

Figure 4

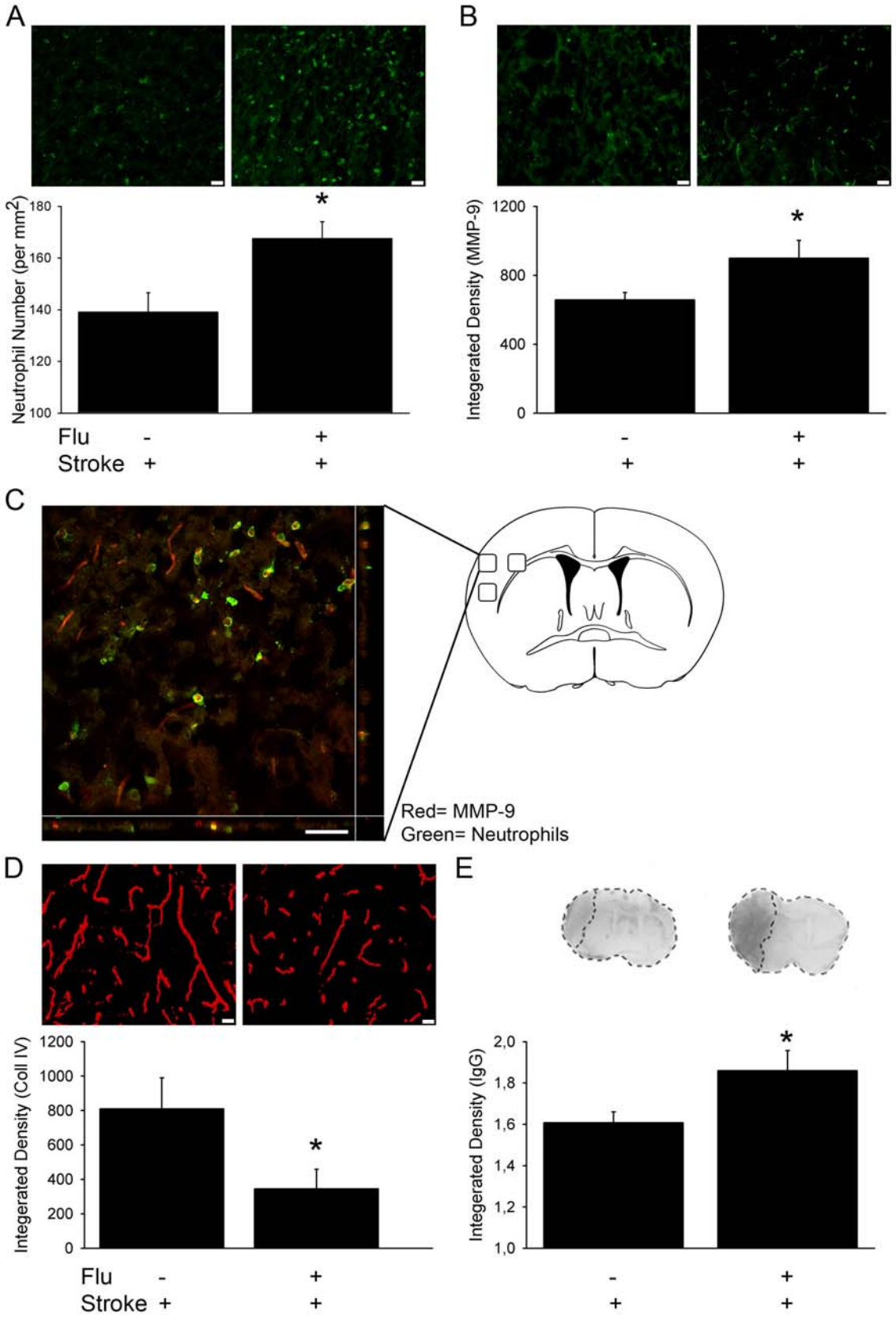
A
B
Neutrophil Number (per mm2)
180
160
140
120
100
*
Integerated Density (MMP-9)
1200
800
400
0
*
Flu - +
Stroke + +
- +
+ +
C
Red= MMP-9
Green= Neutrophils
D
E
Integerated Density (Coll IV)
1200
1000
800
600
400
200
0
*
Integerated Density (IgG)
2,0
1,8
1,6
1,4
1,2
1,0
*
Flu - +
Stroke + +
- +
+ +

Figure 5

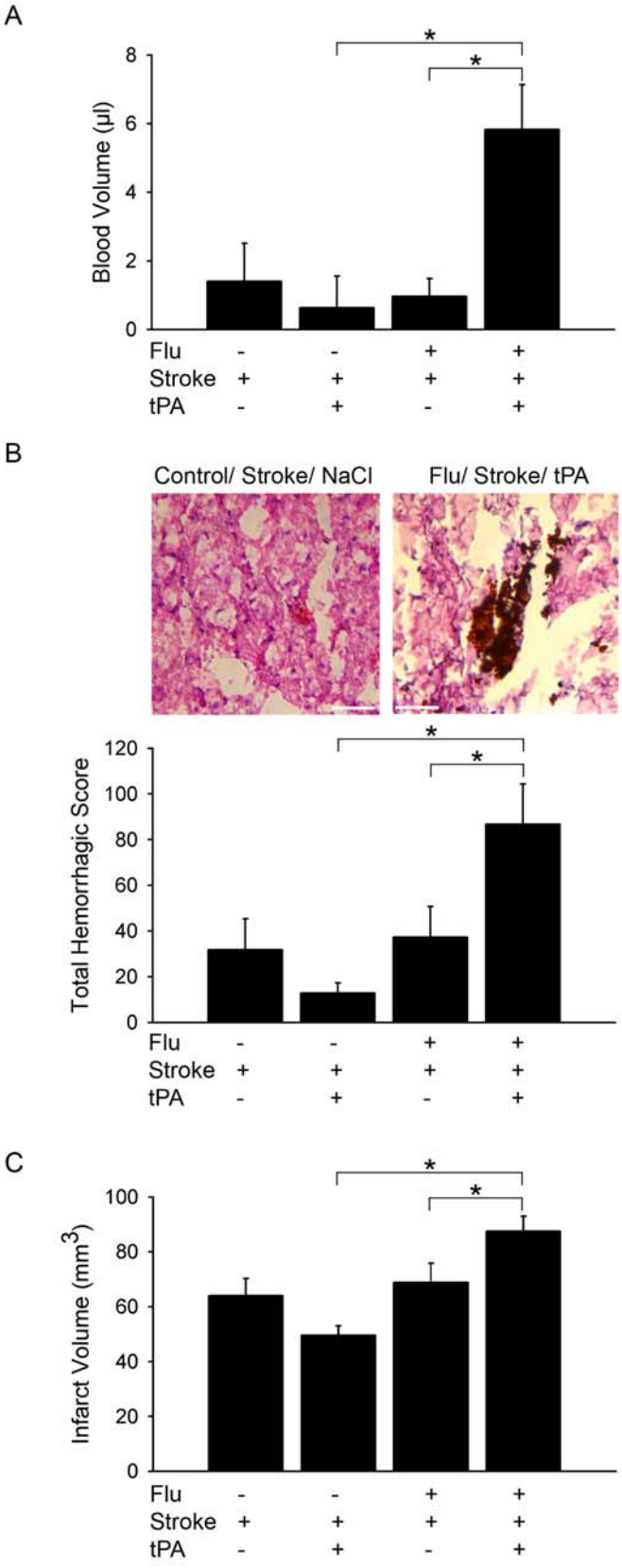
A
Blood Volume (µl)
0
2
4
6
8
*
*
Flu - - + +
Stroke + + + +
tPA - + - +
B
Control/ Stroke/ NaCl
Flu/ Stroke/ tPA
Total Hemorrhagic Score
0
20
40
60
80
100
120
*
*
Flu - - + +
Stroke + + + +
tPA - + - +
C
Infarct Volume (mm3)
0
20
40
60
80
100
*
*
Flu - - + +
Stroke + + + +
tPA - + - +

Figure 6

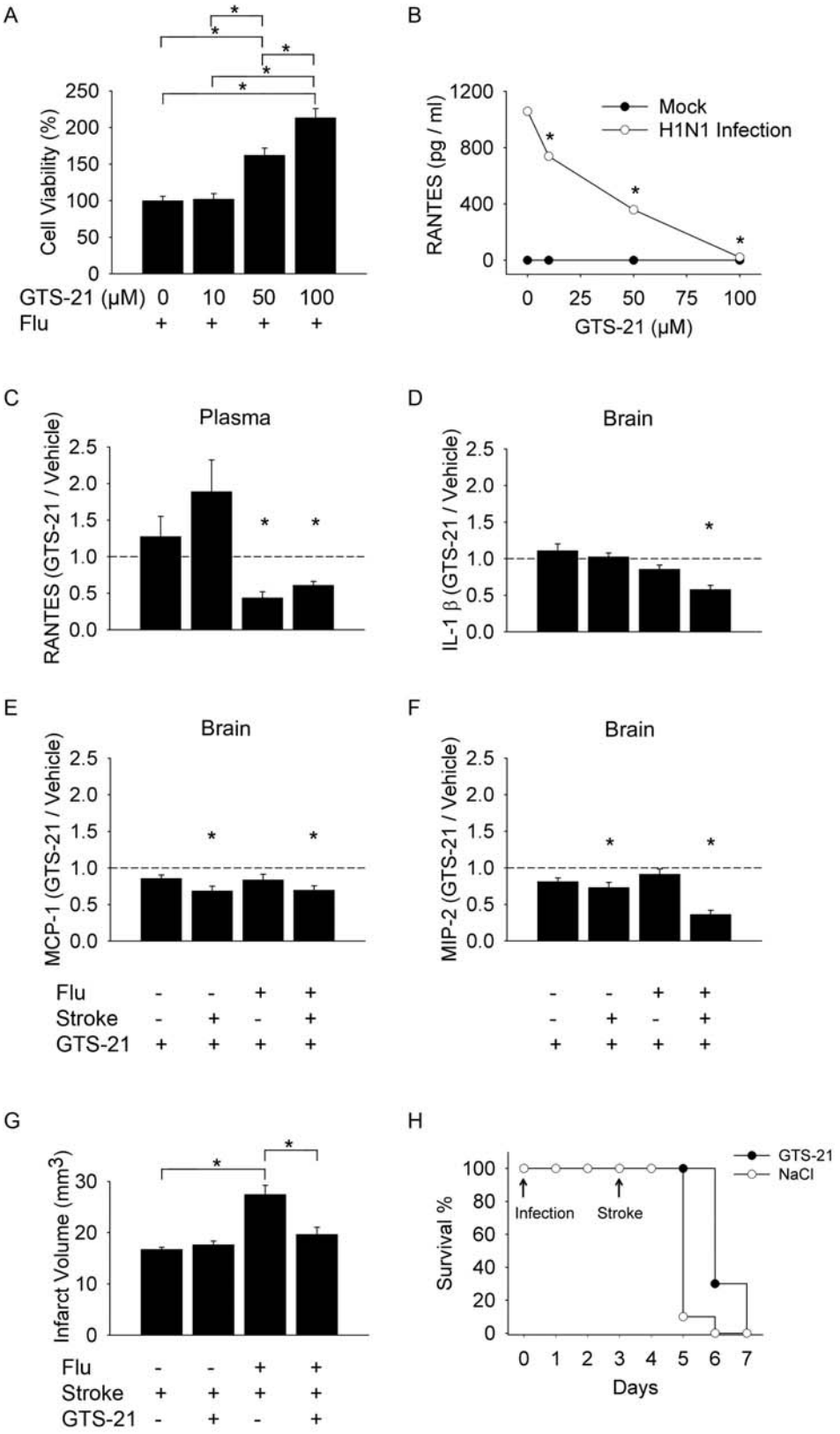
A
Cell Viability (%)
250
200
150
100
50
0
GTS-21 (μM) 0 10 50 100
Flu + + + +
B
RANTES (pg / ml)
1200
800
400
0
Mock
H1N1 Infection
0 25 50 75 100
GTS-21 (μM)
C
Plasma
RANTES (GTS-21 / Vehicle)
2.5
2.0
1.5
1.0
0.5
0.0
D
Brain
IL-1 β (GTS-21 / Vehicle)
E
Brain
MCP-1 (GTS-21 / Vehicle)
Flu - - + +
Stroke - + - +
GTS-21 + + + +
F
Brain
MIP-2 (GTS-21 / Vehicle)
G
Infarct Volume (mm3)
30
20
10
0
Flu - - + +
Stroke + + + +
GTS-21 - + - +
H
Survival %
100
80
60
40
20
0
GTS-21
NaCl
Infection
Stroke
0 1 2 3 4 5 6 7
Days

Supplementary figure 1

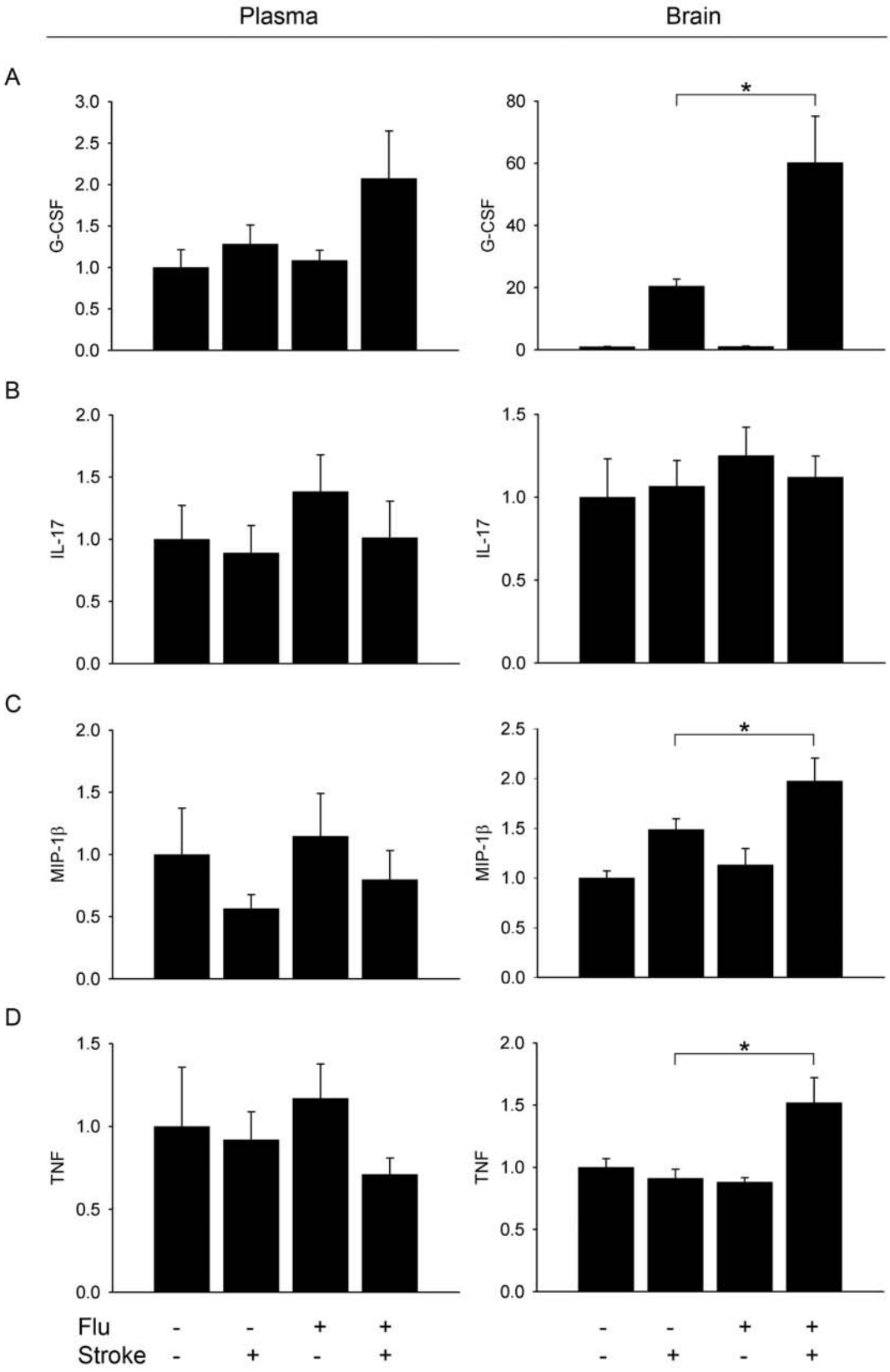

Supplementary figure 2

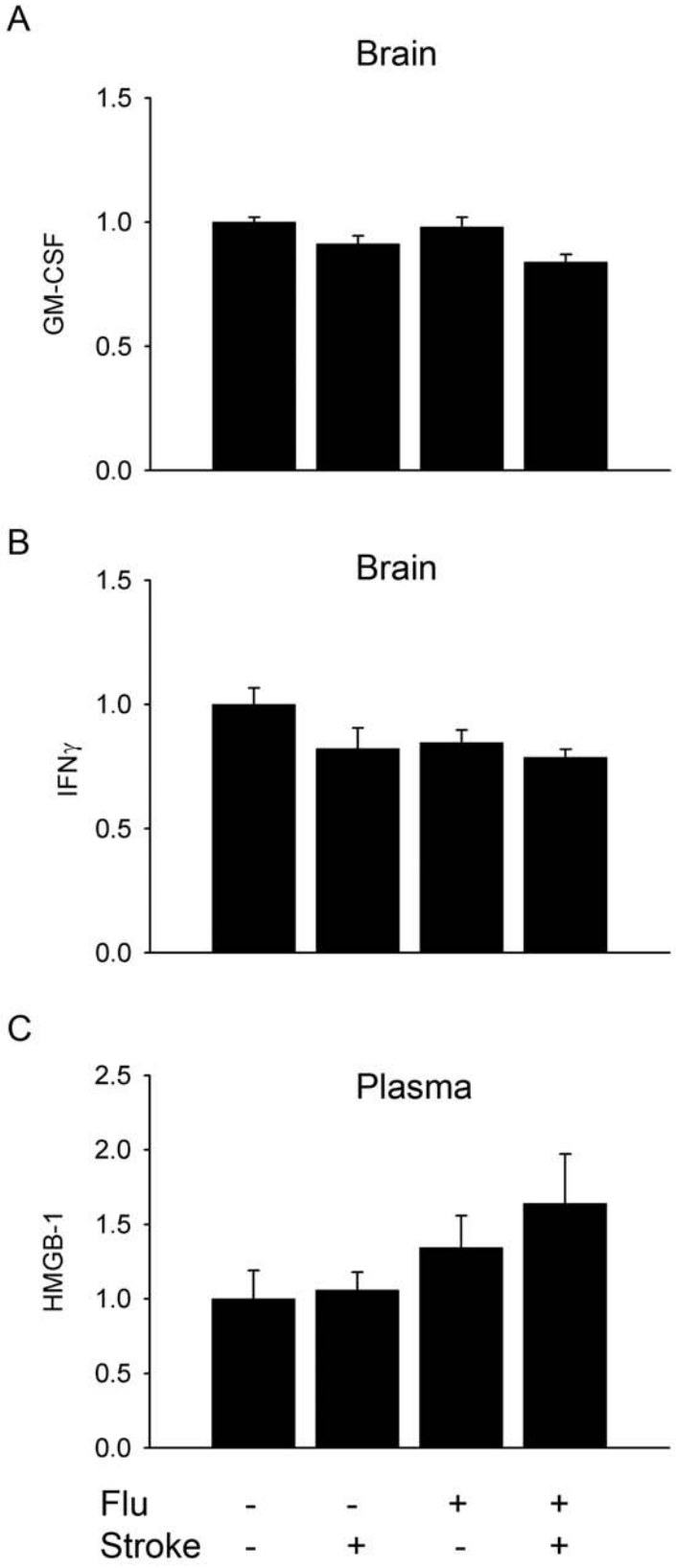

Supplementary figure 3

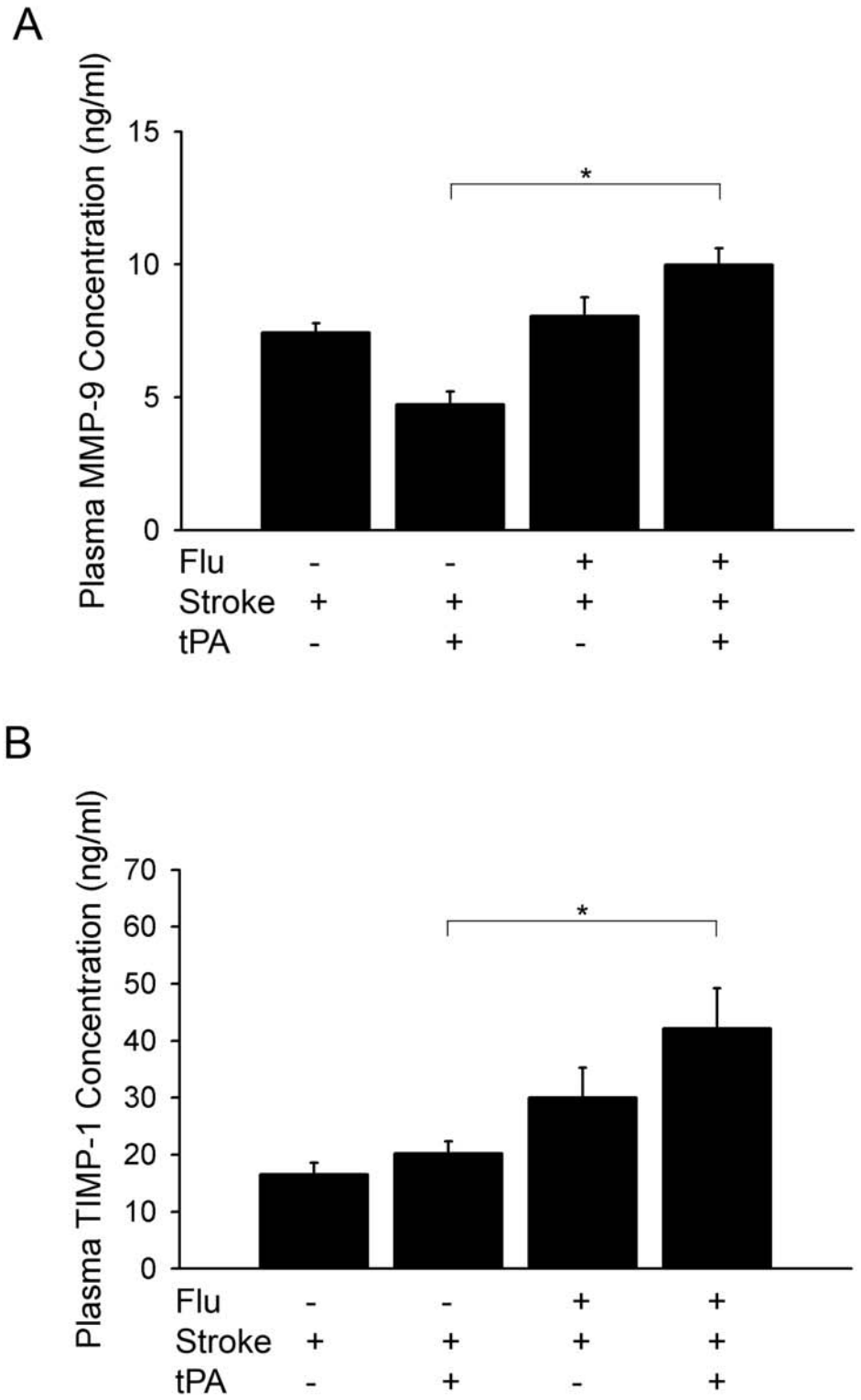

Supplementary figure 4

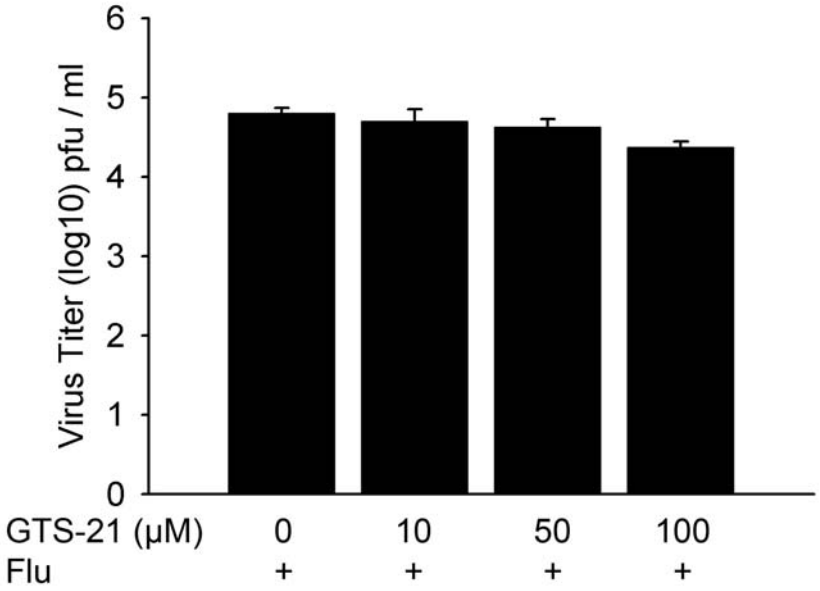

Supplementary figure 5

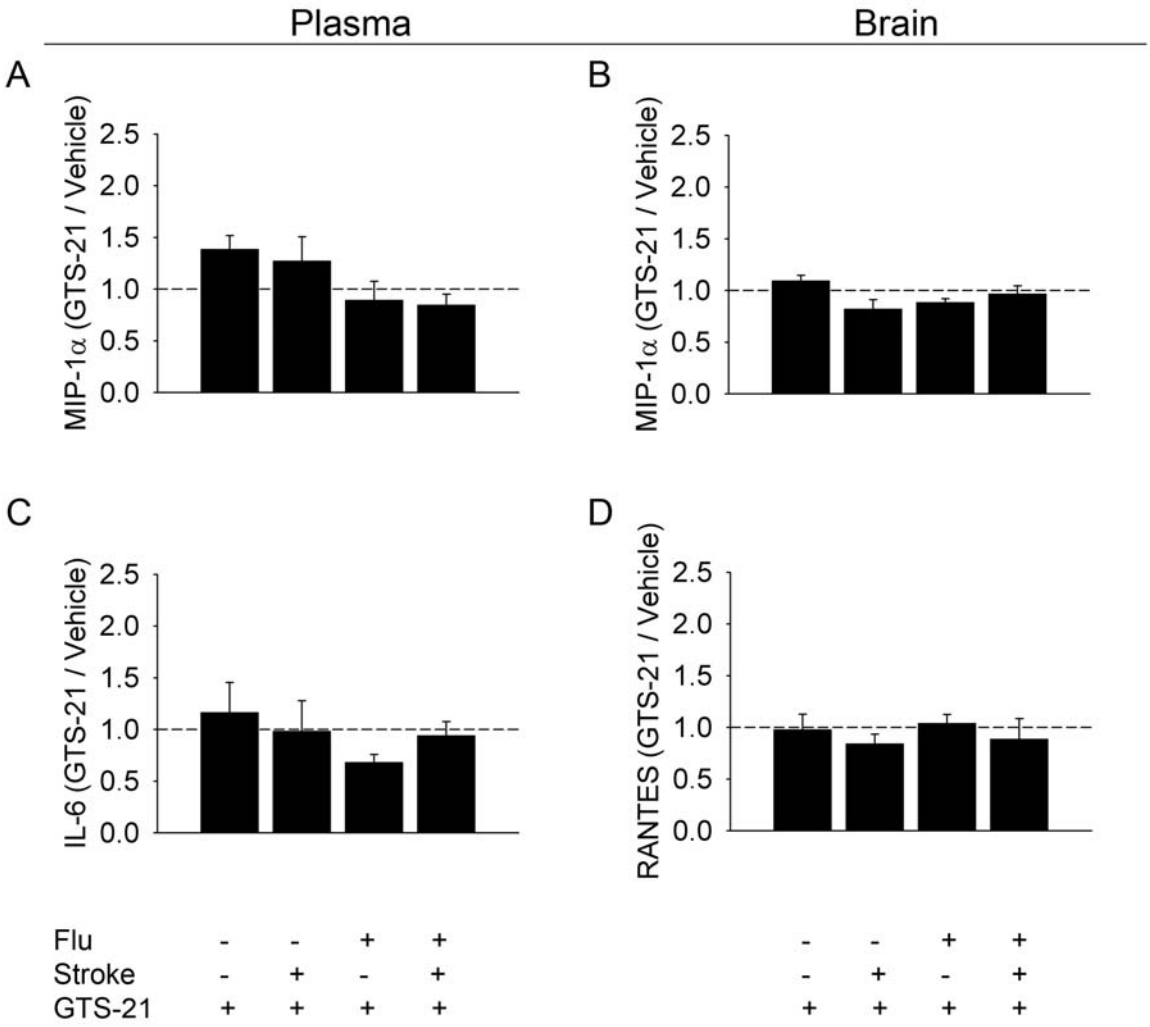

PUBLICATION #4:

Antibodies and CD4$^+$ T-cells mediate cross-protection against H5N1 influenza virus infection in mice after vaccination with a low pathogenic H5N2 strain

Karoline Droebner[1], Emanuel Haasbach[1], Cordula Fuchs[2], Andreas O. Weinzierl[3], Stefan Stevanovic[3], Mathias Büttner[2] and Oliver Planz[1,#]

[1)] Friedrich-Loeffler-Institut, Institute of Immunology, Paul-Ehrlich Str. 28, D-72076 Tübingen, Germany [2)] Bavarian Health and Food Safety Authority, Veterinaerstr. 2, D-85764 Oberschleissheim, Germany 3) Interfacultary Institute for Cell Biology, Department of Immunology, Auf der Morgenstelle 15 D-72076 Tübingen, Germany

[#] Corresponding author: Friedrich-Loeffler-Institut; Institute of Immunology
Federal Research Institute for Animals Health,
Paul-Ehrlich Str. 28
D-72076 Tübingen, Germany
Tel: +49 7071 967 230
Fax: +49 7071 967 105
E-mail: oliver.planz@fli.bund.de

Keywords: cross-protection, H5N1 influenza virus, vaccine strategy

Abstract

A H5N2 low pathogenic avian influenza virus (LPAIV) was isolated from a natural reservoir in Bavaria during a routine screen and was used as a vaccine strain to scrutinize the immune response involved in cross-protection after challenge infection with a H5N1 highly pathogenic avian influenza virus (HPAIV). The challenge virus was also isolated from a natural reservoir in Bavaria. Wild type, antibody deficient (μMT), $CD4^{-/-}$ and $CD8^{-/-}$ mice were infected with the apathogenic H5N2 vaccine strain and challenge infection with a 100-fold MLD_{50} of the H5N1 strain was performed 80 days later. While 100% of the wild type and 100% of the $CD8^{-/-}$ mice stayed healthy, only 50% of the $CD4^{-/-}$ and none of the antibody deficient mice were protected. These results support the view that the humoral immune response and to certain extends the $CD4^{+}$ T helper cells are a prerequisite for cross-protective immunity against H5 influenza virus.

1. Introduction

Unlike the common seasonal influenza A viruses, infection with H5N1 influenza viruses cause severe pathology with high lethality. A sporadic human-to-human transmission of H5N1 viruses is suspected, but not finally proven. Nevertheless, H5N1 continually mutates. Through multiple mutations, which might lead to effective transmission between humans, the virus could acquire the ability to cause a new pandemic [1,2].

Vaccination is the most efficient method for preventing influenza and its severe complications. However, antigenic drift has a major impact on the vaccine effectiveness. Therefore, there is an urgent need for new vaccines that protect against seasonal and in addition potentially pandemic influenza virus strains. Various vaccine approaches are currently under investigation [3]. The ultimate goal is developing a universal influenza vaccine that can also protect against possible pandemic strains like the lethal avian influenza virus A/H5N1. The viral surface proteins hemagglutinin (HA) and neuraminidase (NA) are highly antigenic but also undergo antigenic drift. In order to create a universal vaccine the use of genetically conserved influenza virus antigens as immunogens like M2 and NP is investigated [4-6].

However, at present the development of a universal influenza vaccine remains at a preclinical or clinical phase. Therefore conventional vaccines with a strong focus on cross-protective immunity are the first choice for prophylactic intervention. Different approaches using either inactivated influenza vaccines (IIV) or live-attenuated vaccines (LAIV) were successful in inducing cross-protective immunity in various animal models [7-9]. Furthermore, LAIV's are able to induce cross-protective immunity in healthy adults and children against mutated influenza virus strains [10]. It is under discussion whether broad protection that has been observed using LAIV is due to antibodies against the M2 protein. Moreover, it has also been suggested that the cellular immune response and the mucosal immune response may be involved in protection. Although innate immune reactions play a decisive role, recovery from primary influenza virus infection requires adaptive immunity, but the relative importance of the humoral and the cellular immune mechanisms is controversial [11,12]. Beside reports indicating that the influenza virus specific IgG response is $CD4^+$ T-cell dependent there are also investigations describing $CD4^+$ T-cell independent antibody responses [13]. The cytotoxic T-cell (CTL) response is mainly directed against the M and NP proteins [14]. There are some reports indicating that CTL does not seem to contribute significantly in preventing infection [15,16]. In contrast other investigations point out that a CTL response in addition to

strong antibody formation will be more effective in preventing disease when hetero-subtype cross-protection is demanded [17-19]. Taken together, the puzzle of immunological mechanisms that can lead to robust heterosubtype specific immunity after influenza vaccination is not completely understood.

In the present study, we wanted to scrutinize the role of the humoral and cellular immunity in cross-protection after vaccination with a non-pathogenic H5N2 virus from a naturally infected wild bird. Challenge infection was performed with a lethal dose of a H5N1 highly pathogenic avian influenza virus. Vaccination of wild type and $CD8^+$ T-cell deficient mice was protective against H5N1 lethal infection, whereas vaccination of antibody deficient mice and $CD4^+$ T-cell deficient mice failed to protect against H5N1 infection.

2. Material and Methods

2.1. Mice

Inbred female C57Bl/6, μMT and CD8 knockout mice on a C57Bl/6 background, sv129 and CD4 knockout mice on a sv129 background at the age of 6-8 weeks were obtained from the animal breeding facilities at the Friedrich-Loeffler-Institut, Federal Research Institute for Animal Health, Tübingen, Germany and were used throughout all the experiments.

2.2. Virus

Avian influenza A/mallard/Bavaria/1/2005 (H5N2) (DB1, gene bank acc. No. see table 1) virus grown on Madin-Darby canine kidney (MDCK) cells and A/mallard/Bavaria/1/2006 (H5N1) (MB1, gene bank acc. No. see table 1) virus, grown in embryonated chicken eggs were used throughout this study. Both isolates of the avian influenza A virus were originally obtained from the Bavarian Health and Food Safety Authority, Oberschleissheim, Germany and further propagated at the Friedrich-Loeffler-Institut, Federal Research Institute for Animal Health, Tübingen, Germany.

2.3. *In vitro* infection

MDCK cells were grown in minimal-essential medium (MEM) supplemented with 10% heat-inactivated fetal calf serum (FCS) and antibiotics (100U/ml penicillin and 0.1mg/ml streptomycin). For infection cells were grown overnight in 24 well plates ($8x10^4$ cells/well). Immediately before infection the cells were washed with PBS and subsequently incubated with either MB1 or DB1 virus at a multiplicity of infection (MOI) of 0.001 diluted in PBS/BA (0.2% BA) supplemented with 1mM $MgCl_2$, 0.9mM $CaCl_2$, penicillin and streptomycin for 30 min at 37°C. After 30 min incubation period the inoculum was aspirated and cells were incubated with 1ml MEM containing 0.2% BA, 200U/ml penicillin and 0.2mg/ml streptomycin. For the infection with DB1 1.2μl/ml trypsin was added to the medium. At the given time points (8, 24, 32 and 48 hr past infection) supernatants were collected.

2.4. Infection of mice

For infection of mice, the animals were anaesthetized by intraperitoneal injection of 150μl of a ketamine (Sanofi)/rompun (Bayer) solution (equal amounts of a 2%-rompun-solution and a 10%-ketamin-solution were mixed at the rate of 1:10 with PBS) and infected i.n. with $2x10^3$ pfu/50μl DB1 (H5N2) or $2x10^3$ pfu/50μl MB1 (H5N1). Virus challenge experiments were

performed with $2x10^2$ pfu/50µl DB1 and $2x10^5$ pfu/50µl MB1 (100-fold MLD_{50}). According to the German animal-protection law, the mice were sacrificed as soon as they lost 25-30% of their weight. All animals were monitored for 14 days after infection.

2.5. Influenza virus titration (AVICEL® plaque assay)

To assess the number of infectious particles (plaque titers) in organs and cell culture supernatants a plaque assay using Avicel® was performed in 96-well plates as described by Mastrosovich and colleagues [20]. Virus-infected cells were immunostained by incubating for 1 hr with a monoclonal antibody specific for the influenza A virus nucleoprotein (Serotec) followed by 30 min incubation with peroxidase-labeled anti-mouse antibody (DIANOVA) and 10 min incubation True Blue™ peroxidase substrate (KPL). Stained plates were scanned on a flat bed scanner and the data were acquired by Microsoft®Paint software. The virus titer is given as the logarithm to the basis 10 of the mean value. The detection limit for this test was < 1.7 log10 pfu/ml.

2.6. Hemagglutination inhibition assay

Hemagglutination inhibition assays were carried out in V-bottomed microtiter plates using 50µl of 2.5% suspensions of chicken red blood cells in PBS. Fresh chicken blood was supplemented with 1.6% sodium citrate in sterile H_2O and was centrifuged at 800x g for 10 min at room temperature to separate red blood cells. Thereafter, the cells were washed three times with PBS. Hundred microliter of serum from infected mice was added and serially diluted in PBS, then 50µl of a 1:64 virus dilution ($5x10^5$ pfu/well) was added to the serum. The plate was incubated for 1 hr at 37°C and 5% CO_2. After the incubation period 50µl of chicken erythrocytes were added to the wells. Assays were analysed following 1 hr incubation on ice.

An inhibition of the hemagglutination was indicated, when red blood cells precipitated to the bottom of the plate, while red blood cells incubated with influenza virus or non reactive serum showed a diffuse distribution on the microtiter plates. The results were given as reciprocal of the highest dilution causing detectable inhibition of hemagglutination.

2.7. Statistical analysis

For investigation of the significance of the data, statistical analysis was performed by using the Kaplan-Meier survival analysis and the Cox regression test from WinStat®.

2.7. Neutralisation assay

Fifty µl of influenza virus (DB1 or MB1) were pre-incubated for 30 min at room temperature with 50µl of a serum pool of three mice. Sera from uninfected, DB1 infected (14 days p.i.) and challenged mice (14 days past MB1 infection), were used for this test. For control virus was incubated with PBS. The numbers of infectious particles (plaque titers) were assessed using the Avicel® plaque assay described above.

2.8. Flow Cytometry.

Naive C57Bl/6, µMT and $CD4^{-/-}$ mice or DB1 (H5N2) pre-challenged C57Bl/6, µMT and $CD4^{-/-}$ mice (80 days p.i.), were infected with $2x10^3$ pfu of MB1 (H5N1) virus. Mice were sacrificed at the indicated times after infection, and tissues were removed and mechanically disrupted by passage through a 70µm cell strainer (BD Falcon). Cells ($1x10^6$ cells per sample) were stained with monoclonal antibody to CD8a (clone 53-6.7, BD Bioscience) and MHC class I tetramers ($H\text{-}2D^b$). The MHC class I tetramers containing nucleoprotein (NP) 366–374 peptide predicted for MB1 (ASNENMEAM) or DB1 (ASNENMETM) were used to identify influenza-specific T-cells. Before FACS analysis, erythrocytes were lysed and cells were fixed with FACS lysing solution (BD Bioscience). Flow cytometry was performed on a dual laser FACSCalibur and analysed with Cell Quest software (BD Biosciences).

3. Results

3.1. DB1 (H5N2) and MB1 (H5N1) showed similar virus growth properties *in vitro*

Vaccines based on live attenuated low pathogenic avian influenza viruses (LPAIV) might be promising candidates for effective protection against H5N1 influenza A virus infections. In order to estimate, whether the LPAIV A/mallard/Bavaria/1/2005 (DB1; H5N2) and highly pathogenic avian influenza virus (HPAIV) A/mallard/Bavaria/1/2006 (MB1; H5N1), both isolated from naturally infected wild birds replicate in mammalian cell culture without adaptation *in vitro,* infectivity studies were performed to analyse the amount of progeny virus. MDCK cells that are highly permissive for influenza virus infection were used for infection with DB1 or MB1 viruses at a MOI of 0.001. To determine the amount of progeny virus cell culture supernatants from either DB1 or MB1 infected MDCK cells were collected 8, 24, 36 and 48 hours after infection. Already eight hours p.i., DB1 ($3.2x10^2$ pfu/ml) but not MB1 was detectable in the cell culture supernatant (Fig. 1A). At the later time points both viruses showed similar growth curves whereas MB1 replicated to higher titer. Both viruses reached the maximum titer at 32 hours p.i. (MB1 $9.3x10^7$ pfu/ml; DB1 $4.3x10^6$ pfu/ml). Thereafter, the amount of progeny virus declined in the cell culture supernatant (Fig. 1A). However, infection with DB1 only resulted in progeny virus production, when trypsin was present in the culture medium. In contrast, infection of MDCK cells with MB1 led to virus production in absence of trypsin and yielded similar titers in five consecutive passages. The sequence analyses of both hemagglutinins (HA) revealed a monobasic cleavage site for DB1 HA, while a multibasic cleavage site was found in the HA of MB1 (Fig. 1B).

3.2. Immunocompetent and immunodeficient mice were susceptible to DB1 or MB1 infection

In vitro infection with DB1 and MB1 led to progeny virus production in MDCK cells. We next questioned whether infection of mice with DB1 or MB1 would result in productive virus infection and in manifestation of disease. For *in vivo* studies in mice with either DB1 or MB1 the mouse lethal dose 50% (MLD_{50}) for both influenza virus subtypes was determined. The MLD_{50} for the highly pathogenic H5N1 isolate MB1 in C57Bl/6 mice was $2x10^3$ pfu (Table 1). Using this dose for intranasal infection (i.n.) all mice lost weight and developed clinical symptoms like ruffled fur. A general reduction of their normal activity rate starting 6 days after infection was found (Fig. 2A, open triangle). Lethality in this group was 40%, 2 out of 5 animals died (Fig. 2B, open triangles). Interestingly, mice infected with the low pathogenic H5N2 isolate DB1 neither lost weight (Fig. 2A, black squares) nor developed any apparent

symptoms even at an infectious dose of $5x10^5$ pfu (Table 1). Furthermore, none of the DB1 infected mice died (Fig. 2B, black squares).

Since immunocompetent C57Bl/6 wild type mice showed no symptoms of disease after infection with DB1, we raised the question whether mice that lack an antibody response (μMT) or $CD8^+$ T-cell deficient mice, would also be able to control DB1 infection without clinical symptoms such as immunocompetent mice. Five female wild type, μMT and $CD8^{-/-}$ mice were either infected i.n. with $2x10^3$ pfu DB1 or MB1 virus. The animals were weighted daily and the health status was monitored twice a day.

Infection of μMT mice with DB1 did not result in reduction of the body weight. All of the DB1 infected μMT mice gained weight during the 14 days observation period (Fig. 2C, black squares). None of the infected animals developed signs of disease or even died spontaneously (Fig. 2D, black squares). Infection of μMT mice with the highly pathogenic MB1 virus was accompanied by weight loss and appearance of disease symptoms starting by day 5 p.i. (Fig. 2C, open triangles). The severity of disease symptoms increased until day 8 after infection. By day 10 p.i., 4 out of 5 (80%) of the infected μMT mice died, demonstrating an increased susceptibility to the infection (Fig. 2D, open triangles).

Infection of $CD8^+$ T-cell deficient mice with DB1 did not result in weight loss and the occurrence of clinical symptoms during the infection period (Fig. 2E, black squares) and none of the animals died after the infection (Fig. 2F, black squares). In contrast, after infection with MB1 all $CD8^{-/-}$ mice lost weight and developed disease symptoms (Fig. 2E, open triangles). The first clinical symptoms like ruffled fur, an unnatural posture and a general reduction of the normal activity rates were observed 6 days past infection in this group of animals. Ten days p.i. 3 out of 5 mice died (60%) while the other mice survived infection, recovered from clinical symptoms and regained weight (Fig. 2F, open triangles).

Taken together, the infection experiments revealed an increased susceptibility to the influenza A virus infection with the highly pathogenic MB1 in antibody deficient mice (μMT) and in mice lacking $CD8^+$ T-cells, whereas infection with DB1 showed no pathogenic effects nor changes in behaviour of these mice in direct comparison to infection of wild type mice.

3.3. DB1 infection was restricted to the respiratory tract

Because DB1 infected animals did not develop disease symptoms, the question raised whether DB1 infection is productive in mice and whether infectious virus would be found in various organs. To determine whether productive virus was detectable after infection with low pathogenic DB1, we decided to examine the organs of infected animals to assess the virus

dissemination and the viral tropism in wild type, μMT and $CD8^{-/-}$ mice. Five female mice from each strain were either infected with $2x10^3$ pfu DB1 or MB1. Six days after infection all mice were sacrificed and virus titration from suspensions of different organs was performed as described in material and methods. High viral titers were detected in the lungs of C57Bl/6, μMT and $CD8^{-/-}$ mice six days after DB1 infection, indicating efficient replication without causing any clinical symptoms. C57Bl/6 and μMT mice showed almost the same viral titers in the lungs with 4.9 ± 0.5 log10 pfu/ml or 4.8 ± 0.4 log10 pfu/ml, respectively. In $CD8^{-/-}$ mice DB1 virus titer was slightly increased in the lungs (5.2 ± 0.5 log10 pfu/ml, Table 2). This experiment clearly demonstrated that DB1 efficiently replicated in the lungs of mice, without causing any apparent clinical symptoms.

MB1 virus was detected in the lungs of C57Bl/6 mice showing high titers (4.9 ± 0.3 log10 pfu/ml). A high viral titer was also found in the blood (4.0 ± 0.3 log10 pfu/ml) of infected animals. Interestingly, in addition to its presence in the lungs and blood, MB1 virus was also found to lower extends in livers (2.7 ± 0.3 log10 pfu/ml) and spleens (2.6 ± 0.3 log10 pfu/ml) of wild type mice (Table 3). In contrast, infectious virus was detected only in the lung (5.1 ± 0.2 log10 pfu/ml) and in the blood (3.4 ± 0.3 log10 pfu/ml) of MB1 infected $CD8^{-/-}$ mice. The amount of infectious virus in those animals was not significantly higher when compared to the amount of MB1 detected in the lungs and blood of wild type mice. While the viral load in the lungs of μMT mice (4.9 ± 0.2 log10 pfu/ml) was identical to wild type mice, no virus was detected in the livers, blood or spleens of antibody deficient mice. Interestingly, MB1 virus was detected in the brain of μMT mice (3.3 ± 0.2 log10 pfu/ml) (Table 3). Until now we can not explain the absent viral tropism in spleen and liver of μMT mice. To confirm this observation, this experiment was performed three times with an overall amount of 22 mice per strain. All experiments showed similar results.

3.4. Vaccination of wild type C57Bl/6 mice with DB1

Intranasal infection with DB1 did not lead to any apparent clinical symptoms but virus replicated in the lungs of infected mice. Therefore, we questioned whether infection of mice with a LPAIV from a natural reservoir would lead to solid immunity against a challenge infection with a highly pathogenic H5N1 influenza A virus. Thus, six wild type mice were infected with $2x10^2$ pfu DB1. As demonstrated before, neither clinical symptoms nor weight loss were found after this primary infection. Eighty days later, mice were challenged with $2x10^5$ pfu (100-fold MLD_{50}) of MB1 virus. As a control, a group of naive, age-matched mice received the same lethal dose of MB1 virus. The animals were weighted daily and the health

status was monitored twice a day for 14 days. As expected, wild type mice receiving only MB1 lost 20% of their initial body weight within 7 days after infection (Fig. 3A, open triangles) and died within day 8 and 12 past infection (Fig. 3B, open triangles). Mice that were vaccinated with DB1 and challenged with MB1 showed a moderate weight loss during the first 7 days of the infection (Fig. 3A, black squares), but showed no outward signs of illness. All animals survived the infection with the lethal H5N1 virus (Fig. 3B, black squares); thus, vaccination with DB1 significantly ($p = 0.000653$) protected C57Bl/6 mice against a lethal infection with MB1.

3.5. Vaccination and challenge infection of immunodeficient mice

To gain more information about the role of the immunological mechanisms that were involved in protection against H5N1 virus infection μMT, $CD8^{-/-}$ and in addition $CD4^{-/-}$ mice were also immunized with DB1.

When antibody deficient μMT mice were used for H5N1 challenge infection both the vaccinated (Fig. 4A, black squares) and the naive animals (Fig. 4A, open triangles) started losing weight immediately after challenge infection. Five days past MB1 infection mice of both groups lost already 20% of their body weight. Severe signs of clinical symptoms accompanied the decrease in body weight. Within 11 days past infection vaccinated (Fig. 4B black squares) and unvaccinated (Fig. 4B, open triangles) μMT mice succumbed to infection. In contrast, when $CD8^{+}$ T-cell deficient mice were used for challenge infection the vaccinated mice showed a milder reduction of their body weight (10-12%) until day 5 past infection (Fig. 4C, black squares) and 2 out of 6 mice developed mild clinical symptoms (ruffled fur). Nevertheless, all vaccinated $CD8^{-/-}$ mice survived the 100-fold MLD_{50} H5N1 challenge infection (Fig. 4D, black squares). Naive $CD8^{-/-}$ mice lost body weight (Fig. 4C, open triangles) developed disease symptoms and all mice died (Fig. 4D, open triangles). Vaccination with DB1 significantly ($p = 0.001155$) protected $CD8^{-/-}$ mice from lethal H5N1 infection.

In order to investigate the role of $CD4^{+}$ T-cells in protection against H5N1 influenza virus $CD4^{-/-}$ mice were used for vaccination with $2x10^{2}$ pfu DB1 (H5N2). After a 50 days recover period the mice were challenged with 100-fold MLD_{50} ($2x10^{5}$ pfu) of MB1 virus. As a control, naive littermates were infected with the same lethal dose of MB1 virus. The vaccinated and unvaccinated group of $CD4^{-/-}$ mice lost a significant but similar amount of body weight during the first 7 days of the lethal infection (Fig. 4E). While all unvaccinated animals infected only with MB1 died by day 9 after lethal H5N1 inoculation (Fig. 4F, open

triangles), 50% of the DB1 vaccinated mice recovered from the H5N1 infection, gained weight and survived (Fig. 4F, black squares). Since the $CD4^{-/-}$ mice belong to the sv129 genetic background wild type sv129 mice were used for vaccination experiments, showing similar susceptibility as C57Bl/6 mice to both influenza virus strains (data not shown). These data demonstrated that B-cells and to a lower extend $CD4^{+}$ T-cells but not $CD8^{+}$ T-cells are crucial for cross-protective primary immunity against H5 influenza virus.

To examine, whether vaccination with DB1 would lead to induction of cross-reactive antibodies against the hemagglutinin surface protein, serum from DB1 vaccinated mice was collected at different time points after infection. A hemagglutination inhibition assay was performed with the collected sera. Immunization with DB1 resulted in the production of hemagglutinin (HA) -specific antibodies directed against DB1. First anti-HA antibodies were present in the sera already three days after the infection. The serum titers increased until day 14 past infection. Thereafter, the titer decreased, but anti-HA antibodies were detectable until challenge infection 80 days p.i. Similar pattern of anti HA-antibodies were found after infection of $CD8^{-/-}$ and $CD4^{-/-}$ mice (Fig. 3 C, black bars). Six days past challenge infection vaccinated wild type, $CD8^{-/-}$ and $CD4^{-/-}$ mice showed a rapid increase in serum titers compared to unvaccinated controls against DB1 (Fig. 3C, white bars). The highest anti HA titers were reached by day 14 past infection in the vaccinated wild type, $CD8^{-/-}$ and $CD4^{-/-}$ mice, a time point where all control animals already had succumbed to infection (Fig. 3C, asterisk). These results demonstrated that an increased antibody response was induced in vaccinated mice. In addition to the presence of HA-specific antibodies, a virus neutralization assay revealed the presence of neutralizing antibodies. The antibody specificity after MB1 challenge infection was directed against DB1 and MB1 virus indicating specificity against DB1 and MB1 influenza virus (Fig. 5A, B). To quantify the cross-reactive antibodies elicited in immunized mice the HI titers in the sera of challenged wild type, $CD8^{-/-}$ and $CD4^{-/-}$ mice were compared towards DB1 (Fig. 5C, white bars) and MB1 (Fig. 5C, black bars). The antibodies were specific for both viruses in a nearly analogous manner.

3.6. Detection of influenza virus specific $CD8^{+}$ T-cells after challenge infection.

In order to analyse the role of cellular immune response after challenge infection, tetramer staining was performed to investigate the $CD8^{+}$ T-cell response against the challenge influenza virus infection using the immunodominant epitope ASNENEAM from the viral nucleoprotein (NP). Interestingly, this epitope was found in the NP of MB1, while one amino acid change was detected in DB1 (ASNENETM). Nevertheless, both epitopes were

recognized in similar intensity by virus specific T-cells generated either after DB1 or MB1 infection (data not shown).

Six days after MB1 infection an increase of the amount of $CD8^+$ T-cells was found in μMT and $CD4^{-/-}$ mice compared to wild type mice, whereas no difference in the amount of $CD8^+$ T-cells was found in the spleen six days after challenge infection (Fig. 5D). In contrast, no difference in the amount of $CD8^+$ T-cells in wild type, μMT and $CD4^{-/-}$ mice was found in the lung either after primary MB1 infection or challenge infection (Fig. 5D).

Interestingly, most ASNENEAM specific $CD8^+$ T-cells were detected in μMT mice, either in spleen or lung after primary or challenge infection, while the amount of ASNENEAM specific T-cells in wild type and $CD4^{-/-}$ mice was similar in spleen or lung after primary or challenge infection (Fig 5E).

4. Discussion

The emerging of highly pathogenic avian influenza viruses from the H5N1 subtype and its ability of crossing species barriers and infecting humans raised the strong need for new influenza vaccine approaches, in particular since H5N1 shows a broad antigenic heterogenicity. The development of a vaccine against potentially pandemic influenza will require a substantially different procedure than current strategies that are based on influenza vaccines made from a reassortant seed strain containing the viral hemagglutinin and neuraminidase of the circulating viruses [3]. Safe live-attenuated vaccine strains that provide broader cross-protective immunity against antigenic distinct H5N1 viruses are good candidates for protection covering also avian influenza viruses with pandemic potential [21]. Nevertheless, there are several questions to be answered on the way to design a successful live-attenuated vaccine with broad cross-protective properties. First, the live-attenuated vaccine strain needs to be save, genetically stable and highly immunogenic. In addition, the vaccine should be designed in a way to allow an optimal induction of cross-protective immune responses.

To bring a new light into this discussion, we wanted to scrutinize the immune cell populations involved in cross-protection by the use of immunodeficient mice for vaccination and challenge infection. The mouse model of influenza A virus infection is the best developed experimental system to investigate the immune response after infection, even though experimental influenza virus infection of mice does not resemble the natural infection found in humans and susceptible animal species. Nevertheless, there is increasing support that the

findings in the mouse model are pertinent to the immune mediated mechanisms found in humans during influenza [22,23]. In the present work, the primary vaccinations and the challenge infections were performed with field isolates from birds without prior adaptation to the mammalian host. The avian influenza virus strain DB1 (A/mallard/Bavaria/1/2005; H5N2) was isolated from a healthy duck during a routine monitoring screen. The strategy of using H5N2 subtype viruses as inactivated vaccines is practised worldwide [24]. Here, infection with apathogenic H5N2 led to solid protection and to reduced virus shedding of MB1, a highly pathogenic H5N1 virus (A/mallard/Bavaria/1/2006) which was isolated from a dead mallard [25]. Interestingly, both viruses replicated in cell culture and in the lung of infected mice to similar titers. However, sufficient progeny virus after DB1 infection of MDCK cells was only found in the presence of trypsin after the first culture passage. This might be due to the monobasic cleavage site of the DB1 hemagglutinin. Thus, it was surprising that in the mouse model DB1 and MB1 replicated to similar titers in the lungs. While MB1 infection resulted in severe clinical symptoms and death, no signs of disease were found after DB1 infection. This was a prerequisite for DB1 to be used as a live-attenuated vaccine in the present study.

The challenge infection of DB1 infected/vaccinated wild type mice with 100-fold MLD_{50} of MB1 resulted in protection, while control littermates without vaccination developed disease or even died. This demonstrates that infection with the H5N2 virus acts like modified live vaccination and confers solid cross-protection against H5N1. Nevertheless, the H5 protein of both viruses is highly conserved and share B-cells epitopes (Table 1: accession no.) In contrast, when DB1 vaccinated μMT mice were challenged with MB1 ($2x10^5$ pfu; 100-fold MLD_{50}) all animals developed disease and died. This experiment reveals the important role of the humoral immune response for cross-protective vaccination. It is generally believed that isotype-switched antibodies are neutralizing and protective in challenge infections with influenza A virus and that B-cells are not able to produce neutralizing isotype-switched, influenza-specific antibodies in the absence of $CD4^+$ T-cell help [26-29]. However, other reports demonstrate that B-cells can produce protective isotype-switched antibodies in response to different bacterial and viral infections including influenza A without $CD4^+$ T-cell collaboration. [13,30-32]. Thus, we questioned whether DB1-vaccination would protect mice deficient in $CD4^+$ T-cells against lethal H5N1 infection. Our results demonstrate that only 50% of the $CD4^+$ T-cell deficient mice were protected against H5N1 challenge, indicating a particular role for $CD4^+$ T-cells either by T-cell help for antibody production or by other effector functions. Nevertheless, the fact that similar amounts of HA-specific antibodies could

be detected after challenge infection in $CD4^{-/-}$ mice supports the view for $CD4^+$ T-cell independent antibody response. There are data available that reveal a complex response for influenza virus specific $CD4^+$ T-cells, which results in multiple effector phenotypes. These data imply that the $CD4^+$ T-cells and the memory cells derived from them can display a broad spectrum of functional potentials [33]. Thus, further research is mandatory to understand the role and function of $CD4^+$ helper T-cells during influenza virus infection and in cross-protective immunity in more detail.

After intranasal influenza A virus infection of mice the expansion of naive $CD8^+$ T-cells is tightly depended on antigen localization. Initial activation of $CD8^+$ T-cells occurs during the first 3 days after infection exclusively within the draining mediastinal lymph nodes [34]. Thereafter, the division of the influenza virus primed $CD8^+$ T-cells within the draining lymph nodes occurs between days 3 and 4 after infection and they migrate to the lung and to other regions of the respiratory tract where antigen is present [35]. At the site of virus infection the $CD8^+$ T-cells lyse the infected host cells and exert other effector functions like production of antiviral cytokines [36]. Influenza A virus specific $CD8^+$ T-cells recognize multiple viral epitopes on infected target cells, whereas an epitope from the viral nucleoprotein ($NP^{366-374}$) resembles an immunodominat epitope in C57Bl6 mice ($H2\text{-}D^b$) [37]. A lot of our knowledge was gained in the experimental mouse model but also broad information on common and immunodominant HLA restricted epitopes of circulating non-avian strains is available. Since influenza A virus activates dendritic cells that support the development of $CD8^+$ T-cells via innate immune mechanisms; T helper cells are not necessarily essential for a primary $CD8^+$ T-cell response [38]. These findings suggest that $CD4^+$ T-cell help is not required at the site of the pathological changes if the infection induces a sufficient amount of other immune stimuli. So the question raises, whether $CD8^+$ T-cells are mandatory for cross-protective immunity after vaccination with live-attenuated vaccine candidates. When DB1 vaccinated $CD8^+$ T-cell deficient mice were challenged with MB1 ($2x10^5$ pfu), all mice were protected. While it is of common knowledge that antibodies are required for protective immunity after vaccination, we were surprised by the result that $CD8^+$ T-cells seem not to be necessary for protection against H5N1 challenge infection. It was reported that in µMT mice, the total number of virus-specific CTL's in the alveolar lavage after influenza virus infection is almost comparable to wild type mice [39]. Our results show that the amount of $NP^{366-374}$ epitope specific $CD8^+$ T-cells in lung and spleen was even increased compared to wild type mice after primary and challenge infection. Thus, $CD8^+$ T-cells are unable to counterbalance a missing humoral immune response.

From the present data one might question whether $CD8^+$ T-cells are dispensable for the control of an influenza virus infection? Despite evidence that live-attenuated influenza vaccines and inactivated influenza vaccines induce a cross-reactive cellular immune response in mice and humans, re-infection with homologous or heterotypic influenza viruses can be demonstrated [40,41]. Cell-mediated immunity in particular mediated by $CD8^+$ T-cells can promote viral clearance but in general it will not prevent infection. Already more than 25 years ago it could be shown that the amount of anti-influenza CTL's correlates with viral clearance but not with altered susceptibility to infection or re-infection [41]. Nevertheless, Ulmer and colleagues were able to induce influenza virus nucleoprotein specific $CD8^+$ T-cells by DNA vaccination that were able to protect against hetero-subtype lethal virus challenge in mice [42]. Moreover, vaccines based on immune stimulating complexes (ISCOM's) are able to induce CTL responses in addition to a strong antibody response in humans, but the contribution of $CD8^+$ T-cells for protection in primary infection was not investigated [43].

Taken together, our results support the mandatory role of humoral immune response in protection against influenza virus infection. Consequently, vaccine strategies including live-attenuated vaccines should focus on the induction of an effective antibody mediated immune response accompanied by the helper function of $CD4^+$ T-cells. From our results one might speculate a minor role for $CD8^+$ T-cells in cross-protective primary immunity to influenza virus after vaccination, but their essential contribution for controlling the infection at the place where pathological changes occur, namely in the lung, is indisputable.

Acknowledgments

We would like to thank Carmen Mueller, Isabell Laurich and Ulrich Wulle for excellent technical assistance. This work is part of the EUROFLU consortium activities and of the VIRGIL European Network of Excellence on Antiviral Drug Resistance supported by a grant (LSHMCT-2004-503359) from the Priority 1 "Life Sciences, Genomics and Biotechnology for Health" program in the 6th Framework Program of the EU. Furthermore this research was partially supported by the Federal Government of Germany under the Influenza Research Programm "FSI" and by the BMBF Zoonose program "FluResearchNet"

References

[1] Webby RJ, Webster RG. Are we ready for pandemic influenza? Science 2003 Nov 28;302(5650):1519-22.

[2] Tumpey TM, Maines TR, Van HN, et al. A two-amino acid change in the hemagglutinin of the 1918 influenza virus abolishes transmission. Science 2007 Feb 2;315(5812):655-9.

[3] Cox RJ, Brokstad KA, Ogra P. Influenza virus: immunity and vaccination strategies. Comparison of the immune response to inactivated and live, attenuated influenza vaccines. Scand J Immunol 2004 Jan;59(1):1-15.

[4] Fiers W, De FM, Birkett A, Neirynck S, Min JW. A "universal" human influenza A vaccine. Virus Res 2004 Jul;103(1-2):173-6.

[5] De Filette M, Min JW, Birkett A, et al. Universal influenza A vaccine: optimization of M2-based constructs. Virology 2005 Jun 20;337(1):149-61.

[6] Saha S, Yoshida S, Ohba K, et al. A fused gene of nucleoprotein (NP) and herpes simplex virus genes (VP22) induces highly protective immunity against different subtypes of influenza virus. Virology 2006 Oct 10;354(1):48-57.

[7] Lu X, Edwards LE, Desheva JA, et al. Cross-protective immunity in mice induced by live-attenuated or inactivated vaccines against highly pathogenic influenza A (H5N1) viruses. Vaccine 2006 Nov 10;24(44-46):6588-93.

[8] Lipatov AS, Hoffmann E, Salomon R, Yen HL, Webster RG. Cross-protectiveness and immunogenicity of influenza A/Duck/Singapore/3/97(H5) vaccines against infection with A/Vietnam/1203/04(H5N1) virus in ferrets. J Infect Dis 2006 Oct 15;194(8):1040-3.

[9] Suguitan AL, Jr., McAuliffe J, Mills KL, et al. Live, attenuated influenza A H5N1 candidate vaccines provide broad cross-protection in mice and ferrets. PLoS Med 2006 Sep;3(9):e360.

[10] Carrat F, Flahault A. Influenza vaccine: the challenge of antigenic drift. Vaccine 2007 Sep 28;25(39-40):6852-62.

[11] Doherty PC, Topham DJ, Tripp RA, Cardin RD, Brooks JW, Stevenson PG. Effector CD4+ and CD8+ T-cell mechanisms in the control of respiratory virus infections. Immunol Rev 1997 Oct;159:105-17.

[12] Gerhard W. The role of the antibody response in influenza virus infection. Curr Top Microbiol Immunol 2001;260:171-90.

[13] Lee BO, Rangel-Moreno J, Moyron-Quiroz JE, et al. CD4 T cell-independent antibody response promotes resolution of primary influenza infection and helps to prevent reinfection. J Immunol 2005 Nov 1;175(9):5827-38.

[14] Townsend AR, Rothbard J, Gotch FM, Bahadur G, Wraith D, McMichael AJ. The epitopes of influenza nucleoprotein recognized by cytotoxic T lymphocytes can be defined with short synthetic peptides. Cell 1986 Mar 28;44(6):959-68.

[15] Scherle PA, Palladino G, Gerhard W. Mice can recover from pulmonary influenza virus infection in the absence of class I-restricted cytotoxic T cells. J Immunol 1992 Jan 1;148(1):212-7.

[16] Lawson CM, Bennink JR, Restifo NP, Yewdell JW, Murphy BR. Primary pulmonary cytotoxic T lymphocytes induced by immunization with a vaccinia virus recombinant expressing influenza A virus nucleoprotein peptide do not protect mice against challenge. J Virol 1994 Jun;68(6):3505-11.

[17] Yewdell JW, Bennink JR, Smith GL, Moss B. Influenza A virus nucleoprotein is a major target antigen for cross-reactive anti-influenza A virus cytotoxic T lymphocytes. Proc Natl Acad Sci U S A 1985 Mar;82(6):1785-9.

[18] Rimmelzwaan GF, Fouchier RA, Osterhaus AD. Influenza virus-specific cytotoxic T lymphocytes: a correlate of protection and a basis for vaccine development. Curr Opin Biotechnol 2007 Dec;18(6):529-36.

[19] Kreijtz J, de MG, van BC, Fouchier R, Osterhaus A, Rimmelzwaan G. Cross-recognition of avian H5N1 influenza virus by human cytotoxic T lymphocyte populations directed to human influenza A virus. J Virol 2008 Mar 19.

[20] Matrosovich M, Matrosovich T, Garten W, Klenk HD. New low-viscosity overlay medium for viral plaque assays. Virol J 2006;3:63.

[21] Sakabe S, Sakoda Y, Haraguchi Y, et al. A vaccine prepared from a non-pathogenic H7N7 virus isolated from natural reservoir conferred protective immunity against the challenge with lethal dose of highly pathogenic avian influenza virus in chickens. Vaccine 2008 Apr 16;26(17):2127-34.

[22] Thomas PG, Keating R, Hulse-Post DJ, Doherty PC. Cell-mediated protection in influenza infection. Emerg Infect Dis 2006 Jan;12(1):48-54.

[23] Thomas PG, Brown SA, Yue W, So J, Webby RJ, Doherty PC. An unexpected antibody response to an engineered influenza virus modifies CD8+ T cell responses. Proc Natl Acad Sci U S A 2006 Feb 21;103(8):2764-9.

[24] Marangon S, Cecchinato M, Capua I. Use of vaccination in avian influenza control and eradication. Zoonoses Public Health 2008;55(1):65-72.

[25] Rinder M, Lang V, Fuchs C, et al. Genetic evidence for multi-event imports of avian influenza virus A (H5N1) into Bavaria, Germany. J Vet Diagn Invest 2007 May;19(3):279-82.

[26] Sangster MY, Riberdy JM, Gonzalez M, Topham DJ, Baumgarth N, Doherty PC. An early CD4+ T cell-dependent immunoglobulin A response to influenza infection in the absence of key cognate T-B interactions. J Exp Med 2003 Oct 6;198(7):1011-21.

[27] Scherle PA, Gerhard W. Functional analysis of influenza-specific helper T cell clones in vivo. T cells specific for internal viral proteins provide cognate help for B cell responses to hemagglutinin. J Exp Med 1986 Oct 1;164(4):1114-28.

[28] Wells MA, Albrecht P, Ennis FA. Recovery from a viral respiratory infection. I. Influenza pneumonia in normal and T-deficient mice. J Immunol 1981 Mar;126(3):1036-41.

[29] Justewicz DM, Doherty PC, Webster RG. The B-cell response in lymphoid tissue of mice immunized with various antigenic forms of the influenza virus hemagglutinin. J Virol 1995 Sep;69(9):5414-21.

[30] Szomolanyi-Tsuda E, Welsh RM. T-cell-independent antiviral antibody responses. Curr Opin Immunol 1998 Aug;10(4):431-5.

[31] Szomolanyi-Tsuda E, Le QP, Garcea RL, Welsh RM. T-Cell-independent immunoglobulin G responses in vivo are elicited by live-virus infection but not by immunization with viral proteins or virus-like particles. J Virol 1998 Aug;72(8):6665-70.

[32] Bachmann MF, Hengartner H, Zinkernagel RM. T helper cell-independent neutralizing B cell response against vesicular stomatitis virus: role of antigen patterns in B cell induction? Eur J Immunol 1995 Dec;25(12):3445-51.

[33] Roman E, Miller E, Harmsen A, et al. CD4 effector T cell subsets in the response to influenza: heterogeneity, migration, and function. J Exp Med 2002 Oct 7;196(7):957-68.

[34] Lawrence CW, Ream RM, Braciale TJ. Frequency, specificity, and sites of expansion of CD8+ T cells during primary pulmonary influenza virus infection. J Immunol 2005 May 1;174(9):5332-40.

[35] Lawrence CW, Braciale TJ. Activation, differentiation, and migration of naive virus-specific CD8+ T cells during pulmonary influenza virus infection. J Immunol 2004 Jul 15;173(2):1209-18.

[36] Topham DJ, Castrucci MR, Wingo FS, Belz GT, Doherty PC. The role of antigen in the localization of naive, acutely activated, and memory CD8(+) T cells to the lung during influenza pneumonia. J Immunol 2001 Dec 15;167(12):6983-90.

[37] Turner SJ, Kedzierska K, La Gruta NL, Webby R, Doherty PC. Characterization of CD8+ T cell repertoire diversity and persistence in the influenza A virus model of localized, transient infection. Semin Immunol 2004 Jun;16(3):179-84.

[38] Diebold SS, Kaisho T, Hemmi H, Akira S, Reis e Sousa. Innate antiviral responses by means of TLR7-mediated recognition of single-stranded RNA. Science 2004 Mar 5;303(5663):1529-31.

[39] Kopf M, Brombacher F, Bachmann MF. Role of IgM antibodies versus B cells in influenza virus-specific immunity. Eur J Immunol 2002 Aug;32(8):2229-36.

[40] Brett IC, Johansson BE. Immunization against influenza A virus: comparison of conventional inactivated, live-attenuated and recombinant baculovirus produced

purified hemagglutinin and neuraminidase vaccines in a murine model system. Virology 2005 Sep 1;339(2):273-80.

[41] McMichael AJ, Gotch F, Cullen P, Askonas B, Webster RG. The human cytotoxic T cell response to influenza A vaccination. Clin Exp Immunol 1981 Feb;43(2):276-84.

[42] Ulmer JB, Donnelly JJ, Parker SE, et al. Heterologous protection against influenza by injection of DNA encoding a viral protein. Science 1993 Mar 19;259(5102):1745-9.

[43] Rimmelzwaan GF, Baars M, van AG, van BR, Osterhaus AD. A single dose of an ISCOM influenza vaccine induces long-lasting protective immunity against homologous challenge infection but fails to protect Cynomolgus macaques against distant drift variants of influenza A (H3N2) viruses. Vaccine 2001 Oct 12;20(1-2):158-63.

Figure legends

Figure 1: A: Progeny virus titer of high pathogenic MB1 (H5N1) (open triangles) and low pathogenic DB1 (H5N2) (black squares) influenza viruses after infection on MDCK cells with MOI 0.001. Detection limit was <1.7 log10 pfu/ml. This experiment was performed three times. B: Nucleic acid sequence analyses. The MB1 isolate contains a cleavage site with multiple basic amino acids. This polybasic cleavage site is an attribute for HPAI viruses. DB1 revealed a monobasic cleavage site, characteristic for LPAI viruses.

Figure 2: Susceptibility of immunocompetent and immunodeficient mice to DB1 or MB1 infection. Five mice from each group were infected i.n. with $2x10^3$ pfu of the low pathogenic H5N2 strain DB1 or with $2x10^3$ pfu of the highly pathogenic H5N1 strain MB1. Course of average body weight of wild type (A), µMT (C) and $CD8^{-/-}$ (E) animals after infection with DB1 (black squares) or MB1 (open triangles). Survival rates of wild type (B), µMT (D) and $CD8^{-/-}$ (F) mice. The graph represents one experiment with five mice. The experiment was performed twice with similar results.

Figure 3: Immunization of C57Bl/6 mice. Groups of six C57Bl/6 mice were infected i.n. with $2x10^2$ pfu DB1. Eighty days past DB1 infection, the animals were challenged with 100-fold MLD_{50} of the highly pathogenic MB1 virus (black squares). Controls (littermates) were only infected with MB1 (open squares). A: Weight progress. B: Survival rates. C: Production of anti HA-specific antibodies directed against DB1 in C57Bl/6, $CD4^{-/-}$ and $CD8^{-/-}$ mice. Serum samples were collected at different time points past infection from immunized (black bars) and control (white bars) animals. * = at this time point all animals succumbed to infection. The results are given as the reciprocal of the highest dilution causing detectable inhibition of hemagglutination. This experiment was performed twice with similar results

Figure 4: Immunization of immunodeficient mice. Six animals of each group were immunized i.n. with $2x10^2$ pfu DB1. Eighty days past DB1 infection ($CD4^{-/-}$ 50 days p.i. since neither DB1 virus nor antibody titer was detectable), the animals were challenged with 100-fold MLD_{50} of the highly pathogenic MB1 virus. Controls (littermates) were infected with MB1. Weight progress from µMT (A), $CD8^{-/-}$ (C) and $CD4^{-/-}$ (E) mice infected with DB1 (black squares) or MB1 (open triangles). Survival curves from µMT (B), $CD8^{-/-}$ (D) and $CD4^{-/-}$ (F) mice. For statistical analysis the Cox-regression test was used.

Figure 5: *In vitro* neutralisation assay. To test the ability of different sera to inhibit DB1 (A) or MB1 (B) virus an *in vitro* neutralisation assay was performed with sera from C57Bl/6 mice. Virus was incubated for 30 min at room temperatur with serum from uninfected mice (white bars), DB1 infected mice 14 days past infection (pale gray bars) and challenged mice 14 days past infection (dark gray bars). For control virus was incubated with PBS (black bars). The numbers of infectious particles were assessed by plaque titration. The bars represent the mean values of three different experiments. (C) Comparison of the HI titers in the serum-pool (n = 5) of immunized C57Bl/6, $CD8^{-/-}$ and $CD4^{-/-}$ mice 14 days past challenge infection towards DB1 (white bars) and MB1 (black bars). The results are given as the reciprocal of the highest dilution causing detectable inhibition of hemagglutination. Flow cytometry for $CD8^{+}$ T-cells and NP-specific $CD8^{+}$ T-cells in the lungs and spleens of MB1 infected (n=4) C57Bl/6, µMT and $CD4^{-/-}$ mice 6 days past MB1 infection and challenged C57Bl/6, µMT and $CD4^{-/-}$ (n=3) also 6 days past MB1 infection. Cells were obtained from spleens and lungs of infected mice and assayed for the presence of $CD8^{+}$ T-cells (C) and $NP^{366-374}$-specific $H2D^{b}$ restricted $CD8^{+}$ T-cells determined by tetramer staining (D).

Tables

Table 1: Overview of the used avian influenza A virus strains.

Species	Subtype	Abbreviation	Accession-No.*	MLD_{50} (pfu)
A/mallard/Bavaria/1/2006	H5N1	MB1	DQ458992	$2x10^3$
A/mallard/Bavaria/1/2005	H5N2	DB1	DQ387854	$> 5x10^5$

* Accession number based on hemagglutinin.

Table 2: Distribution of DB1 virus after infection of mice.

Day 6 p.i.	Lung	Brain	Kidney	Liver	Spleen	Blood	Heart
C57Bl/6	4.9 ± 0.5	< 1.7	< 1.7	< 1.7	< 1.7	< 1.7	< 1.7
µMT	4.8 ± 0.5	< 1.7	< 1.7	< 1.7	< 1.7	< 1.7	< 1.7
$CD8^{-/-}$	5.2 ± 0.5	< 1.7	< 1.7	< 1.7	< 1.7	< 1.7	< 1.7

Virus titer is given as pfu per 1ml 10% organ-homogenate.

Table 3: Distribution of MB1 virus after infection of mice.

Day 6 p.i.	Lung	Brain	Kidney	Liver	Spleen	Blood	Heart
C57Bl/6	4.9 ± 0.3	< 1.7	< 1.7	2.7 ± 0.3	2.6 ± 0.3	4.0 ± 0.3	< 1.7
µMT	4.9 ± 0.2	3.3 ± 0.2	< 1.7	< 1.7	< 1.7	< 1.7	< 1.7
$CD8^{-/-}$	5.1 ± 0.2	< 1.7	< 1.7	< 1.7	< 1.7	3.4 ± 0.3	< 1.7

Virus titer is given as pfu per 1ml 10% organ-homogenate.

Figures

Figure 1

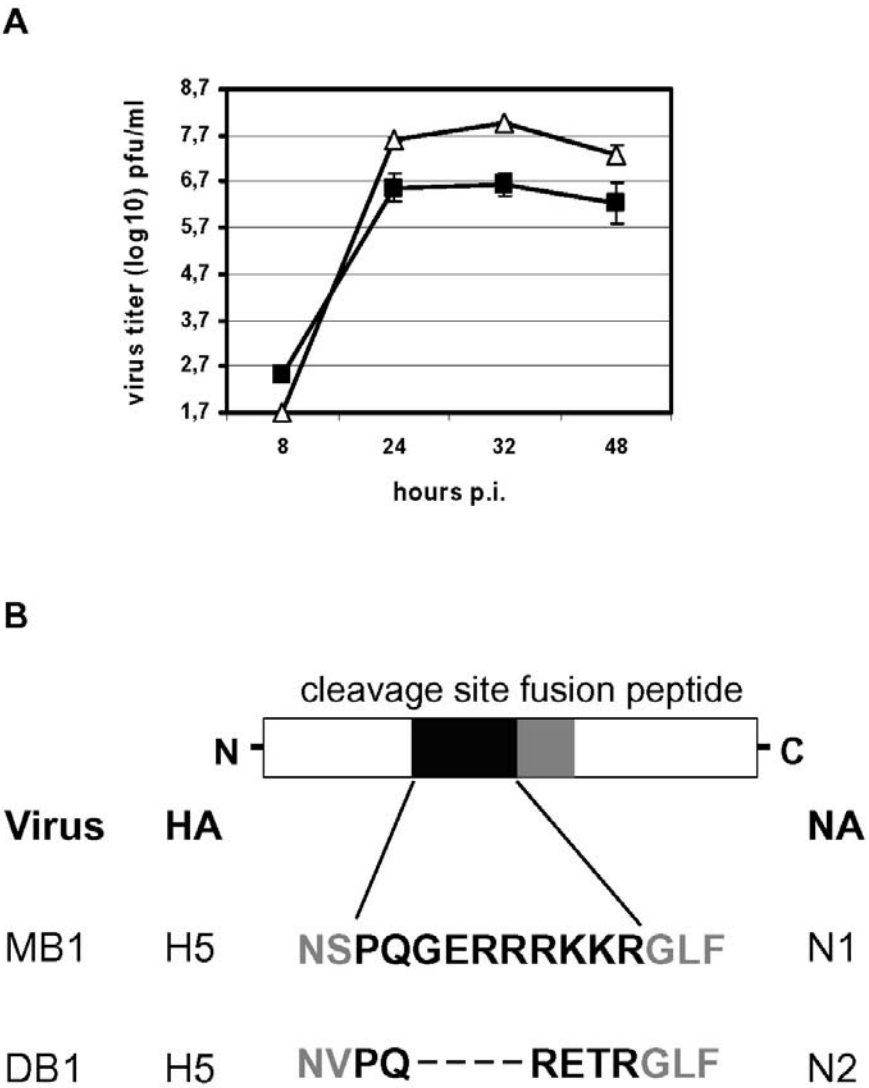

Figure 2

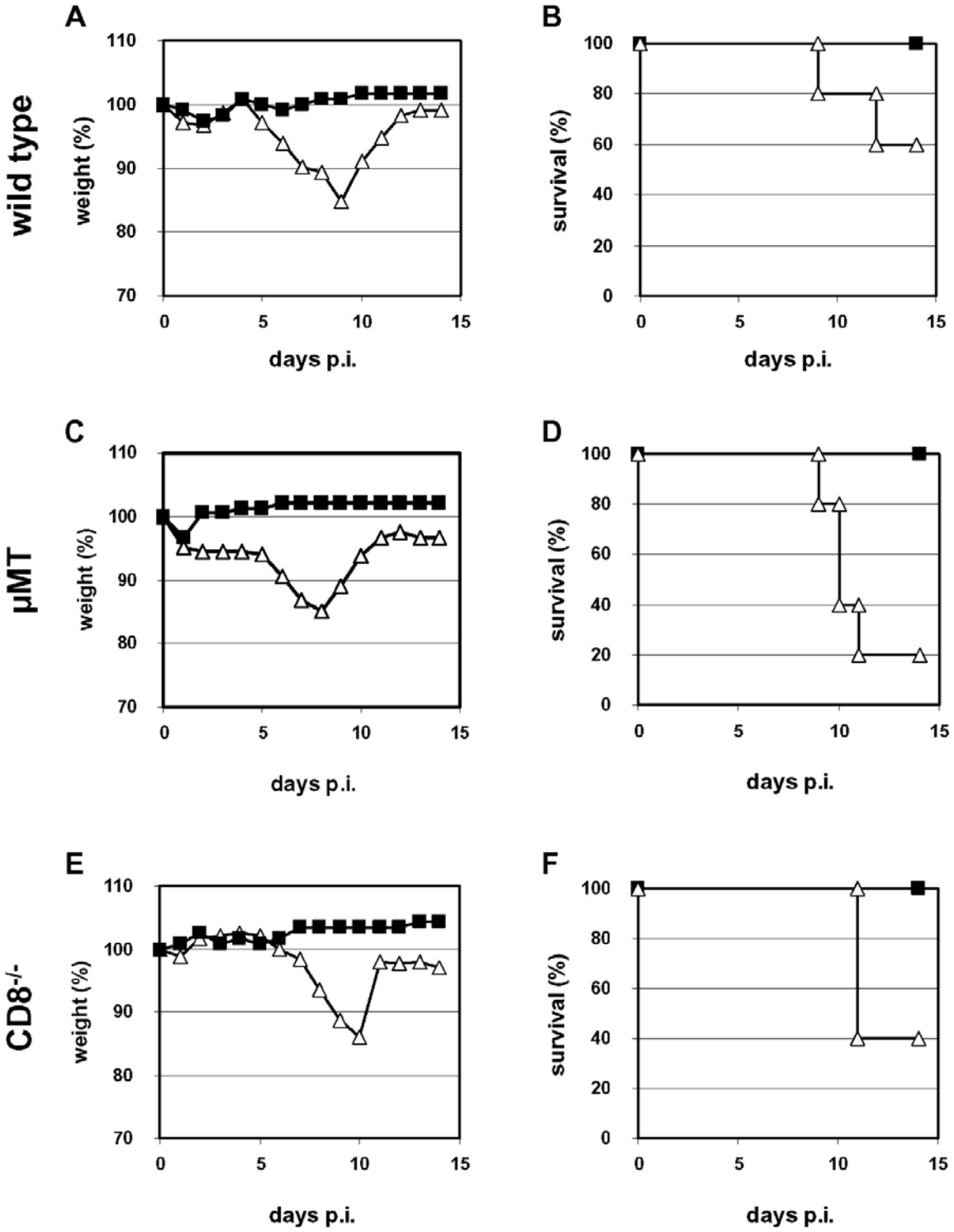
A
B
C
D
E
F
wild type
µMT
CD8-/-
weight (%)
survival (%)
days p.i.
110
100
90
80
70
60
40
20
0
5
10
15

Figure 3

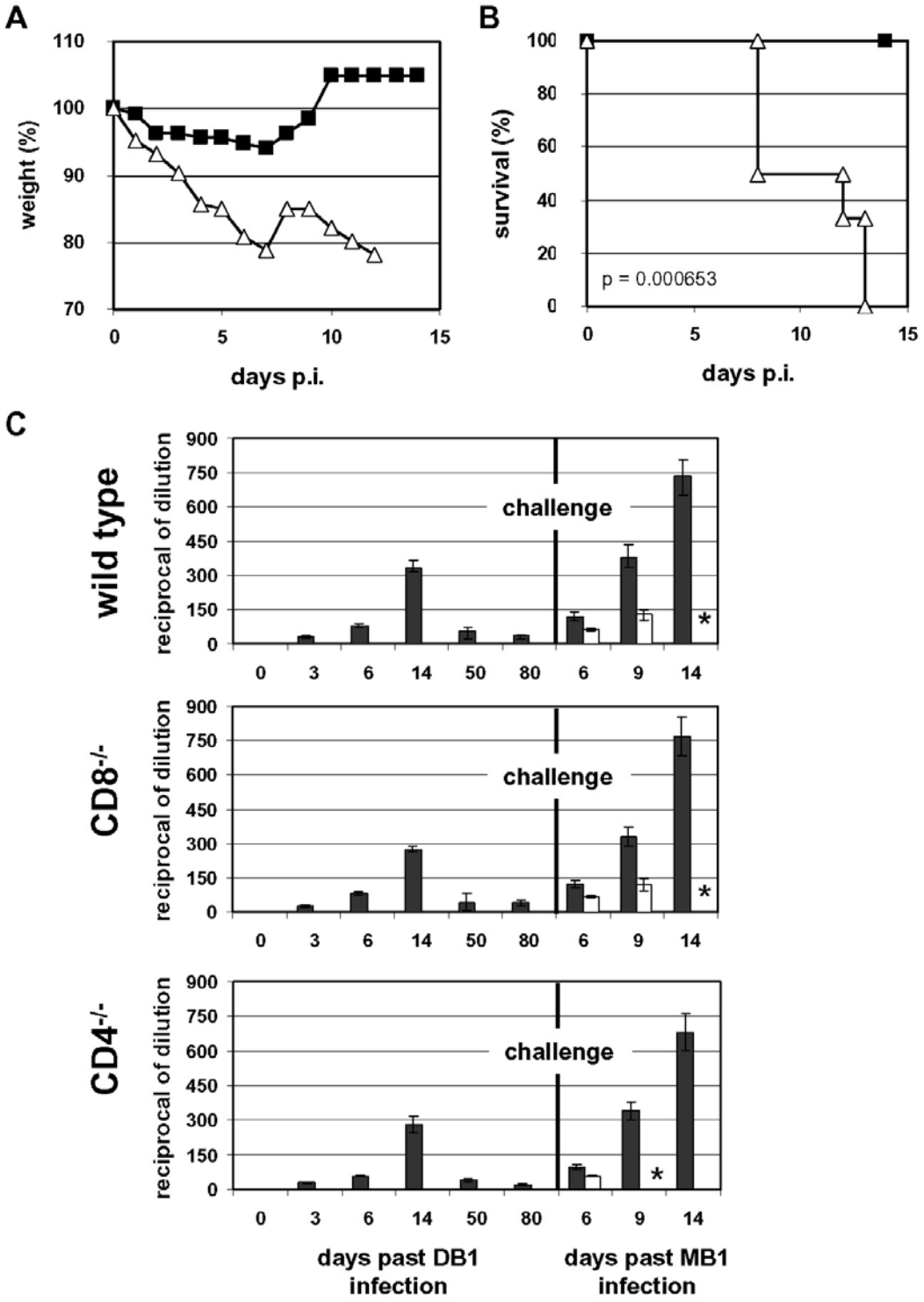
A
weight (%)
days p.i.
B
survival (%)
p = 0.000653
days p.i.
C
wild type
CD8-/-
CD4-/-
reciprocal of dilution
challenge
days past DB1 infection
days past MB1 infection

Figure 4

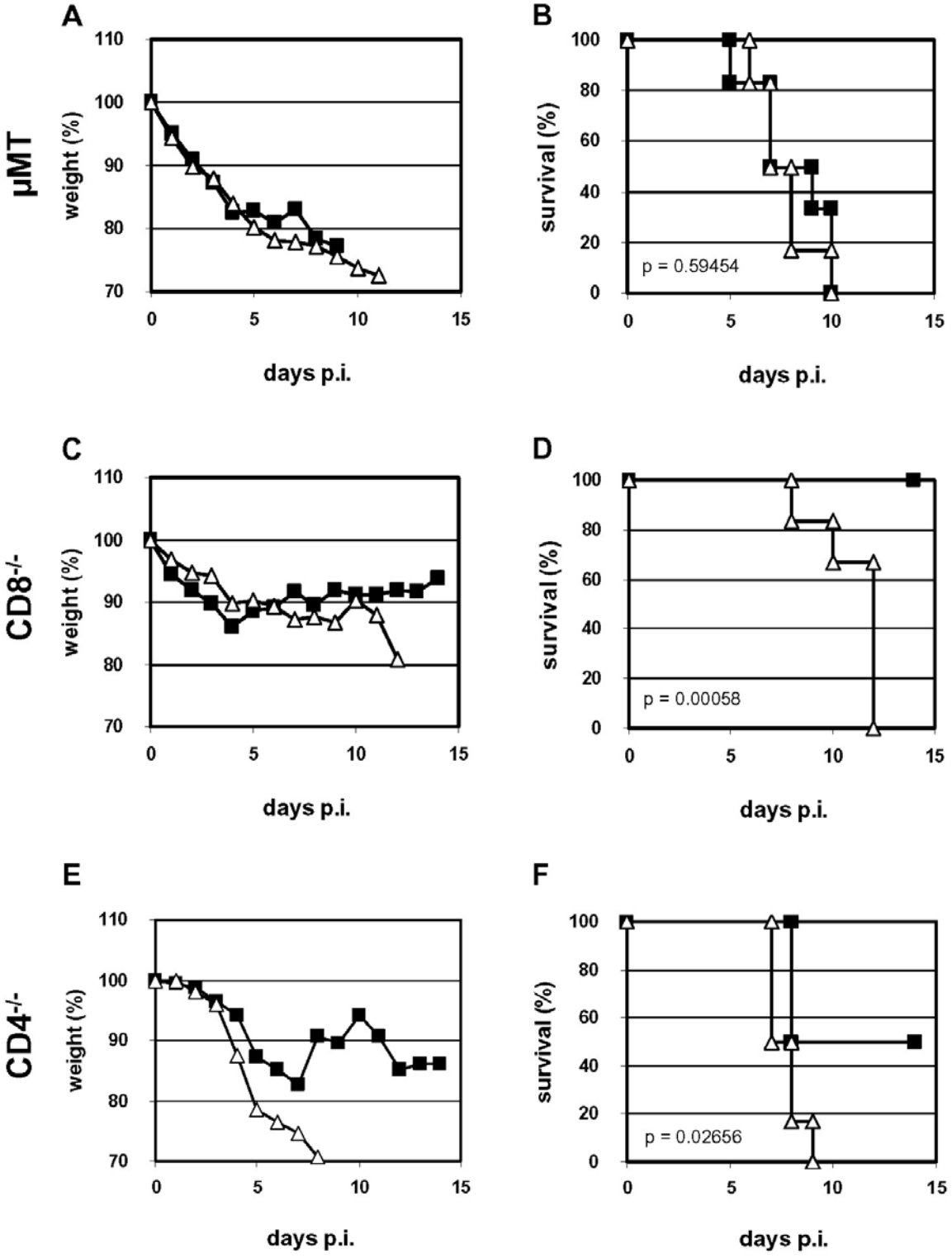
A
B
C
D
E
F
μMT
CD8-/-
CD4-/-
weight (%)
survival (%)
days p.i.
p = 0.59454
p = 0.00058
p = 0.02656

Figure 5

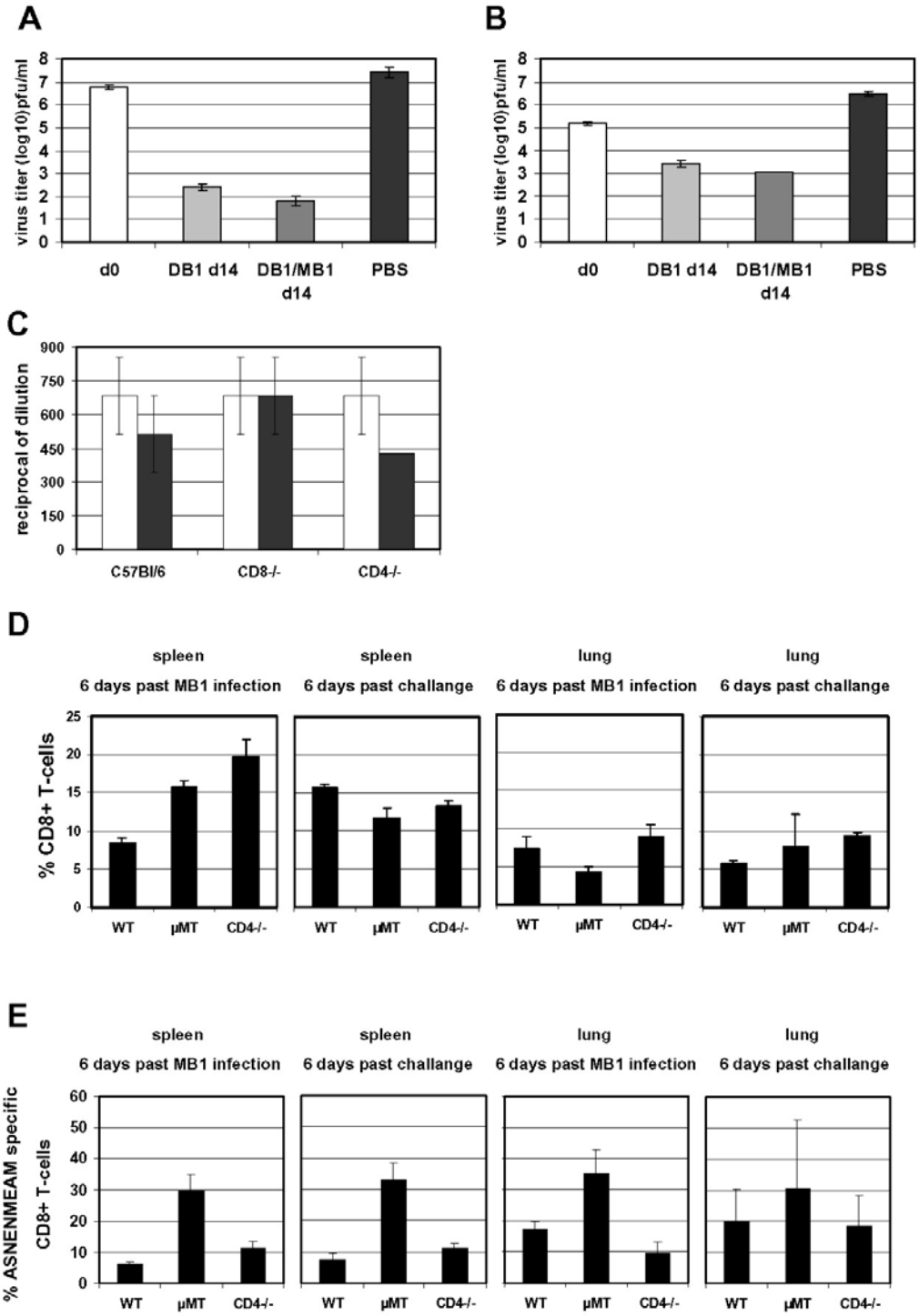
A
virus titer (log10)pfu/ml
d0
DB1 d14
DB1/MB1 d14
PBS
B
virus titer (log10)pfu/ml
d0
DB1 d14
DB1/MB1 d14
PBS
C
reciprocal of dilution
C57Bl/6
CD8-/-
CD4-/-
D
spleen
6 days past MB1 infection
spleen
6 days past challange
lung
6 days past MB1 infection
lung
6 days past challange
% CD8+ T-cells
WT
µMT
CD4-/-
E
spleen
6 days past MB1 infection
spleen
6 days past challange
lung
6 days past MB1 infection
lung
6 days past challange
% ASNENMEAM specific CD8+ T-cells
WT
µMT
CD4-/-

PUBLICATION #5:

Highly pathogenic influenza virus infection of the thymus interferes with T lymphocyte development

Annette B. Vogel[*], Emanuel Haasbach[*], Sarah J. Reiling[*], Karoline Droebner[*], Karin Klingel[†] and Oliver Planz[*#]

[*] Friedrich-Loeffler-Institut, Institute of Immunology, Paul-Ehrlich Str. 28, D-72076 Tuebingen, Germany

[†] Department of Molecular Pathology, University Hospital, D-72076 Tuebingen, Germany

[#]Corresponding author: Friedrich-Loeffler-Institut; Institute of Immunology,
Federal Research Institute for Animals Health,
Paul-Ehrlich Str. 28
D-72076 Tuebingen, Germany
Tel: +49 7071 967 254
Fax: +49 7071 967 105
E-mail: oliver.planz@fli.bund.de

Keywords: H5N1 influenza A virus, pandemic H1N1v, DC, thymus, lymphopenia

Abstract

Highly pathogenic avian influenza A viruses (HPAIV) cause severe disease in humans. Still the basis for their increased pathogenesis particularly with regards to the younger population remains unclear. Additionally, the recent pandemic H1N1v outbreak in 2009 demonstrated the urgent need for a better understanding about influenza virus infection. In the present study we demonstrated that HPAIV infection of mice led not only to lung destruction but also to functional damage of the thymus. Moreover, respiratory dendritic cells (RDCs) in the lung functioned as targets for HPAIV infection being able to transport infectious virus from the lung into the thymus. In addition the pandemic H1N1v influenza virus was able to infect RDCs without a proper transport to the thymus. Especially the strong interference of HPAIV with the immune system is devastating for the host and can lead to severe lymphopenia. In summary, from our data we conclude that highly pathogenic influenza viruses are able to reach the thymus via dendritic cells and to interfere with T lymphocyte development. Moreover, this exceptional mechanism might not only be found in influenza virus infection but also might be the reason of the increased immune evasion of some new emerging pathogens.

Introduction

Influenza A virus infection causes severe disease in humans and is a major topic in clinical health. While epidemic outbreaks of human influenza viruses cause over < 300.000 death worldwide per year (Maines et al., 2008), the recent swine origin influenza virus (SOIV) H1N1v pandemic outbreak demonstrates the full threat of influenza virus infection. So far SOIV infection in humans worldwide causes rather mild clinical symptoms though over 18.000 deaths in humans have been reported (WHO). In contrast, infection with the highly pathogenic avian influenza virus (HPAIV) H5N1 is more fatal to humans. Till today, 499 confirmed cases have been reported while 295 of them were lethal mainly in South East Asia (WHO). This fatality rate of roughly 59 percent demonstrates the urgent need to get a closer inside into the pathogenesis of HPAIV infections in humans, since H5N1 influenza virus is still considered as a potential pandemic strain. Moreover, a reassortant between H5N1 and pandemic H1N1v influenza virus might be a candidate for a serious pandemic influenza virus strain with high morbidity and more devastating high fatality rate.

While annual epidemic outbreaks typically affect people with an impaired immune system (e.g. elderly, infants and immunosuppressed people), severe influenza after HPAIV infection is mostly found in young and middle-aged people (Smallman-Raynor and Cliff, 2007), (bdel-Ghafar et al., 2008). Human infection cluster of H5N1 outbreaks with an average age of 13.7 and 15.4 years have been reported (Tran et al., 2004), (Kandun et al., 2006). The same phenomenon was found for the “Spanish Flu” pandemic (Taubenberger et al., 2001) and the 2009 pandemic H1N1v strain (CDC, 2009. The reason for this altered host specificity remains unclear. One hallmark of H5N1 infection in humans is a strong reduction of lymphocytes, also known as lymphopenia. Lymphopenia is a common feature of some infectious diseases, in particular with new emerging pathogens (Chuang et al., 2008), (Baize et al., 2009). The mechanism of lymphopenia induced after H5N1 influenza virus infection is largely unknown. Remarkably, H5N1 influenza virus seems to reduce the effector function of $CD8^+$ T cells by an insufficient perforin expression (Hsieh and Chang, 2006). Moreover, it was reported that H5N1 viruses are able to infect cells of the immune system, leading to an impaired adaptive immune response (Korteweg and Gu, 2008. As a consequence the unbalance between innate and adaptive immune response might lead to a second hallmark of H5N1 infection, namely hypercytokinemia which is an increase of proinflammatory cytokines and chemokines in the lung (Maines et al., 2008).

The thymus, where T cell development takes place, presents an organ that is highly active during childhood, but stays functionally in young adults. The human thymus has its highest activity phase in an age group from 0 to 10 years and shows a major activity drop in the population older than 39 years. Nevertheless the thymus remains still active in the elderly population (Geenen et al., 2003), (Hale et al., 2006).

Bone marrow originated common lymphoid progenitor cells reach the cortical area of the thymus and become $TCR^{+}CD4^{+}CD8^{+}$ thymocytes. At this stage, the positive selection takes place. During this process thymocytes with a TCR that does not recognize self major histocompartibility complex (MHC get lost. Surviving thymocytes migrate into the medulla of the thymus were self-peptides are presented. Thymocytes that recognize presented antigen undergo apoptotic processes and will be eliminated. Only thymocytes which do not recognize MHC class I or II presented self-peptide become naive T lymphocytes and migrate to the periphery. During the highly active life phase, the T lymphocyte production rate of the thymus ranges from 2×10^{8} to 1.8×10^{10} cells per day in humans (Hollander and Peterson, 2009. Macrophages and dendritic cells in the thymus are also involved in the process of negative selection. It was a given fact for a long time that both cell types have their origin in the bone marrow and migration out of the thymus is an one way event. However, recent reports demonstrated that dendritic cells with extrathymic origin migrate also from the periphery into the thymus (Li et al., 2009). The uptake of foreign antigens by DCs and the transport of these antigens into the thymus results in a development of a T cell tolerance against foreign antigens (Bonasio et al., 2006).

Fatal H5N1 influenza virus infection in mice results in massive lung damage originated by infiltrating immune cells namely macrophages and neutrophiles (Perrone et al., 2008). T lymphocytes only play a secondary role for this damage. Moreover, $CD8^{+}$ T lymphocytes have a poor cytotoxic profile after influenza virus infection (Harari et al., 2009) and lymphopenia can be observed (Maines et al., 2008). We hypothesize that the influenza virus itself plays an active role in these findings. A conceivable mechanism could be the direct interference with the thymus as the primary lymphoid organ for T lymphocyte development.

In the present study we were able to demonstrate that highly pathogenic influenza viruses abuse the homing process of DCs into the thymus after infecting respiratory DCs (RDCs) in the lung. RDCs migrated into the thymus after activation by the infection with HPAIV and thereby interfere with the T lymphocyte selection processes. That way a reduced cellular immune response against the invading pathogen and the predominantly increased disease symptoms in younger people might be explained. Moreover, the atrophic process of the

thymus observed during HPAIV infection, is a common feature of severe diseases like AIDS, Rabies and Chagas disease (Savino et al., 2007). Our results give rise to the assumption that this mechanism of increased pathogenesis is not only due to influenza viruses with pandemic potential, but also to infections with other new or reemerging pathogens like FMDV, Chikungunya, SARS and West Nile Virus (Borgherini et al., 2007), (Salguero et al., 2005), (Panesar, 2008), (Law et al., 2005), (Cunha, 2004).

Materials and Methodes

Mice. Inbred C57BL/6 and C57BL/6-Tg(ACTB-EGFP)1Osb/J (C57BL/6-GFP^{+}) mice at the age of 8 to 10 weeks were obtained from the animal breeding facilities at the Friedrich-Loeffler-Institute, Federal Research Institute for Animal Health, Tuebingen, Germany and were used throughout all the experiments. The C57BL/6-Tg(ACTB-EGFP)1Osb/J mouse strain was originally obtained from Charles River Germany (Wiga).

Virus and infection. Two different highly pathogenic avian influenza virus strains were used throughout this study. The mouse-adapted avian influenza A/FPV/Bratislava/79 (H7N7) virus was grown on Madin-Darby canine kidney (MDCK) cells. The Bratislava strain of the H7N7 avian influenza A virus was originally obtained from the Institute of Virology, Justus-Liebig University, Giessen, Germany. The avian influenza A H5N1 virus A/mallard/Bavaria/1/2006 grown in embryonated chicken eggs was originally obtained from the Bavarian Health and Food Safety Authority, Oberschleissheim, Germany. Like the H5N1 strain, the low pathogenic avian influenza virus (LPAIV) strain A/mallard/Bavaria/1/2005 (H5N2) was also obtained from the Bavarian Health and Food Safety Authority, Oberschleissheim, Germany and propagated on MDCK cells (Droebner et al., 2008). The SOIV strain A/Regensburg/D6/09 (H1N1v) was obtained from the Friedrich-Loeffler-Institut, Federal Research Institute for Animal Health, Riems, Germany was grown on MDCK cells.
All animal studies were approved by the Institutional Animal Care and Use Committee of Tuebingen. For infection of mice, the animals were anaesthetized by intraperitoneal injection of 200 µl of a ketamine (Sanofi) -rompun (Bayer)-solution (equal amounts of a 2%-rompun-solution and a 10%-ketamin-solution were mixed at the rate of 1:10 with PBS) and infected intranasal (i.n.) with a 10-fold MLD_{50} specific for each HPAI virus strain ($2x10^3$ pfu for H7N7, $2x10^4$ pfu for H5N1). For both, the low pathogen H5N2 and the H1N1v strain, $1x10^4$ pfu (< MLD_{50}) was used for infection.

Antibodies and flow cytometry analysis. The following fluorochrome conjugated antibodies were purchased from BD Bioscience: mAbs to mouse CD4 (L3T4), CD8a (Ly-2), CD11C (Integrin αx chain), CD3 (CD3ε chain), Siglec-F and CD103. Additionally, goat anti-influenza A antibody (AbD Serotec) and donkey anti-goat Alexa Fluor 647 (Invitrogen) were used. For flow cytometry analysis, a single-cell suspension was stained in FACS-buffer (PBS, 2% FCS, EDTA, pH 7.5) with required fluorochrome conjugated antibodies for 30 min at

4°C. After the incubation time, cells were washed and analyzed by the FACSCalibur (BD Bioscience).

Quantitative real-time PCR (qRT-PCR). Total RNA was isolated from the cell homogenate of organs using TRIZOL reagent (Invitrogen). 1 µg RNA was used for qRT-PCR to determine the expression of Gapdh, CXCL12, CCL25, ICAM-1, and V-CAM using the QuantiFast SYBR Green RT-PCR Kit (Qiagen) according to the manufacturer's protocol and the SmartCycler™ System and software (Cepheid, Sunnyvale, CA). The following specific primer for qRT-PCR were used: Mm_Gapdh_2_SG, Mm_Cxcl12_1_SG, Mm_Ccl25_1_SG, Mm_Icam1_1_SG and Mm_Vcam1_1_SG (Qiagen). The protocol for qRT-PCR was an initial incubation at 50°C for 10 min after that 95°C for 3 min, followed by 40 cycles of 95°C for 10s, 60°C for 30 sec. Afterwards, melt curve data were collected from 40°C to 90°C at a ramping rate of 0.2°C per second and finally cooling to 40°C was performed. The relative expression values were normalized to the expression value of the housekeeping gene Gapdh.
Detection of viral M-protein RNA was performed as previously described (Spackman et al., 2002) using the following oligonucleotides: 5-AGA TGA GTC TTC TAA CCG AGG TCG-3' (forward), 5'-TGC AAA AAC ATC TTC AAG TYT CTG-3' (reverse) and 5'-Tet-TCA CCC CTC AAA GCC GA-BHQ-1-3' (sonde; Metabion, Germany).

***In vitro* cytotoxicity assay.** Effector cytotoxic $CD8^+$ lymphocyte activity was measured by in *vitro* cytotoxicity assay. Therefore, five mice were infected with a 10-fold MLD_{50} of H7N7 or H5N1 virus. 6 days p.i., mice were sacrificed and leukocytes from the lung and thymus were isolated. Meanwhile, $H2b^b$ MC57 target cells were loaded with the immunodominant peptide $NP_{366-374}$ in a concentration of 10 µg/ml and labeled with 0.2 mCi of ^{51}Cr at 37°C for 1 h. For all avian influenza virus strain the peptide ASENMEAM was used, for pandemic H1N1v the peptide ASNENVEIM was utilized. Target cells were co incubated with the isolated leukocytes at various effector-to-target ratios in a final volume of 200 µl/well. After 5 h, supernatant was collected and measured for the presence of released ^{51}Cr using the micro-beta counter (Wallace). The percentage of ^{51}Cr release was calculated according to the formula previously described (Planz et al., 1993).

Influenza virus titration AVICEL® plaque assay). The titration in 96 well plates was performed as described previously (Droebner et al., 2008). Briefly, organs from sacrificed mice were homogenized in a ten percent homogenate in saline buffer and target cells were incubated with the homogenate. For H5N2 and H1N1v, trypsin was added during the

incubation period (Gibco). Thereafter, cells were immunostained by incubating for one hour with a monoclonal antibody specific for the influenza A virus nucleoprotein (AbD Serotec) followed by 30 min incubation with peroxidase-labeled anti-mouse antibody (DIANOVA). Labelling was visualized by 10 min incubation with True BlueTM peroxidase substrate (KPL). Stained plates were scanned on a flat bed scanner and the data were acquired by PhotoStudio5.5 (ArcSoft) software. Stained foci were counted. The virus titer is given as the logarithm to the base 10 of the mean value. The detection limit for this test was <1.7 log 10 ffu/ml.

***In situ* histology**. For *in situ* hybridization various organs including lung, thymus, brain, heart and kidney were removed, fixed over night in 4% buffered paraformaldehyde and embedded in paraffin. 5 µm thick tissues sections were used for *in situ* stainings.

***In situ* hybridization.** Influenza RNA in tissues was detected using single-stranded ^{35}S-labeled RNA probes which were synthesized from a bluescript KS+ vector containing a fragment of the NP gene (nt.1077 to nt.1442) of A/FPV/Rostock/34 (H7N1) as previously described (Gabriel et al., 2009). Control RNA probes were obtained from a transcription vector containing the plasmid of coxsackievirus B3 (pCVB3-R1; (Klingel et al., 1992). Pretreatment, hybridization, and washing conditions of dewaxed paraffin tissue sections were performed as described previously (Klingel et al., 1992). Slide preparations were subjected to autoradiography, exposed for three weeks at 4°C and counterstained with hematoxylin/eosin.

Preparation of single cell suspension for DC isolation. Isolation of DCs was performed as described previously (Hao et al., 2008). Mice were sacrificed and lungs were perfused with 10 ml phosphate-buffered saline (PBS). Afterwards lungs or thymi were minced and digested in RPMI 1640 medium (Gibco) together with 0.125% collagenase II (Roche) for 30 min at 37°C in 5% CO_2. Thereafter, the minced and digested fractions were passed through a 70 µm BD cell strainer (BD Bioscience) and washed three times. The cell pellets were resuspended in PSA containing 2 mM EDTA and 0.5% bovine serum albumin for the following DC purification steps.

Purification of RDCs and DCs. RDCs were isolated as previously described (Hao et al., 2008). Briefly, alveolar macrophages were removed by incubating the counted cells with a PE-labeled anti-SiglecF antibody. Thereafter, magnetic microbeads were used for cell

separation according to the manufacturer's protocol (Miltenyi Biotec GmbH). Cells were labeled with a magnetic anti-PE-microbead and separated by negative selection using an Auto-MACS Separator (Miltenyi Biotec GmbH). In the next step, the SiglecF$^-$ fraction was incubated with anti-CD11c magnetic microbeads and CD11c$^+$ SiglecF$^-$ cells were obtained by positive selection according to the manufacturer's protocol (Miltenyi Biotec GmbH). Isolation of thymus DCs was accomplished similar to the isolation steps of RDCs. In contrast to the RDC purification protocol, SiglecF$^+$ macrophages were not depleted in the thymus.

Adoptive transfer. Donor C57BL/6-GFP$^+$ mice were infected with the H7N7 influenza virus and scarified 3 days after infection. 4.5x10^6 CD11c$^+$SiglecF$^-$ cells were isolated from the lung of C57BL/6-GFP$^+$ mice and were injected i.n. into C57BL/6 wildtype recipient mice. Two days later, C57BL/6 recipient mice were also scarified and both lung and thymus were harvested. Single cell suspensions were generated and CD11c$^+$ cells were isolated using magnetic microbeads according to the manufacturer's protocol (Miltenyi Biotec GmbH). Purification was analyzed with a FACSCalibur (BD Bioscience). Cells were surveyed by immunofluorescence.

Immunofluorescence. Isolated CD11c$^+$ cells were fixed for 30 min in 4% buffered paraformaldehyde at 4°C. The fixed cells were washed twice with PBS and incubated with DAPI. Afterwards, cells were washed again, mounted with ProLong Gold Antifade Medium (Invitrogen) and were analyzed by the Apotome Care Invert Microscope Labovert FS (Leitz) and the AxioVision Rel 4.5 (Carl Zeiss Imaging).

Immunohistology. 2 µm thin slides were obtained from paraffin embedded organs. Sialic acid staining was performed as previously described (Droebner et al., 2007). Briefly, the staining of sialic acid α-2.6 linked to galactose was performed with *Sambucus nigra* agglutinin, while for sialic acid α-2.3 linked to galactose *Maackia amurensis* agglutinin was utilized (Vector Laboratories). Signal detection was visualized by ABC- and DAB kit according to the manufacturer's protocol (Vector Laboratories). For viral detection, slides were incubated with the goat α-influenza A antibody (AbD Serotec) and the ImmPRESS™ REAGENT Anti-Goat Ig Kit (Vector Laboratory) was used for secondary staining. Substrate reaction was accomplished with DAB kit (Vector Laboratory) and counterstaining was performed with hematoxylin Gill II (Carl Roth GmbH). The staining was evaluated by microscope (Leitz) and photographed with the DC 300 (Leica).

Statistical analysis. Error bars are given as the standard error of the mean. For the investigation of significant differences (p-value <0.05), paired *t-test* was performed.

Results

H5N1 influenza virus interferes with T lymphocyte development

To investigate the mechanism of influenza virus mediated lymphopenia, mice were infected for 6 days with either H7N7 or H5N1, two highly pathogenic avian influenza virus strains, the pandemic H1N1v human influenza strain or with a low pathogenic H5N2 virus of avian origin. Thereafter, the animals were sacrificed and the morphology of the thymus was analyzed. During infection with either H7N7 or H5N1 virus the thymus underwent a strong atrophic process that led to a drastically reduced size already 6 days after virus infection (Fig. 1A,B lower panel) which was not found after H1N1v or H5N2 influenza virus infection (Fig. 1C,D lower panel). H7N7 infection led to an 84% reduction of the total leucocyte count (Fig. 1E white bar). After H5N1 infection the total leucocyte amount was even more drastically reduced to less than 5% compared to total leucocytes of the thymus of uninfected mice (Fig. 1E vertical line bar). No significant leucocyte depletion could be observed after H5N2 or H1N1v infection (Fig. 1E, grey and horizontal line bar). Analysis of cells within the thymus revealed that especially the $CD4^+CD8^+$ thymocytes population was nearly absent after HPAIV infection. While $CD4^+CD8^+$ thymocytes of control, H5N2 and H1N1v infected mice presented about 80% to 85% of the cells in the thymus and extinguished about 1×10^8 cells. This population was reduced to 5% dropped to around 1×10^6 thymocytes after H7N7 but also H5N1 infection (Fig. 1F; Supplementary Fig. 1). These results suggested that HPAIV infection of mice interferes with T lymphocyte development or thymocyte progenitor cells. Since the bone marrow is the source for thymocytes progenitor cells, we next investigated whether highly pathogenic avian influenza virus is present in the bone marrow using quantitative real-time PCR to detect viral RNA. However, no viral nucleic acid could be found in the bone marrow in mice 3 and 6 days after infection with either H7N7 or H5N1 (data not shown). These results indicated that the bone marrow itself is not targeted by HPAIV influenza virus infection. To further investigate the influence of influenza virus infection of the thymus, expression of chemokines (CXCL12, CCL25) and cell adhesion molecules (ICAM-1, VCAM-1) that are involved in T lymphocyte development were analyzed. Infection of mice with H7N7 led to a strong down regulation of mRNA encoding for CXCL12 and CCL25 which are produced by thymic epithelial cells in the cortex and the medulla (Fig. 2A). The mRNA encoding for either CXCL12 or CCL25 was less reduced after H5N1 infection. In contrast ICAM-1 mRNA expression at day 6 was even slightly increased (Fig. 2B). No strong alterations of the thymus or thymocyte development were found after

H5N2 or H1N1v influenza virus infection (Fig. 2C and D). These results indicate that the thymus T lymphocyte development is altered during an HPAIV infection and give rise to the assumption that the function of thymic epithelial cells is impaired. Thus HPAIV infection affects the thymus and could interfere with the thymic homeostasis.

Presence of influenza virus specific $CD8^+$ T cells in the thymus after HPAIV infection

The previous results allowed the idea that the altered function of the thymic epithelial cells might have an influence on the impaired T lymphocyte development in the thymus after HPAIV infection including the dramatic loss of $CD4^+CD8^+$ thymocytes. Therefore, we next questioned whether the activation status of the immune lymphocytes in the thymus was altered after influenza virus infection. While in the thymus of uninfected mice the amount of activated thymocytes is less than 5% within this population, the number increased up to about 50% after H5N1 or H7N7 infection. No significant change of the thymocyte activation was observed after H5N1 or H1N1v influenza virus infection. However, HPAIV infection also changed the activation status based on CD69 expression of the single positive lymphocyte populations in the thymus. While there was no strong increase of the activated $CD4^+$ T lymphocyte population, the activated $CD8^+$ T lymphocyte fraction rose from 23% of uninfected mice up to 47% of H5N1 infected mice (Supplementary Fig 2). To determine whether activated $CD8^+$ T lymphocytes in the thymus were specific for influenza virus, an *in vitro* cytotoxicity assay was performed using target cells labeled with the immunodominant peptide $NP_{366-377}$ derived from the viral nucleoproteins (Fig. 3). As a control, influenza virus specific $CD8^+$ T lymphocytes could be detected in the lung of mice after either H5N1, H7N7, H1N1v or H5N2 influenza virus infection (Fig. 3 A-D, black solid line). Most surprisingly after H7N7 and H5N1 infection of mice nucleoprotein specific $CD8^+$ T lymphocytes were also found in the thymus (Fig. 3A,B grey solid line). In contrast, no $NP_{366-377}$ specific $CD8^+$ T cells were notable in the thymus after H5N2 or H1N1v infection (Fig. 3C,D grey solid line). These results demonstrated that after infection with both HPAIV strains functional influenza virus specific cytotoxic $CD8^+$ T lymphocytes were present in the thymus to recognize infected target cells in an MHC class I restricted manner.

Infectious H5N1 and H7N7 influenza viruses are present in the thymus

The above results indicate a direct interaction of H5N1 and H7N7 influenza virus with the thymus. Avian influenza viruses require Siaα2-3gal as a receptor. Siaα2-6gal is a prerequisite for infection with human influenza viruses. To determine whether the thymus of mice and

humans are sensible for avian or human influenza virus infection, immunohistology was performed to scrutinize the distribution of Siaα2-3gal and Siaα2-6gal. In addition to lung and mediastinal lymph nodes, Siaα2-3gal and Siaα2-6gal expression was found in the thymus of both species, whereas especially the medulla region showed positive signals for Siaα2-3gal and Siaα2-6gal (Fig. 4A, B). To analyze whether infectious influenza virus is present in the thymus of mice, virus infectivity assays were performed. H7N7 and H5N1 influenza virus was found to high titers in the lung and to moderate titers in the med. LN's and in the thymus. In addition virus was present in the spleen after H7N7 but not after H5N1 infection. In the lung of H1N1v infected mice, comparable titers to H5N1 and H7N7 infected mice were found in the lung. In contrast only low amounts of infectious virus were present in the med. LN's. In only one out of four thymi few infectious virus particles could be detected. After H5N2 influenza virus infection low amounts of virus were found in the lung and only one out of four mice revealed some infectious particles in the med. LN's. No virus was found in the thymus. (Table I). Quantitative real-time PCR (qRT-PCR) was used to confirm the data achieved by virus infectivity assay after HPAIV infection and to observe the progression of viral load in the lymphoid organs (Fig. 5A). The results demonstrate viral nucleic acid in the thymus of mice after infection with the HPAIV virus strains. In addition, viral RNA was imaged by *in situ hybridization* in the lung and thymus (Fig. 5B). The *in situ* hybridization experiments confirm the existence of viral footprints in both organs after H5N1 and H7N7 influenza virus infection and localized the infectivity in the thymus to the cortico-medullary junctions. By imaging the regions of the thymus which are virus positive, the question appears which route of infection the virus uses to reach these specific thymus cells.

Infection of lung dendritic cells by H5N1, H7N7 and human pandemic H1N1v influenza virus

Circulating DCs in addition to mature peripheral T lymphocytes can re-enter the thymus after the uptake of antigenic material in the periphery (Bonasio et al., 2006). Next to this DC attribute, it was demonstrated that DCs are a target for influenza virus infection (Hao et al., 2008). To investigate whether DCs harbor influenza virus, mice were sacrificed and respiratory DCs were isolated 3 days after infection. DCs were identified by $CD11c^{+}$ and $SiglecF^{-}$ staining. CD11c is found on DCs and macrophages. SiglecF, a sialic acid binding immunoglobulin-like lectin, is expressed by macrophages but not by dendritic cells. Flow cytometry analysis demonstrated a high infection rate of DCs either after H5N1 or H7N7 influenza virus and to a lower extends also after pandemic H1N1v infection (Fig. 6A,B).

H5N1 virus infected about 19.0% of DCs in the lung, while 13.5% of DCs were infected with H7N7 influenza virus. Only 9.2% DCs were infected with the H1N1v virus strain. In contrast, after H5N2 influenza virus infection of mice no $CD11c^+$ cells harbored viral footprints. To define the DC subpopulation being the target for influenza virus in more detail, DCs were stained against CD103 which is a marker for mucosal DCs (Fig. 6A; middle row). The flow cytometry analysis demonstrated that the $CD11c^+/CD103^+/SiglecF^-$ DC population is a preferred target for influenza virus. Nevertheless $CD11c^+/CD103^+/SiglecF^-$ DC's present roughly only 13% a of the dendritic cell population (data not shown). Our results indicate that macrophages are not the obvious main target for influenza virus infection. These findings suggest a potential role of migrating DCs in the viral spread to the thymus.

To investigate whether lung DCs migrate to the thymus after infection with HPAIV, DCs from H7N7 infected C57BL/6-GFP^+ mice were isolated and transferred into the lungs of GFP^- mice (Fig. 7A). Three days after the transfer, recipient mice were sacrificed and GFP^+ DCs were isolated from the lung and thymus. Isolated DCs were characterized by immunofluorescence. The analysis clearly demonstrated that GFP^+CD11c^+ cells were detectable in lung and most interesting in the thymus of recipient wildtype mice, providing evidence that respiratory DCs migrate to the thymus after infection with HPAIV (Fig. 7B). These results strongly propose a model by which HPAIV hitchhike DCs in the lung for trafficking into the thymus, leading to alterations of the antigen presentation for developing thymocytes.

Discussion

A common feature of human infection with pandemic avian influenza virus is a strong reduction of T lymphocytes. This feature, called lymphopenia, is also found in some other infectious diseases, in particular with new emerging pathogens (Chuang et al., 2008),(Baize et al., 2009). Nevertheless, the reason and mechanism for the declining number of lymphocytes remains unclear (Coskun et al., 2010). To investigate a possible mechanism for lymphopenia after influenza virus infection we focused on the thymus as a primary lymphoid organ. We hypothesized that highly pathogenic influenza A virus infection of mice interferes with T lymphocyte development and selection processes in the thymus which consequently leads to an impaired cellular immune response. The hypothesis was developed, since the morphology of the thymus revealed massive destruction after H5N1 and H7N7 influenza virus infection of mice but not after pandemic H1N1v and low pathogenic H5N2 influenza virus infection. As a consequence reduced or even missing naive T lymphocytes outflow could lead to the observed lymphopenia. We speculate a direct involvement of the highly pathogenic avian influenza A virus. Two reasons for such a dysregulation followed by the destruction of the T lymphocyte producing site might be possible. First, the virus stops the influx of T lymphocyte progenitor cells directly by infecting the bone marrow which is the source of T cell progenitors. Second, influenza virus infection interferes with T lymphocyte development directly in the thymus. Since quantitative real-time RT-PCR experiments revealed no traces of viral RNA in the bone marrow, we can exclude that the observed phenomenon is due to infection of the bone marrow. The hypothesis that HPAIV interferes with T lymphocyte development was supported by the findings that the expression of chemokines (CXCL12, CCL25) and cell adhesion molecules (ICAM-1, VCAM-1) involved in T cell development was drastically reduced after HPAIV but only slightly after H1N1v or H5N2 influenza virus infection. CXCL12, which is recognized by the CXCR4 receptor, is an essential prerequisite for functional thymocytes migration (Savino et al., 2002). CXCL12 is produced by both cortical and medullar epithelial cells and recent studies underline the urgent need for CXCL12/CXCR4 pathway in T lymphocyte development *in vivo* (Ara et al., 2003). In single positive $CD4^{-}CD8^{+}$ or $CD4^{+}CD8^{-}$ T lymphocytes the expression rate of CXCR4 is reduced which supports the outflow of naive T lymphocytes into the periphery (Suzuki et al., 1999). The importance of this signal pathway becomes apparent in studies with *Trypanosoma cruzi* which is the causative agent of Chagas disease and also infects the thymus. Here, the up regulation of CXCL12 in the thymus seems to lead to an outflow of immature T lymphocytes

into the periphery (Mendes-da-Cruz et al., 2006). The surprising finding that highly pathogenic avian influenza A virus infection interferes with this important signal gave reason to believe that the virus affects the thymus structure and function directly. Therefore, the question was raised whether HPAIV is able to infect the thymus. Using immunohistochemistry, we clearly demonstrated that especially the thymus medulla is positive for both Siaα2-3gal and Siaα2-6gal, a prerequisite for influenza virus infection. Moreover, we were able to demonstrate infectious virus and viral RNA in the thymus, particularly in the cortico-medullary junction and medulla, the place where negative selection occurs. After H1N1v infection virus was found in the thymus of one mouse to a low amount. This result gives rise to the assumption that this new emerging human pandemic influenza virus strain has the ability to infect the thymus. Nevertheless, from our data we speculate that a so far unknown "viral-piece" is still absent in this recent pandemic H1N1v strain to induce fatal disease. This observation could underline the fact, that pandemic H1N1v has a high morbidity coming with a mild illness while fatale cases are fairly rare (Cao et al., 2009).

The amount of activated T cells after HPAIV infection was increased in the thymus after influenza virus infection including influenza virus NP-specific $CD8^+$ T cells. The existence of activated, influenza virus specific $CD8^+$ T lymphocytes in the thymus is crucial and might lead to organ destruction via an immunopathological mechanism. Whether these cells were primed in the thymus or moved into the thymus as active virus-specific T cells remains unclear. The fact that the expression of chemokines and chemoattractants involved in T lymphocyte development was altered might argue in favor for the possibility that already activated T cells might move back from the periphery into the thymus. The re-entry of mature and even activated T lymphocytes has been described elsewhere (Hale and Fink, 2009), (Hardy et al., 2001). Still, the question how the virus is being transported into the thymus is unanswered at this point. The former paradigm of the thymus as a "one-way street" is important for a functional development of T lymphocytes. By that way the organism assures that only self-peptides are presented on the MHC-complexes during thymocytes selection processes. However, recent studies revealed that selected lymphoid populations can migrate into the thymus within the cortico-medullary junction allowing foreign antigens to reach the thymus (Mori et al., 2007). This could be important for oral tolerance against nutrition antigens (Song et al., 2006). Also, the evidences rise that an organism is able to develop a tolerance against an intravenous, intrathymic but also intranasal injected high dose antigen by deletion of antigen-specific thymocytes and induction of apoptosis of T lymphocytes in secondary lymphoid organs (Liblau et al., 1996), (Marodon et al., 2006). By reaching the

thymus, non-self antigens can generate a suppressive Treg population, which could also have an suppressive effect on the previously generated existing peripheral T cell precursor population (Cabarrocas et al., 2006). It also might be possible that highly pathogenic avian influenza viruses assemble a suppressive Treg population by migrating into the thymus. Because of the implausibility that the virus can pass the barrier between periphery and thymus by itself without causing a systemic infection, a carrier cell is more likely. In a recent publication Gabriel and colleagues demonstrated that a murine T cell line can be infected by influenza viruses *in vitro* (Gabriel et al., 2009). Moreover, the virus used in this study was also able to infect macrophages *in vitro* and *in vivo* (Gabriel et al., 2009). In our *in vivo* study, macrophages were not the major target for infection. More interestingly, it's been reported that dendritic cells can be infected by influenza viruses *in vitro* (Hao et al., 2008). Because of the DC function to migrate continuously into the LN but also in the thymus (Li et al., 2009) with or without having contact and being activated by an antigen, thymic dendritic cells play a major role in establishing tolerance by negative selection of thymocytes and induction of Tregs (Proietto et al., 2008). We hypothesized that DCs are the carrier cell type for influenza viruses. We first tested whether different influenza viruses were able to infect DCs in the lung. Flow cytometry analysis was used to demonstrate a high rate of infection of DCs by the H5N1 and H7N7 strains and to lower extends by H1N1v infection. Low pathogenic H5N2 virus infection of DCs could not be detected. Our results demonstrate that the infection of DC's with HPAIV also includes the $CD103^+$ DC subpopulation for which an induction of peripheral Tregs has already been described (Coombes et al., 2007). Since $CD103^+$ mucosal DC's only present 13% (data not shown) of the total DC population we cannot exclude that the virus strains used in this study are specialized on $CD11c^+/CD103^+$ subpopulations.

The adoptive transfer experiment using GFP^+ lung DCs further strengthen our hypothesis that DCs can migrate from the lung into the thymus. Flow cytometry and immunofluresence revealed the presence of GFP^+ cells in the thymus of HPAIV infected wild type mice. Nevertheless from our immunofluoresence data, we cannot exclude that these respiratory dendritic cells in the thymus undergo apoptotic processes either due to influenza virus infection or $CD8^+$ T cell response. From these results we hypothesize that activated, HPAIV infected DCs move from the lung into local, mediastinal lymph nodes where viral replication can take place. In a second step, DCs move further on into the thymus, where influenza virus infected DCs first reach the cortico-medullary junction and the medulla the place of negative selection processes. Thymic antigen presenting cells in the thymus, namely DCs but also thymic epithelial cells are responsible for the selection processes (Proietto et al., 2009). We

conclude that $CD45^-$ epithelial cells in the medulla are the first target for infection since viral footprints in the $CD45^+$ thymocyte population were absent (data not shown). Epithelial cells are critical for the development of T lymphocytes. These stroma cells give the structure for a working positive and negative selection of outgoing naive T lymphocytes. An interference with $CD45^-$ cells can lead to a dysregulation of T lymphocytes development especially in the younger population when the thymus is still highly active. One result could be a reduced or even missing immune response against new antigens that break through the mechanical barriers of our immune system. The pandemic H1N1v strain doesn't reach the thymus consistently which could be due to a missing pathogenesis factor, since virus titer is even higher in the lung of H1N1v infected mice compared to viral titers in the lung after H5N1 and H7N7 infection.

We propose a mechanism, where highly pathogenic avian influenza virus has the ability to infect dendritic cells in the lung. This migrating cell type can now transport the virus to secondary lymphoid organs like lymph nodes, but more important to the primary lymphoid organ: the thymus. In both cases, the infected cell can not only support the virus to spread to selected targets but also present viral antigens as pseudo self peptides. That way, an additional clonal deletion of influenza specific T lymphocytes can take place in the thymus. The collapse of the thymocytes developing signal network could be due to the fact that stromal cells in the thymus are a target for the virus (Fig. 8). Additionally, influenza specific Tregs could be generated that suppress already existing T lymphocyte activity against viral epitopes. The existence of Tregs needs to be analyzed in further studies to assure this assumption.

Taken together, the infection of dendritic cells demonstrates a very effective way to evade the immune system and could be the reason for fatal influenza virus infection that leads to lymphopenia and the strong influx of innate immune cells (Perrone et al., 2008). The fact that the Siaα2-3gal and Siaα2-6gal lectins that function as the receptor for influenza virus infection are also expressed in human thymus (Fig. 4), makes the transfer of the described mouse model to the pathogenic situation in humans likely. The resent pandemic H1N1v outbreak which also causes lymphopenia in severe clinical cases demonstrates that this described mechanism might not only be restricted to highly pathogenic avian influenza viruses but might be a general feature of severe influenza (Perez-Padilla et al., 2009).

Acknowledments

We thank Carmen Mueller, Isabell Laurisch, Mirijam Steck, Ulrich Wulle, and Martina Sauter for their excellent technical assistance.

Footnote

This work is part of the EUROFLU consortium activities and of the VIRGIL European Network of Excellence on Antiviral Drug Resistance supported by a grant (LSHMCT-2004-503359) from the Priority 1 “Life Sciences, Genomics and Biotechnology for Health” program in the 6th Framework Program of the EU. Furthermore, this research was partially supported by the Federal Government of Germany under the Influenza Research Programm “FSI” and by the BMBF Zoonose program “FluResearchNet”.

References

1. Ara, T., M.Itoi, K.Kawabata, T.Egawa, K.Tokoyoda, T.Sugiyama, N.Fujii, T.Amagai, and T.Nagasawa. 2003. A role of CXC chemokine ligand 12/stromal cell-derived factor-1/pre-B cell growth stimulating factor and its receptor CXCR4 in fetal and adult T cell development in vivo. *J. Immunol.* 170: 4649-4655.

2. Baize, S., P.Marianneau, P.Loth, S.Reynard, A.Journeaux, M.Chevallier, N.Tordo, V.Deubel, and H.Contamin. 2009. Early and strong immune responses are associated with control of viral replication and recovery in Lassa virus-infected cynomolgus monkeys. *J. Virol* 83: 5890-5903.

3. Abdel-Ghafar, A.N., T.Chotpitayasunondh, Z.Gao, F.G.Hayden, D.H.Nguyen, J.de, A.Naghdaliyev, J.S.Peiris, N.Shindo, S.Soeroso, and T.M.Uyeki. 2008. Update on avian influenza A (H5N1) virus infection in humans. *N. Engl. J. Med.* 358: 261-273.

4. Bonasio, R., M.L.Scimone, P.Schaerli, N.Grabie, A.H.Lichtman, and U.H.Von Andrian. 2006. Clonal deletion of thymocytes by circulating dendritic cells homing to the thymus. *Nat. Immunol.* 7: 1092-1100.

5. Borgherini, G., P.Poubeau, F.Staikowsky, M.Lory, M.N.Le, J.P.Becquart, C.Wengling, A.Michault, and F.Paganin. 2007. Outbreak of chikungunya on Reunion Island: early clinical and laboratory features in 157 adult patients. *Clin. Infect. Dis.* 44: 1401-1407.

6. Cabarrocas, J., C.Cassan, F.Magnusson, E.Piaggio, L.Mars, J.Derbinski, B.Kyewski, D.A.Gross, B.L.Salomon, K.Khazaie, A.Saoudi, and R.S.Liblau. 2006. Foxp3+ CD25+ regulatory T cells specific for a neo-self-antigen develop at the double-positive thymic stage. *Proc. Natl. Acad. Sci. U. S. A* 103: 8453-8458.

7. Cao, B., X.W.Li, Y.Mao, J.Wang, H.Z.Lu, Y.S.Chen, Z.A.Liang, L.Liang, S.J.Zhang, B.Zhang, L.Gu, L.H.Lu, D.Y.Wang, and C.Wang. 2009. Clinical features of the initial cases of 2009 pandemic influenza A (H1N1) virus infection in China. *N. Engl. J. Med.* 361: 2507-2517.

8. CDC. 2009. Update: Novel Influenza A (H1N1) Virus Infection --- Mexico, March--May, 2009. *MMWR* 58: 585-589.

9. Chuang, V.W., T.Y.Wong, Y.H.Leung, E.S.Ma, Y.L.Law, O.T.Tsang, K.M.Chan, I.H.Tsang, T.L.Que, R.W.Yung, and S.H.Liu. 2008. Review of dengue fever cases in Hong Kong during 1998 to 2005. *Hong. Kong. Med. J.* 14: 170-177.

10. Coombes, J.L., K.R.Siddiqui, C.V.rancibia-Carcamo, J.Hall, C.M.Sun, Y.Belkaid, and F.Powrie. 2007. A functionally specialized population of mucosal CD103+ DCs induces Foxp3+ regulatory T cells via a TGF-beta and retinoic acid-dependent mechanism. *J. Exp. Med.* 204: 1757-1764.

11. Coskun, O., I.Y.Avci, K.Sener, H.Yaman, R.Ogur, H.Bodur, and C.P.Eyigun. 2010. Relative lymphopenia and monocytosis may be considered as a surrogate marker of pandemic influenza a (H1N1). *J. Clin. Virol.* 47: 388-389.

12. Cunha, B.A. 2004. Differential diagnosis of West Nile encephalitis. *Curr. Opin. Infect. Dis.* 17: 413-420.

13. Droebner, K., C.Ehrhardt, A.Poetter, S.Ludwig, and O.Planz. 2007. CYSTUS052, a polyphenol-rich plant extract, exerts anti-influenza virus activity in mice. *Antiviral Res.* 76: 1-10.

14. Droebner, K., E.Haasbach, C.Fuchs, A.O.Weinzierl, S.Stevanovic, M.Buttner, and O.Planz. 2008. Antibodies and CD4(+) T-cells mediate cross-protection against H5N1 influenza virus infection in mice after vaccination with a low pathogenic H5N2 strain. *Vaccine* 26: 6965-6974.

15. Gabriel, G., K.Klingel, O.Planz, K.Bier, A.Herwig, M.Sauter, and H.D.Klenk. 2009. Spread of infection and lymphocyte depletion in mice depends on polymerase of influenza virus. *Am. J. Pathol.* 175: 1178-1186.

16. Geenen, V., J.F.Poulin, M.L.Dion, H.Martens, E.Castermans, I.Hansenne, M.Moutschen, R.P.Sekaly, and R.Cheynier. 2003. Quantification of T cell receptor rearrangement excision circles to estimate thymic function: an important new tool for endocrine-immune physiology. *J. Endocrinol.* 176: 305-311.

17. Hale, J.S., T.E.Boursalian, G.L.Turk, and P.J.Fink. 2006. Thymic output in aged mice. *Proc. Natl. Acad. Sci. U. S. A* 103: 8447-8452.

18. Hale, J.S. and P.J.Fink. 2009. Back to the thymus: peripheral T cells come home. *Immunol. Cell Biol.* 87: 58-64.

19. Hao, X., T.S.Kim, and T.J.Braciale. 2008. Differential response of respiratory dendritic cell subsets to influenza virus infection. *J. Virol.* 82: 4908-4919.

20. Harari, A., F.B.Enders, C.Cellerai, P.A.Bart, and G.Pantaleo. 2009. Distinct profiles of cytotoxic granules in memory CD8 T cells correlate with function, differentiation stage, and antigen exposure. *J. Virol.* 83: 2862-2871.

21. Hardy, C.L., D.I.Godfrey, and R.Scollay. 2001. The effect of antigen stimulation on the migration of mature T cells from the peripheral lymphoid tissues to the thymus. *Dev. Immunol.* 8: 123-131.

22. Hollander, G.A. and P.Peterson. 2009. Learning to be tolerant: how T cells keep out of trouble. *J. Intern. Med.* 265: 541-561.

23. Hsieh, S.M. and S.C.Chang. 2006. Insufficient perforin expression in CD8+ T cells in response to hemagglutinin from avian influenza (H5N1) virus. *J. Immunol.* 176: 4530-4533.

24. Kandun, I.N., H.Wibisono, E.R.Sedyaningsih, Yusharmen, W.Hadisoedarsuno, W.Purba, H.Santoso, C.Septiawati, E.Tresnaningsih, B.Heriyanto, D.Yuwono, S.Harun, S.Soeroso, S.Giriputra, P.J.Blair, A.Jeremijenko, H.Kosasih, S.D.Putnam, G.Samaan, M.Silitonga, K.H.Chan, L.L.Poon, W.Lim, A.Klimov, S.Lindstrom, Y.Guan, R.Donis,

J.Katz, N.Cox, M.Peiris, and T.M.Uyeki. 2006. Three Indonesian clusters of H5N1 virus infection in 2005. *N. Engl. J. Med.* 355: 2186-2194.

25. Klingel, K., C.Hohenadl, A.Canu, M.Albrecht, M.Seemann, G.Mall, and R.Kandolf. 1992. Ongoing enterovirus-induced myocarditis is associated with persistent heart muscle infection: quantitative analysis of virus replication, tissue damage, and inflammation. *Proc. Natl. Acad. Sci. U. S. A* 89: 314-318.

26. Korteweg, C. and J.Gu. 2008. Pathology, molecular biology, and pathogenesis of avian influenza A (H5N1) infection in humans. *Am. J. Pathol.* 172: 1155-1170.

27. Law, H.K., C.Y.Cheung, H.Y.Ng, S.F.Sia, Y.O.Chan, W.Luk, J.M.Nicholls, J.S.Peiris, and Y.L.Lau. 2005. Chemokine up-regulation in SARS-coronavirus-infected, monocyte-derived human dendritic cells. *Blood* 106: 2366-2374.

28. Li, J., J.Park, D.Foss, and I.Goldschneider. 2009. Thymus-homing peripheral dendritic cells constitute two of the three major subsets of dendritic cells in the steady-state thymus. *J. Exp. Med.* 206: 607-622.

29. Liblau, R.S., R.Tisch, K.Shokat, X.Yang, N.Dumont, C.C.Goodnow, and H.O.McDevitt. 1996. Intravenous injection of soluble antigen induces thymic and peripheral T-cells apoptosis. *Proc. Natl. Acad. Sci. U. S. A* 93: 3031-3036.

30. Maines, T.R., K.J.Szretter, L.Perrone, J.A.Belser, R.A.Bright, H.Zeng, T.M.Tumpey, and J.M.Katz. 2008. Pathogenesis of emerging avian influenza viruses in mammals and the host innate immune response. *Immunol. Rev.* 225: 68-84.

31. Marodon, G., S.Fisson, B.Levacher, M.Fabre, B.L.Salomon, and D.Klatzmann. 2006. Induction of antigen-specific tolerance by intrathymic injection of lentiviral vectors. *Blood* 108: 2972-2978.

32. Mendes-da-Cruz, D.A., J.S.Silva, V.Cotta-de-Almeida, and W.Savino. 2006. Altered thymocyte migration during experimental acute Trypanosoma cruzi infection: combined

role of fibronectin and the chemokines CXCL12 and CCL4. *Eur. J. Immunol.* 36: 1486-1493.

33. Mori, K., M.Itoi, N.Tsukamoto, H.Kubo, and T.Amagai. 2007. The perivascular space as a path of hematopoietic progenitor cells and mature T cells between the blood circulation and the thymic parenchyma. *Int. Immunol.* 19: 745-753.

34. Panesar, N.S. 2008. What caused lymphopenia in SARS and how reliable is the lymphokine status in glucocorticoid-treated patients? *Med. Hypotheses* 71: 298-301.

35. Perez-Padilla, R., l.R.-Z.de, L.S.Ponce de, M.Hernandez, F.Quinones-Falconi, E.Bautista, A.Ramirez-Venegas, J.Rojas-Serrano, C.E.Ormsby, A.Corrales, A.Higuera, E.Mondragon, and J.A.Cordova-Villalobos. 2009. Pneumonia and Respiratory Failure from Swine-Origin Influenza A (H1N1) in Mexico. *N. Engl. J. Med* 361: 680-689.

36. Perrone, L.A., J.K.Plowden, A.Garcia-Sastre, J.M.Katz, and T.M.Tumpey. 2008. H5N1 and 1918 pandemic influenza virus infection results in early and excessive infiltration of macrophages and neutrophils in the lungs of mice. *PLoS. Pathog.* 4: e1000115.

37. Planz, O., T.Bilzer, M.Sobbe, and L.Stitz. 1993. Lysis of major histocompatibility complex class I-bearing cells in Borna disease virus-induced degenerative encephalopathy. *J. Exp. Med.* 178: 163-174.

38. Proietto, A.I., D.S.van, and L.Wu. 2009. The impact of circulating dendritic cells on the development and differentiation of thymocytes. *Immunol. Cell Biol.* 87: 39-45.

39. Proietto, A.I., D.S.van, P.Zhou, A.Rizzitelli, A.D'Amico, R.J.Steptoe, S.H.Naik, M.H.Lahoud, Y.Liu, P.Zheng, K.Shortman, and L.Wu. 2008. Dendritic cells in the thymus contribute to T-regulatory cell induction. *Proc. Natl. Acad. Sci. U. S. A* 105: 19869-19874.

40. Salguero, F.J., M.A.Sanchez-Martin, S.F.az-San, A.A.de, and N.Sevilla. 2005. Foot-and-mouth disease virus (FMDV) causes an acute disease that can be lethal for adult laboratory mice. *Virology* 332: 384-396.

41. Savino, W., M.Dardenne, L.A.Velloso, and S.yse Silva-Barbosa. 2007. The thymus is a common target in malnutrition and infection. *Br. J. Nutr.* 98 Suppl 1: S11-S16.

42. Savino, W., D.A.Mendes-da-Cruz, J.S.Silva, M.Dardenne, and V.Cotta-de-Almeida. 2002. Intrathymic T-cell migration: a combinatorial interplay of extracellular matrix and chemokines? *Trends Immunol.* 23: 305-313.

43. Smallman-Raynor, M. and A.D.Cliff. 2007. Avian influenza A (H5N1) age distribution in humans. *Emerg. Infect. Dis.* 13: 510-512.

44. Song, F., Z.Guan, I.E.Gienapp, T.Shawler, J.Benson, and C.C.Whitacre. 2006. The thymus plays a role in oral tolerance in experimental autoimmune encephalomyelitis. *J. Immunol.* 177: 1500-1509.

45. Spackman, E., D.A.Senne, T.J.Myers, L.L.Bulaga, L.P.Garber, M.L.Perdue, K.Lohman, L.T.Daum, and D.L.Suarez. 2002. Development of a real-time reverse transcriptase PCR assay for type A influenza virus and the avian H5 and H7 hemagglutinin subtypes. *J. Clin. Microbiol.* 40: 3256-3260.

46. Suzuki, G., H.Sawa, Y.Kobayashi, Y.Nakata, K.Nakagawa, A.Uzawa, H.Sakiyama, S.Kakinuma, K.Iwabuchi, and K.Nagashima. 1999. Pertussis toxin-sensitive signal controls the trafficking of thymocytes across the corticomedullary junction in the thymus. *J. Immunol.* 162: 5981-5985.

47. Taubenberger, J.K., A.H.Reid, T.A.Janczewski, and T.G.Fanning. 2001. Integrating historical, clinical and molecular genetic data in order to explain the origin and virulence of the 1918 Spanish influenza virus. *Philos. Trans. R. Soc. Lond B Biol. Sci.* 356: 1829-1839.

48. Tran, T.H., T.L.Nguyen, T.D.Nguyen, T.S.Luong, P.M.Pham, V.C.Nguyen, T.S.Pham, C.D.Vo, T.Q.Le, T.T.Ngo, B.K.Dao, P.P.Le, T.T.Nguyen, T.L.Hoang, V.T.Cao, T.G.Le, D.T.Nguyen, H.N.Le, K.T.Nguyen, H.S.Le, V.T.Le, D.Christiane, T.T.Tran, d.J.Menno, C.Schultsz, P.Cheng, W.Lim, P.Horby, and J.Farrar. 2004. Avian influenza A (H5N1) in 10 patients in Vietnam. *N. Engl. J. Med.* 350: 1179-1188.

Figure legends

Figure 1. Morphology of the thymus after influenza virus infection in mice. Visual atrophy of the thymus after infection with high pathogenic H7N7 (*A*), H5N1 (*B*), virus strains but not by low pathogenic H5N2 *(C)* or pandemic H1N1v *(D)* influenza virus. All mice were sacrified 6 days post infection. Images show uninfected control C57BL/6 thymus (upper panel) in comparison to thymus of infected mice (lower panel) *E.* Total number of counted leucocytes in the thymus after influenza virus infection. Number of animals; control: n=8; H7N7: n = 9; H5N1: n = 9; H5N2 n = 4, H1N1v n = 4. * Paired t-test revealed significant reduction compared to control ($p < 0.025$). *F.* Changes of the thymocyte populations and single positive T lymphocytes 6 days after HPAIV influenza virus infection analyzed by flow cytometry. Thymus population after H5N2 and H1N1v are not listed here, but show comparable distribution to controls. Four mice per group were used in the experiments. The experiment was performed three-times.

Figure 2. Decreased mRNA levels of chemokines involved in T lymphocyte development after (*A*) H7N7 or (*B*) H5N1 but not after H5N2 *(C)* or H1N1v *(D)* infection using quantitative real-time RT-PCR. Analysis was performed 3 or 6 days post infection and ΔΔct-values compared to uninfected controls were evaluated (n = 3 to 4). *Paired t-test revealed significant difference to uninfected controls ($p < 0.05$).

Figure 3. *In vitro* cytotoxicity assay of influenza virus specific $CD8^+$ lymphocytes. ^{51}Chrom labeled MC57 targets cells were loaded with the immunodominant influenza peptide $NP_{366-374}$. NP specificity of $CD8^+$ T lymphocytes isolated from lung and thymus 6 days after infection with (*A*) H7N7, (*B*) H5N1, (*C*) H5N2 or (*D*) H1N1v were determined by the ^{51}Chrom release of lysed target cells.

Figure 4. Immunohistological detection of sialic acids in the lung, mediastinal lymph node and thymus of C57BL/6 mice (*A*) and the mesenterial lymph node and thymus of humans (*B*). Avian influenza viruses recognize Siaα2-3gal while human influenza viruses use Siaα2-6gal as a receptor for infection. Magnification: 20x.

Figure 5. Detection of viral mRNA. (*A*) Expression levels of viral matrix protein mRNA after H7N7 (left) or H5N1 (right) infection in the lung and lymphatic organs. Analysis was

performed from day 0 till day 6 post infection. Ct-values for every day are relative to the control ct-value of each organ. (*B*) *In situ* hybridization for the localization of viral RNA in lung and thymus**.** Numerous alveolar and bronchial epithelial cells are positive in mice infected with H7N7 and H5N1. In the thymus, H7N7 and H5N1 infected cells are located in the cortico-medullary junction (Abbreviation used in this figure: *M = medulla; C = cortex; J = cortico-medullary junction*).

Figure 6. Detection of influenza virus infected dendritic cells in the lung. (*A*) Samples were collected 3 days post infection and determined by flow cytometry. After depletion of SiglecF$^+$ cells, CD11c$^+$ cells were isolated and additionally stained for the mucosal CD103$^+$ DC subpopulation (middle row). Infection was confirmed by intracellular staining against influenza A antigens using a polyclonal antibody. *(B*) Percentage of cell populations analyzed by flow cytometry.

Figure 7. Adoptive transfer of GFP$^+$ dendritic cells into H7N7 (10-fold MLD_{50}) influenza virus infected wildtype mice. *(A)* Experimental design: DCs from infected C57BL/6-GFP expressing mice were isolated 3 days after infection and transferred in lungs of wildtyp C57BL/6 mice. Recipient mice were sacrificed 2 days after transfer and GFP$^+$ dendritic cells found in the lung and thymus (less than 1%) were visualized by immunofluorescence *(B*).

Figure 8. Proposed mechanism how HPAIV and possibly pandemic H1N1v could reach the thymus without causing a systemic infection. Influenza virus is able to infect DC's in the lung. Activated and infected DCs migrate into the lymph node where the antigen presentation and a first viral replication phase take place. Additionally, DCs migrate into the thymus where they support the viral spread and the depletion of influenza peptide specific thymocytes by antigen presentation. As a result, the amount of T lymphocytes is reduced.

Supplementary Figure 1. Calculated number of (*A*) CD4+ or (*B*) CD8+ T lymphocytes and (*C*) DP thymocytes 3 or 6 days after influenza virus infection. The quantity was evaluated by the total number of leukocytes divided by the gated quotient of the flow cytometry analysis as shown in Fig. 1. Paired t-test revealed significant difference compared to control (*$p < 0.05$; **$p < 0.01$). Five independent experiments yielded consistent results.

Supplementary Figure 2. Investigation of CD69+ activated (*A*) CD4+ or (*B*) CD8+ T lymphocytes and (*C*) DP thymocytes in the thymus. The analysis shows an increase of activated CD8+ lymphocyte after H5N1 infection and a strong boost of activated DP thymocytes after HPAIV infection on day 6 p.i. Paired t-test revealed significant differences compared to control (*$p < 0.05$; **$p < 0.01$). 3 mice were tested in three different experiments.

ABBREVIATIONS

DC = dendritic cell
DP = double positive
H1N1v = A/Regensburg/D6/09
H5N1 = A/Mallard/Bavaria/1/2006
H5N2 = A/mallard/Bavaria/1/2005
H7N7 = A/FPV/Bratislava/79
HPAIV = highly pathogenic avian influenza virus
LN = lymph node
LPAIV = low pathogenic avian influenza virus
Treg = Regulatory T cell

Table

Table I: *Distribution of the viral load 6 d post infection of C57BL/6 mice*

	Lung	Mediastinal LN	Thymus	Spleen	Brain
H7N7	**5.24 ± 0.19**	**3.71 ± 0.24**	**3.85 ± 0.23**	**3.61 ± 0.22**	**< 1.7**
H5N1	**5.29 ± 0.06**	**3.80 ± 0.35**	**2.84 ± 0.21**	**< 1.7**	**< 1.7**
H5N2	**2.91 ± 0.52**	**2.05 ± 0.31***	**< 1.7**	**< 1.7**	**< 1.7**
H1N1	**5.65 ± 0.49**	**2.22 ± 0.77**	**1.82 ± 0.10***	**3.27 ± 0.28**	**< 1.7**

Virus titers are given as the logarithm in focus forming units per 1ml organ homogenate.

[a]Low amounts of virus were detected in one out of four organs (H5N2 med LN: 3.12 ffu/ml; H1N1 thymus: 2.01 ffu/ml).

Figures

Figure 1

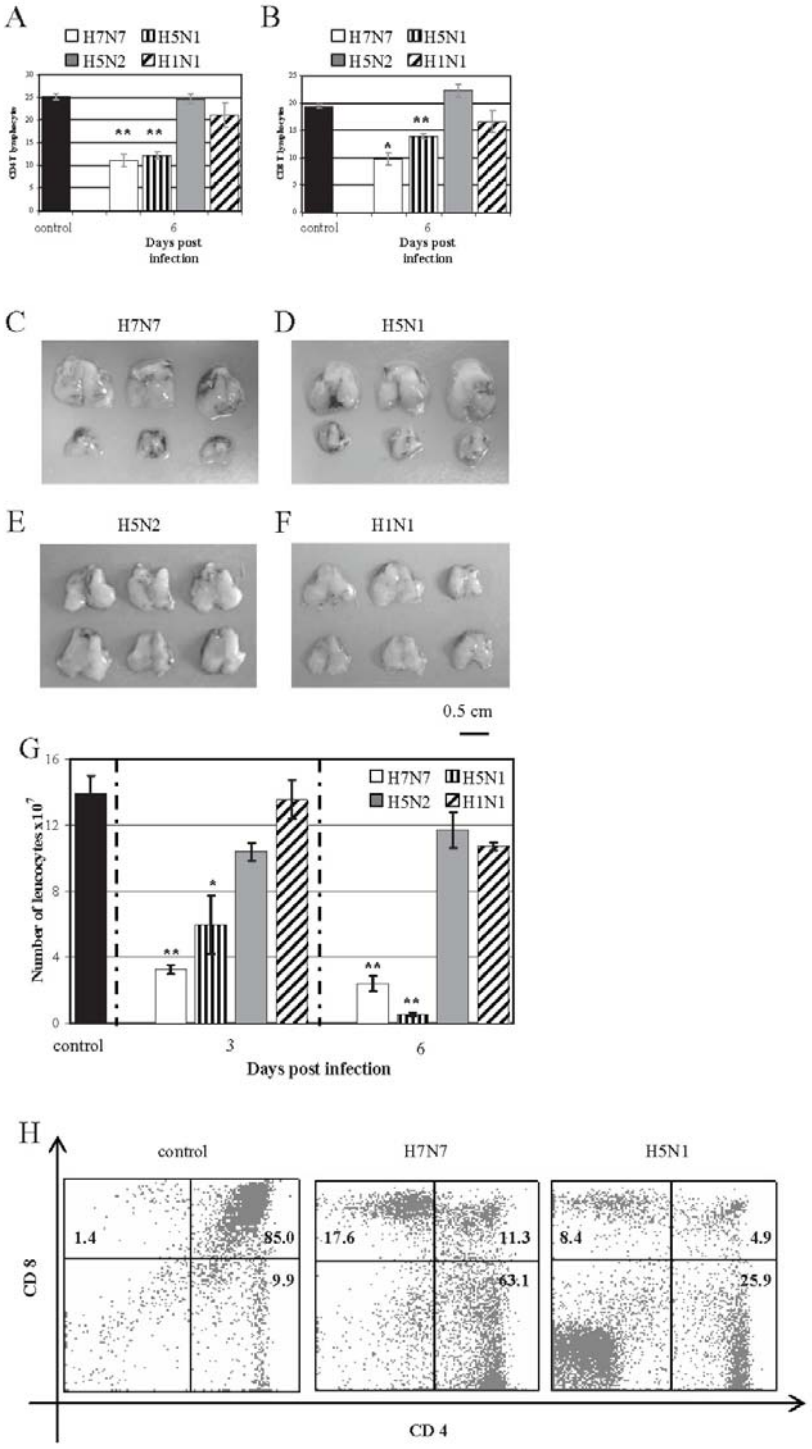

Figure 2

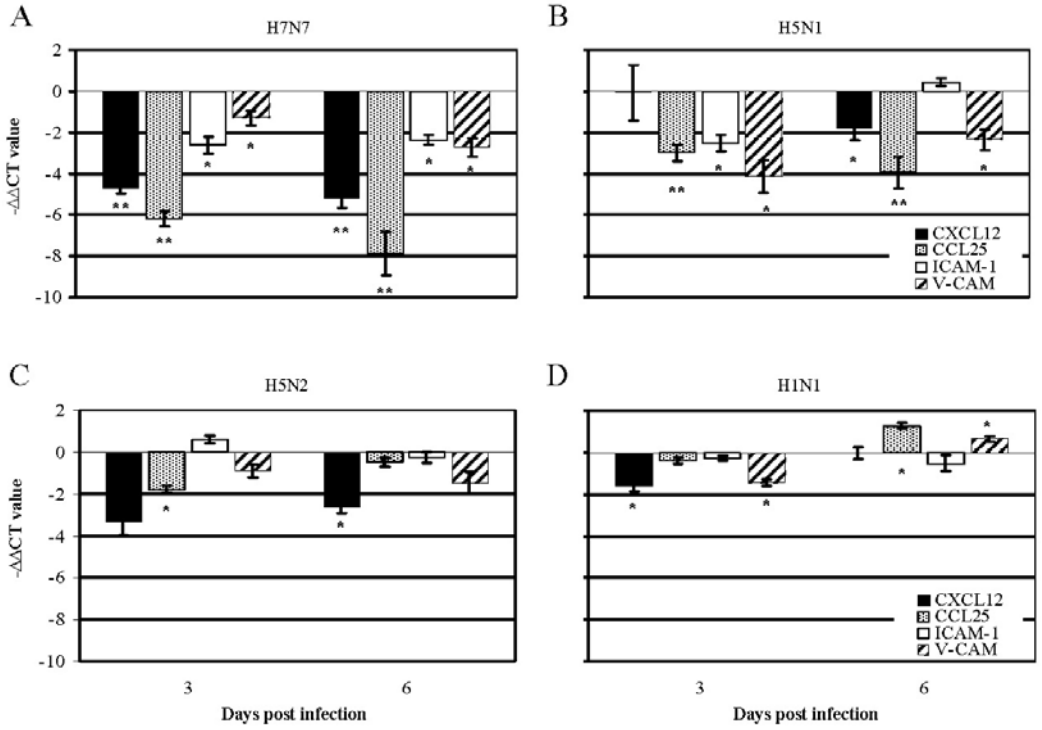

Figure 3

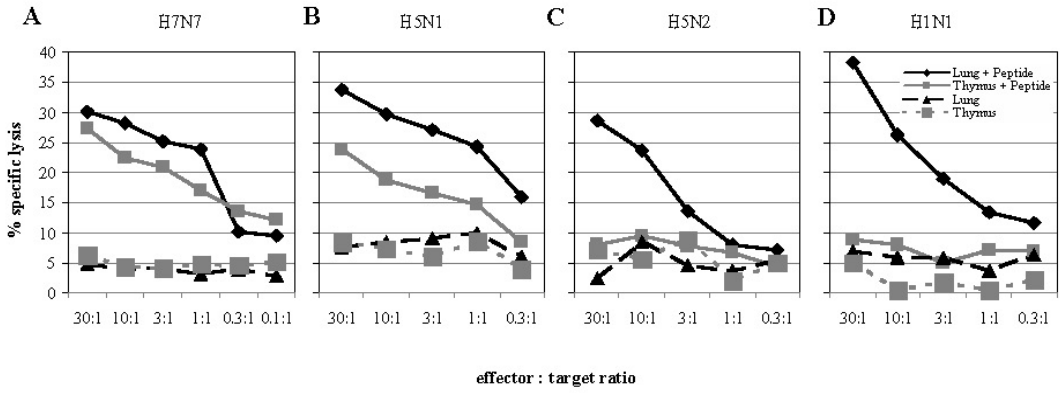

Figure 4

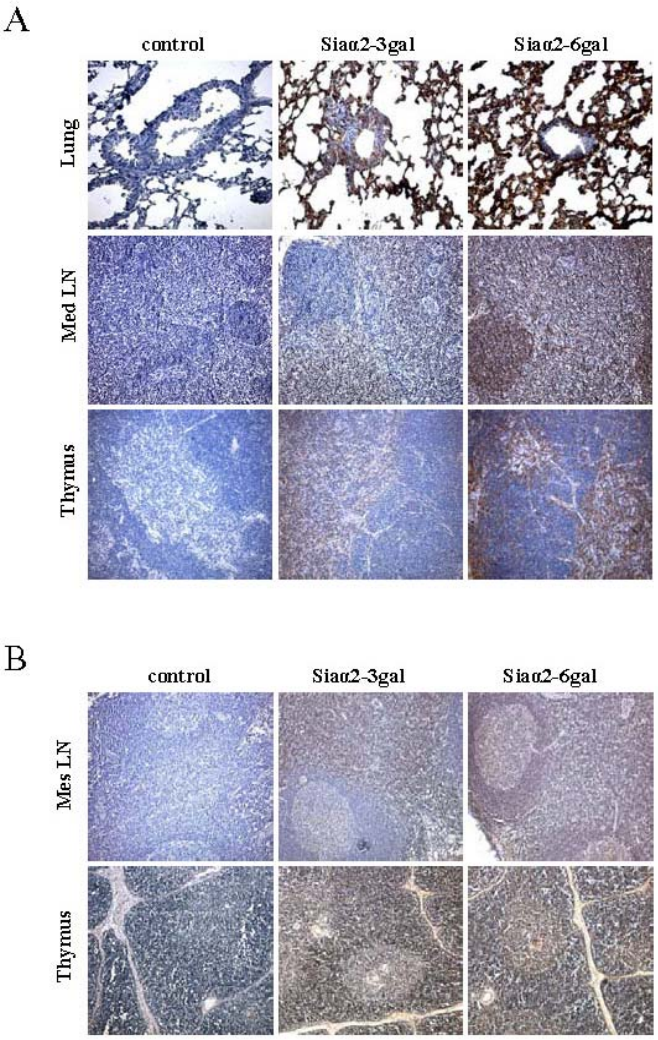
A
control
Siaα2-3gal
Siaα2-6gal
Lung
Med LN
Thymus
B
control
Siaα2-3gal
Siaα2-6gal
Mes LN
Thymus

Figure 5

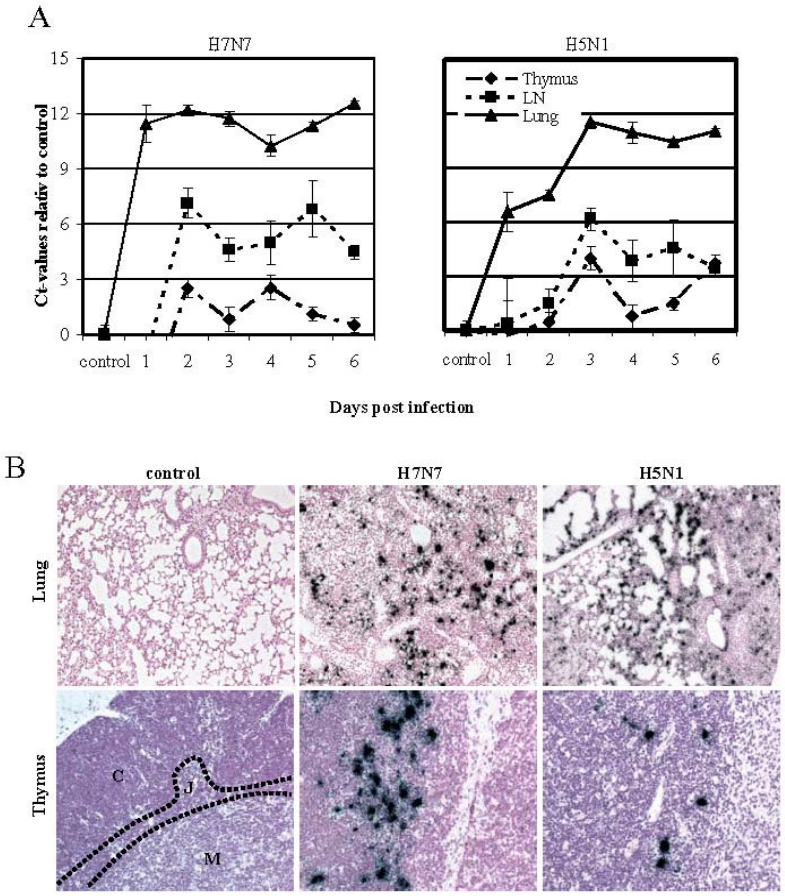
A
H7N7
H5N1
Thymus
LN
Lung
Ct-values relativ to control
15
12
9
6
3
0
control 1 2 3 4 5 6
Days post infection
B
control
H7N7
H5N1
Lung
Thymus
C
J
M

Figure 6

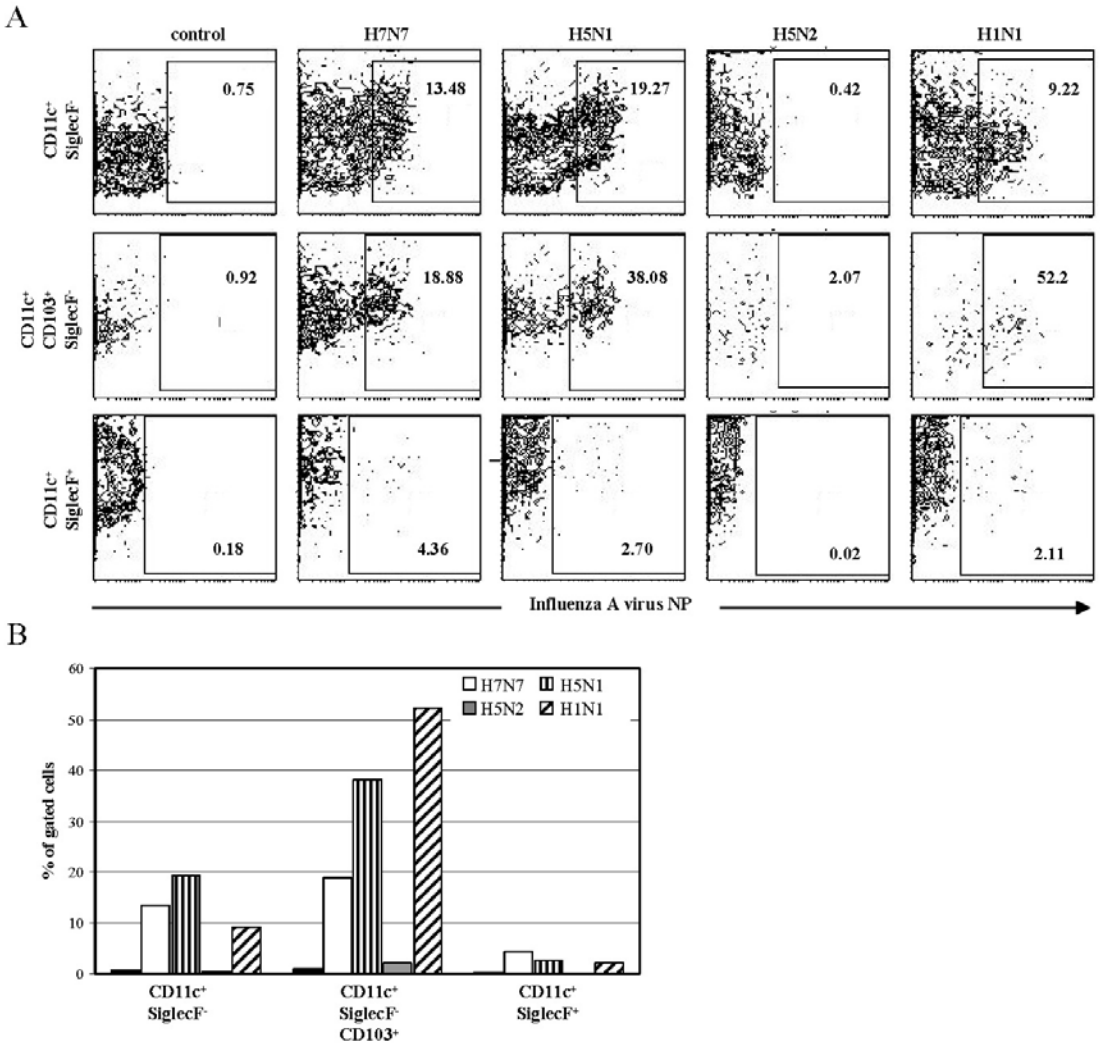
A
control
H7N7
H5N1
H5N2
H1N1
CD11c+ SiglecF-
0.75
13.48
19.27
0.42
9.22
CD11c+ CD103+ SiglecF-
0.92
18.88
38.08
2.07
52.2
CD11c+ SiglecF+
0.18
4.36
2.70
0.02
2.11
Influenza A virus NP
B
H7N7
H5N1
H5N2
H1N1
% of gated cells
0
10
20
30
40
50
60
CD11c+ SiglecF-
CD11c+ SiglecF- CD103+
CD11c+ SiglecF+

Figure 7

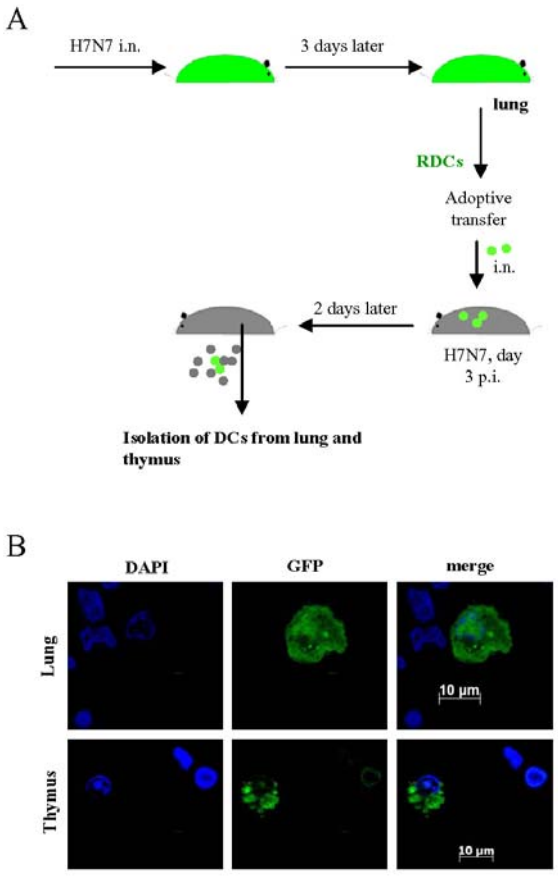

Figure 8

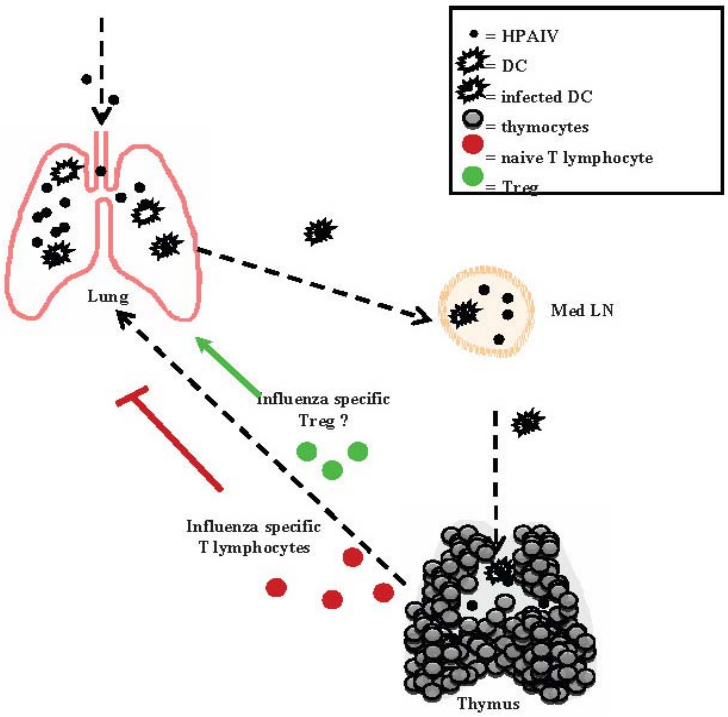

Supplementary figure 1

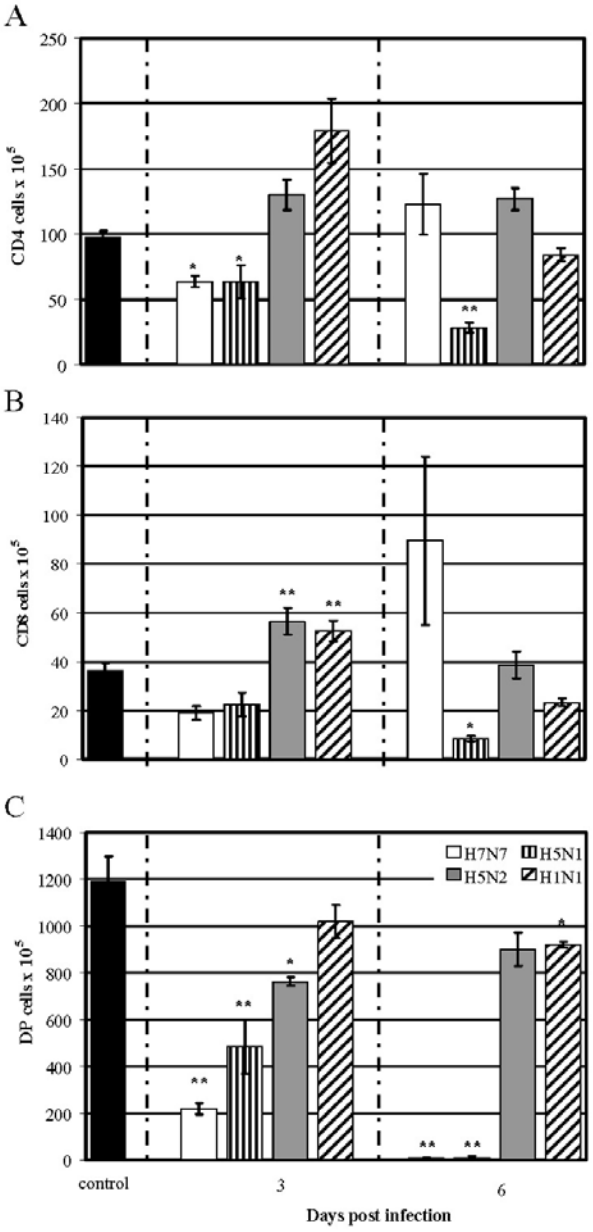

Supplementary figure 2